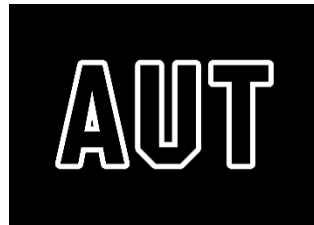


# **Achieving Thermal Comfort Using Intelligent Windows in Buildings**

**Manoj Kumar Pokhrel**



School of Engineering, Computer and Mathematical Sciences

Auckland University of Technology

A thesis submitted to Auckland University of Technology in fulfilment  
of the requirement for the degree of  
*Doctor of Philosophy*

January 2021

## Abstract

In temperate climatic conditions, residents often ventilate their houses naturally by opening windows. Though numerous studies have examined ventilation in buildings, few have attempted to modulate naturally ventilated spaces' thermal behaviour actively using just the windows. Maintaining a house's thermal comfort characteristics by modulating natural ventilation is particularly challenging, as accurately predicting natural ventilation is a complicated task, and the solution is not explicit. This is due to various non-linear, dynamic and unpredictable environmental and operating factors that influence natural ventilation's driving forces (wind and buoyancy). Furthermore, the potential for natural ventilation to regulate thermal behaviour using windows and its influence on convective heat transfer from indoor surfaces is also not explicit.

To address this issue, this work utilised a coupled thermal and network airflow to perform a building performance evaluation. In the first instance, the work examined the potential for regulating the thermal behaviour of a single-sided naturally ventilated model house by opening or shutting a window considering the NZ climatic, building and operating conditions. The study identified significant scope for regulating the thermal behaviour by opening windows. The range improved considerably for a relatively airtight and insulated house during the summer period. However, the work realised that such thermal-airflow model's robustness needs greater scrutiny; particularly the method for determining the indoor surface's convective heat transfer coefficient.

To scrutinise natural ventilation's influence on the heat transfer process, the research considered the case of a single-sided partly open air-filled cubicle enclosure with a heated floor (analogous to a room exposed to solar radiation). In doing this, Computational Fluid Dynamics (CFD) was used to determine a relationship to describe the heat transfer by natural convection from the floor surface. The relationship showed that the heat transfer can be expressed in terms of the Nusselt number ( $Nu$ ), Rayleigh number ( $Ra$ ) and window opening factor ( $WOF$ ) or aspect ratio  $\left(\frac{d'}{D'}\right)$ , and expressed in the form of either  $Nu = 0.1593 \cdot Ra^{0.33} \cdot WOF^{0.18}$  or  $Nu = 0.17 \cdot Ra^{0.33} \cdot \left(\frac{d'}{D'}\right)^{0.18}$ . The

work also observed that there was a significant variation in flow fields in 3D space resulting in a non-uniform distribution of floor heat flux on the spatial spectrum.

From this, it was apparent that there was a need to understand the added influence of wind conditions. Thus, the research further examined the flow in, and heat transfer from the floor of, the same enclosure developed in the CFD environment while considering the impact of outdoor wind conditions (wind speed and direction). The investigation showed that changes in the wind conditions could significantly change flow regimes and temperature distributions inside the space, leading to a significant variation in the convective heat transfer from the floor. This micro analysis of computational model deduced another relationship to estimate the heat transfer coefficient for the floor ( $h_{c, floor}$ ) of a naturally ventilated building as a function of wind speed at a meteorological height ( $V_m$ ) and direction ( $\phi$ ), and can be expressed as:

$$h_{c, floor} = a + (b \cdot V_m) + (c \cdot \phi) + (d \cdot V_m^2) + (e \cdot V_m \cdot \phi) + (f \cdot \phi^2).$$

Hence, the robustness of the building's thermal airflow model was improved by including these specifically deduced convective heat transfer relationships to systematically analyse the effect of buoyancy and wind. A dimensionless Archimedes Number ( $Ar$ ) was used to determine the dominant effect (wind or buoyancy) causing the airflow through the opening and switch the respective heat transfer relationships for the floor. Further analysis of the dynamic simulations reconfirmed the potential of regulating thermal behaviour by actively modulating window openings.

Finally, a solution for maintaining a house's thermal comfort characteristics by modulating natural ventilation required a technique that could adjust the opening area while encompassing the complexity, dynamics, and non-linearity associated with the natural ventilation driving forces and the building thermal behaviour. The work addressed this issue by applying an artificial intelligence technique – Artificial Neural Network (ANN), using a co-simulation environment of Transient System Simulation (TRNSYS) and Matrix Laboratory (MATLAB). The ANN-based model, trained using the dynamic simulations database, was used to actuate window intelligently and modulate the natural ventilation to maintain the indoor thermal comfort level during the summer months. The intelligent window actuating model helped ensure the ventilated space's thermal comfort condition for more than 90% instances during the summer period.

Furthermore, the research work confirmed that expanding the ANN technique to control additional heating equipment ensured the ventilated space's thermal comfort for more than 96% instances over the year.

In summary, the use of the new correlations describing the heat transfer processes in the building and ANN appear to offer a positive outlook in the development of intelligent control of actuated windows for the next generation naturally ventilated sustainable buildings. The study also provides a significant benefit to delivering a better-built environment by achieving better thermal comfort, building energy efficiency and indoor air quality.

## Table of Contents

<b>ABSTRACT .....</b>	<b>I</b>
<b>LIST OF FIGURES.....</b>	<b>VII</b>
<b>LIST OF TABLES .....</b>	<b>XI</b>
<b>ATTESTATION OF AUTHORSHIP .....</b>	<b>XII</b>
<b>ACKNOWLEDGEMENTS .....</b>	<b>XIV</b>
<b>NOMENCLATURE .....</b>	<b>XV</b>
<b>CHAPTER 1 INTRODUCTION .....</b>	<b>1</b>
1.1 BACKGROUND .....	1
1.2 THESIS OUTLINE .....	4
1.3 PUBLICATIONS .....	5
<b>CHAPTER 2 LITERATURE REVIEW.....</b>	<b>7</b>
2.1 INTRODUCTION .....	7
2.2 THERMAL COMFORT .....	7
2.3 NATURAL VENTILATION .....	10
2.4 BUILDING PERFORMANCE MODELLING .....	15
2.5 THE NOTION OF SMART AND INTELLIGENT BUILDINGS.....	20
2.6 APPROACHES FOR CONTROLLING THERMAL BUILDING ENVIRONMENT.....	22
2.7 CURRENT RESEARCH STATUS OF AUTOMATIC WINDOW ACTUATION.....	24
2.8 RESEARCH QUESTION .....	28
<b>CHAPTER 3 EXAMINING THERMAL COMFORT BEHAVIOUR OF A NATURALLY VENTILATED MODEL HOUSE ...</b>	<b>30</b>
3.1 INTRODUCTION .....	30
3.2 BUILDING PERFORMANCE MODELLING IN TRNSYS.....	31
<b>3.2.1 Thermal modelling of building in TRNSYS: Type-56 component.....</b>	<b>31</b>
<b>3.2.2 Ventilation modelling of building in TRNSYS.....</b>	<b>34</b>
3.3 METHODOLOGY .....	39
3.4 DESCRIPTION OF THE MODEL .....	41
<b>3.4.1 Physical and geographical description .....</b>	<b>41</b>
<b>3.4.2 Occupancy .....</b>	<b>42</b>
<b>3.4.3 Envelope airtightness.....</b>	<b>42</b>
<b>3.4.4 Envelope thermal resistance.....</b>	<b>42</b>
<b>3.4.5 Window and opening area .....</b>	<b>43</b>
<b>3.4.6 Input weather database .....</b>	<b>44</b>
<b>3.4.7 Heat transfer models .....</b>	<b>44</b>

3.5	RESULTS AND DISCUSSION .....	46
3.6	ROBUSTNESS, APPLICABILITY AND GENERALISABILITY OF THE RESULTS.....	55
3.7	REMARKS.....	57
<b>CHAPTER 4 THE INFLUENCE OF BUOYANCY FORCES ON THE HEAT TRANSFER BEHAVIOUR OF THE FLOOR ....</b>		<b>58</b>
4.1	INTRODUCTION .....	58
4.2	INTERNAL SURFACE CONVECTIVE HEAT TRANSFER BEHAVIOUR .....	59
4.3	METHODOLOGY .....	62
4.4	RESULT AND DISCUSSION .....	67
4.5	EMPIRICAL RELATIONSHIP AND THE ROBUSTNESS OF THE RESULT .....	74
4.6	REMARKS.....	75
<b>CHAPTER 5 THE INFLUENCE OF THE WIND CONDITIONS ON THE HEAT TRANSFER BEHAVIOUR OF THE FLOOR</b>		<b>77</b>
.....		<b>77</b>
5.1	INTRODUCTION .....	77
5.2	METHODOLOGY .....	78
5.3	MODEL VALIDATION .....	82
5.4	RESULTS AND DISCUSSION.....	85
5.5	REMARKS.....	91
<b>CHAPTER 6 IMPROVING THE ROBUSTNESS OF THE NATURALLY VENTILATED HOUSE MODEL.....</b>		<b>92</b>
6.1	INTRODUCTION .....	92
6.2	CONVECTIVE HEAT TRANSFER RELATIONSHIP FOR A FLOOR .....	93
6.3	METHODOLOGY .....	99
6.4	RESULTS .....	103
6.5	REMARKS.....	113
<b>CHAPTER 7 DEVELOPING AND APPLYING INTELLIGENT CONTROL CONCEPT .....</b>		<b>115</b>
7.1	INTRODUCTION .....	115
7.2	ARTIFICIAL NEURAL NETWORKS .....	116
7.3	METHODOLOGY .....	120
7.3.1	<i>Developing ANN-NARX model of the house</i> .....	121
7.3.2	<i>Optimising the architecture of the ANN-NARX model</i> .....	122
7.3.3	<i>Applying the ANN-NARX model predictive control strategy</i> .....	126
7.4	RESULTS AND DISCUSSION.....	127
7.4.1	<i>Examining the predicting capability of air temperature time series by ANN</i> .....	127
7.4.2	<i>Applying the ANN-NARX model for intelligently actuating a window</i> .....	132
7.4.3	<i>Expanding the ANN capability for heating</i> .....	140
7.5	REMARKS.....	150

<b>CHAPTER 8 CONCLUSIONS AND RECOMMENDATIONS .....</b>	<b>151</b>
8.1 CONCLUSIONS .....	151
8.2 RECOMMENDATIONS .....	156
<b>CHAPTER 9 REFERENCES .....</b>	<b>160</b>

## List of Figures

Figure 2-1. Schematics of PMV Calculation .....	9
Figure 2-2. Natural ventilation driving force wind (adapted from [40]) .....	11
Figure 2-3. Natural ventilation driving force buoyancy (adapted from [40]) .....	11
Figure 2-4. Typical distribution of pressure field around a building (adapted from [43]).....	12
Figure 2-5. Thermal buoyancy between two points on the opposite side of leakage (Adapted from [44]).....	14
Figure 2-6. Modelling structure of building thermal performance evaluation .....	16
Figure 2-7. A typical dynamic building simulation procedure (adapted from [52] ) .....	17
Figure 2-8. Overview of the heat transfer process in building simulation program (adapted from [53]).....	18
Figure 3-1. A typical representation of information flow in TRNSYS (adapted from [81]).....	31
Figure 3-2. A typical representation of information flow in Type 56 .....	32
Figure 3-3. Schematics of heat flux applied in Type-56 standard approach (adapted from [80, 84, 85]) .....	33
Figure 3-4. A typical bi-directional vertical velocity profile in Large Vertical Opening (adapted from [44, 45])...	37
Figure 3-5. Coupled thermal and airflow modelling approach in TRNSYS-COMIS environment.....	40
Figure 3-6. 3D building model.....	42
Figure 3-7. Effect of WOF on PMV and temperature in an average-airtight house .....	46
Figure 3-8. Effect of WOF on PMV and temperature in an ultra-airtight house.....	47
Figure 3-9. Effect of WOF on the relative humidity in an average-airtight house .....	48
Figure 3-10. Effect of WOF on the relative humidity in an ultra-airtight house .....	48
Figure 3-11. PMV variation with airtightness with shut (left) & open (right) windows.....	50
Figure 3-12. PMV variation with airtightness with shut (left) & open (right) windows.....	51
Figure 3-13. PMV variation with airtightness with shut (left) & open (right) windows.....	52
Figure 3-14. PMV frequency distribution for an average airtight house .....	53
Figure 3-15. PMV frequency distribution for an average airtight house .....	53
Figure 3-16. Thermal comfort distribution for a range of WOF & airtightness values .....	54
Figure 3-17. Thermal comfort distribution for a range of WOF & airtightness values .....	55
Figure 4-1. Schematic representation of the computational domain and model .....	63
Figure 4-2. Mesh sensitivity study .....	65
Figure 4-3. Isometric view of air filled enclosure .....	66
Figure 4-4. Front and side views of the enclosure.....	66
Figure 4-5. Velocity vectors.....	67
Figure 4-6. Air temperature contours .....	67
Figure 4-7. Velocity vectors.....	68
Figure 4-8. Air temperature contours .....	68
Figure 4-9. Velocity vectors.....	69
Figure 4-10. Air temperature contours .....	69

Figure 4-11. Velocity vectors.....	70
Figure 4-12. Air temperature contours.....	70
Figure 4-13. Velocity vectors.....	70
Figure 4-14. Air temperature contours.....	70
Figure 4-15. Velocity vectors.....	71
Figure 4-16. Air temperature contours.....	71
Figure 4-17. High-resolution temperature.....	72
Figure 4-18. Spatial distribution of floor heat.....	72
Figure 4-19. Average Nu with respect to WOF and Ra.....	74
Figure 5-1. Schematic representation of the computational domain and model.....	80
Figure 5-2. An example of the time-averaged estimation of the floor heat flux (wind speed 4m/s at 120°).....	81
Figure 5-3. Schematic representation of the 3D air space and the mid-Isoplane ( $x = 1.4$ m).....	82
Figure 5-4. Surface averaged pressure coefficient with respect to wind direction.....	83
Figure 5-5. Localised pressure coefficient distribution on a closed enclosure [face orthogonal to upstream wind at 0° angle of attack].....	84
Figure 5-6. Localised pressure coefficient distribution on a closed enclosure (face orthogonal to upstream wind at 0° angle of attack) (Adapted from TPU (n. d.).....	84
Figure 5-7. Velocity vectors.....	85
Figure 5-8. Air temperature contours.....	85
Figure 5-9. Velocity vectors.....	86
Figure 5-10. Air temperature contours.....	86
Figure 5-11. Velocity vectors.....	87
Figure 5-12. Air temperature contours.....	87
Figure 5-13. Effect of external wind speed on the floor's average Nu number [Wind condition at reference height of 10 m and angle of attack 0°].....	88
Figure 5-14. Velocity vectors [Wind speed = 4 m/s, angle of attack = 180°].....	90
Figure 5-15. Air temperature [Wind speed = 4 m/s, angle of attack = 180°].....	90
Figure 5-16. Effect of varying wind direction on the floor's average Nu Number [Wind speed of 4 m/s at a reference height of 10 m].....	91
Figure 6-1. Floor CHTC with respect to WOF and temperature difference for the buoyancy-driven case.....	94
Figure 6-2. Average floor Nu with respect to different wind reference conditions at the height of 10 m.....	97
Figure 6-3. Average floor CHTC with respect to different wind reference conditions at the height of 10 m.....	98
Figure 6-4. Floor average heat transfer behaviour with respect to the square root of Ar.....	101
Figure 6-5. Flowchart for switching floor convective heat transfer correlations.....	103
Figure 6-6. Percentage thermal comfort duration ( $-0.7 < PMV < 0.7$ ) with respect to WOF.....	104
Figure 6-7. Percentage of thermal comfort duration ( $-0.7 < PMV < 0.7$ ) with respect to WOF.....	105
Figure 6-8. Percentage of thermally uncomfortable hot duration ( $PMV > 0.7$ ) with respect to WOF & airtightness (Ravg 2.01, January).....	106

<i>Figure 6-9. Percentage of thermally uncomfortable hot duration (PMV&gt;0.7) with respect to WOF &amp; airtightness (Ravg 3.4, January).....</i>	<i>107</i>
<i>Figure 6-10. Percentage of thermally uncomfortable cold (PMV&lt;-0.7) duration with respect to WOF &amp; airtightness (Ravg 2.01, January).....</i>	<i>108</i>
<i>Figure 6-11. Percentage of thermally uncomfortable cold (PMV&lt;-0.7) duration with respect to WOF &amp; airtightness (Ravg 3.4, January).....</i>	<i>109</i>
<i>Figure 6-12. Percentage of thermally comfortable and uncomfortable duration (with respect to WOF &amp; airtightness (Ravg 2.01, January).....</i>	<i>110</i>
<i>Figure 6-13. Percentage of thermally comfortable and uncomfortable duration (with respect to WOF &amp; airtightness (Ravg 2.6, January).....</i>	<i>111</i>
<i>Figure 6-14. Percentage of thermally comfortable and uncomfortable duration (with respect to WOF &amp; airtightness (Ravg 3.22, January).....</i>	<i>112</i>
<i>Figure 6-15. Percentage of thermally comfortable and uncomfortable duration (with respect to WOF &amp; airtightness (Ravg 3.4, January).....</i>	<i>112</i>
<i>Figure 7-1. Typical structure of the MLP-ANN (adapted from [150]) .....</i>	<i>117</i>
<i>Figure 7-2. A typical ANN-NARX structure .....</i>	<i>120</i>
<i>Figure 7-3. Neural network performance with default architecture .....</i>	<i>122</i>
<i>Figure 7-4. Sensitivity of average minimum squared error values for different values hidden layers and delays .....</i>	<i>123</i>
<i>Figure 7-5. Sensitivity of average regression values for different values hidden layers and delays .....</i>	<i>123</i>
<i>Figure 7-6. The sensitivity of training time for different values of hidden layers and delays .....</i>	<i>124</i>
<i>Figure 7-7. The sensitivity of regression values of supplementary tests for different values of hidden layers and delays.....</i>	<i>125</i>
<i>Figure 7-8. The optimum neural network architecture.....</i>	<i>125</i>
<i>Figure 7-9. A schematic demonstrating the co-simulation strategy of ANN and coupled thermal &amp; airflow model .....</i>	<i>126</i>
<i>Figure 7-10. Indoor air temperature from the ANN and TRNSYS model (WOF 0.75, AVG house with Ravg 3.2, first week of January and July).....</i>	<i>128</i>
<i>Figure 7-11. Indoor air temperature from the ANN and TRNSYS model (WOF 0.4, AVG house with Ravg 3.2, first week of January and July).....</i>	<i>129</i>
<i>Figure 7-12. Indoor air temperature from the ANN and TRNSYS model (WOF 0.1, AVG house with Ravg 3.2, first week of January and July).....</i>	<i>130</i>
<i>Figure 7-13. Indoor air temperature from the ANN and TRNSYS model (WOF 0.1, UAT house with Ravg 3.2, October).....</i>	<i>131</i>
<i>Figure 7-14. Actuator performance for the model (AVG house with Ravg 3.2) for a typical day in January ....</i>	<i>132</i>
<i>Figure 7-15. Frequency distribution of PMV after using window actuator (AVG house with Ravg 3.2 for first week of January).....</i>	<i>133</i>

<i>Figure 7-16. Frequency distribution of PMV for fixed WOF 0.75 (AVG house with <math>R_{avg}</math> 3.2 for first week of January) .....</i>	<i>134</i>
<i>Figure 7-17. Thermal comfort distribution of house (<math>R_{avg}</math> 3.2) with and without window control for first week of January .....</i>	<i>135</i>
<i>Figure 7-18. Actuator performance for the model (AVG house with <math>R_{avg}</math> 3.2) for a typical day in July .....</i>	<i>136</i>
<i>Figure 7-19. Frequency distribution of PMV after using window actuator (AVG house with <math>R_{avg}</math> 3.2 for first week of July) .....</i>	<i>137</i>
<i>Figure 7-20. Frequency distribution of PMV with window shut (WOF value 0) of the model (AVG house with <math>R_{avg}</math> 3.2 for first week of July) .....</i>	<i>137</i>
<i>Figure 7-21. Thermal comfort distribution of house (<math>R_{avg}</math> 3.2) with and without window control for first week of July.....</i>	<i>138</i>
<i>Figure 7-22. Impact of window control on thermal comfort distribution of house (AVG house with <math>R_{avg}</math> 3.2 for first week of each month).....</i>	<i>139</i>
<i>Figure 7-23. Performance of actuator and heating device working together for the model (AVG house with <math>R_{avg}</math> 3.2) for a typical day in January .....</i>	<i>141</i>
<i>Figure 7-24. Frequency distribution of PMV after using window actuator (AVG house with <math>R_{avg}</math> 3.2 for first week of January).....</i>	<i>142</i>
<i>Figure 7-25. Thermal comfort distribution of house (<math>R_{avg}</math> 3.2) with and without window control and heater control for first week of January.....</i>	<i>143</i>
<i>Figure 7-26. Performance of actuator and heating device working together for the model (AVG house with <math>R_{avg}</math> 3.2) for a typical day in July.....</i>	<i>144</i>
<i>Figure 7-27. Frequency distribution of PMV applying both auxiliary heating device and window actuation (AVG house with <math>R_{avg}</math> 3.2 for first week of July).....</i>	<i>145</i>
<i>Figure 7-28. Performance of window fixed opening (WOF 0.25) with intelligent control of the heating device for the model (AVG house with <math>R_{avg}</math> 3.2) for a typical day in July.....</i>	<i>146</i>
<i>Figure 7-29. Frequency distribution of PMV applying auxiliary heating device and fixed window opening at WOF value of 0.25 (AVG house with <math>R_{avg}</math> 3.2 for first week of July).....</i>	<i>147</i>
<i>Figure 7-30. Thermal comfort distribution of house (<math>R_{avg}</math> 3.2) with and without window control and heater control for first week of July .....</i>	<i>148</i>
<i>Figure 7-31. Impact of intelligent control of both window and auxiliary heater on thermal comfort distribution of house (AVG house with <math>R_{avg}</math> 3.2 for first week of each month).....</i>	<i>149</i>
<i>Figure 7-32. Impact of intelligent control only on the auxiliary heater on thermal comfort distribution of house (AVG house with <math>R_{avg}</math> 3.2 for first week of each month) .....</i>	<i>149</i>

## List of Tables

<i>Table 2-1 Thermal comfort-related quantities definition and ranges [adapted from [31]</i> .....	8
<i>Table 2-2. Thermal comfort categories according to EN ISO 7730 [35]</i> .....	10
<i>Table 3-1. Building facade description</i> .....	43
<i>Table 3-2. Default values of constants and exponents [80]</i> .....	45
<i>Table 3-3. Parameters for calculating heat transfer coefficient for external surface materials [95]</i> .....	45
<i>Table 3-4 Monthly mean values of the conditions for Ravg 2.01, AVG and Ravg 3.4 UAT</i> .....	49
<i>Table 4-1 Convective heat transfer behaviour of floor due to buoyancy-driven force</i> .....	73
<i>Table 5-1 Effect of wind speed on heat transfer behaviour from the floor</i> .....	88
<i>Table 6-1. Default values of constants and exponents [80]</i> .....	95
<i>Table 6-2. Constants of polynomial Equation (6-4) for the different range of wind direction</i> .....	99
<i>Table 6-3 Floor average Nu and Ar with respect to increasing wind speed</i> .....	101
<i>Table 7-1 Input quantities for the ANN model</i> .....	121
<i>Table 7-2. Comfort period proportion for different values of WOF and window actuation (AVG house with Ravg 3.2 for first week of January)</i> .....	134

## **Attestation of Authorship**

I hereby declare that this submission is my own work and that, to the best of my knowledge and belief, it contains no material previously published or written by another person (except where explicitly defined in the acknowledgements), nor materials which to a substantial extent has been submitted for the award of any other institution of higher learning.

Manoj Kumar Pokhrel



## Acknowledgements

I would like to gratefully thank and acknowledge the following people, without whom I would not have been able to complete this research, and without whom I would not have made it through my PhD degree!

The mechanical engineering department at Auckland University of Technology, especially to my supervisor Associate Professor Dr Tim Anderson, whose insight and knowledge into the subject matter steered me through this research. And special thanks to Professor Dr Tek Tsing Lie, whose encouragement as a mentor supervisor helped me reach this destination. I would also like to thank Dr Jonathan Currie for his insightful brief about optimal and predictive intelligent control systems during my initial research work stage. I would also like to thank the good people at the Fairview System Limited, particularly the research and design team who provided me with the opportunity to work with the team and help me understand the commercial prospect of the project. I would also like to thank Callaghan Innovation, New Zealand, for supporting the project.

My colleagues at the Auckland University of Technology, who have supported me for the past four years of study! My work colleague and supervisor at Auckland Transport, who have always encouraged me to complete this additional piece of work than the regular office work. My biggest thanks to my family for all the support you have dedicated to me throughout the period of this research. For my kids, Manashi and Manaslu sorry for being even grumpier than normal whilst I wrote this thesis! And for my wife Sujata, thanks for all your support, without which I would have stopped these studies a long time ago. You have been amazing! And to my mother, who always encouraged me to this PhD a long time ago.

# Nomenclature

## Abbreviations

<b>Abbreviation</b>	<b>Description</b>
ANN	Artificial Neural Network
NZ	New Zealand
ACH	Air Changes per Hour
WHO	World Health Organization
NZBC	New Zealand Building Code
IAQ	Indoor Air Quality
AUT	Auckland University of Technology
CI	Callaghan Innovation
TRNSYS	Transient Simulation System Tool
CFD	Computational Fluid Dynamics
WOF	Window Opening Factor
MATLAB	Matrix Laboratory
CHTC	Convective Heat Transfer Coefficient
PMV	Predicted Mean Vote
PPD	Percentage of People Dissatisfied
ASHRAE	American Society of Heating Refrigeration and Air conditioning
DOE	Department of Energy
COMIS	Conjunction with Multizone Infiltration Specialists
PID	Proportional Integrate D
HVAC	Heating Ventilation and Air Conditioning
MPC	Model (based) Predictive Control
NMPC	Non-Linear Model Predictive Control
FL	Fuzzy Logic
HBM	Heat Balance Method
NL	Neutral level

DTY	Draughty
UAT	Ultra Airtight
AVG	Average Airtight
AT	Airtight
LKY	Leaky
LVO	Large Vertical Opening
TMY	Typical Meteorological Year
BES	Building Energy Simulation
SST	Shear Stress Transitional
SIMPLEC	Semi-Implicit Method for Pressure Linked Equations-Consistent
PRESTO	Pressure Staggering Option
MLP	Multi-Layer Perceptron
DLP	Double Layer Perceptron
MSE	Mean Square Error
NARX	Nonlinear Autoregressive with Exogenous Input
GHR	Global Horizontal Radiation
R	Regression
WC	Window Control
HC	Heater Control
RBF	Radial Basis Function
ANFIS	Artificial Neuro-Fuzzy Inference System

## List of Symbols and Definitions

<b>Symbol</b>	<b>Definition</b>
$M$	Metabolic rate
$Clo$	Clothing insulation
$v$	Relative air velocity
$T_r$	Mean radiant temperature
$T_a$	Indoor air temperature
$P_w$	Vapour pressure of water in ambient air
$C_p$	Pressure coefficient on a building surface
$(x, y, z)$	A point on a building surface
$P(x, y, z)$	The surface pressure on the façade at point $(x, y, z)$
$P_0$	Static (atmospheric) pressure
$P_{dyn}$	Wind-induced dynamic pressure
$\rho_o$	The density of outside ambient air
$V$	Reference wind velocity at a building location
$z$	Reference height of a building
$\emptyset$	Wind direction
$V(h)$	Wind speed at a height $h$
$V(h_0)$	Wind speed at a reference height $h_0$
$\alpha$	Wind velocity profile exponent
$T$	Temperature
$P$	Pressure
$\rho$	Density
$Z$	Height
$P_A$	Reference pressure at zone A
$P_B$	Reference pressure at zone B
$\rho_A$	Reference air density at zone A
$\rho_B$	Reference air density at zone B
$T_A$	Reference air temperature at zone A
$T_B$	Reference air temperature at zone B

$Z_A$	Reference height at zone A
$Z_B$	Reference height at zone B
$P_i$	Local pressure at a point $i$
$P_j$	Local pressure at a point $j$
$Z_i$	Local height at a point $i$
$Z_j$	Local height at a point $j$
$P_{stack}$	Pressure difference induced by the stack effect
$T_{a,predicted}$	Predicted inside room temperature
$LUB$	FORTTRAN logical unit for reading the *.bui file written by TRNBUILD
$T^* - MODE$	Switch for calculation of star network in TRNSYS
$A_{op}$	The weighting factor for operative room temperature in TRNSYS
$q_{s,o}$	Net heat flux into the wall at an outside surface
$q_{c,e}$	Convective heat flux
$q_{r,e}$	Longwave radiation heat flux
$q_{s,e}$	Absorbed incident solar radiation heat flux
$T_{sky}$	Sky temperature
$f_{s,sky}$	View factor to the sky
$T_{sgrd}$	Fictive ground temperature
$q_{s,i}$	Transient conduction heat flux at the inside surface
$q_{s,j}$	Radiation heat flux absorbed at the inside surface $j$
$q_{u,j}$	Users specified heat flux at the inside surface $j$
$q_{r,j}$	Net radiative heat flux from an inside surface $j$ to all other inside surfaces
$q_{c,j}$	Convective heat flux at the inside surface $j$
$T_{star,i}$	Star temperature of zone $i$
$T_{a,i}$	Ambient air temperature at zone $i$
$R_{star,i}$	Star resistance of zone $i$
$Q_{inf,i}$	Infiltration gain from outside to zone $i$
$Q_{v,i}$	Ventilation gain from the user's defined ventilation source
$Q_{gain,i}$	Convective heat gain from people, equipment, illumination etc.
$Q_{cplg,i}$	Ventilation gain due to coupling with other zones

$Q_{solair,i}$	Convection gain to the internal air due to the fraction of solar radiation entering an air node through an external window
$Q_{ISHCCI,i}$	convective gain to the internal air due to absorbed solar radiation on all internal shading devices of the zone
$\dot{m}_{im}$	Air mass flow through the $i^{\text{th}}$ flow path of the $m^{\text{th}}$ node
$\dot{m}$	Air mass flow rate
$C_s$	Air mass flow coefficient
$N$	Airflow exponent
$\Delta P$	Pressure difference
$\Delta P(z)$	The pressure difference across an opening connecting two zones
$\dot{m}_{AB}$	Air mass flow rate from zone A to B
$C_d$	Discharge coefficient
$H'$	Height of a rectangular opening
$W'$	Width of a rectangular opening
$\rho(z)$	Air density at point $z$ on Z-axis
$w(z)$	Width of the opening at point $z$ on Z-axis
$_{AB}$	Subscript defining flow direction from zone A to B
$_{BA}$	Subscript defining flow direction from zone B to A
$V(Z)$	Air velocity at point $z$ on Z-axis
$\dot{m}_{BA}$	Air mass flow rate from zone B to A
$Re$	Reynolds number
$Gr$	Grashof Number
$V_0$	Wind speed at a building reference height
$\vartheta$	Viscosity of air
$D_r$	Depth of the room
$T_m$	Mean of absolute ambient and room air temperature
$R - value$	The thermal resistance value of building façade component
$R_{avg}$	Weighted average envelope thermal resistance value of all the façade components of a house
$R \approx NZBC$	The thermal resistance value of facade components according to the New Zealand building code standard schedule method for non-solid construction
$h_{c,j}$	Convective heat transfer coefficient for inside surface $j$

$T_{s,j}$	The temperature at inside surface j
$n$	Exponent representing flow regime
$C$	Constant representing the geometry of the surface
$T_{s,f}$	The temperature at the inside floor surface
$T_{s,c}$	The temperature at inside ceiling surface
$h_{c,e}$	Convective heat transfer coefficient at the outside of the exterior walls and roof
$V_m$	Wind velocity at meteorological station height (10 m)
$a_1$	Coefficient to estimate envelope exterior heat transfer for different materials
$a_2$	Coefficient to estimate envelope exterior heat transfer for different materials
$a_3$	Coefficient to estimate envelope exterior heat transfer for different materials
$T_o$	Outdoor ambient air temperature
$RH_o$	Outdoor air relative humidity
$RH_a$	Indoor zone air relative humidity
$INF_{WINDOW}$	Natural ventilation through the window
$q$	Rate of convection heat transfer per unit surface area
$h_c$	Convective heat transfer coefficient
$\Delta T$	The temperature difference between the surface and the surrounding
$Nu$	Nusselt Number
$L_c$	Characteristic length
$k$	Thermal conduction of air at the film air properties
$g$	Gravitational acceleration
$\beta$	Coefficient of thermal expansion
$Ra$	Rayleigh number
$Pr$	Prandtl number
$\nu$	Momentum diffusivity
$\alpha'$	Thermal diffusivity
$L$	Length of the room cavity
$W$	Width of the room cavity
$H$	Height of the room cavity

$\approx$	Approximately
$y^+$	A non-dimensional wall distance for a wall-bounded flow
$k - \omega$	A two-equation turbulence model including transported variables of turbulent kinetic energy ( $k$ ) and specific dissipation ( $\omega$ )
$k - \omega SST$	A two-equation eddy viscosity model
$x$	The distance along X-Axis of the cartesian coordinate system
$y$	The distance along Y-Axis of the cartesian coordinate system
$z$	The distance along Z-Axis of the cartesian coordinate system
$h_{c, floor}$	Floor average convective heat transfer coefficient
$d'$	Opening height
$D'$	Overall enclosure height
$T_{s, floor}$	Inside surface temperature of the floor
$T_o$	Outside ambient air temperature
$T_{s, ceiling}$	Inside surface temperature of the ceiling
$Ar$	Archimedes Number
$a$	Constant value defined for different ranges of wind direction
$b$	Constant value defined for different ranges of wind direction
$c$	Constant value defined for different ranges of wind direction
$d$	Constant value defined for different ranges of wind direction
$e$	Constant value defined for different ranges of wind direction
$f$	Constant value defined for different ranges of wind direction
$\Delta T$	The temperature difference between the indoor floor surface to outdoor ambient
$T_{av}$	Average of the indoor room floor surface and outdoor ambient temperature
$h_o$	Building reference height
$h_m$	Meteo mast reference height
$\Delta T'$	The temperature difference between the indoor floor surface to indoor ambient
$K$	Number of outputs of a typical ANN model
$I$	Number of inputs of a typical ANN model
$J$	Number of hidden layers neurons of a typical ANN model
$w_{kj}$	Weight from neuron $z_j$ to neuron $y_k$ of a typical ANN model

$c_k$	Bias for the neurons $y_k$ of a typical ANN model
$w_{ji}$	Weight from neuron $x_i$ to neuron $z_j$ of a typical ANN model
$b_j$	Bias for the neurons $z_j$ of a typical ANN model
$f_y$	Non-linear activation function with a sigmoid shape
$f_z$	Non-linear activation function with a sigmoid shape
$y(t)$	Output or target time series of a typical ANN-NARX structure
$x(t)$	Inputs time series of a typical ANN-NARX structure
$d'$	Past values of the input, output or target time series
$W_{nn}$	The typical weight of ANN-NARX structure
$b_{nn}$	Typical biases of ANN-NARX structure
$D_{nn}$	Typical delay of ANN-NARX structure
$HRS$	Hours of the day
$OCC$	A random number of occupants
$GHR$	Global horizontal radiation

# Chapter 1 Introduction

## 1.1 Background

In New Zealand (NZ), there are approximately 1.6 million residential houses [1] typically constructed with metal roofs mounted on timber frames, a large floor area and little or no insulation. This housing stock has a considerable variation in airtightness (0.3 to 0.9 Air Changes per Hour (ACH)) [2, 3]. If compared with the standard passive house airtightness requirement of 0.03 ACH (0.6 ACH at 50Pa) [4], the best air-tight houses in NZ leak approximately ten times more than this. As most of these houses are very old and were developed with or without any compliance with the then prevailing building codes, there is a wide variation in building fabric characteristics and envelope thermal resistance in the current residential housing stock of NZ.

Inadequate thermal resistance and airtightness of the envelope causes most of the winter cold and damp in NZ homes leading to an uncomfortable and unhealthy interior living space. Typically, the NZ houses are damp due to a diverse range of indoor, outdoor and construction related moisture sources [5, 6, 7]. However, the inherent characteristics of the housing stock and relatively low quality makes most of them perform poorly, in terms of thermal comfort and indoor air quality in winter, without an auxiliary heating means [2]. Some of the studies state that the indoor air temperature of the typical NZ house is relatively low in the winter compared to the range of 18-24°C suggested by World Health Organization (WHO) [8, 9]. The indoor relative humidity is usually above 65% in the winter, providing an ideal condition for mould growth [8, 10]. These studies have identified that the inadequate amount of heating and insulation [8, 11] are the primary rationale behind it. These generic characteristics of NZ houses mean more energy is required to maintain a minimum level of thermal comfort year-round.

There has been a gradual introduction of mechanical ventilation systems mostly limited to the kitchen, bathroom and laundry in post-1970s construction. Most of the window(s) in the NZ houses built pre-1970s have wooden single-glazed double-hung, casements with awning type, with aluminium-framed designs introduced more recently [2, 12]. NZ has a mild temperate climate having a mean annual outdoor air temperature in the range of 10°C-16°C [13] which is lower than the generally accepted indoor

comfortable temperature range of 19-27°C [14]. This climatic condition has led to 90% of the NZ houses relying on natural ventilation through windows in the summer to improve the indoor comfort condition. Both positive pressure/roof cavity or balanced pressure/heat recovery mechanical ventilation systems are popular in NZ and are installed in approximately 10% of residential houses [12]. Another study on the introduction of positive pressure ventilation systems in Auckland indicates that they help significantly to sustain the exposure to an indoor temperature above 18°C [1].

The building codes in New Zealand (NZBC) require the compliance with modest ventilation [15, 16, 17, 18, 19] thermal insulation [20, 21] and performance-based energy efficiency [22, 23, 24] for new buildings. However, the NZ building codes [15, 22, 20, 23, 21, 24, 16] do not enforce achieving any minimum indoor air temperature, Indoor Air Quality (IAQ), air-tightness or moisture level for residential houses. Combined with the poor performance of the existing housing stock, these issues result in many NZ homes being cold and unhealthy for much of the year, thereby exposing occupants to the risk of developing health issues [12]. That said, it is traditional to ventilate residential houses passively by opening windows [2] in the summer and using heating appliances (electric, gas, oil heater and heat pumps) during winter evenings to achieve the occupants' thermal comfort and reduce the risk of developing health issues. However, the effectiveness of these manual/standard practices to achieve thermal comfort is not known.

According to the thermal comfort definition, local air velocity may play a role in determining the thermal comfort in a space. Therefore, natural ventilation of a building can influence the thermal comfort level by removing excess heat by direct cooling [25]. Finding a solution to control the natural ventilation by regulating the openable window area might help maintain the thermal comfort condition in the occupied space. However, this is particularly challenging, as the solution is not explicit. The reason is the non-linear relationship between buoyancy and wind driving forces of natural ventilation [26, 27]. Additionally, ambient environmental factors, building geometry, the terrain around the buildings and the dimensions of adjacent obstacles can also impact the natural ventilation of a building. Furthermore, the combined effect of the two driving forces of the natural ventilation may be reinforcing or resisting each other [27].

Given that no legal definition of “thermal comfort” is enforced by code in NZ, and the status of the “thermal comfort” dynamics for NZ houses is not well understood, there is need to examine the thermal comfort characteristics of a typical NZ residential building. In particular, an improved knowledge base of the thermal comfort regulation potential of naturally ventilated typical NZ houses for a range of operating conditions including different levels of envelope airtightness, thermal resistance, window opening area, wind conditions and occupancy is needed to conceive possible solutions. It is well understood that the opening or closing the windows and the operation of the heating appliances are usually dependent on the occupants’ movements and the set-point temperatures. However, the viability of regulating the thermal behaviour of residential houses of NZ by automatically operating windows and modulating natural ventilation is not well understood, nor extensively researched.

In this context, there is a need to understand better the potential of modulating natural ventilation by intelligently and actively operating windows to maintain indoor thermal comfort. Further research might be necessary to understand the potential of leveraging an optimum use of both the natural ventilation and the heating by actively operating both the windows and the heating appliances to maintain the indoor thermal comfort year-round.

Assessing these issues, along with the current housing stock in terms of the operating conditions, there is a significance in achieving thermal comfort using intelligent windows in buildings. The successful outcome of this research may address not only the thermal comfort issue of the residential house but also other peripheral issues like IAQ, energy-efficiency, moisture, dampness, mould and asthma. In this respect, the work aims to build-up a robust scientific base for the commercial development of an “intelligent” window system. Moreover, this research could be a milestone to obtain a comprehensive better-built environment at both the local and the global level.

## 1.2 Thesis outline

The following paragraph presents the structure of the thesis:

- Chapter 1 presents a background in terms of rationale and significance of the study. The chapter also contains an executive summary of the thesis, including significant research contributions and outcome.
- Chapter 2 presents a brief review of the literature and fundamentals behind thermal comfort and natural ventilation leading to the building modelling approaches. The review further explores the existing control methods for building thermal environment, and establishes the research scope and objectives.
- Chapter 3 examines the thermal comfort characteristics of a naturally ventilated house model. The results obtained in this chapter indicate that there is a possibility of regulating the thermal behaviour of naturally ventilated houses in a temperate climate region. The work presented in this chapter recommends examining the influence of natural ventilation on the indoor surface convective heat transfer coefficient (CHTC) at a micro-level.
- Chapter 4 presents an investigation on the influence of buoyancy-driven airflow on the floor convective heat transfer of a partially opened cubical enclosure. The microanalysis presented in this chapter with the numerical approach of CFD confirms that natural ventilation greatly influences the convective heat transfer behaviour of the floor. The examination develops an empirical relationship for modelling convective heat transfer behaviour of a hot floor applicable to a buoyancy-driven single-sided natural ventilated building performance modelling. The work recommends investigating the influence of outdoor wind conditions further.
- Chapter 5 presents an expansion of the numerical experiment with CFD, including the influence of outdoor wind conditions. The investigation confirms that both wind speed and direction significantly influences the natural ventilation through a single-sided opening.
- Chapter 6 develops a methodology to include the outcome of the numerical results presented in Chapter 4 and Chapter 5 in terms of empirical correlations. This work helps encapsulate the influence of the outdoor conditions on floor

convective heat transfer behaviour in the coupled thermal-airflow building performance model originally developed in Chapter 3. The re-examination of the model validates that there is a significant scope of regulating the thermal behaviour of naturally ventilated residential houses by controlled opening of windows. It also demonstrates that the regulating capacity improves considerably for a relatively airtight and insulated house during the summer period. The work results in a compiled database of the outcome of the dynamic simulations for various operating conditions.

- Chapter 7 applies the results and inputs from the dynamic simulations of the thermal-airflow model from Chapter 6 to develop and examine an ANN-based model predictive control algorithm for actuating window of the model house. The examination confirms that there is a significant potential of the ANN technique to predict and actuate the window intelligently, thereby modulating the natural ventilation to maintain a comfortable thermal environment of the occupied space during summer. The chapter also presents the expansion of the control technique to regulate an additional auxiliary heating appliance.
- Chapter 8 provides the conclusions in terms of the contributions of this study to the scientific knowledge, and the recommendations for further work.

### **1.3 Publications**

The PhD research work resulted in the following eight peer-reviewed scientific publications during the study.

M. K. Pokhrel, T. N. Anderson, J. Currie and T. T. Lie, "Examining the Thermal Comfort Characteristics of Naturally Ventilated Residential Buildings in New Zealand," in *Asia Pacific Solar Research Conference*, Canberra, Australia, 2016.

M. K. Pokhrel and T. N. Anderson, "Spatial Distribution of Heat Transfer in Naturally Ventilated Buildings Surfaces," in *10th Australasian Natural Convection Workshop (10 ANCW)*, Auckland, New Zealand, 2017.

M. K. Pokhrel, T. N. Anderson, J. Currie and T. T. Lie, "An Intelligent System for Actuating Windows of Naturally Ventilated Residential Houses," in *51st International Conference of the Architectural Science Association (ANZAScA)*, Wellington, New Zealand, 2017.

M. K. Pokhrel, T. N. Anderson and T. T. Lie, "Improving the Robustness of the Thermal Models of Natural Ventilated Buildings," in *The Asia-Pacific Solar Research Conference 2017*, Melbourne, Australia, 2017.

M. K. Pokhrel, T. N. Anderson and T. T. Lie, "Improving Thermal Comfort Regulating Potential in Naturally Ventilated Residential House," in *Asia Pacific Solar Research Conference*, Sydney, Australia, 2018.

M. K. Pokhrel, T. N. Anderson and T. T. Lie, "Influence of wind on indoor convective floor heat transfer of single-sided naturally ventilated cubical enclosures," in *52nd International Conference of the Architectural Science Association (ANZAScA)*, Melbourne, 2018.

M. K. Pokhrel, T. N. Anderson and T. T. Lie, "MAINTAINING THERMAL COMFORT OF A SINGLE-SIDED NATURALLY VENTILATED MODEL HOUSE BY INTELLIGENTLY ACTUATING WINDOWS," in *The 24th International Conference of the Association for Computer-Aided Architectural Design Research in Asia (CAADRRIA) 2019*, Wellington, 2019.

M. K. Pokhrel, T. N. Anderson and T. T. Lie, "The effect of wind on the convective heat transfer from the floor of single-sided naturally ventilated cubical enclosures," *Architectural Science Review*, 2020.

## Chapter 2 Literature Review

### 2.1 Introduction

This chapter introduces a brief review on the periphery of subjects related to the research title 'Achieving Thermal Comfort using Intelligent Windows in Buildings'. The following subsections describe a review focused on thermal comfort, natural ventilation, building performance modelling and building environment control methods. The rationale and significance of the study presented in the previous Chapter 1, along with the literature review included in this chapter, help formulate the research question and articulates the specific objectives and methodology of the research.

### 2.2 Thermal Comfort

The human body has an effective thermoregulatory system that works to maintain the temperature at approximately 37°C for thermal comfort [28, 29]. If the body becomes too hot or too cold, the thermoregulatory system tries to maintain the core temperature by increasing or decreasing blood flow close to the skin, by sweating to lose heat through evaporative cooling or shivering to provide heat with muscular activity. [28]. To maintain the thermal comfort condition of the body, a combination of body core and skin temperature must provide a sensation of thermal neutrality and also the heat produced by metabolism must be equal to the heat given off by the body [14, 28, 29].

Fanger, having comprehensively researched on different conditions and parameters, defined the concept of "thermal comfort" as "that condition of mind that expresses satisfaction with the thermal environment and is assessed by subjective evaluation" [30], leading to a thermal comfort index known as Predicted Mean Vote (PMV) and the Percentage of People Dissatisfied (PPD).

Fanger introduced a set of non-linear equations [30] requiring iteration(s) to describe the thermal comfort of the human body by considering the heat balance of the human body and empirical relationships he developed for the physiological parameters i.e, the skin temperature and the sweat evaporation, depending on the internal heat production [30]. With the help of these equations, it is possible to find a condition of neutral comfort for an average person in every condition of activity level and clothing thermal

resistance and every combination of air and radiant temperature, humidity and relative air velocity [30].

The PMV index considers various quantities, physical activity, physiological and psychological factors [30] for assessing thermal comfort, as shown in Equation (2-1) and described in Table 2-1.

$$f(M, Clo, v, T_r, T_a, P_w) = 0 \quad (2-1)$$

In examining Equation (2-1), it is apparent that local air velocity plays a role in determining the thermal comfort in a space. In this respect, natural ventilation of a building may influence the thermal comfort level by removing excess heat thereby providing direct cooling [25].

Table 2-1 Thermal comfort-related quantities definition and ranges [adapted from [31]]

Symbol	Quantity	Units	Typical range	Typical values
$M$	Metabolic rate	W/m <sup>2</sup>	46-232	70 W/m <sup>2</sup> = 1.2 met for sedentary activity
$Clo$	Clothing insulation	m <sup>2</sup> K/W	0-0.31	0.155 (m <sup>2</sup> K/W)=1 Clo
$v$	Relative air velocity	m/s	0-1	0.1 m/s
$T_r$	Mean radiant temperature	°C	10-40	Variable
$T_a$	Air temperature	°C	10-30	Variable
$P_w$	Vapour pressure of water in ambient air	Pa	0-2700	Relative humidity 50%

The PMV index predicts the thermal sensation as a function of two human conditions: human activity and clothing insulation, and four thermal environmental variables: Indoor air temperature, air humidity, air velocity and mean radiant as shown in Figure 2-1.

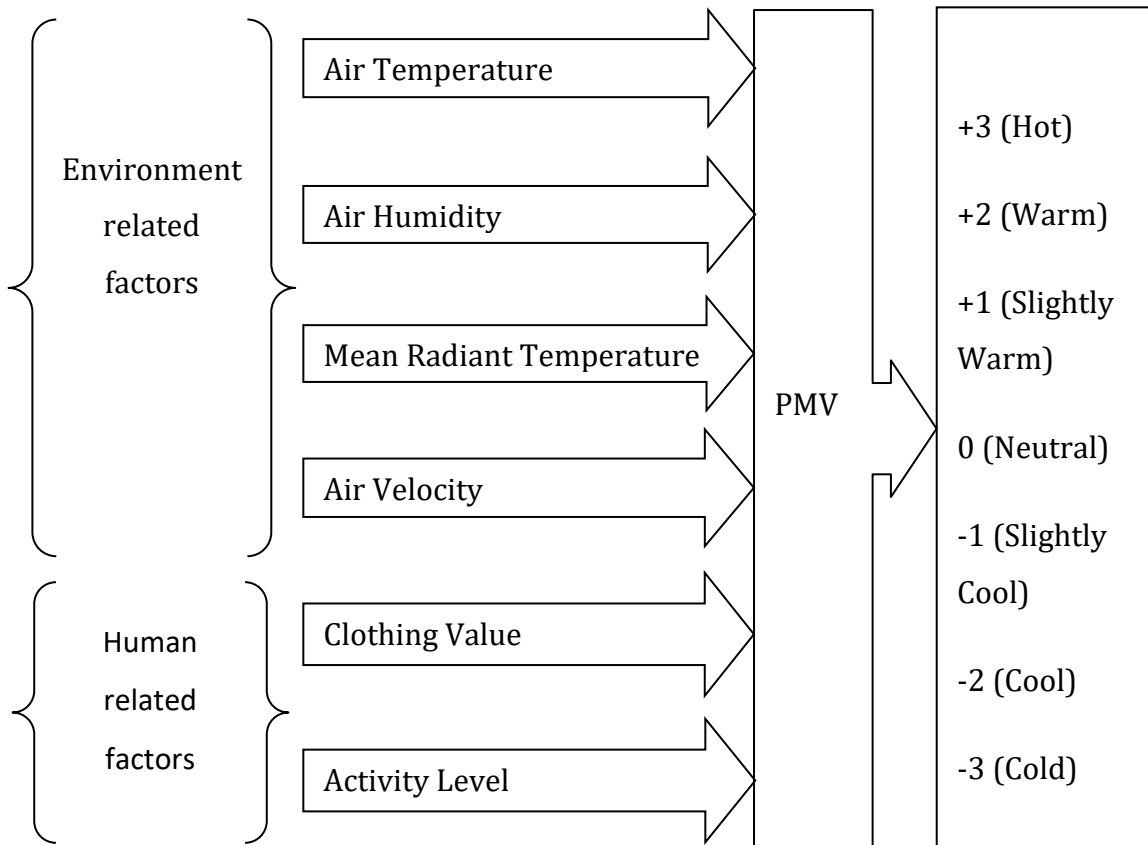


Figure 2-1. Schematics of PMV Calculation

That said, there is a disparity between the PMV scale and the thermal sensation of the user of a free-floating building (no heating or cooling) described in the literature [32, 33]. As such, an alternative thermal comfort theory based on behavioural and psychological adaptive principles exists: “if a change occurs such as to produce discomfort, people react in ways which tend to restore their comfort” [32, 34]. The adaptive theory proposes two comfort zones corresponding to 90% and 80% thermal acceptability depending on the effective outdoor temperature and (or) the dry bulb outdoor temperature [14, 32, 33].

Nevertheless, the American Society of Heating Refrigeration and Air Conditioning Engineers (ASHRAE) standard 55 considers Fanger’s comfort theory and defines the condition of operative temperature and humidity where 80% of passive or slightly active persons find the environment thermally acceptable [14]. The comfort zone relies on measurements under stable conditions and corresponds to thermal sensation ranging from -0.5 to +0.5 [14] on the comfort scale of Fanger. The ASHRAE standard 55 [14] also recognises the adaptive comfort model for naturally ventilated buildings.

Similarly, the European Standard EN ISO 7730 [35] also identifies the PMV index and categorises the thermal comfort zones, as presented in Table 2-2.

Table 2-2. Thermal comfort categories according to EN ISO 7730 [35]

Categories	PMV range	PPD range
A	$\pm 0.2$	<6
B	$\pm 0.5$	<10
C	$\pm 0.7$	<15

Irrespective of some critics, the broader recognition of the PMV thermal comfort assessment approach in the various standards and research studies, the PMV index can be used to assess the thermal comfort of a naturally ventilated building. The PMV values under category “C” of Table 2-2 could fit for the research related to the naturally ventilated building. The higher range of the PMV values for the naturally ventilated building could address the higher adaptive capability of people accustomed to a natural ventilation environment as equivalent to the adaptive principle. Having recognised all these factors and benefits of using the PMV thermal comfort index, it can be used as the performance indicator factor for the thermal comfort evaluation of naturally ventilated residential buildings in this study.

### 2.3 Natural Ventilation

Natural ventilation uses the natural forces of wind and buoyancy to introduce fresh air and distribute it effectively in buildings for the benefit of the occupants [36]. It can ensure or supplement the supply of fresh air for breathing, ventilation of contaminants, thermal conditioning and moisture dissipation [36]. Natural ventilation with controlled airflow rate through a building can maintain a desired IAQ and influence the thermal comfort level by removing excess heat either by direct cooling or by using the building thermal mass [25]. It can be a cost-effective, energy-efficient alternative technique to conventional mechanical ventilation [37, 38]. Its effect is mainly due to the existing pressure distribution resulting pressure difference around and within the building primarily due to the wind or thermal buoyancy as shown in Figure 2-2 and Figure 2-3 or combination of them [26, 39, 28].

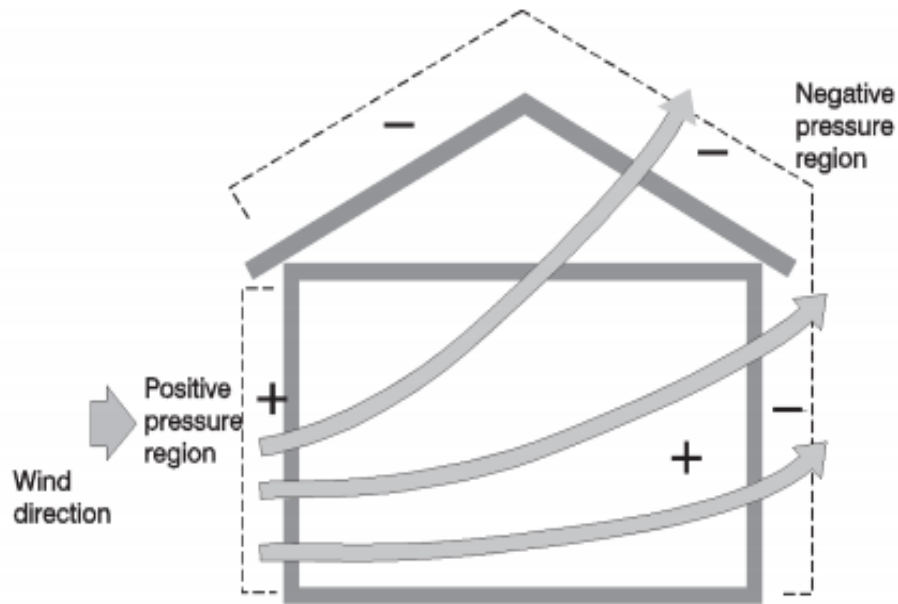


Figure 2-2. Natural ventilation driving force wind (adapted from [40])

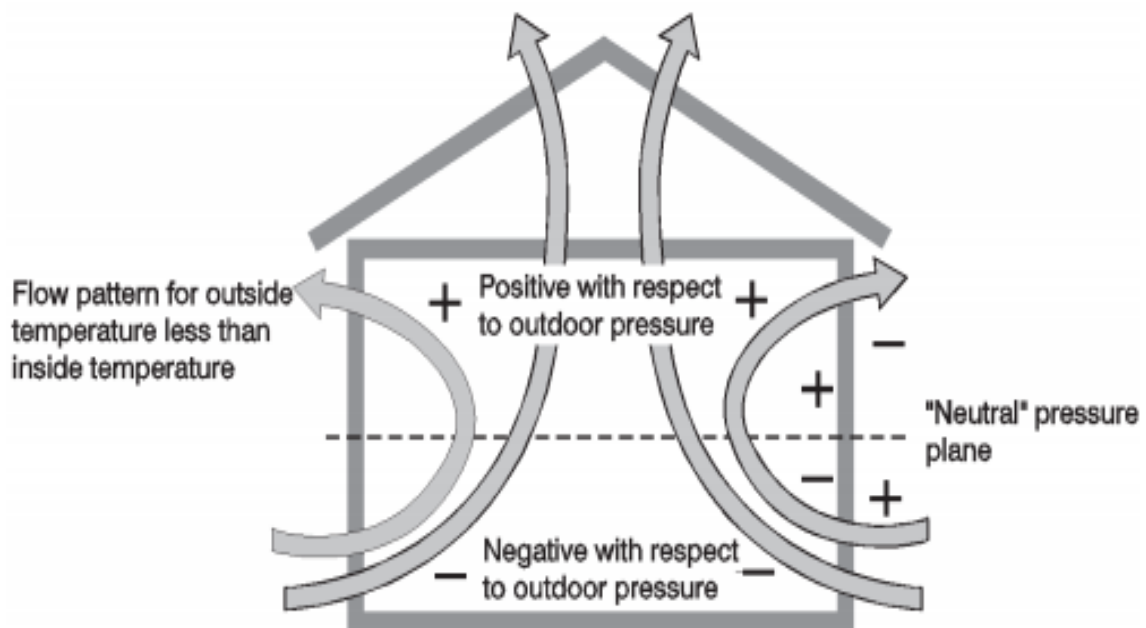


Figure 2-3. Natural ventilation driving force buoyancy (adapted from [40])

Ambient environmental factors like wind conditions, temperature, solar radiation and relative humidity are dynamic and non-linear, resulting in fluctuations of the driving forces of natural ventilation. Similarly, building dimensions and type, size, number and

location of the openings on the building façade, opening angle and area varies according to the architectural design of the building. This dissimilarity in design and external environmental characteristics results in variations in the distribution of openings in a building's shell, and through the building's inner pathway, leading to a difference in the effective area and the resistance for transfer of airflow. However, opening a window influences the transient behaviour of ACH, air temperature and ventilation efficiency [41]. In addition to this, the activities of occupants can also lead to significant differences in pressure distribution inside a building. Also, the terrain around the buildings and adjacent obstacle dimensions vary according to the geographic location of the building and these influence the natural ventilation through the building. Therefore, considering all these factors, predicting natural ventilation through a building is very complicated [42].

By its nature, the wind flows produce not only pressure field but also a velocity field around a building. However, a description of the pressure field around a building is very complicated even for a simple geometry impinged by a vertical wind profile, as illustrated in Figure 2-4 [43].

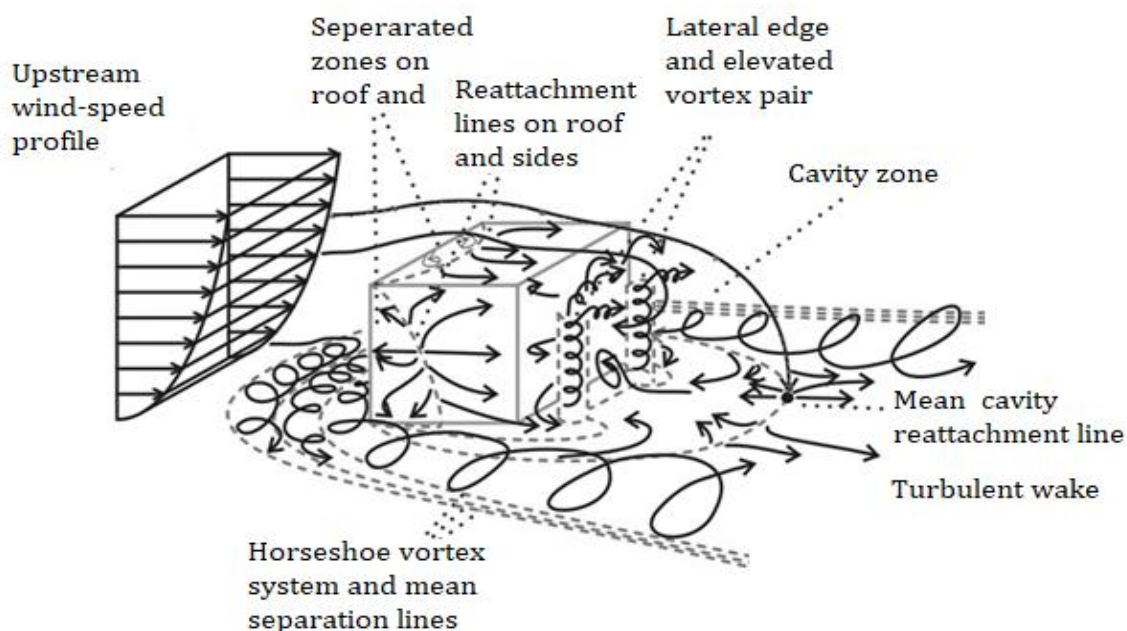


Figure 2-4. Typical distribution of pressure field around a building (adapted from [43]).

Despite this complexity, Bernoulli's equation helps to estimate the pressure generated by the wind at the outdoor surface of a building in terms of a dimensionless pressure coefficient [44]. The ratio of the dynamic pressure on a surface to the dynamic pressure in the undisturbed flow pattern at a reference height defines the pressure coefficient as described in Equations (2-2) and (2-3) [44, 45].

$$C_p(x, y, z) = \frac{P(x, y, z) - P_0(z)}{P_{dyn}(z)} \quad (2-2)$$

$$P_{dyn}(z) = \frac{1}{2} \rho_o(z) V^2 \quad (2-3)$$

Where,  $C_p(x, y, z)$  = Pressure coefficient at a point  $(x, y, z)$  on a building surface

$P_{dyn}(z)$  = Reference dynamic pressure at height  $(z)$  [Pa] for a given wind direction  $(\phi)$

$P(x, y, z)$  = Surface pressure on the façade at point  $(x, y, z)$  [Pa]

$P_0(z)$  = Static (atmospheric) pressure on the height  $z$  [Pa]

$V$  = Reference wind velocity at building location with reference height  $z$  [m/s]

$\rho_o$  = Density of outdoor ambient air at height  $z$  [kg/m<sup>3</sup>]

The  $C_p$  for a particular point on a building's envelope depends on many parameters (wind velocity profile, wind incident angle, density, building geometry-frontal and side aspect ratio, building exposure/sheltering) [46]. The  $C_p$  data sets are available from the published databases [45, 47, 48, 49] or analytic expressions [50] for a simple geometrical shape of building [46].

Generally, a meteorological station measures wind speed at a standard height (10 m), but it is possible to estimate the wind speed at different heights as necessary. According to the atmospheric boundary layer principle, the roughness of the terrain, surface surrounding the building (ground and other structures) and atmospheric stability influence the vertical profile of wind speed [44, 45]. Researchers generally use a

logarithmic law or power-law, as shown in equation (2-4) [44, 45] to determine the wind speed at different heights.

$$V(h) = V(h_0) \left[ \frac{h}{h_0} \right]^\alpha \quad (2-4)$$

Where,  $V(h)$  = Wind speed at height  $h$  [m/s]

$V(h_0)$  = Wind speed at reference height  $h_0$  [m/s]

$\alpha$  = Wind velocity profile exponent that increases with increasing roughness of the solid boundary

Besides the wind effect, thermal buoyancy also causes a differential pressure in a building [44]. The thermal buoyancy is due to density differences between different zones of a building. The density is mainly a function of temperature and the moisture content of the air. Figure 2-5 demonstrates a typical building having two zones A and B with reference pressure ( $P$ ), density ( $\rho$ ), temperature ( $T$ ) and height ( $Z$ ) on the opposite sides (A and B) of an opening.

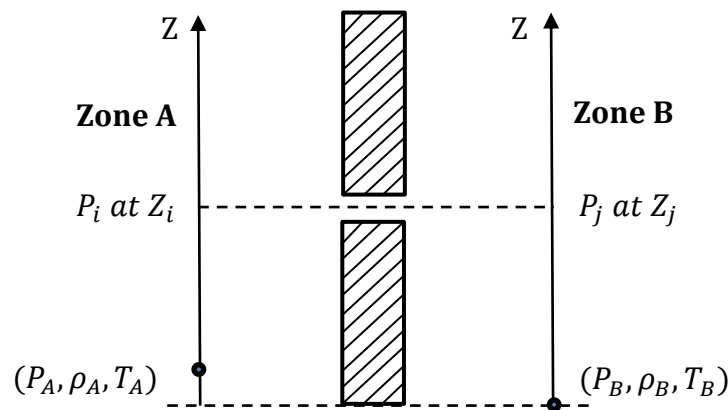


Figure 2-5. Thermal buoyancy between two points on the opposite side of leakage (Adapted from [44])

The thermal buoyancy  $P_{stack}$  can be incorporated in the equation of the local pressure difference between two points  $P_i$  and  $P_j$  as Equation (2-5) and further expressed as Equation (2-6) [44].

$$P_i - P_j = P_A - P_B + P_{stack} \quad (2-5)$$

$$P_{stack} = \rho_A \cdot g (Z_A - Z_i) - \rho_B \cdot g (Z_B - Z_j) \quad (2-6)$$

The pressure field driven by the wind on building surface is usually unsteady due to the turbulent characteristic of the wind flow in the lower layers of the atmosphere and the differential pressure due to the thermal buoyancy that depends on density field [44]. Therefore, it is difficult to simulate the wind pressure field exactly. However, the variation and range of thermal buoyancy phenomena over time are relatively predictable. The combined effect of these two driving forces of natural ventilation could be reinforcing or resisting each other [26, 27]. Therefore, the wind effect could enhance or hinder the natural ventilation in the building depending on the strength and direction of the wind, size and location of the window(s) and the temperature difference between the internal and external environment [26, 27]. As a result, accurately predicting the natural ventilation of a building is a complicated task.

## 2.4 Building performance modelling

Generally, researchers characterise building models by either static or dynamic thermal behaviour. By simplifying the thermal model, they use the static thermal behaviour approach for modelling steady-state conditions when all the internal and external inputs are controllable. The dynamic approach models the transition of internal and external information and outputs of the building system and helps understanding of the thermal exchange generally used for simulation purposes [51, 52].

Researchers categorise the building modelling approaches broadly into three categories. The first category, “white-box”, is based on the laws of physics to describe the set of phenomena of residential building and permits high fidelity modelling of the building system. The complexity of this approach depends mainly on the chosen precision`s levels of the known phenomena associated with the building system to be modelled. Irrespective of the application of fundamental principles to reflect physical significance, the white-box models always possess errors associated with random variables which are due to unknown parameters such as window openings and air exchange rates in natural ventilation [51, 52].

The second approach, “black-box”, is based on observation and relies on statistical and measurement strategies to describe the set of the phenomena. These provide little insight into the dynamics dictating the system behaviour of building as their performances depend on the training data used as input. However, they do not need to have much knowledge of the building geometry or the complex physical phenomena to deduce the thermal performance. Therefore, compared to physical approaches, the black-box approach requires less information about the building and may appear easier to deploy. The third category is a hybrid method (grey-box), which uses both physical and statistical modelling techniques [51, 52].

Building performance simulation tools (TRNSYS, Energy Plus, DOE, ESP-r) often use dynamic methods with “white box” approach to capture building dynamics (thermal dynamics of the envelope, system dynamics of control strategies) [52]. They predict the output (performance indicators) based on first principles (calculation model) with given conditions as input and building characteristics (influencing factors) as shown in Figure 2-6.

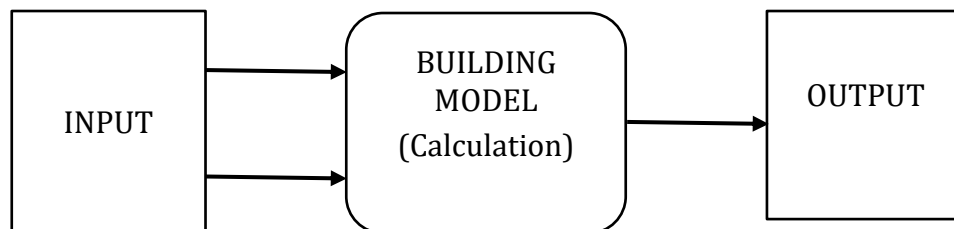


Figure 2-6. Modelling structure of building thermal performance evaluation

The influencing factors (weather, building, system and components) as inputs, transfer to the simulation engine included with mathematical simulation algorithms.

Subprograms like building load, system and plant are generally included in the simulation engine to perform the whole building simulation either in a simultaneous or sequential procedure to determine defined outputs in terms of performance indicators as shown in Figure 2-7.

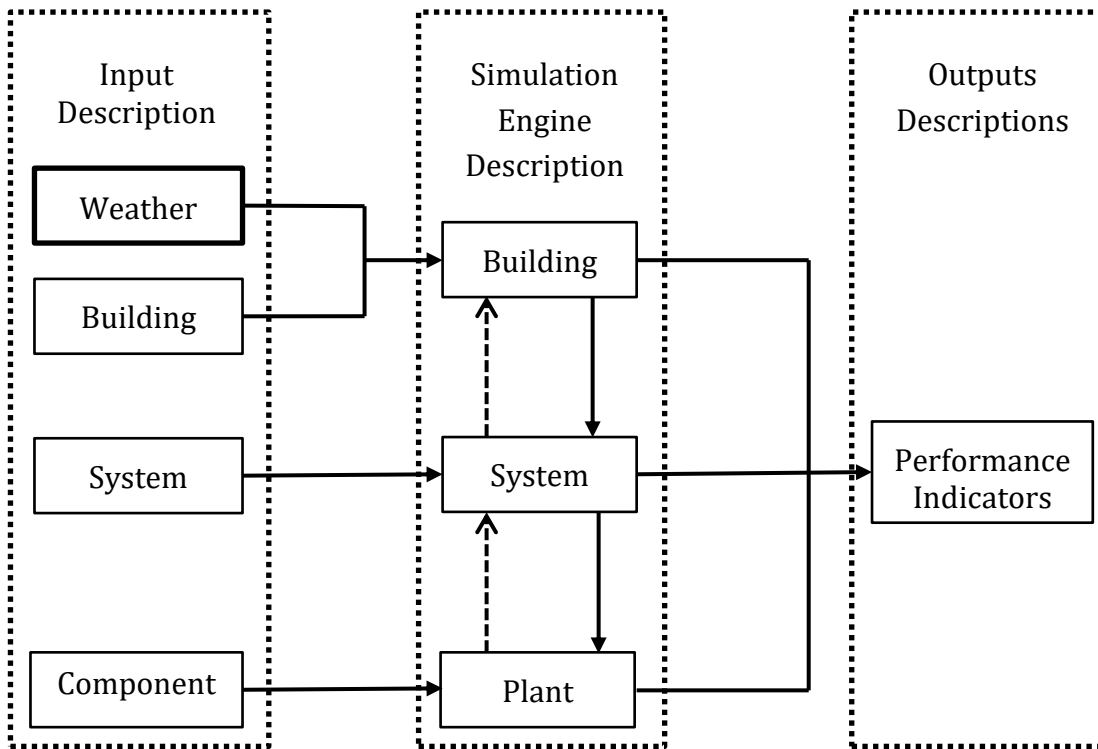


Figure 2-7. A typical dynamic building simulation procedure (adapted from [52] )

These building simulation programmes solve a set of heat balance equations for an unknown surface of an enclosed space in terms of the air temperatures based on the law of conservation of energy. As illustrated in Figure 2-8 [53], the outside surfaces exchange heat through convection with the air and radiation with its surroundings. The heat then flows through the building envelope to, or from, the external boundary conditions. The net positive heat then conducts through the wall into the zones of the building where radiation and convection occur on the inside surfaces. The radiation heat transfer occurs between the surface nodes, while the convection occurs between surfaces and the air node they face. Bulk convection from infiltration, ventilation and between zones or air nodes occurs only on the air nodes [53].

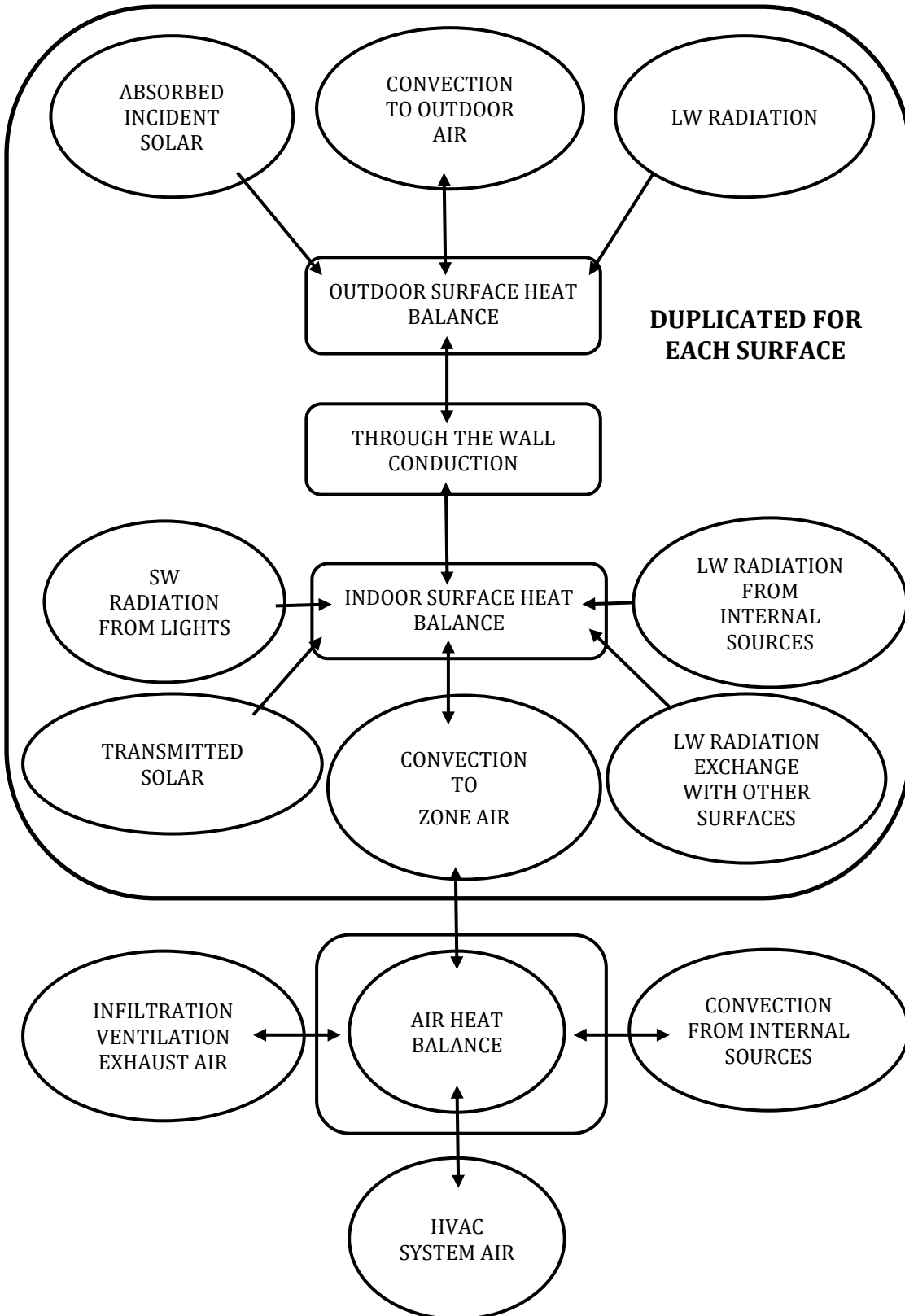


Figure 2-8. Overview of the heat transfer process in building simulation program (adapted from [53])

Despite the complexities of predicting natural ventilation, this inverse dynamic modelling approach can help to evaluate the thermal behaviour of the naturally ventilated house and is able to provide the necessary evidence of the assessment. However, it requires assessing the transient information of the natural ventilation in terms of bulk ventilation at the air node(s) of the zone(s) at each time step. The coupling of the bulk ventilation information with the air temperature of the zone defines the complete thermal behaviour of the zone at each time step, including the effect of natural ventilation.

In this respect, the model/field experimental method assessing time-average airflow rate, analytical or empirical calculation method for simplified building geometry and opening, micro assessment method with a numerical approach using CFD [42] can be coupled to the thermal building model to assess the natural ventilation aspect of the modelling. Obviously, the higher the fidelity of the model, the greater the computational resources and time necessary for running the simulation.

Thus, the problem of assessing and predicting the natural ventilation of the building is possible. Though it is subject to different levels of simplification according to the accuracy requirement of the application. The balance of accuracy and detail needs to be weighted from the perspective of the research objective. From a natural ventilation control research perspective, the simpler the model, the easier the control design and implementation(s), leading to a higher possibility of technology transfer for the application. Furthermore, from a direct application perspective of this particular research, an opening or group of openings in the room or a group of rooms or a zone of a residential building need to be controlled to maintain thermal comfort within a prescribed range of thermal comfort performance indicator factors. Thus, the spatial requirement of the assessment should identify at least one average value of performance indicator factor for a standard room or zone of a residential building.

A coupled thermal-airflow modelling approach in a multi-zone and network flow dynamic simulation environments that considers a space within a zone as one homogenous node could be employed with reasonable accuracy to assess the thermal behaviour of a naturally ventilated room or zone. In this context, TRNSYS in conjunction with Multizone Infiltration Specialists (COMIS) [54] might be able to assess the thermal

performance of a natural ventilation residential house as a room/group of rooms/zone with reasonable accuracy.

## **2.5 The notion of smart and intelligent buildings**

The notion of an intelligence or 'smart' associated with buildings emphasises a distinct identity and building characteristics compared to typical buildings. However, both the terms can be considered evolutionary in nature mostly used interchangeably with diverse interpretations and inferences [55]. Most of the interpretations in this context are highly influenced by the possibility of harnessing available cutting edge technologies at the time and location to fulfil the chosen set of multidimensional performance indicators cost effectively [55]. One line of thought includes intelligence as a component of smartness [56] while the other line is just the opposite considering smartness as a component of intelligence [55, 57].

Buckman et al. [56] proposed the smart building as a concept that indicates the ability of the building to integrate intelligence, enterprise, control, and materials and design flexibly to allow the building to adapt and prepare for the event before they occur. These characteristics and inherited information from a broader range of sources help meet the drivers for building progression in energy, efficiency, longevity, comfort and satisfaction [56]. The term 'intelligence' refers to how building operation information is gathered and responded to, while the term 'control' refers to the interaction between the occupants and the building. Similarly, the term 'material' refers to the building physical form, and 'enterprise' refers to how building use information is collected and used to improve occupant performance [56]. A successful operation of a smart building requires adapting in response to internal and external information gathered from a range of sources for building use. The term 'adaptability' is the core of the smart building.

In contrast to the smart building, Buckman et al. considered the intelligent buildings meet the drivers to building progression by focusing on intelligent systems that reactively utilise information; control, enterprise, and building materials and construction are developed largely independently of the intelligent systems [56]. The term 'reactive' is the core of the intelligent building. In summary, Buckman et al. [56]

presents a line of thinking that considers the lower bounds of smart buildings as the upper bounds of intelligent buildings [56].

In contrast to the above definition, work by Ghaffarianhoseini et al. [55, 57] suggests the notion of the intelligent building as a more holistic concept encompassing the features concentrating on the performance of the building or the quality of service that the building provides. Buildings that are highly responsive and possess significant potentials of automatic monitoring and control system for maintaining optimum ambient environment can be considered as intelligent building [55]. However, at the same time, they enshrine the concept of including human values, well-being, health, quality of life and respond to ever-increasing demands of society while reducing the environmental impacts [55]. Considering the performance, service and system thinking Ghaffarianhoseini et al. [55] proposed four categories of performance indicators (Smartness and technology awareness, economic and cost efficiency, personal and social sensitivity and environmental responsiveness) to encompass the concept of intelligence in building. This line of thinking proposes smartness as an indicator of intelligent buildings.

In the NZ context, in addition to the adherence to existing sustainability rating schemes for modern building (Green star, NABERS etc.) with embedded automation as a standard, the intelligent building requires including a greater level of security and human dimensions (dynamism, casualness, privacy, flexibility, creativity, etc.) [55] compared to a standard building.

Irrespective of the smart or intelligent notion being used to define the relatively advanced building, this research considers the term 'intelligent' window in the title and throughout the thesis for maintaining consistency. The intelligent window is envisaged as a sub-system of the next generation sustainable intelligent or smart building. The function of an intelligent window is to actuate the window actively to modulate a residential house's natural ventilation as a component to help maintain thermal comfort. The research expects to contribute to developing an intelligent window responsive to the dynamics and non-linearity of outdoor, indoor environment and building thermal behaviour.

## 2.6 Approaches for controlling thermal building environment

Researchers categorise approaches for controlling the indoor building environment as conventional, computational intelligence and agent-based intelligent control systems [58, 59]. The ON/OFF room temperature control is the simplest type of control [58, 60] that switches the heating or cooling devices in a room according to an error between a set point and the room temperature with a suitable hysteresis curve. It does not contain any information about the dynamics of the building, and cannot respond to weather predictions and thermal discomfort [58, 60].

On the contrary, weather-compensated control is a feedforward control, which also does not contain any information about the building dynamics [60]. The control sets the temperature of the heating or cooling medium according to the outside temperature employing predetermined heating or cooling curve. Despite the lack of dynamics in control, this is a long-used and proven control strategy; its advantage is its robustness and simple tuning [60].

The Proportional-Integrate-Derivative (PID) control system is a feedback control that considers information about the system dynamics, temperature error and some “history” [60]. These controllers are robust and allow accurate tuning, but they cannot reflect the outside weather effects [60]. Therefore, PIDs are not standard in Heating Ventilation and Air Conditioning (HVAC) control [43].

The application of these controllers is unlikely from a control perspective considering the comprehensive definition of thermal comfort and the complexities of natural ventilation. The major problem is to address the dynamic environmental conditions, in particular, variations of wind velocity and direction, solar radiation, outside temperature; these require continuous changes of the controlled parameter like airflow through the window(s).

To overcome these limitations, researchers worked for optimum and predictive control strategies for buildings during 1980s and 1990s. To use these techniques a model of the building is necessary. Particularly, mathematical analysis of the thermal behaviour of a building generally results in non-linear models and most importantly, these models

differ from one building to another. Therefore, no further industrial development has followed these scientific studies because of implementation issues [59].

Further, researchers have developed control techniques similar to adaptive control inbuilt with weather prediction models and optimising algorithms to establish optimal strategies for integrated control of window devices such as blinds, vents windows and heating devices [58, 59, 61]. Although issues of implementation call for an explicit model of the building, difficulties in monitoring and controlling parameters caused by nonlinear features, less user-friendliness are impeding its application.

Model (based) Predictive Control (MPC) is a method of advanced control that originated in the process industries for heating control [60]. The MPC strategy requires a “model” of the process to calculate a control signal by optimising an objective function subject to some constraints. It solves the optimisation problem in a receding horizon fashion. Applying the concept to a naturally ventilated building might need to include an objective function as a trade-off between minimising energy consumption and maximising thermal comfort. The room PMV error can act as feedback. Ideally, it requires developing a non-linear building “model” for the thermal comfort computation, prediction, optimisation and window(s) control.

Nevertheless, the MPC strategy may be feasible if the non-linearity terms in the building, “model” are simplified to a linear “model” by approximations. Research related to building HVAC control with the help of Nonlinear Model Predictive Control (NMPC) demonstrated that the NMPC control technique could reduce energy consumption and maintain the indoor temperature and humidity set points [62]. However, the study is limited to the control of only a mechanical HVAC system.

In complicated systems, where mathematical modelling cannot adequately describe a system in real-time, an advanced control system with computational intelligence techniques like Fuzzy Logic (FL) and/or the ANN may be useful [58, 59]. These techniques have their strengths and weaknesses specific to the problem and type of solution sought from the perspective of their capabilities. The integration of these techniques leading to a hybrid solution could increase the strength and overcome each other’s weakness [63]. Researchers used an ANN-based modelling approach in some of the earlier studies related to the naturally ventilated building to address the

complexities and the non-linearity associated with the natural ventilation [64, 65, 66, 67, 68]. However, those studies applying the ANN technique were limited to designing, optimising and predicting different quantities of the building rather than using the ANN technique for controlling the building environment.

Studies on a self-commissioned neuro-fuzzy building heating control system [69, 70] used an ANN-based predictive control concept. The researchers used a model-based predictive and adaptive control strategy with an ANN for adaptation of the control model to real conditions (climate, building characteristics, and user's behaviour). The Neuro-Fuzzy control system [70], used an optimum heating control policy depended on a dynamic programming algorithm. The method required an extensive computational processing power limiting detailed discretisation of the state variables of the indoor air temperature and heating command [70]. However, the controller did not deal with a building thermal system comprising natural ventilation, cooling or direct prediction of a thermal comfort index like PMV. Nevertheless, computation processing power has increased a lot since the late 1990s. The concept using presently available computation processing power might be helpful to find a solution of intelligently actuating windows of the naturally ventilated house in order to maintain thermal comfort.

## **2.7 Current research status of automatic window actuation**

The development of the window control sub-systems as part of the next generation of intelligent houses is an emerging trend. Hou et al. [71] proposed a smart electric push-pull window system composed of an actuator, a control system, a data acquisition system, a data processing system, a weather website, and a window. Based on the real-time weather information collected from the internet, and a set of pre-defined expert rules, the control system processed data intelligently to actuate the window to a certain predetermined width in order to adjust and improve the temperature, humidity, air quality and lighting in the house. Similarly, Sun et al. [72] proposed microprocessor driven intelligent window control system integrated with a variety of sensors to address some pre-defined functions and threshold. The author targeted automatic opening or closing functions to prevent slant rain coming inside, gas leakage above pre-set threshold, buzzing anti-theft alarm, monitor indoor environment etc. Zhang et al. [73] applying the same concept designed an automatic window-closing control system that

based on single-chip microcomputer as the control core. The design realised the automatic window control through the cooperation of temperature sensor, humidity sensor, wind sensor, infrared sensor, particle size detection sensor, infrared sensor, buzzer alarm, motor driver and other auxiliary modules.

Medeiros et al. [74] proposed a system of automated and sensor-monitored smart windows for smart home scenarios following an Internet of Things (IoT) enabled approach. The system consists of actuating unit, sensors and microcontroller unit following an IoT and reacting to the surrounding environment. Users can use the system to close or open the windows through a mobile App or via Web, or the windows can act autonomously according to data collected from the installed sensors. It was noted that the system can be industrialized by using an engine and reduction box that meet the required torque specifications of larger and heavier windows.

This review on intelligent windows system provides only electric actuating solution of the window. These solutions are merely an automatic switching control based on the information of the local environment through integrated sensors and set threshold. These systems do not possess optimisation, adaptive or predictive capabilities and are not responsive to the dynamic and non-linear building thermal and environmental behaviours.

Stazi et al. [75] employed a modified version of Humphreys adaptive comfort algorithm to develop an automatic window opening and closing system to optimise IAQ and thermal comfort in classroom environment. The research adapted the algorithm including CO<sub>2</sub> concentration and reducing the dead band and confirmed that the system guarantees low CO<sub>2</sub> levels, thermal comfort and users' satisfaction. The adaptive model need to be corrected and re adjusted for any change in building dynamics limiting the prospect of its sustained use. To overcome these limitations Han et al. [76] proposed the use of novel reinforcement learning (RL) technique for improving occupant comfort by window opening or closing. The model-free characteristic of RL avoids the disadvantage of implementing inaccurate or complex models for the environment, showing a potential in the application of intelligent control for buildings.

Fiorentini et al. [77] presented an effective platform for testing naturally ventilation control strategy based on model predicting control for a mixed mode building in a

simulation environment of building simulation software ESP-r and the Building Control Virtual Test Bed (BCVTP). They extended the integration to control window openings. The researchers claim that the platform allows any complex multi-zone and multi-sensor window control strategy to be simulated in an integrated manner with any potential building design. Fiorentini [78] used simulations and experiments to demonstrate the development, implementation and performance investigation of an adaptive comfort-oriented control strategy for natural ventilation and mechanical air conditioning management in a residential mixed-mode building. The algorithm can optimise window opening percentage according to adaptive thermal comfort criteria. The algorithm can also dynamically optimise the heating or cooling set-point targeting a desired PMV index objective if natural ventilation cannot maintain desired thermal comfort. In natural ventilation mode, the controller required solving an airflow network (thermal and airflow model) of the building in real time to predict the temperature of the air mix to optimise the window opening tracking the temperature target.

Chen et al. [79] demonstrated the development of an advanced data-driven MPC algorithm to regulate hybrid ventilated buildings. This study was based on numerical simulations implementing a non-linear MPC using an ANN to model the dynamic behaviour. The researcher employed ANN over other mathematical models and demonstrated the best performance considering both prediction performance and computation time comparisons. The research used a particle swarm optimisation algorithm to optimise the control sequence and used a stochastic model to calculate an optimum position of windows based on the outdoor temperature.

These studies have demonstrated the potential effectiveness of MPC regulation for building performance in hybrid mode rather than standalone residential set-up. Some of these studies used stochastic thermal comfort models to calculate the window opening position and apply the MPC based control algorithm to drive the window actuator. These simple adaptive thermal comfort models are based on occupant behaviour in different outdoor air conditions tested in other regions and climatic conditions. An adjustment of the thermal comfort model might be necessary before directly applying them to the calculation of the optimum window positions for the climate and build typologies of interest. Some of these studies require building simulations to be performed in real-time to calculate the optimum window opening position, a

proposition that seems to be challenging from a broader deployment perspective. Building simulations for natural ventilation is also challenging, as finding a robust solution for accurately predicting natural ventilation is a complicated task due to driving forces and variables' dynamic and non-linear nature.

Nevertheless, the review of building control and automatic window control indicates that there is a possibility of using an ANN tool for solving the complexity and non-linearity of evaluating the thermal behaviour of the naturally ventilated building. Investigating the case of developing a naturally ventilated building model with the ANN technique and deploying it as a simplified model to intelligently actuate the window might be helpful to realise the objectives of this thesis.

## 2.8 Research Question

The literature review found that the occupants of residential houses located in the maritime temperate climatic regions like NZ manually open or shut the window(s) to modulate the airflow and exploit the cooling potential of the natural ventilation to maintain thermal comfort during summer. The occupants use heating appliances along with natural ventilation to maintain both the thermal comfort and the IAQ in winter. The review further identifies that automation of the opening and shutting of the window(s) with some feedback on the building thermal comfort might be necessary to utilise natural ventilation for optimally maintaining thermal comfort.

The review work identifies that complexity and non-linearity exists in the computation and prediction of both natural ventilation and the thermal comfort of naturally ventilated houses. The complexity and non-linearity are the major hindrances to devising automatic systems to open or shut window(s). Nevertheless, the review identifies a macro-spatial building thermal modelling method to sufficiently capture the effect of natural ventilation and compute the thermal comfort condition of a residential building in the TRNSYS simulation environment. The review also identifies the possibility of exploiting the knowledge base of building thermal modelling by utilising an artificial intelligence tool called the ANN. The author expects to address the issue associated with the complexity and non-linearity of natural ventilation and thermal comfort, to investigate the possibility of development of a simple control system based on the ANN predictive capability. The review did not find any earlier studies that use the potential of an ANN and predictive control to actively control window(s) in order to modulate the natural ventilation and maintain the thermal comfort of the residential house.

As such, the research work defines an overarching research question as:

***“How can we actively control the window (s) to modulate the natural ventilation of a residential house and as a component in maintaining thermal comfort?”***

To find the answers to the research question, the author divides the research question into the following specific objectives.

- 1) Examine the thermal comfort characteristics of a single-sided naturally ventilated model house
- 2) Investigate the influence of the driving forces (thermal buoyancy and wind) of natural ventilation and develop specific relationship(s) to improve the estimation of heat transfer behaviour of the floor of a single-sided partially opened model enclosure
- 3) Improve the robustness of the single-sided naturally ventilated model house by applying the specifically developed relationship(s) for estimating convection heat transfer behaviour of the floor and re-examine the thermal comfort characteristics
- 4) Develop and apply an intelligent control concept based on an Artificial Neural Network (ANN) to actuate the window to modulate the natural ventilation and maintain the thermal comfort of the naturally ventilated model house.

The research question of this study is relatively broad compared to the objectives. This approach was taken in order to focus on the crux of the problem and explore the possible solutions. Therefore, the research work uses the NZ context (housing types, construction method, climate, standards, building codes) to identify the thermal comfort dynamics of NZ residential houses. The research work intends to evaluate the potential of the regulating thermal comfort of the naturally ventilated house situated in the temperate climate conditions of Auckland, New Zealand.

The following chapters describe how these specific objectives are realised in determining the answers to the research question.

## **Chapter 3 Examining thermal comfort behaviour of a naturally ventilated model house**

### **3.1 Introduction**

The definition of thermal comfort reveals that local air velocity also plays a role in determining the thermal comfort in a space. In terms of a residential house, natural ventilation can influence the thermal comfort level by removing excess heat using direct cooling. However, analytically evaluating natural ventilation is particularly challenging, as the solution is not explicit. Determining a solution requires the heat and mass transfer assessment to be driven by complex and non-linear phenomena associated with the natural ventilation driving forces of wind and thermal buoyancy, along with other related factors. Moreover, maintaining the indoor thermal comfort characteristics of a house by modulating natural ventilation further raises the complexity. Before finding any solution, the potential of regulating the thermal behaviour of the building under different building operating conditions needs to be examined.

This chapter presents the evaluation of the regulating potential of thermal behaviour of a simple model house by opening or shutting the windows, thereby modulating the controlled portion of the natural ventilation. This work dynamically simulates the performance of the model house in TRNSYS environment utilising coupled thermal and airflow simulations. These simulations examine the variation of thermal comfort of a model single sided naturally ventilated house, equivalent to the size of a typical room, under NZ climatic conditions and for various operating conditions. To achieve this, the simulations examine thermal comfort in terms of the PMV of the room with various WOF, different air-tightness values and different levels of envelope thermal resistance.

## 3.2 Building performance modelling in TRNSYS

TRNSYS is a relatively advanced tool being used to simulate dynamic systems, mainly building, solar and thermal systems. It consists of a suite of programs, including a dedicated interface for transferring building inputs (TRNBuild.exe) [80]. It uses the concept of “component” recognised as types; and these types are solved separately in their subroutines within the simulation engine, at every time-step [80, 81]. They consist of mathematical equations representing a physical description of the heat and mass transfer process of the component. These physical equations require inputs and parameters for generating the results. While the information can change every time step, the outputs are averaged over the time-step [80, 81]; and the parameters such as size and constant material properties remain fixed values. Input is usually output from another type or vice versa, as illustrated in Figure 3-1; and requires finding solutions iteratively by convergence at time steps. In the simulation studio, these types, connections, additional equations, start time, time-step, length of the simulation and convergence criteria are defined creating input deck file that the solver uses to perform simulations [80].

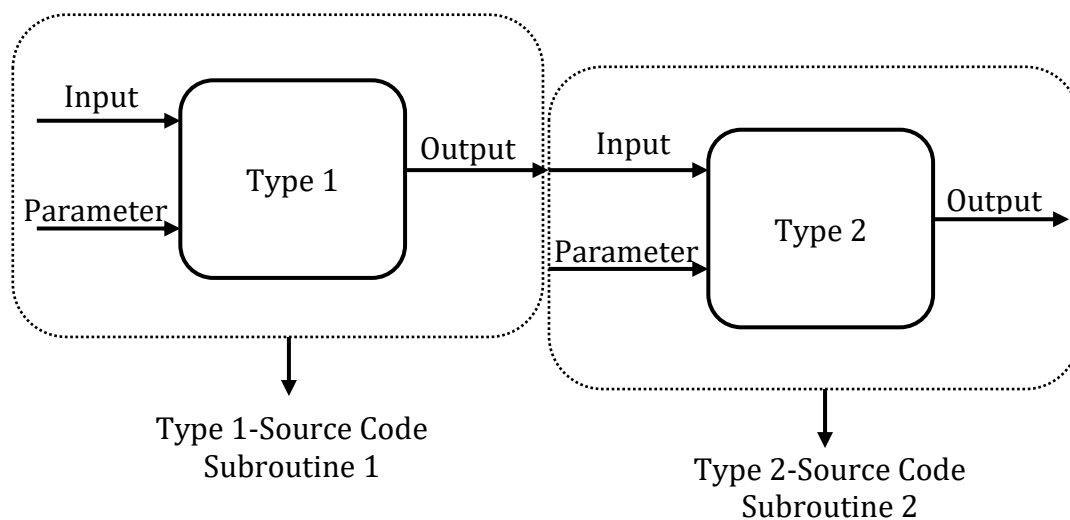


Figure 3-1. A typical representation of information flow in TRNSYS (adapted from [81])

### 3.2.1 Thermal modelling of building in TRNSYS: Type-56 component

The standard component included in the TRNSYS program, known as Type-56 [80], can model both the thermal behaviour of a simple house with a single zone, and a very

complex building divided into different thermal zones. Figure 3-2 illustrates a typical representation of the information flow of the Type-56 component. An integral program suite (TRNBuild) collects and pre-processes necessary building information, automatically creating input file describing building (\*.BLD) and a file describing the wall characteristics in terms of transfer function coefficients (\*.TRN) along with other necessary parameters (\*.BUI, LUb, T\*-Mode, A<sub>op</sub>) [80]. There is a provision to define required outputs in TRNBuild. The TRNSYS program calls the TRNBuild subroutine before each building simulation automatically generating an information file (\*.INF) with a list of required inputs and available outputs [80].

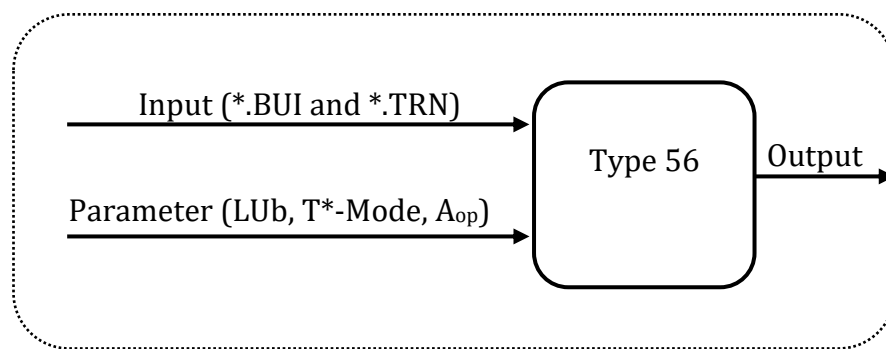


Figure 3-2. A typical representation of information flow in Type 56

Type 56 utilises a heat balance method (HBM). It consists of three crucial energy balance equations-indoor air, exterior surface and interior surface for a typical zone. These energy balance equations are based on the fundamentals of heat transfer process-conduction, convection and radiation and are solved simultaneously for unknown surface and air temperatures for an enclosed space [80].

Figure 3-3 demonstrates a schematic of the essential heat fluxes applied in a typical Type 56 standard building model. At the exterior surface, the sum of convective and radiative heat transfer gives the total heat transfer. Figure 3-3 illustrates the net heat flux ( $q_{s,o}$ ) into the wall at the outside surface as the combination of convective ( $q_{c,e}$ ), longwave radiative ( $q_{r,e}$ ), and absorbed incident solar radiation ( $q_{s,e}$ ) heat fluxes. Similarly, for external surfaces, the long-wave radiation exchange at the outside surface is considered explicitly using a sky temperature ( $T_{sky}$ ), with a view factor to the sky, ( $f_{s,sky}$ ) and a fictive ground temperature ( $T_{sgrd}$ ) with a view factor ( $1 - f_{s,sky}$ ) for each external surface. The z-transfer function (one-dimensional heat conduction method [80,

82, 83] ) approximates the transient conduction heat flux ( $q_{s,i}$ ) at the inside surface (walls) comprising a zone.

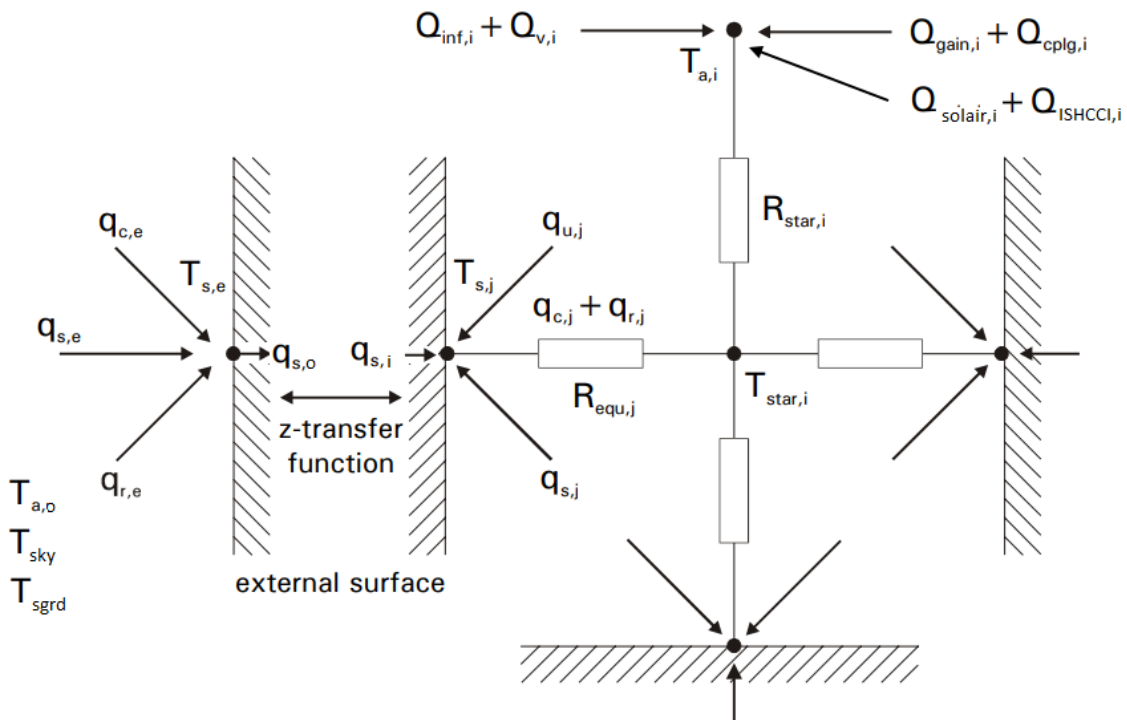


Figure 3-3. Schematics of heat flux applied in Type-56 standard approach (adapted from [80, 84, 85])

The solar radiative and longwave radiative gains from inside objects, furniture and people are approximated in terms of radiation heat flux ( $q_{s,j}$ ) absorbed at the inside surface  $j$ . The user can specify any particular heat flux ( $q_{u,j}$ ) to the surface  $j$ .

Furthermore, the star network method [80, 85, 84] approximates the longwave radiation exchange between the surfaces within a specific zone. As such, the net radiative heat flux ( $q_{r,j}$ ) from an inside surface  $j$  to all other inside surfaces and the convective heat flux ( $q_{c,j}$ ) at the inside surface,  $j$ , is calculated. The star temperature ( $T_{star,i}$ ) links the interior surface temperatures by equivalent resistances ( $R_{equ,j}$ ) for the surface  $j$ . The star temperature ( $T_{star,i}$ ) in turn, is linked to the zone air temperature ( $T_{a,i}$ ) by means of a star resistance ( $R_{star,i}$ ). Area ratios are used in these approximations to find the absorption factors between all surfaces.

Similarly, Figure 3-3 also illustrates bulk heat transfer to the zone in terms of various gains. This includes the infiltration gain from the outside air ( $Q_{inf,i}$ ), ventilation gain

from user-defined ventilation source ( $Q_{v,i}$ ), internal convective heat gain (people, equipment, illumination, radiators) ( $Q_{gain,i}$ ), ventilation gain due to coupling with other zones ( $Q_{cplg,i}$ ), convective gain to the internal air due to the fraction of solar radiation entering an air node through external windows ( $Q_{solair,i}$ ) and the convective gain to the internal air due to absorbed solar radiation on all internal shading devices of the zone  $Q_{SHCCI,i}$ .

### 3.2.2 Ventilation modelling of building in TRNSYS

TRNSYS uses COMIS [44] to model natural ventilation, infiltration and exfiltration through building flow components by applying a network approach. This method assumes the flow as steady, inviscid and incompressible [44]. In parallel, an equivalent pressure difference profile represents turbulence effects; and a single coefficient represents the effective area of the opening [86]. Similarly, linear density stratification exists on both sides of the opening [44]. Due to these considerations, COMIS predicts the single-sided ventilation with a reasonable accuracy comparable to other network airflow models even for relatively high wind speeds and small temperature difference [86].

The program models the airflow through the building by pressure nodes (zones) that are interconnected by non-linear conductance's in terms of airflow paths (links) modelling the cracks or openings [87]. These models combine the effect of wind and buoyancy to estimate the pressure difference and the solution is based on mass conservation at each zone or pressure node [87, 88], as shown in Equation (3-1).

$$\sum_{i_m=1}^{j_m} \dot{m}_{im} = 0 \quad (3-1)$$

Where,  $\dot{m}_{im}$  = Air mass flow through the  $i^{\text{th}}$  flow path of the  $m^{\text{th}}$  node

An appropriate equation describes a mass flow rate through airflow components (crack, large vertical opening) as a function of pressure difference, establishing a specific flow path. A fixed boundary condition represents the outside of the building (external node) for a one-time step with the help of the pressure coefficients that relate the wind pressure at the building to the wind velocity [89]. Using a non-linear system of flow

equation with the Newton-Rapson method with an appropriate relaxation factor, the pressures of the internal nodes in the airflow network are solved to determine the different airflow rates [89].

The small openings, like cracks on joints in the fabric or openings are the uncontrollable-air type components of natural ventilation. Analytically defining airflow rate through a crack under real conditions is quite complicated due to the involvement of several influencing parameters and airflow regimes depending on the shape of the crack and pressure difference [44]. However, applying a simple power-law ensures that most of the situations of uncontrolled ventilation can be defined as a function of pressure difference as in Equation (3-2) [44, 45].

$$\dot{m} = C_s \cdot (\Delta P)^N \quad (3-2)$$

Where,  $\dot{m}$  = Air mass flow rate (kg/s)

$C_s$  = Air mass flow coefficient (kg/s/Pa)

N = Air flow exponent (0.5 to 1)

A regression fit to experimental measurements derives these constants and exponents, including any correction factors to allow for differences in the conditions of the air, particularly temperature.

However, large vertical openings (windows or doors) installed on the building envelope facing the outside environment or installed between two zones of a building are controllable-air type natural ventilation. Due to the possibility of simultaneous bi-directional airflow with many influencing factors, natural ventilation through large openings is complicated [44]. Broadly, they are classified into two categories – those which induce steady flow due to their mean value and those whose effect is of a fluctuating nature [44].

The first category includes the effects of mean wind velocity, steady gravitational flows due to density gradients and the impact of boundary layer flows developed in an enclosure [44, 90]. The COMIS estimates mass flow through the opening as a function of the main characteristics of air on both side of the opening, considering Bernoulli's

assumption and including the influence of temperature stratification. In addition to this, most of the steady-state configurations can be well represented by linear density stratifications [44].

The second category includes the unsteady flow behaviour through large openings due to either slow evolution of boundary conditions or the fluctuating airflow due to fluctuating pressures or velocities [44]. Assuming that the flow develops instantaneously and considering Bernoulli's flow theory, COMIS describes and solves the steady-state flow of the dynamic process corresponding to the boundary conditions of each time step [44]. A successive imposition of new boundary conditions at each time step provides the subsequent solutions of the dynamic process. The time step varies according to available environmental datasets such as hourly wind speed and direction, occupancy schedule or changes of the thermal state of the building. Coupling or integrating the developments of the thermal model with airflow model in each time step provides a complete thermal and airflow dynamic process [44].

In single-sided natural ventilation, or when the wind direction is parallel to the openings in two parallel facades, the fluctuating effects can be significant. These are mainly due to the impact of turbulence due to local wind on the incoming wind to the opening or eddy penetration into the building of opening itself [44]. The turbulence in airflow along an opening causes pulsating flow resulting pressure fluctuations of the inside air of the enclosure [44]. Different types of windows, like awning (top-hinged), hopper (bottom-hinged) or casement (side-hung) or sliding create different natures of obstruction to the airflow resulting in complexity on quantifying the airflow. These unsteady situations due to turbulence effects and a high number of influencing parameters on the development of eddies on the building facades make the problem very complex. Nevertheless, researchers [86, 88, 91, 92, 93] have acquired some empirical know-how on this problem from the experiment in real configurations and this has been useful to some extent.

Now, the pressure difference  $\Delta P(z)$  [Pa] across an opening connecting the two zones, A and B, can be estimated in general by Equation (3-3).

$$\Delta P(z) = P_A - P_B + P_{dyn} + P_{stack} \quad (3-3)$$

- Where,  $P_A$  = Reference pressures at zone A [Pa]
- $P_B$  = Reference pressures at zone B [Pa]
- $P_{dyn}$  = Wind-induced pressure (0 for internal opening and according to Equation (2-3) for external opening) [Pa]
- $P_{stack}$  = Pressure difference induced by the stack effect [Pa]

As illustrated in Figure 3-4, a function of height ( $z$ ) expresses the vertical velocity profile. A neutral plane level (NL) intersects at a point on the vertical of the opening where the pressure difference across the opening is zero. Figure 3-4 along with the Equations (3-4) and (3-5) [44, 45] describe the estimation of the mass airflow by integrating the velocity profile.

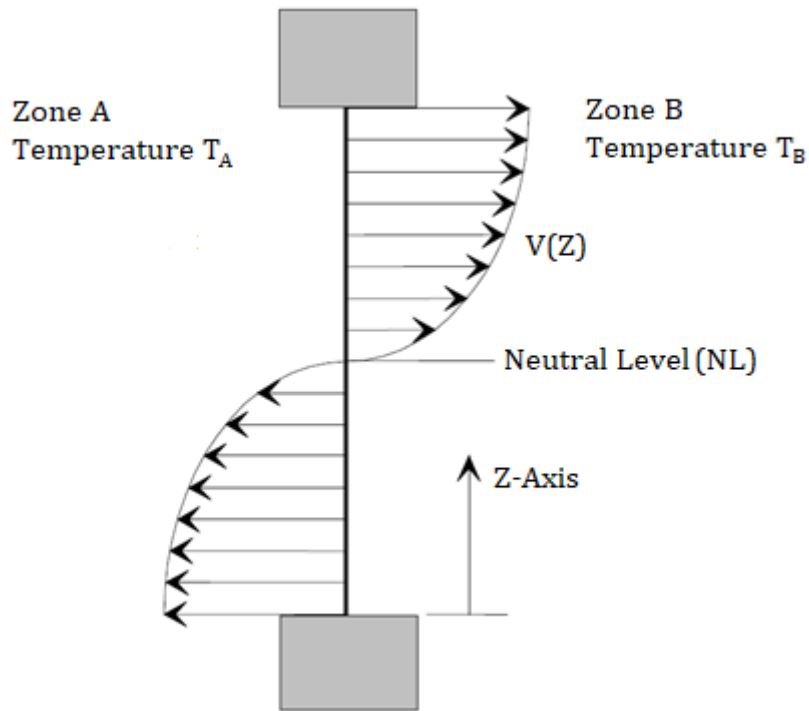


Figure 3-4. A typical bi-directional vertical velocity profile in Large Vertical Opening (adapted from [44, 45])

$$\dot{m}_{AB} = C_d \int_0^H \sqrt{2\rho(z)f_{AB}(z)} \cdot w(z) \cdot dz \quad (3-4)$$

With:

$$f_{AB}(z) = \begin{cases} \Delta P(z) & ,if \ \Delta P(z) > 0 \\ 0 & ,if \ \Delta P(z) < 0 \end{cases}$$

$$\dot{m}_{BA} = C_d \int_0^H \sqrt{2\rho(z)f_{BA}(z)} \cdot w(z) \cdot dz \quad (3-5)$$

With:

$$f_{BA}(z) = \begin{cases} -\Delta P(z) & ,if \ \Delta P(z) < 0 \\ 0 & ,if \ \Delta P(z) > 0 \end{cases}$$

Where,  $C_d$  = Discharge coefficient

$w(z)$  = Width of the opening at the height  $z$  [m]

$AB$  or  $BA$  = Flow direction across zone A and B

The opening angle, height and width of the opening define the geometry of the different types of windows. As such, the  $w(z)$  function in the Equations (3-4) and (3-5) describes the type of window and the effective opening area it might create while operating.

Constant values of width-  $W'$  [m] and Height-  $H'$  [m] define a rectangular opening.

The discharge coefficient  $C_d$  in Equations (3-4) and (3-5) compensates for the deviation of the flow from the ideal condition, taking account of both contraction and frictional loss of an opening [45, 91]. Flow properties like flow angle, Reynolds number and turbulence; geometric properties like porosity (opening to wall ratio), location and type of opening; and friction losses all contribute to the deviation from the ideal condition [45]. The value of  $C_d$  is highly dependent on an opening size such that the greater the opening, the higher the  $C_d$  [94]. The  $C_d$  value varies from 0.61 for sharp-edged orifices to 0.98 for trumpet-shaped nozzles type opening [44]. The  $C_d$  can also include contribution of many non-linear factors. Dascalaki [88] included wind fluctuation by adjusting  $C_d$  as Equation (3-6) for single-sided openings.

$$C_d = \begin{cases} C_w, & if \ 0.6 \leq C_w \leq 1.5 \\ 0.6, & if \ C_w < 0.6 \\ 1.5, & if \ 1.5 < C_w \end{cases} \quad (3-6)$$

With:

$$C_w = 0.08 \left( \frac{Gr}{Re^2} \right)^{-0.38} \quad (3-7)$$

$$Re = \frac{V_0 \cdot D_r}{\vartheta} \quad (3-8)$$

$$Gr = \frac{g \cdot \Delta T \cdot H'^3}{T_m \cdot \mu^2} \quad (3-9)$$

Where,  $Re$  = Reynolds number

$Gr$  = Grashof number

$V_0$  = Wind velocity [m/s]

$\vartheta$  = Viscosity of air [m<sup>2</sup>/s]

$D_r$  = Depth of the room (distance between the opening and the opposite wall) [m]

$T_m$  = Mean of absolute ambient and room air temperature [K]

### 3.3 Methodology

This work intends to examine the thermal comfort characteristics of a naturally ventilated single-sided simple model house. The examination is expected to help understand the relative influences of variations of internal and external operating conditions on the thermal behaviour of naturally ventilated house by using the numerical experiment method. This chapter approaches the issue at a macro level with a research-oriented recognised dynamic building simulations software tool TRNSYS. The tool is one of the industry-standard software used to set the acceptable range for ASHRAE Standard 140 [95].

The software package TRNSYS integrated with a COMIS simulation can develop a multi-zone coupled thermal and airflow model, to predict airflow through openings and the temperature and PMV for a zone, based on heat and mass conservation laws and its well-mixed assumption [54]. In addition to the uncontrolled ventilation effect, the COMIS helps to explore the influence of controlled natural ventilation of the building space.

This approach considers the space of the model house as one homogenous node having the same temperature and pressure connected and to outside only through the window. As illustrated in Figure 3-5, the model calculates the node air temperature in the thermal model (TRNSYS-Type 56) at each time-step and passes to the airflow model (COMIS), so that the model uses updated information to estimate node pressure and mass flow.

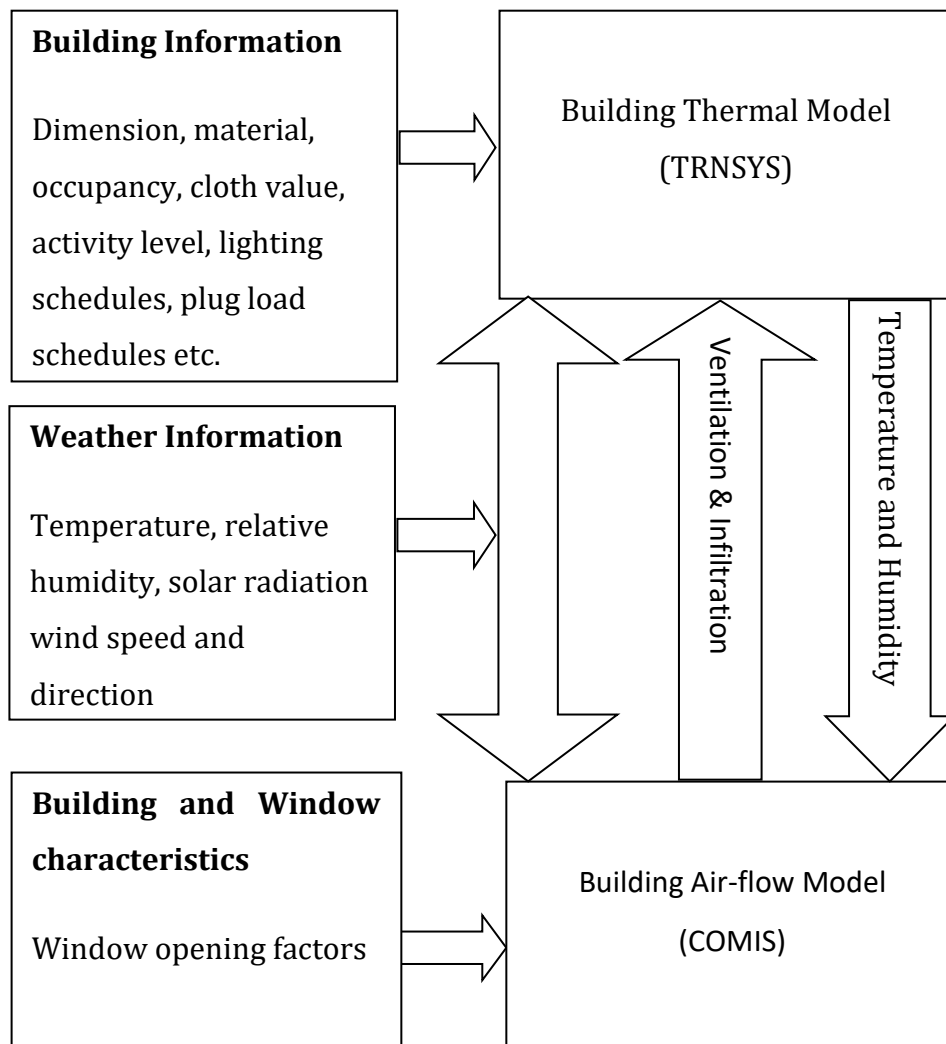


Figure 3-5. Coupled thermal and airflow modelling approach in TRNSYS-COMIS environment

The spatial requirement of identifying at least one average value of thermal PMV for a standard room or zone of a residential building is sufficient to reveal an overall scope for regulating thermal comfort of the natural ventilated room or zone. As such, the

multi-zone coupled thermal-airflow modelling approach with a TRNSYS-COMIS simulation can provide an average value of PMV to assess thermal comfort behaviour.

For the post-processing assessment of thermal comfort, the PMV range ( $-0.7 < PMV < 0.7$ ) which has a relatively a higher value on the comfort scale, is considered in this research as acceptable to people accustomed to naturally ventilated environments. This leads characterising thermal comfort index for uncomfortable hot as ( $PMV \geq 0.7$ ) and uncomfortable cold as ( $PMV \leq -0.7$ ).

### **3.4 Description of the model**

#### **3.4.1 Physical and geographical description**

A house with a single room with external dimensions, 3 m length, 3 m width, 3.6 m reference height (including 0.6 m of the subfloor space), acts as a model for this study, as shown in Figure 3-6. The selected dimension ensure a minimum standard floor-to-ceiling height of a typical residential house in Auckland [96, 97]. The minimum internal space volume of the model is 18.75 m<sup>3</sup>. The interior volume of the room varies according to the selection of the envelope's thickness to model different levels of envelope thermal resistance. The smaller room size is relatively more susceptible to the minor influence of house operation conditions than the big size resulting in the simulations capturing minor changes due to the possible small disturbances. In this regard, the selected physical size of the model, meets both the minimum residential size requirement of a room and is expected to provide sufficient and resolution of the thermal behaviour than large size rooms.

It is assumed that the model house is located in Auckland NZ at 36.85° S, 174.76° E, with each wall oriented toward the cardinal directions and a single window on the north face. The house is located in an urban terrain with obstacles at distances less than a few times the house's height, similar to the typical suburban area where most residential dwellings exist. The simulations include this shielded condition by considering the wind velocity profile coefficient of 0.313 [89]. On the other hand, the weather station's location is regarded as a relatively open terrain with a wind velocity profile coefficient of 0.14 [89].

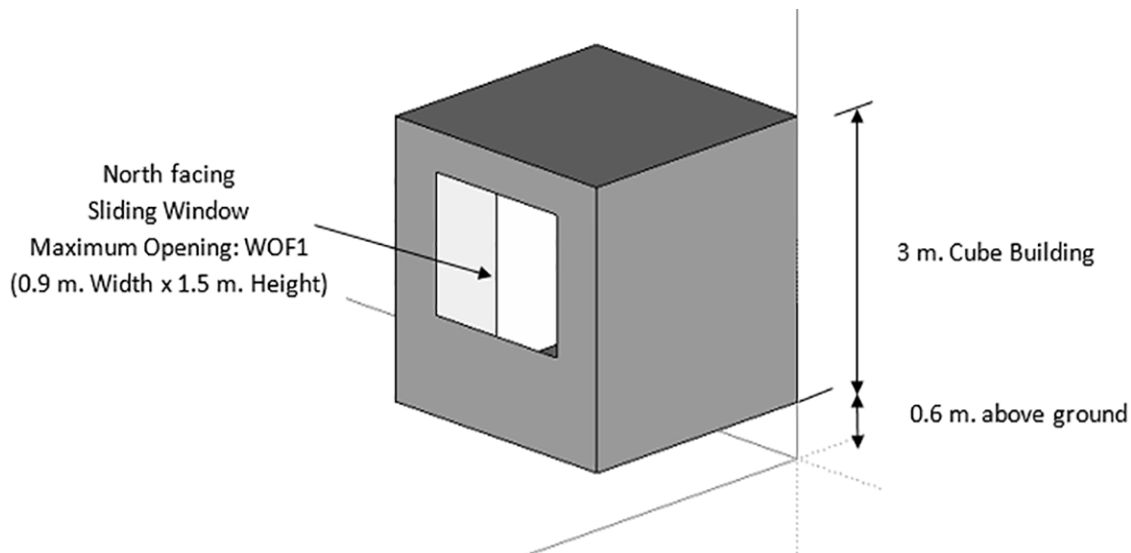


Figure 3-6. 3D building model

### 3.4.2 Occupancy

The modelling work assumes that 0 to 5 occupants, producing heating of 100W per person (sensible-60W and latent-40W), occupy the room randomly. This rate of heat gain is equivalent to the activity level of an occupant seated at rest inside the house [80], making the threshold of internal heat gain from 0 to 500 watts. This random occupancy model can produce a broader range of internal heat gains. It also helps test the influence of extreme occupancy and any virtual electric loads that might appear in the actual operation of the house.

### 3.4.3 Envelope airtightness

Considering the wide variability in air-tightness of NZ housing stock [3], the modelling discretises the envelope airtightness level from the least airtight-Draughty (DTY) house with 0.9 ACH to the most airtight – Ultra Airtight (UAT) house with 0.03 ACH. While doing this, the model also considers un-controlled infiltration equivalent to intermediate airtightness levels defined as Airtight (AT) (0.3 ACH), Average (AVG) (0.5 ACH) and Leaky (LKY) (0.7 ACH) houses. The UAT airtightness level case approximately satisfies a passive house airtightness standard [4].

### 3.4.4 Envelope thermal resistance

Table 3-1 presents the building facade baseline thermal resistance ( $R - value$ ) (Case 1) just meeting the current standard schedule method for non-solid construction [24]. This baseline results in a weighted average envelope thermal Resistance ( $R_{avg}$ ) value of the house equivalent to 2.01. Further,  $R - value$  of 2.6 (Case 2), 3.2 (Case 3) and 3.6 (Case 4), define as intermediate insulation layers on the envelope components (wall, roof, and floor) to explore the overall improved average envelope  $R_{avg}$  values of 2.6, 3.22 and 3.44 respectively.

Table 3-1. Building facade description

Building Facade	Description	R-Values			
		Case 1 $R \approx NZBC$	Case 2 $R 2.6$	Case 3 $R 3.2$	Case 4 $R 3.6$
External Wall	Timber frame direct fixed cladding	1.9	2.4	3.1	3.2
Floor	Suspended floor with lining under the joists and gap between insulation and lining	1.3	3.1	3.5	3.8
Roof	Timber frame skillion roof	2.9	3	3.4	3.8
Window	Vertical double glazed sliding window (1.8 m. width x 1.5 m. height) Northern wall	0.34	0.34	0.34	0.34
Area weighted average envelope resistance ( $R_{avg}$ )		2.01	2.6	3.22	3.44

### 3.4.5 Window and opening area

The model uses the wall average pressure coefficient  $C_p$  values for low rise buildings with a length to width ratio of 1:1 and a shielded condition [98]. In the process, COMIS solves a system of nonlinear equations to determine the node pressures and the mass flow in each link using air mass conservation in each node.

Large Vertical Opening (LVO type 1) [44], models a sliding window with a maximum opening size of 0.9 m (width) by 1.5 m (height) as shown in Figure 3-6 to achieve the ventilation. In doing this, a WOF value of 1 defines fully open and 0 fully shut operating state of the window. Further, intermediate WOF values of 0.1, 0.25, 0.4, 0.5, and 0.75 help to determine the effect of various opening area on the thermal conditions.

### 3.4.6 Input weather database

The ambient boundary conditions for the simulations is the weather for a typical year in Auckland, NZ. Diffuse and direct solar irradiation, air temperature and humidity, wind speed and direction are input parameters on an hourly basis for a whole year. Because of the relatively long data interval, uncertainties arise, especially on partially cloudy days where the actual amount of direct solar irradiation might vary from minute to minute. When simulation time steps are shorter than one hour, a linear interpolation helps derive data for each time step. In this regard, the model uses the Typical Meteorological Year (TMY) with the format of type.tm2 for Auckland (Airport.tm2). The weather file might not capture a worst-case scenario as such days are relatively rare. Similarly, the microclimate condition of the exact building location might differ compared to the meteorological station; this might raise a level of uncertainties on dynamic simulation results.

### 3.4.7 Heat transfer models

This initial examination uses the standard approach of modelling heat transfer process (conduction, convection and radiation) of a building with TRNSYS-Type 56 model. In this approach, the convective heat transfer process depends on the temperature difference between surface and fluid and direction of heat flow for internal surfaces. As such, this work uses the default empirical relationship of the form as of Equation (3-10).

$$h_{c,j} = \frac{C}{3.6} |T_{s,j} - T_{a,i}|^n \quad (3-10)$$

Where,  $h_{c,j}$  = CHTC for inside surface  $j$  [K].hr/m<sup>2</sup>.K]

$C$  = Constant representing geometry of the surface

$n$  = Exponent representing flow regime

$T_{a,i}$  = Ambient air temperature at zone  $i$  (K)

$T_{s,j}$  = Temperature at inside surface  $j$  (K)

The modelling uses the default values of the constants and exponents for the vertical and horizontal surfaces CHTC(s) as listed in Table 3-2.

Table 3-2. Default values of constants and exponents [80]

Surface	Thermal status	Constant (C) [k]/m <sup>2</sup> K]	Exponent (n)
Floor	Hot ( $T_{s,f} - T_{a,i} > 0$ )	7.2	0.31
Floor	Cold ( $T_{s,f} - T_{a,i} < 0$ )	3.888	0.31
Ceiling	Hot ( $T_{s,c} - T_{a,i} > 0$ )	3.888	0.31
Ceiling	Cold ( $T_{s,c} - T_{a,i} < 0$ )	7.2	0.31
Vertical	Any	5.76	0.3

The heat transfer coefficient at the outside of the exterior walls and roof varies with the wind speed. Thus, the modelling considers that the external heat transfer coefficient depends on outer surface material and wind velocity according to the Equation (3-11) [95].

$$h_{c,e} = a_1 + a_2 \times V_m + a_3 \times (V_m)^2 \quad (3-11)$$

Where,  $V_m$  = Wind velocity at meteorological station height (10 m)

Table 3-3 presents the coefficients  $a_1$ ,  $a_2$  and  $a_3$  for different materials; the modelling work considers the coefficient related to wood for external surfaces exposed to the environment.

Table 3-3. Parameters for calculating heat transfer coefficient for external surface materials [95]

Surface Material	$a_1$	$a_2$	$a_3$
Stucco	11.58	5.894	0
Brick	12.49	4.065	0.028
Concrete	10.79	4.192	0
Wood (Clear Pine)	8.23	4	-0.057
Smooth plaster	10.22	3.1	0
Glass	8.23	3.33	-0.036

Similarly, the modelling sets the heat transfer coefficient of the floor to a minimal value, considering the surface temperature equivalent to the ground temperature.

### 3.5 Results and discussion

After developing the thermal model of the single-sided naturally ventilated house, the dynamic simulations help to explore the performance of the model and the occupied space for a range of conditions. In this respect, Figure 3-7 and Figure 3-8 show the effect of the window at various fixed values of WOF(s), on the PMV in an average and in ultra- airtight houses respectively for a typical summer day in January. January represents a peak summer month in NZ, when the need for ‘cooling’ by natural ventilation is greatest. Figure 3-7 and Figure 3-8 show that the PMV follows the air temperature in the zone closely, thus illustrating that the zone air temperature ( $T_a$ ) is one of the critical factors for assessing thermal comfort in the space.

Figure 3-7 and Figure 3-8 show that the window infiltration ( $INF_{WINDOW}$ ) initially increases at a low rate for small WOF (0-0.5), then increases sharply for WOF 0.75 and again rises slowly up to WOF 1. At the early stage, the open area restricting the balance of in and outflow from the space limits the infiltration rate. At the later stage, the small temperature and pressure difference (between outside and inside) slows the infiltration rate.

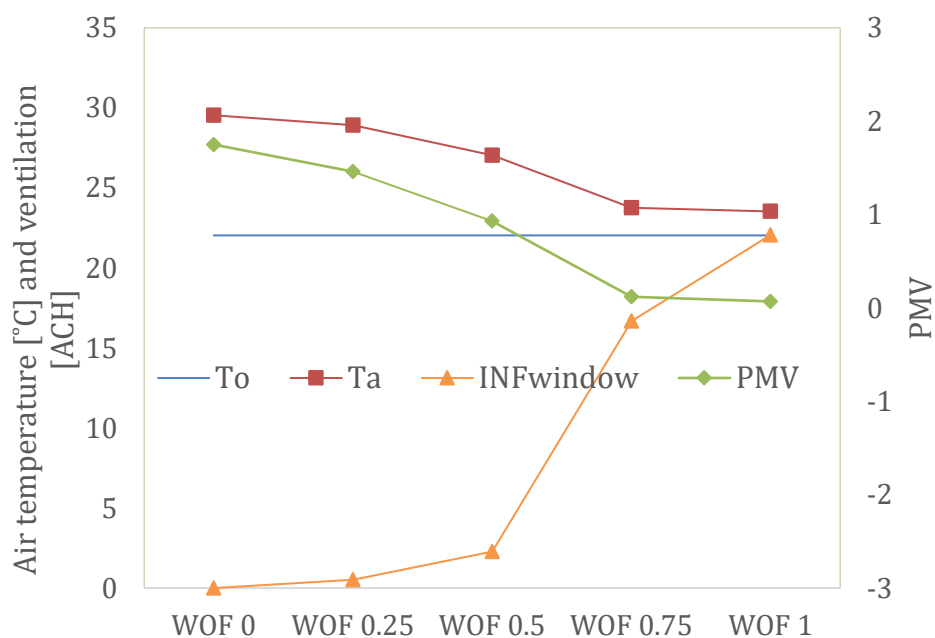


Figure 3-7. Effect of WOF on PMV and temperature in an average-airtight house  
( $R_{avg}$  2.01, January)

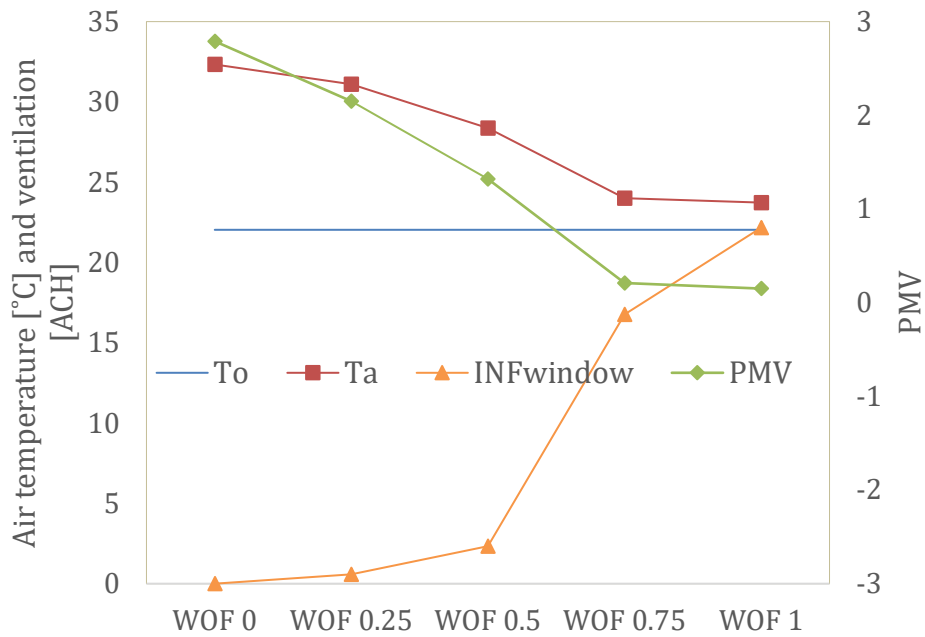


Figure 3-8. Effect of WOF on PMV and temperature in an ultra-airtight house  
( $R_{avg}$  3.4, January)

Figure 3-7 and Figure 3-8 also illustrate that there is a relatively higher potential in a well-insulated house for regulating indoor air temperature and thermal comfort behaviour of the occupied space by opening windows. It is apparent that the opening of the window (WOF 0.75 or higher) can reduce the relatively high indoor air temperature ( $T_a$ ), irrespective of envelope thermal insulation  $R_{avg}$  2.01 or  $R_{avg}$  3.4. The closing of the window (WOF value 0) or small opening (WOF value less than 0.25) generally raises the indoor temperature. An increase in WOF helps bring the zone air temperature close to the outdoor ambient air temperature ( $T_o$ ) such that a further increase more than a WOF of 0.75 has a negligible effect on the difference.

Exploring this idea, Figure 3-9 and Figure 3-10 demonstrate that the zone relative humidity ( $RH_a$ ) falls sharply with small WOF(s) as the vapour pressure difference between the outside and inside moves towards zero. An increase in WOF helps bring the zone air relative humidity close to the outdoor ambient air relative humidity ( $RH_o$ ) such that a further increase more than a WOF of 0.75 has a negligible effect on the difference.

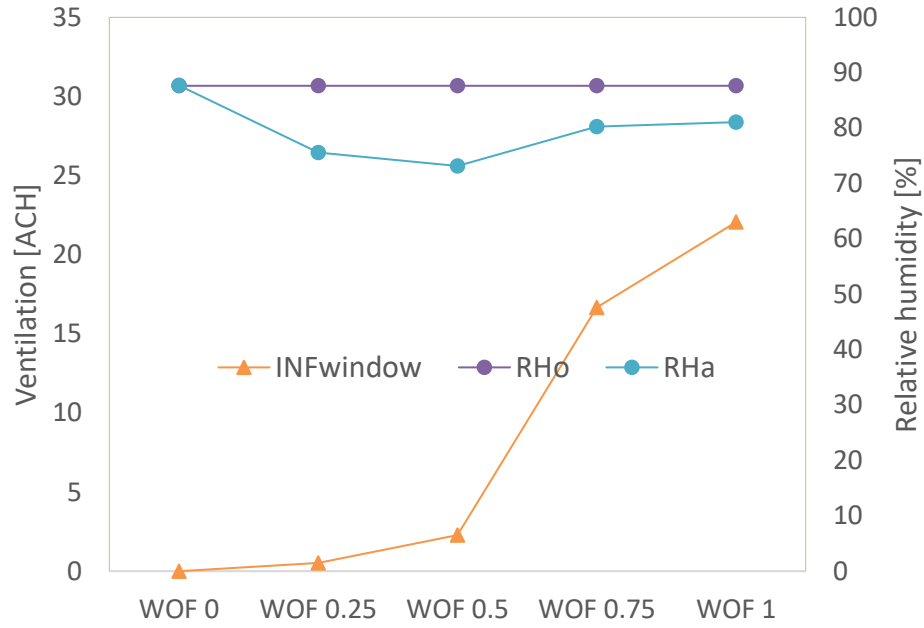


Figure 3-9. Effect of WOF on the relative humidity in an average-airtight house  
( $R_{avg}$  2.01, January)



Figure 3-10. Effect of WOF on the relative humidity in an ultra-airtight house  
( $R_{avg}$  3.4, January)

Table 3-4 presents the mean monthly values of the zone temperature ( $T_a$ ) and relative humidity ( $RH_a$ ). The table includes both the average-airtight (AVG) house with an average envelope thermal resistance ( $R_{avg}$  2.01) and ultra-airtight (UAT) house with an average envelope thermal resistance ( $R_{avg}$  3.4), with the window closed, related to the outdoor ambient conditions ( $T_o, RH_o$ ). When compared with the standard range of thermal comfort index ( $-0.7 < PMV < 0.7$ ) for a naturally ventilated building, the summer months from November to March have the highest potential for improving the PMV by the opening window in the house with  $R_{avg}$  2.01. The results also indicate that a well-insulated house ( $R_{avg}$  3.4) has a risk of overheating the occupied space from September to April. However, the natural ventilation free cooling potential can also apply from September to April for a well-insulated house with  $R_{avg}$  3.4. Moreover, it is also apparent that by not operating windows, additional steps are required to remove moisture from the building to avoid problems associated with the high relative humidity of the air in the zone.

Table 3-4 Monthly mean values of the conditions for  $R_{avg}$  2.01, AVG and  $R_{avg}$  3.4 UAT

Monthly Mean	Month												
	$R_{avg}$	January	February	March	April	May	June	July	August	September	October	November	December
$T_o$ [°C]		20	20	19	16	13	11	10	11	13	14	16	18
	2	31	30	29	25	22	19	19	20	22	24	27	29
$T_a$ [°C]	3.4	37	37	35	31	27	24	24	25	28	30	34	36
	2	2.0	1.9	1.5	0.3	-0.7	-1.5	-1.7	-1.3	-0.6	0.0	1.0	1.6
PMV	3.4	4.6	4.3	3.6	2.1	1.0	0.0	-0.2	0.4	1.2	2.0	3.3	4.2
$RH_o$ [%]		73	75	76	79	80	82	83	81	80	78	77	76
	2	80	82	88	95	98	99	100	99	97	93	87	82
$RH_a$ [%]	3.4	100	100	100	100	100	100	100	100	100	100	100	100

Most NZ houses do not have the higher level of airtightness described previously (UAT). Therefore, Figure 3-11 illustrates the distribution of PMV for the modelled space with open and shut windows during January for a typical NZ timber house meeting a minimum envelope average thermal resistance  $R_{avg}$  2.01. When the window opens, the

effect of airtightness is less significant, and all buildings exhibit a similar overall comfort distribution, in terms of hot ( $>0.7$ ) and cold hours ( $<-0.7$ ).

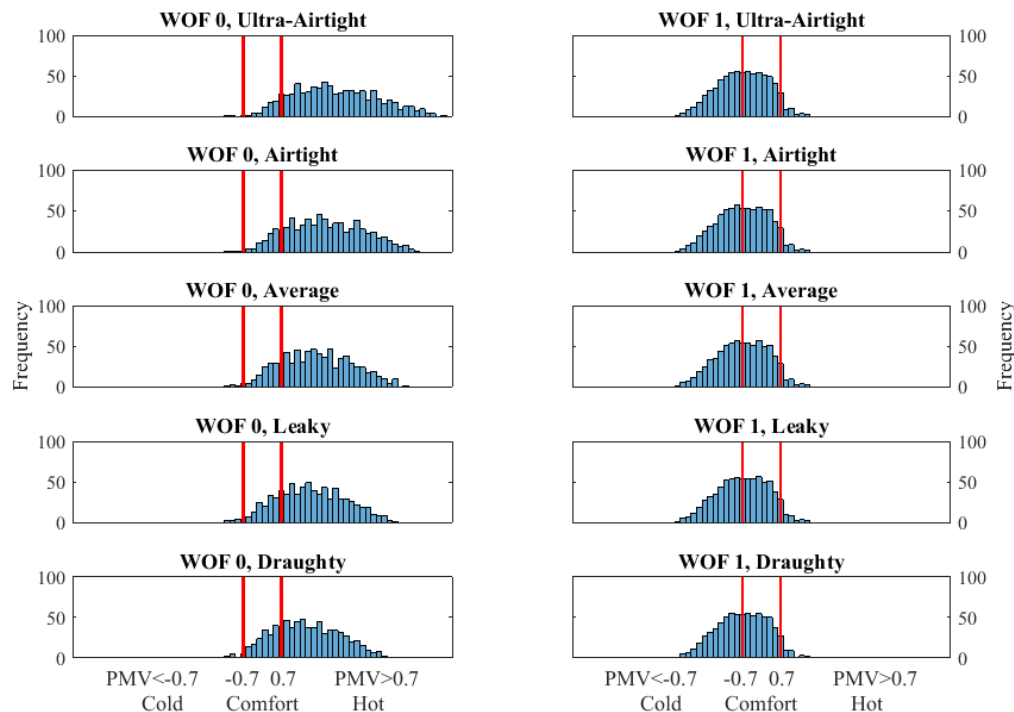


Figure 3-11. PMV variation with airtightness with shut (left) & open (right) windows  
( $R_{avg}$  2.01, January)

Figure 3-12 illustrates the distribution of PMV for the modelled space with open and shut windows during January for the higher level of envelope thermal resistance ( $R_{avg}$  3.4). Figure 3-12 shows that the distribution of PMV moves towards hot ( $>0.7$ ) when the window shuts, indicating the prevalence of uncomfortably hot indoor conditions. This undesirable hot condition is worst in the UAT house and gradually reduces with decreasing the airtightness level. Irrespective of the higher envelope thermal resistance, when the window opens, the effect of both the insulation and airtightness become less meaningful, and all buildings exhibit a similar overall comfort distribution, in terms of hot ( $>0.7$ ) and cold hours ( $<-0.7$ ). This indicates a better prospect of thermal comfort regulation potential by regulating window openable area in a well-insulated and airtight house.

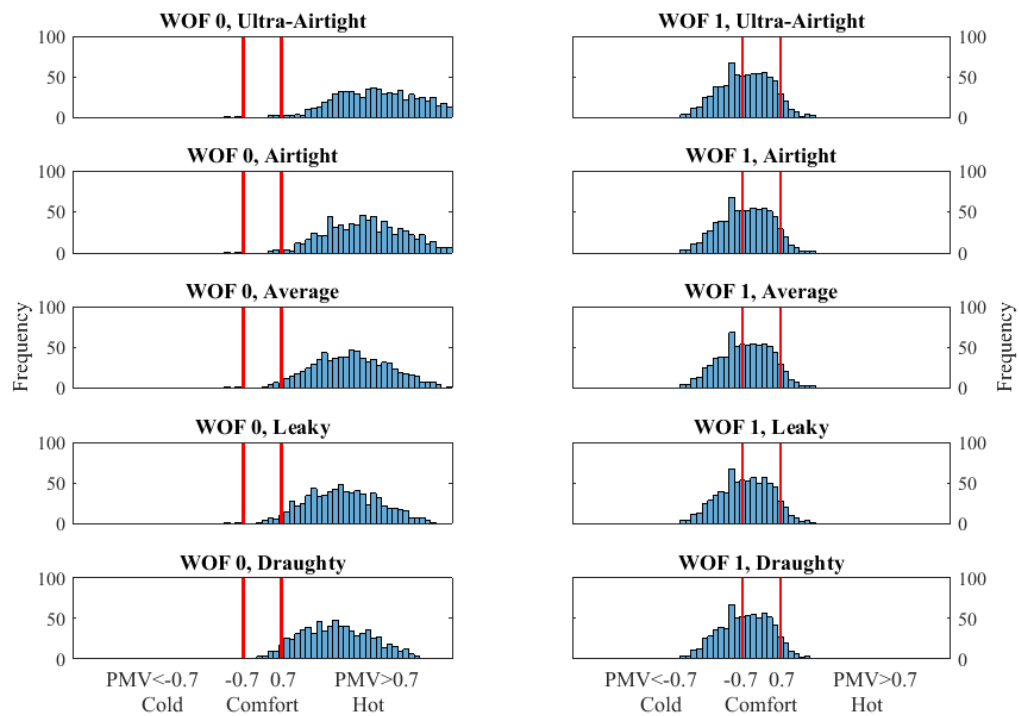


Figure 3-12. PMV variation with airtightness with shut (left) & open (right) windows ( $R_{avg}$  3.4, January)

Figure 3-13, illustrates the distribution of thermal comfort for the modelled space with open and shut windows during July for envelope thermal resistance ( $R_{avg}$  3.4). The Figure 3-13 shows that the PMV stays in the comfort zone when the window closes for an airtight house (UAT) compared to the worst airtight house (DTY). Again, irrespective of higher envelope thermal resistance, when the window opens, the effects of both the insulation and airtightness are diminished, and all buildings exhibit a similar overall comfort distribution, in terms of hot (>0.7) and cold hours (<-0.7).

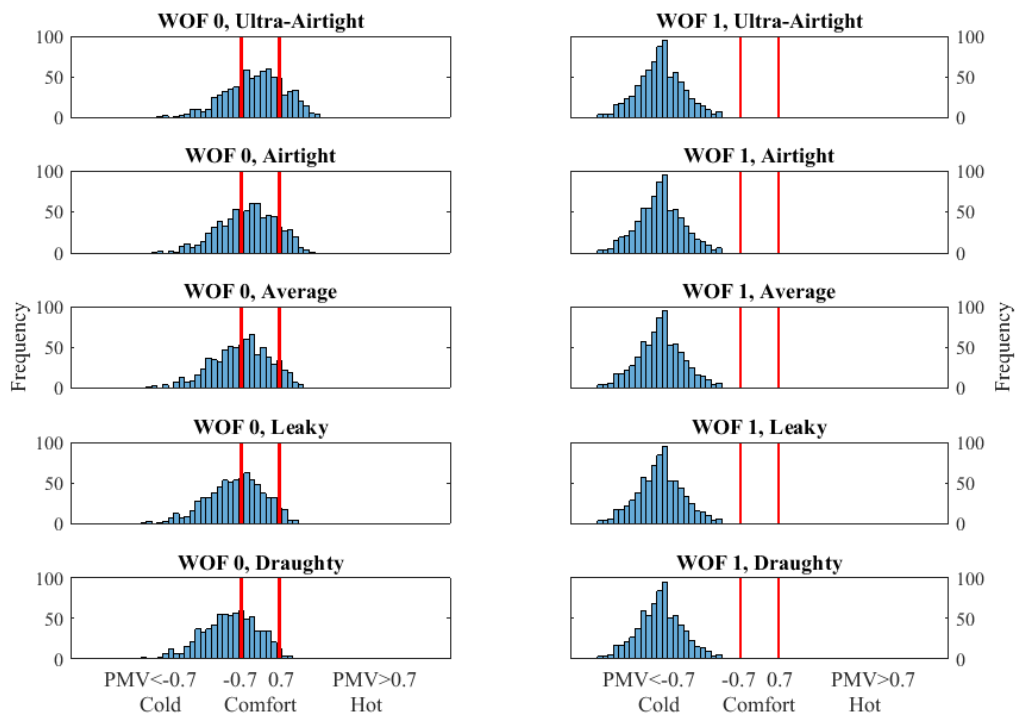


Figure 3-13. PMV variation with airtightness with shut (left) & open (right) windows ( $R_{avg}$  3.4, July)

Considering the use of natural ventilation further, Figure 3-14 and Figure 3-15 show the PMV distribution for January and July for  $R_{avg}$  2.01 and  $R_{avg}$  3.4 house respectively and this illustrates the comfort levels over the year, considering varying the WOF 0-1 for the average (AVG) airtight house.

The frequency of getting uncomfortably warm and hot indoor conditions decreases and comfortable thermal condition increases with the increase in WOF at the expense of an increase in the frequency of uncomfortable cold situation for the peak summer month of January. However, an increase in the WOF diminishes the probability of getting thermal comfort condition in peak winter month of July.

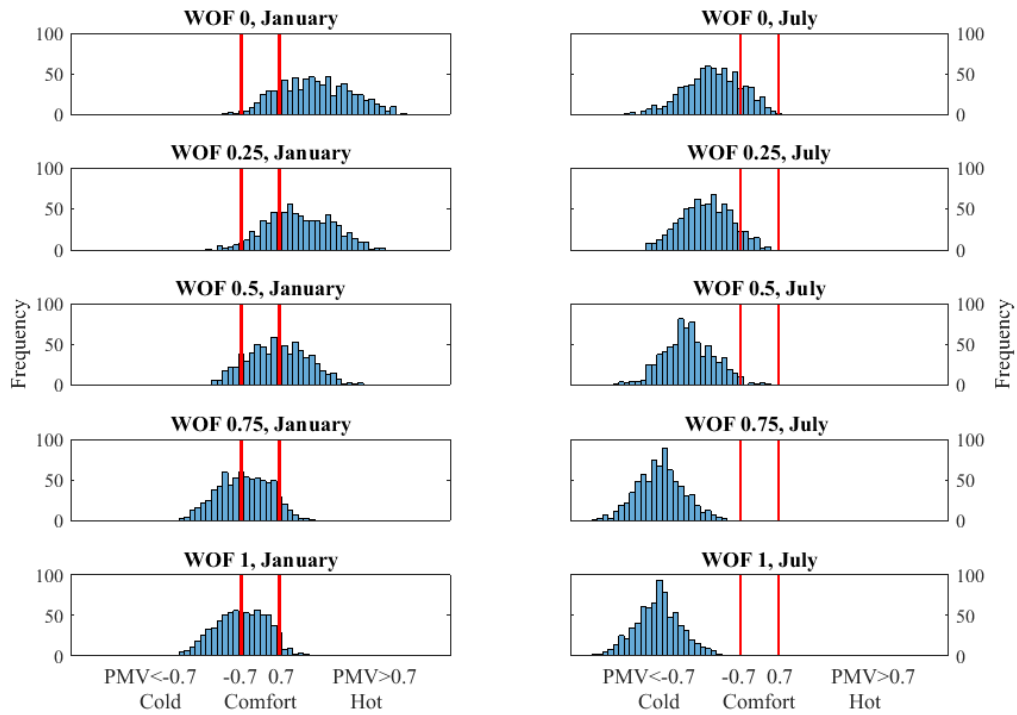


Figure 3-14. PMV frequency distribution for an average airtight house ( $R_{avg}$  2.01, January & July)

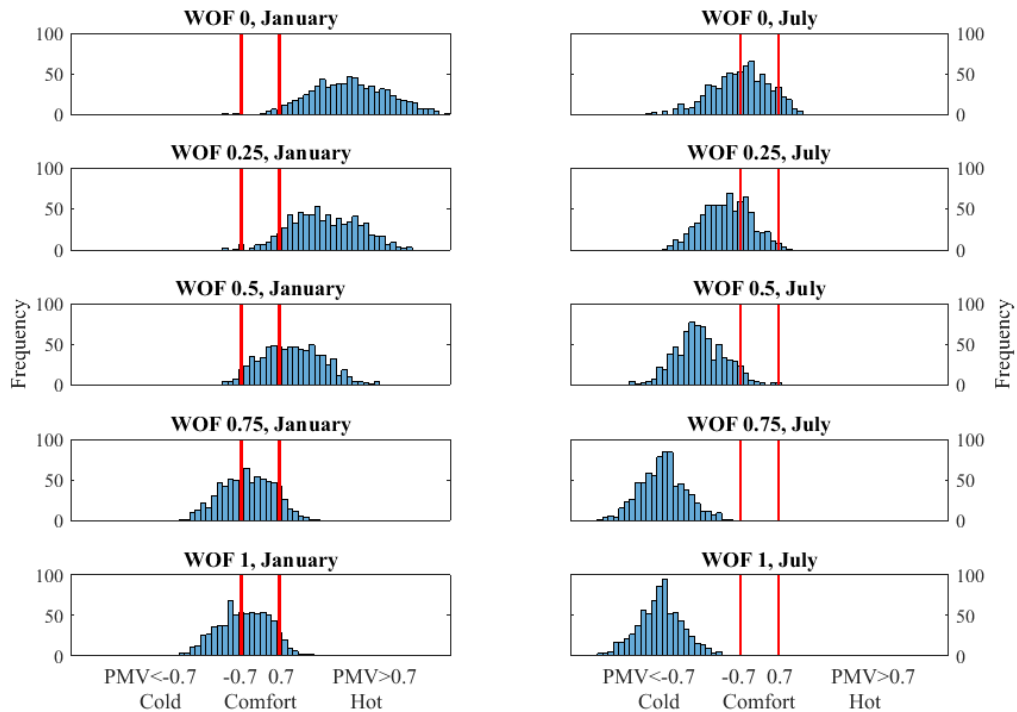


Figure 3-15. PMV frequency distribution for an average airtight house ( $R_{avg}$  3.4, January & July)

Considering the thermally comfortable period together, with both the thermally uncomfortable hot and cold duration, Figure 3-16 and Figure 3-17 demonstrate the impact of the increasing envelope airtightness, window opening factors and the thermal resistance values from  $R_{avg}$  2.01 to  $R_{avg}$  3.4 respectively.

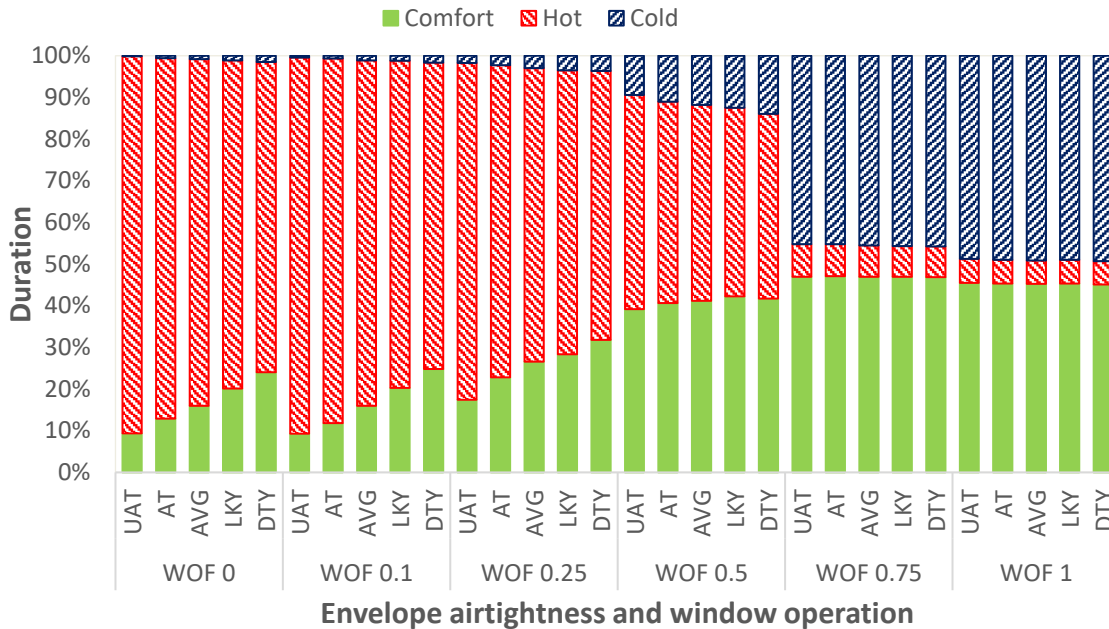


Figure 3-16. Thermal comfort distribution for a range of WOF & airtightness values ( $R_{avg}$  2.01, January)

Figure 3-16 and Figure 3-17 show that there is an overall increase in the thermally uncomfortable hot and decrease in cold duration indicating a better prospect of regulating thermal behaviour of the undesirable hot period in the well-insulated house. These results confirm that window position (WOF 0.75) provides a maximum of 47-49% thermal comfort duration irrespective of any envelope airtightness and thermal resistance values. It reveals that a large proportion of the instances (more than 51%) still fall into either an uncomfortable cold or hot range despite having an insulated and airtight house. It illustrates the limited prospect of any position of fixed openable area for improving the thermal comfort of the naturally ventilated house.

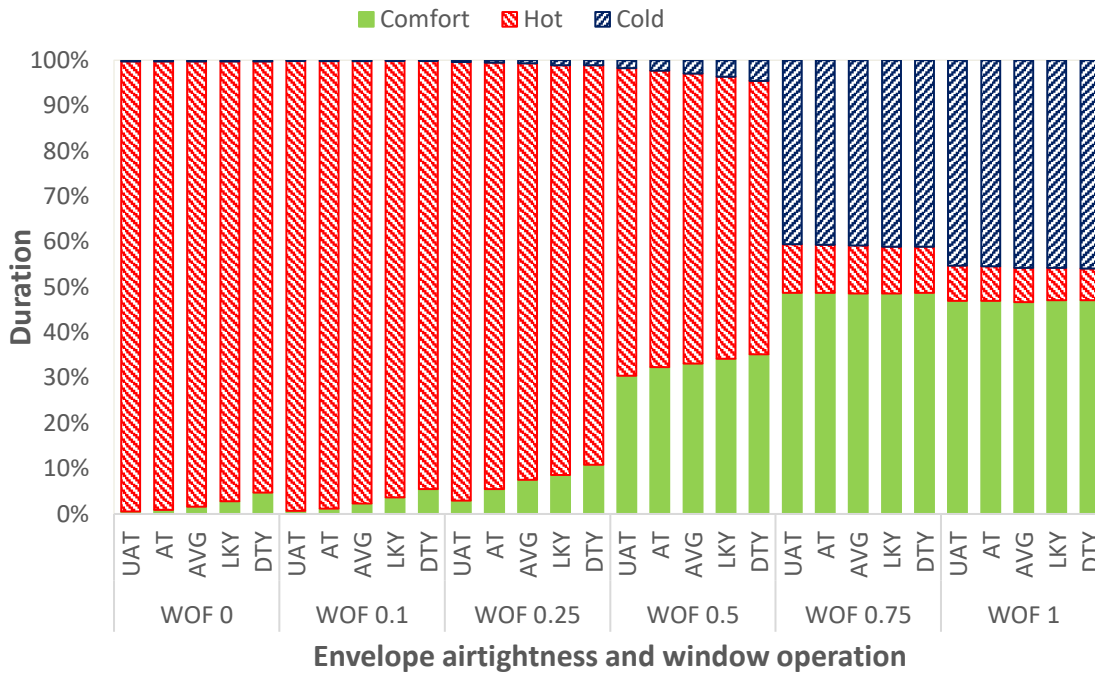


Figure 3-17. Thermal comfort distribution for a range of WOF & airtightness values ( $R_{avg}$  3.4, January)

Examining the results further, focusing on the percentage of the undesirable hot periods, Figure 3-16 and Figure 3-17 indicate that envelope airtightness can also play a significant role in regulating the thermal comfort behaviour of the naturally ventilated house. However, the degree of thermal regulation potential reduces with reducing airtightness level. Therefore, further opening the window increases the uncomfortable cold periods, and there is a better resilience towards uncomfortable-cold periods in a well-insulated house.

### 3.6 Robustness, applicability and generalisability of the results

ASHRAE Standard 140 [95] specifies a standard method of test for evaluating the technical capabilities and applicability of software used in calculating the thermal performance of buildings and their HVAC systems [95]. Building simulation tools are "validated" by running them through a series of tests described in ASHRAE Standard 140. TRNSYS is one of the industry-standard software tools used to set the acceptable range for ASHRAE Standard 140. Many published and peer-reviewed numerical experiments are carried out by researchers using the building model Type 56 of TRNSYS software.

This work also used the building model Type-56 to explore the problem of single-sided natural ventilation in a simple building set-up in association with another TRNSYS model, Type 157a. In addition, the work examined the model's response to variations of internal or external parameters over some range of interest following numerical experiment methodology. The objective of the assessment was to understand the relative influences of variations of internal and external operating conditions on the thermal behaviour of naturally ventilated house through the coupled use of Type 56 and Type 157a.

The results produced in this chapter are sufficient to confirm that there is a scope for regulating the thermal behaviour of naturally ventilated houses as set out in the first objective of the research and move to the next objective. However, this work identifies that the TRNSYS building mathematical model greatly simplifies the heat transfer behaviour of interior surface exposed to natural ventilation. Greater scrutiny and specific treatment on the heat transfer behaviour of building internal surface exposed to natural ventilation might help further improve the robustness of the building simulation models and the accompanying results. Addressing the issue could be useful to improve the robustness of the building performance simulation tools for evaluating thermal performance of naturally ventilated buildings. In overall, the outcomes presented in this chapter establishes an excellent base to find solutions for improving the robustness of the thermal building models and actuating solutions set out as other specific objectives of this research.

Other than what the research contemplated under the scope of this research objective, there are still many open-ended questions on thermal comfort dynamics of naturally ventilated NZ houses. Using this base, researchers can further explore the subject to improve the knowledge base about the thermal comfort dynamics of naturally ventilated NZ houses operated in complex real-life conditions. Finding all the answers requires increasing the complexity of the building model (multiple zones) and the associated operating conditions (cross window, adjacent window, natural and mechanical hybrid ventilation, plug loads, occupancy schedules, various house orientation, location of the window, size and type of windows etc.). The work might help better inform planners and policymaker to conceive necessary instruments and standards to improve the thermal performance of the existing housing stock of NZ.

### 3.7 Remarks

The coupled multi-zone thermal and airflow simulations can capture the effect of natural ventilation through a window in terms of the PMV thermal comfort index of a residential house located in a mild climatic zone like Auckland. The indoor air temperature and relative humidity might reduce to the limit equivalent to the ambient air temperature and relative humidity by opening a window in the daytime summer months. This potentially can help maintain the indoor thermal comfort level of a residential house within an acceptable thermal comfort range. There is a significant scope of regulating the thermal behaviour of naturally ventilated residential houses in mild climatic conditions. Furthermore, there is greater scope for achieving this in a relatively airtight and insulated house, in particular by opening windows during the summer period. Interpreting the results in terms of the newly built or refurbished houses (relatively higher thermal resistance and airtightness than the average houses) in Auckland or NZ, the potential scope for regulating thermal behaviour is promising.

However, this simplified approach of examining the thermal behaviour of the natural ventilated building possesses a risk of higher uncertainty of the investigation. This is due to the assumptions that the convective heat transfer relationships from the indoor surface depend on the natural convection mechanism ideally developed in the closed room operating conditions. However, a partially opened naturally ventilated building would result in a stream of airflow exchange from outdoor to indoor and vice-versa through the opening. This stream of incoming airflow with the dynamic outdoor weather condition, in particular, the outdoor air temperature, relative humidity, wind speed and direction might result in a completely different convective heat transfer behaviour on the indoor building surfaces.

Therefore, the robustness of such thermal-airflow models needs greater scrutiny; particularly, the method for determining the indoor surface CHTC.

## **Chapter 4 The influence of buoyancy forces on the heat transfer behaviour of the floor**

### **4.1 Introduction**

To calculate the heat transfer from surfaces within a space, many Building Energy Simulation (BES) programs utilise coupled multi-zone thermal and airflow network models to predict the airflow through an opening of, and indoor air temperatures within, naturally ventilated buildings [54]. By applying this approach, this research has already confirmed that a BES program (TRNSYS coupled with COMIS) can capture the thermal behavior of a single-sided naturally ventilated house [99].

Depending on the type and cause of driving force, the ventilation strategy (natural, forced or mixed), employed in a particular building can influence the indoor airflow pattern and convective heat transfer behaviour at the indoor surfaces. Besides, the natural ventilation strategy can follow the principle of single-sided, cross and adjacent sided flow leading to different airflow patterns inside the building. These airflow patterns might result in different convective regimes and heat transfer behaviour from the internal building surfaces. An ideal convective heat transfer model or correlation might not adequately describe all these different environmental and operational situations of the building. Therefore, the robustness of such thermal-airflow models, particularly, the method for determining the indoor-floor surface CHTC, needs greater scrutiny.

This chapter presents an initial numerical examination of the heat transfer and flow-fields in a standard room with a single-sided window by utilising CFD. The thermal buoyancy effect between floor and above due to floor and external temperature difference produces the convection heat transfer on the floor surface. The work examines the influence of thermal buoyancy and window opening factor on the heat transfer behaviour of the partly open room, in particular, the floor. In addition, the work aims to develop a specific empirical relationship to improve the robustness of thermal models of naturally ventilated buildings. However, the investigation presented in this chapter does not consider possible effects due to external wind, the transient temperature inside the space, thermal mass of the envelope, solar gains, internal heat

loads and furnishings/flow restrictions in the interior spaces. All of these factors are important and might influence the heat transfer behaviour of the floor significantly. The subsequent Chapter 5 provides a further effect of wind conditions on the heat transfer behaviour of the floor.

## 4.2 Internal surface convective heat transfer behaviour

Newton's law of cooling (Equation (4-1)) defines the basic principle behind the convective heat transfer [100] of building surfaces.

$$q = h_c \cdot \Delta T \quad (4-1)$$

Where,  $q$  = Rate of convection heat transfer per unit surface area  
[W/m<sup>2</sup>]

$h_c$  = CHTC [W/m<sup>2</sup>.K]

$\Delta T$  = Temperature difference between the surface and the surrounding fluid sufficiently far from the surface [K]

A significant challenge for this simple equation is identifying the value of the CHTC because various factors (the flow regime, the properties of the fluid, and the geometry of the specific system under consideration) influence the CHTC [100].

The driving force behind the natural convection is the buoyancy force created due to the surface-to-air temperature difference leading to density differences of adjacent layers of air. In this regard, researchers [101, 102, 103, 104, 105] have developed numerous correlations for modelling the natural convection heat transfer to and from internal building surfaces. Further to that, researchers [106, 107] specify that either majority of correlations available in BES depend on isolated horizontal and vertical flat plate surfaces or, at most, they are dependent on the temperature difference between opposite surfaces, or surface and zone air.

These correlations depend on "typical" rectangular or cubical closed building enclosure geometries. The choice of the heat transfer correlation for convection coefficients strongly affects the energy use and thermal comfort predictions of BES programs analyses [108, 106, 109]. Directly applying these available correlations over-simplifies

the estimation of internal surfaces' heat transfer behavior in naturally ventilated houses which are partially opened rather than completely sealed; and therefore applying these existing empirical relationships might lead the potential assessment with a high level of uncertainty.

Most of these correlations are expressed in terms of Nusselt number ( $Nu$ ) (Equation (4-2) [100] and Grashof number ( $Gr$ ) (Equation (4-3) [100] for respective heated surfaces as demonstrated [105].

$$Nu = \frac{h_c \cdot L_c}{k} \quad (4-2)$$

Where,  $Nu$  = Non-dimensional number representing CHTC

$L_c$  = Characteristic length [m]

$k$  = Thermal conductive of air obtained at the film air properties [W/m K]

$$Gr = \frac{g \cdot \beta \cdot \Delta T \cdot L_c^3}{\vartheta^2} \quad (4-3)$$

Where,  $Gr$  = Non-dimensional Grashof number representing natural convection heat transfer effect

$g$  = Gravitational acceleration [m/s<sup>2</sup>]

$\beta$  = Coefficient of thermal expansion [1/K]

$\vartheta$  = Viscosity of air [m<sup>2</sup>/s]

Similarly, some researchers express the average CHTC over a surface in the form of a non-dimensional empirical relationship of Nusselt ( $Nu$ ) and Raleigh number ( $Ra$ ) as demonstrated in the Equation (4-4) [100].

$$Nu = C \cdot Ra^n \quad (4-4)$$

Where,  $Ra$  = Non-dimensional Rayleigh number representing natural convection heat transfer process

$C$  = Constant representing the geometry of the surface

$n$  = Exponent representing flow regime approximately (laminar =  $\frac{1}{4}$  and turbulent =  $\frac{1}{3}$ )

In these works,  $Ra$  is recognised as a multiplication of  $Gr$  and Prandtl Number ( $Pr$ ) as in Equation (4-5).

$$Ra = Gr \cdot Pr \quad (4-5)$$

Where,  $Pr$  = Non-dimensional Prandtl number

Similarly, the Prandtl number ( $Pr$ ) is the ratio of momentum diffusivity ( $\nu$ ) to the thermal diffusivity ( $\alpha'$ ), as shown in Equation (4-6).

$$Pr = \frac{\nu}{\alpha'} \quad (4-6)$$

In this respect, Bilgen and Muftuoglu computationally examined the flow in an open, square cavity with multiple slots. They found that the  $Nu$  and the volume flow rate both increased with  $Ra$  and with the opening ratio [110]. Further studies by Prakash et al. have delivered an empirical relationship of heat transfer as a function of  $Ra$ , opening ratio and inclination for open cavities of different geometries [111]. Anderson and Norris [112, 113, 114] developed an empirical relationship in terms of  $Nu$ ,  $Ra$  and the opening ratio and for a threshold of  $1 \times 10^8 \leq Ra \leq 5 \times 10^8$  and characteristic length of 1 m; and recommended a further three-dimensional numerical study with a broader range of  $Ra$ .

Research conducted by Rincón-Casado et al. [107], mainly focusing on the application in building performance simulation software, resulted in separate correlations as a function of enclosure aspect ratio and a particular  $Ra$  number range for laminar and turbulent regimes for wall, ceiling and floor by performing numerical simulations.

Applying these correlations can improve predictions of convective heat transfer behaviour of indoor building surfaces in BES software, particularly in turbulent regimes.

Despite these numerous correlations available for modelling the convective heat transfer behaviour of internal surfaces of the building, this review was not able to find a suitable heat transfer correlation applicable to a buoyancy-driven naturally ventilated building. In particular, if the floor has been heated by solar radiation and is exposed to the external environment, none of these existing correlations can accurately determine the resulting convective heat transfer from the floor.

### 4.3 Methodology

To explicitly identify the influence of buoyancy-driven natural ventilation on the convective heat transfer behaviour at the floor, the research did not consider other influences like solar radiation, wind speed, 3D heat source etc., at this stage. This helps the resulting empirical relationship capture the impact of disturbances (buoyancy due to floor and outdoor temperature, WOF) on the convective heat transfer behaviour of the floor within the threshold of the selected boundary conditions. It is difficult to establish a rationalisation of the result if the research considers all the possible source of disturbances simultaneously. The study expects to build up the model increasing complexity step-by-step in future. In order to develop an understanding of how buoyancy affects the heat transfer from the floor of an open space, the velocity, temperature, and pressure fields of the partially opened room-like space must be determined. Thus this research work created a computational model of a three-dimensional air-filled room using a commercial finite-volume CFD solver (ANSYS Fluent V17.2). The research work further employs the Navier–Stokes equations, which describe the fluid motion for a given set of boundary conditions. These equations, along with the turbulence model and energy equation, are solved at each node of the mesh. The flow field was considered to be steady and the fluid incompressible. The Boussinesq approximation was employed, that is, the thermophysical properties of the fluid are assumed to be constant, with the exception of the density variation in the buoyancy term.

As shown in Figure 4-1, the dimensions of the room are  $L = 2.4$  m,  $W = 2.4$  m and  $H = 2.4$  m. The model's size represents the internal cavity dimension compared to the size of

the model presented in Chapter 4 that are external. The selected height of the enclosure represents a minimum standard full-scale floor-to-ceiling height of a typical residential house in Auckland [96]. The cubical shape represents a typical room geometry with a floor area ( $\sim 6 \text{ m}^2$ ) and meets the minimum floor area requirement ( $4.5 \text{ m}^2$ ) by legislation in NZ [97]. The selected size is relatively small compared to the standard room size of a residential building but expected to provide a sufficient full-scale representation of the enclosure model for assessing flow characteristics due to buoyancy-driven natural ventilation.

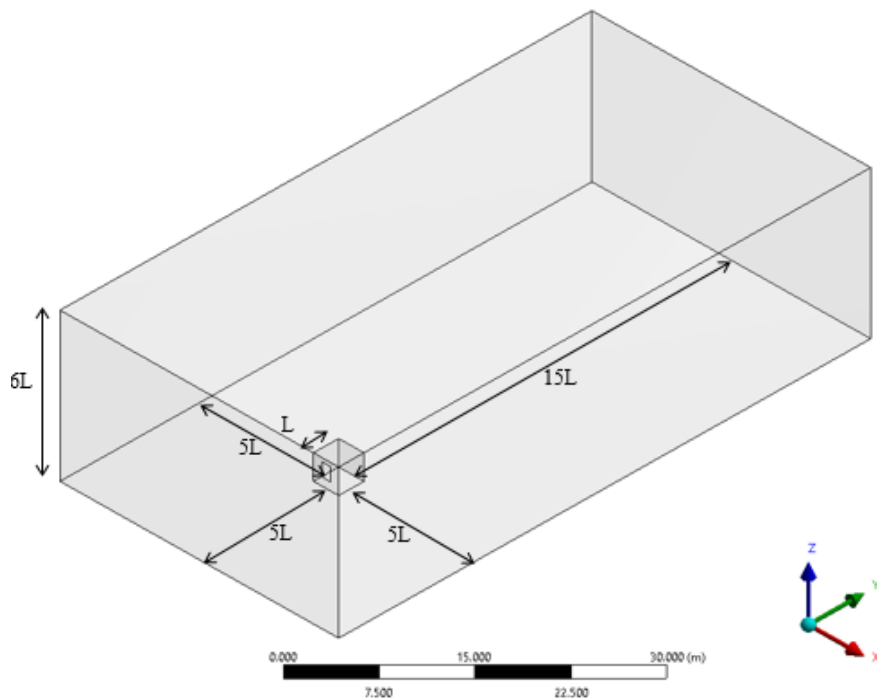


Figure 4-1. Schematic representation of the computational domain and model

A simulation domain with open boundaries (a distance of  $5L$  upstream of the external wall, as well as to the sides and top and  $15L$  downstream from the rear wall), encompass the room space. Assuming the floor to have a temperature of  $35^\circ\text{C}$  and other walls as adiabatic, the simulation work examines three ambient temperature conditions ( $10^\circ\text{C}$ ,  $15^\circ\text{C}$  and  $20^\circ\text{C}$ ) with characteristic length equal to the height of the cube ( $2.4 \text{ m}$ ). The floor and outdoor air temperature boundary condition produce a temperature difference of  $15^\circ\text{C}$  to  $25^\circ\text{C}$ . The assumption produces a buoyancy effect with  $Ra$  range as  $1.9 \times 10^{10} \leq Ra \leq 3.6 \times 10^{10}$ . The selection of the buoyancy range provides a simplified base to representing an analogy of a naturally ventilated single room with

underfloor heating or where the floor is heated by solar radiation. The upstream wall contains a single window ( $W' = 0.9$  m and  $H' = 1.5$  m) that is equivalent to the WOF value of 1. Other WOF values of 0.75, 0.5 and 0.25 help simulate the effect of reducing the opening area of the window. In order to account for the wide range of flow directions and convection regimes (natural, mixed, forced) that might appear inside the enclosure, the computational model applies a predominantly unstructured 3D tetrahedron mesh type. A numerical mesh sensitivity helps establish a grid-independent solution, with the discretising process resulting in  $\approx 4.1$  million control volumes in the computational domain.

In order to resolve the boundary layer close to the floor, the modelling work constructs several layers of inflating prismatic cells, as suggested by [115]. As such, the height of the first layer is 0.5 mm, and the remaining cells depend on a stretching factor of 1.1. This ensures that the average  $y^+$  value is significantly less than 1 ( $\approx 0.3$ ). This discretisation scheme with high aspect ratio cells near the wall helps to capture or resolve the strong transverse gradient of the solution within the boundary layer with less numerical diffusion. The scheme is also capable of modelling the buoyancy-driven flow in cavities with an internal heat source [116]. A mesh sensitivity study (Figure 4-2) ensures the results are as mesh independent as possible before finalising the number of control volumes. The discretisation work also provides grid distribution in the boundary layer with several layers in the laminar sublayer and buffer layer as described by [117].

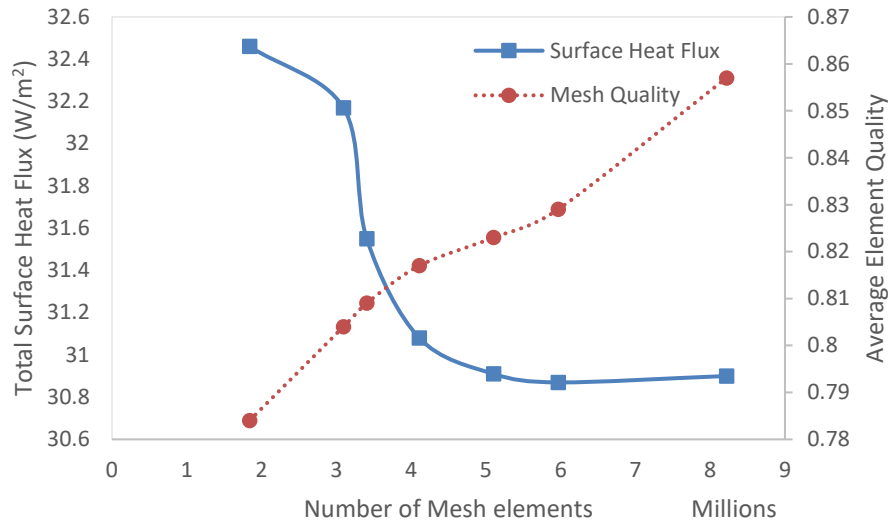


Figure 4-2. Mesh sensitivity study

The steady-state  $k - \omega$  Shear Stress Transitional (SST) with Low Reynolds Number viscous model, addresses the turbulence field. The Semi-Implicit Method for Pressure Linked Equations-Consistent (SIMPLEC) scheme resolves the coupling between pressure and velocity distribution. Spatial discretisation considers the Pressure Staggering Option (PRESTO) pressure scheme, and other variables employ a second-order linear upwind difference scheme. This process mirrors that of [118, 119], which illustrates that the  $k - \omega$  SST turbulence model is one of the most accurate models to capture the effect of natural convection heat transfer from an enclosure.

The convergence criterion ensures the reduction of all scaled solution residuals under a threshold of  $10^{-3}$  for all 12 cases. For all cases, the simulation work considers six different Isoplanes, as shown in Figure 4-3 to post-process the 3D behaviour of the flow fields inside the enclosure. While doing this, the isoplanes ( $x = 1.4$  m and  $y = 1.4$  m) refer to the mid-longitudinal and transverse section of the enclosure, respectively. Similarly, the simulation considers additional isoplanes at ( $x = 0.6$  m,  $y = 0.6$  m and  $y = 2.2$  m) to observe the specific flow fields close (0.4 m) to the vertical walls, as shown in Figure 4-3. The isoplanes ( $x = 1$  m), which is a longitudinal plane near to the window side edge help observe the flow fields on the cusp of the directly exposed and unexposed region of the opening. The front and side view of the enclosure, as shown in Figure 4-4, illustrates the position of the opening with WOF value of 1.

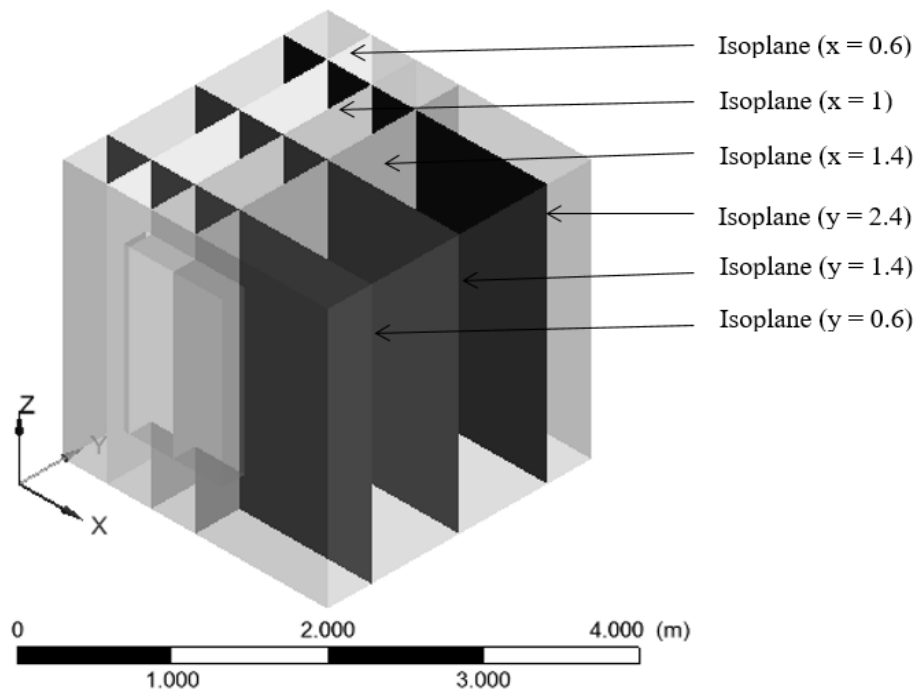


Figure 4-3. Isometric view of air filled enclosure

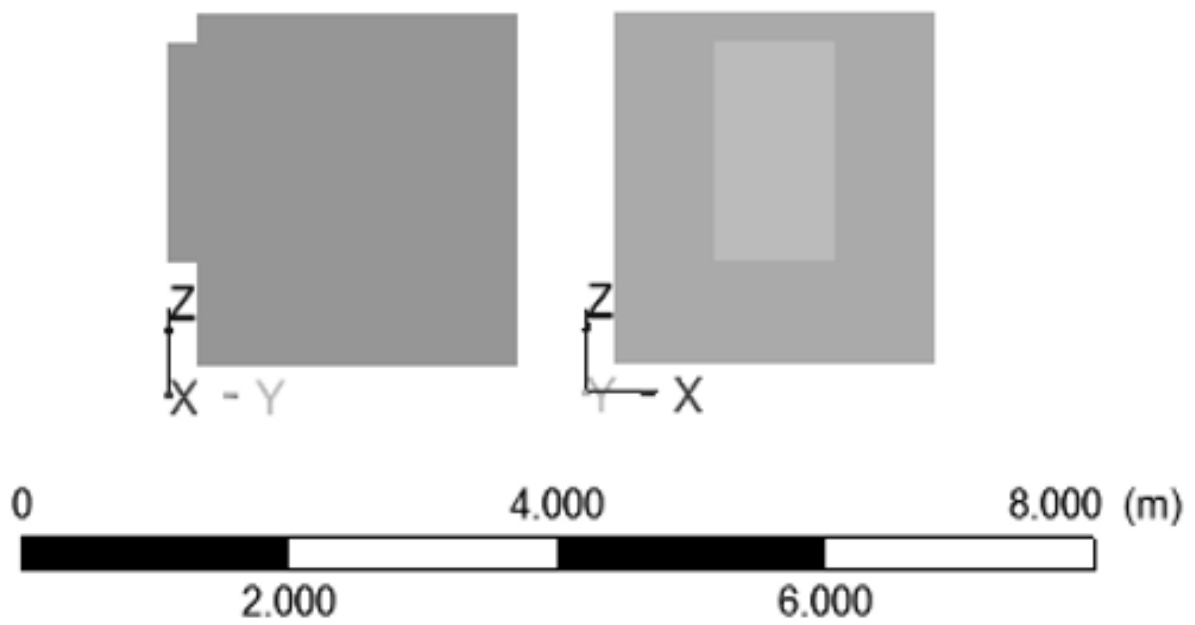


Figure 4-4. Front and side views of the enclosure

#### 4.4 Result and discussion

The examination of the flow on six isoplanes (defined in Figure 4-3) identifies that the flow behaviours are within the threshold of WOF values and  $Ra$  number considered. However, the intensity of them appears to vary in nature. As such, the investigation selects the case with WOF value of 1 and  $Ra$   $1.93 \times 10^{10}$  to demonstrate and define a typical three-dimensional flow field behaviour. While doing this, Figure 4-5 illustrates the velocity vector on the isoplanes ( $x = 1.4$  m).

It is evident from the distribution that flow on this plane is recirculating in nature due to the buoyancy effect. However, the lower part of the opening draws a significant fresh air plume from outside the enclosure to maintain continuity as air exits the room due to buoyancy. It contributes significantly to the turbulent flow on the floor adjacent to the window resulting in a higher velocity.

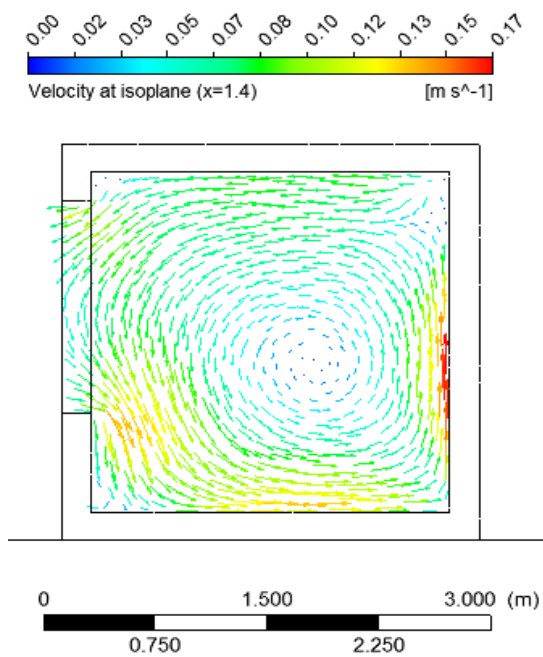


Figure 4-5. Velocity vectors  
[Isoplane  $x = 1.4$  m]

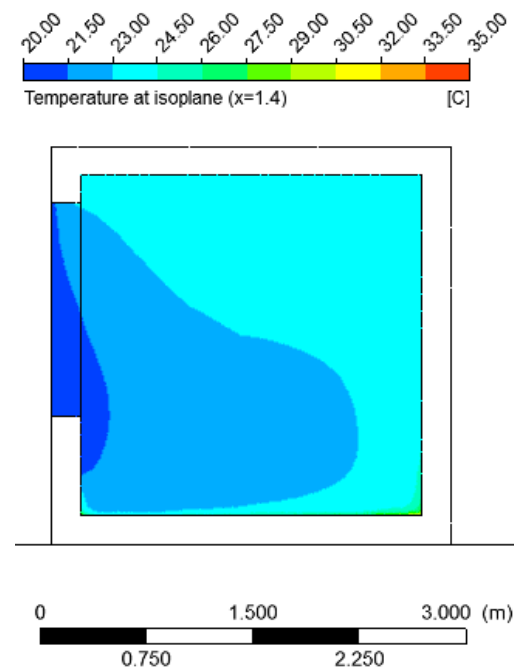


Figure 4-6. Air temperature contours  
[Isoplane  $x = 1.4$  m]

Figure 4-6 illustrates contours of the air temperature inside the cavity at the isoplane ( $x = 1.4$  m). The contours indicate an increasing level of temperature from the inlet opening (window) towards the opposite wall, and from the floor to the ceiling of the cavity.

This uneven distribution of velocity and temperature indicate that the resulting heat transfer from the floor at the intersection of the plane and floor surface is relatively non-uniform and weakening in nature as it moves away from the opening.

Furthermore, observing the velocity flow fields on isoplane ( $x = 1$  m) as shown in Figure 4-7, the recirculating nature due to the buoyancy effect has a similar distribution throughout the width of the opening. However, the tendency of the recirculation process covers the entire height of the enclosure as it moves away from the directly exposed opening interior space. A similar temperature distribution profile results in a weakening of the influence of the incoming air plume temperature, as demonstrated in Figure 4-8.

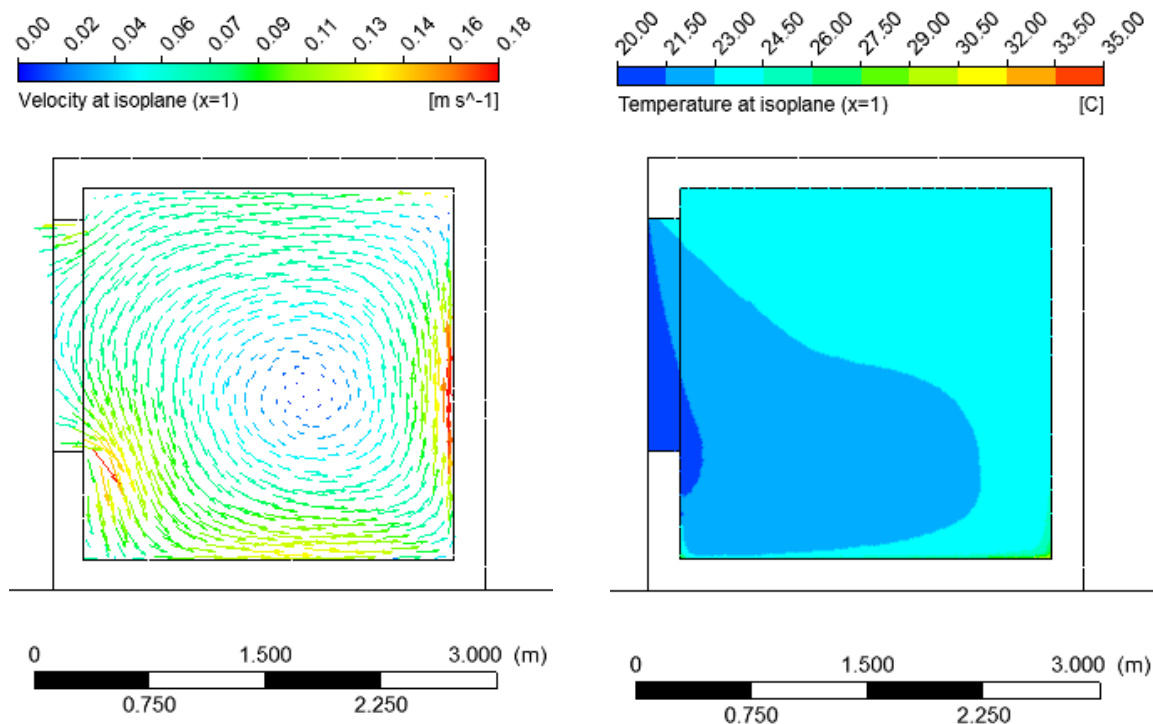


Figure 4-7. Velocity vectors  
[Isoplane  $x = 1$  m]

Figure 4-8. Air temperature contours  
[Isoplane  $x = 1$  m]

While scrutinising the velocity vector behaviour further away from the mid-plane and close to the sidewall (isoplane  $x = 0.6$  m), Figure 4-9 illustrates that the recirculation flow covers the entire height of the enclosure. However, the temperature distribution varies significantly and is limited to two regions in most of the enclosure, as shown in Figure 4-10.

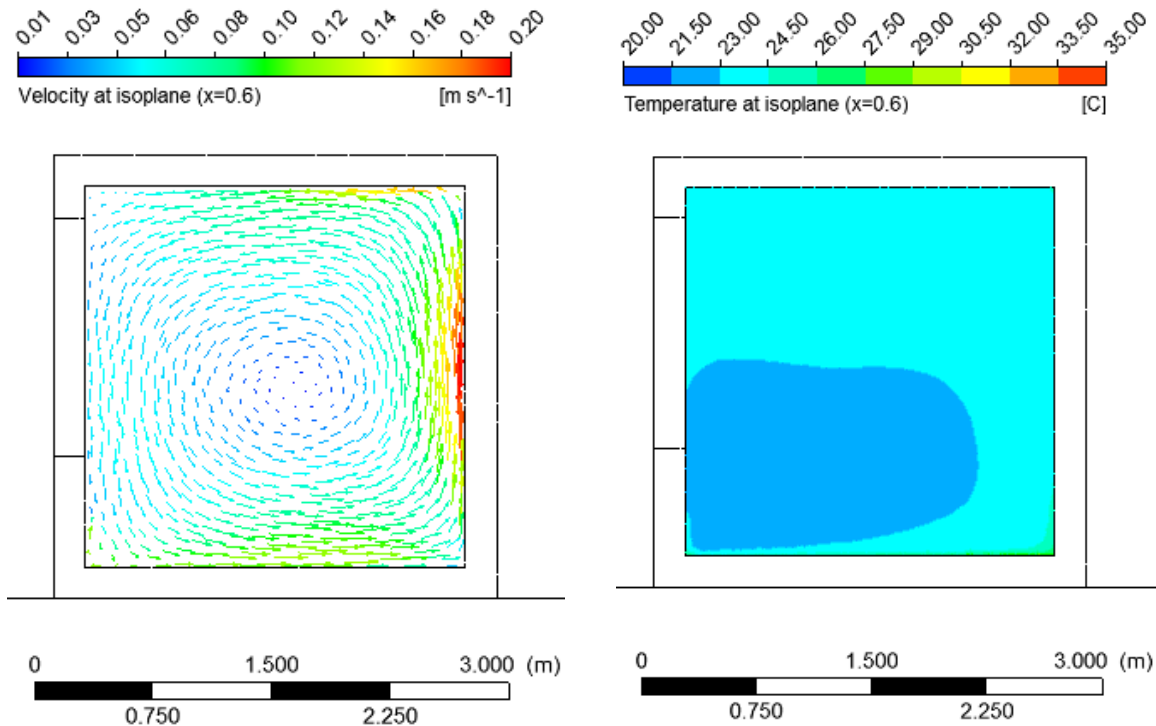


Figure 4-9. Velocity vectors  
[Isoplane  $x = 0.6$  m]

Figure 4-10. Air temperature contours  
[Isoplane  $x = 0.6$  m]

Examining the convection process further, Figure 4-11 and Figure 4-12 demonstrate the velocity flow field and temperature distribution contour on isoplane ( $y = 0.6$  m) representing the lateral distribution close to the wall next to the opening. Figure 4-11 illustrates that the incoming airflow from the opening initially draws from the bottom part towards the floor with a relatively higher velocity and splits into two regions creating small recirculation zones laterally on either side of the enclosure space not directly exposed to the opening. Similarly, Figure 4-12 shows the two zones of the temperature distribution, indicating the apparent influence of the outside air plume with relatively lower temperature.

Exploring this further, Figure 4-13 and Figure 4-14 demonstrate the flow fields on isoplane ( $y = 1.4$  m) representing the lateral distribution in the middle section of the enclosure. This corroborates that the intensity of the incoming flow decreases as the flow moves away from the opening, Figure 4-13 shows a similar trend of velocity vector as in Figure 4-11, however with weak intensity.

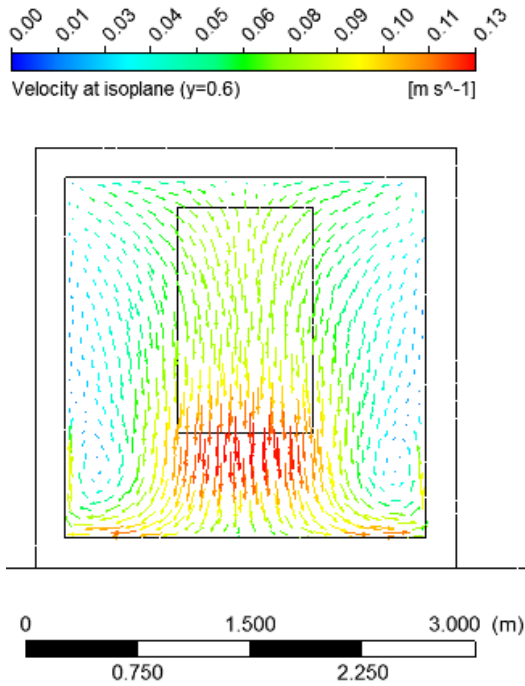


Figure 4-11. Velocity vectors  
[Isoplane y = 0.6 m]

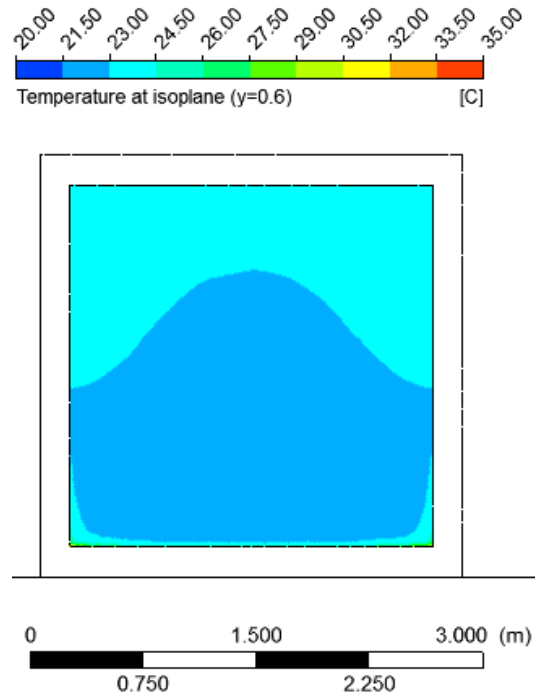


Figure 4-12. Air temperature contours  
[Isoplane y = 0.6 m]

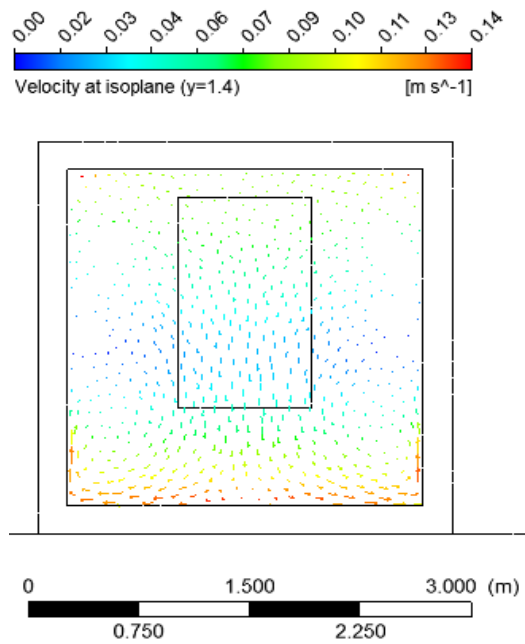


Figure 4-13. Velocity vectors  
[Isoplane y = 1.4 m]

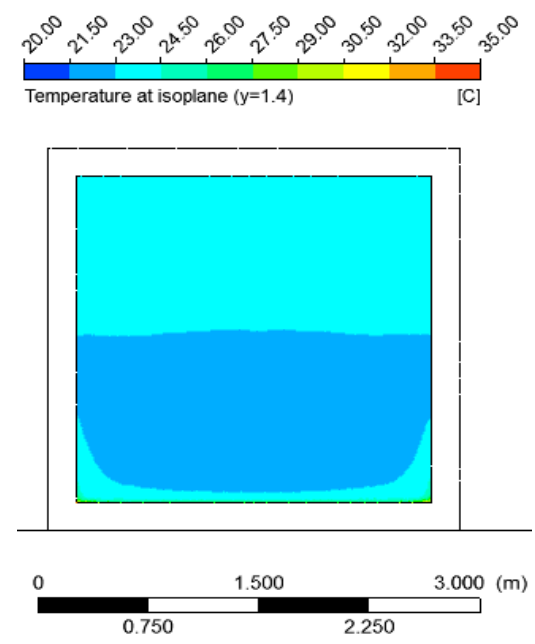


Figure 4-14. Air temperature contours  
[Isoplane y = 1.4 m]

Following the similar trend of decreasing intensity as it moves away from the wall with an opening, Figure 4-14 shows the temperature distribution with reduced influence from the outdoor air temperature leading to the presence of two-temperature zones.

Further examination, Figure 4-15 and Figure 4-16, demonstrates the flow fields on Isoplane ( $y = 2.2$  m) located farthest away from the wall with the opening. The velocity vectors observed on this plane indicates that the flow rises towards the roof from the floor and draws towards the top mid of the Isoplane location ultimately aligning to exit to the outside environment from the top section of the opening. Observing, Figure 4-16, it is evident that the temperature distribution is uniform on this plane, as the incoming cold air plume from the opening does not directly influence it.

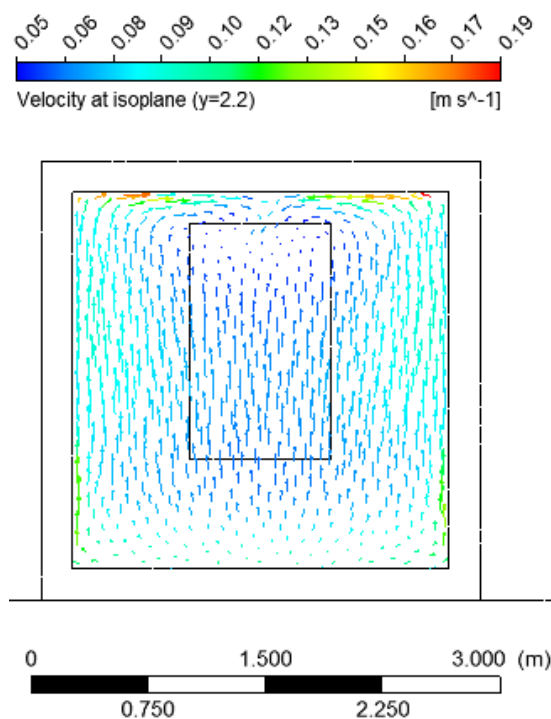


Figure 4-15. Velocity vectors  
[Isoplane  $y = 2.2$  m]

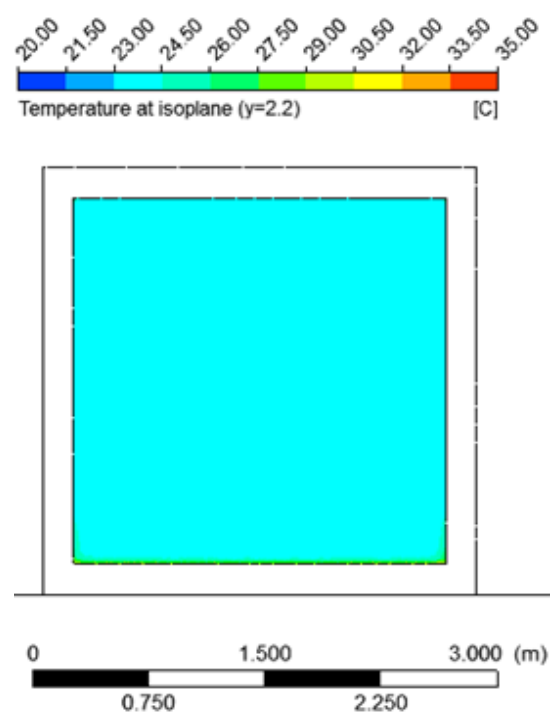


Figure 4-16. Air temperature contours  
[Isoplane  $y = 2.2$  m]

Figure 4-17 presents a very close observation of a typical temperature profile with a high resolution near to the floor at the middle of isoplane ( $x = 1.4$  m). A steep graduation of decreasing temperature profile prevails adjacent to (approximately within 50 mm height) of the floor. A wide variation of air temperature persists in the enclosure. The air temperature tends to be relatively higher in the regions above the opening top edge throughout the enclosure, and in the area adjacent to the opposite

vertical wall of the opening. The temperature of the air follows the path of the plume. The plume enters the enclosure through the bottom portion of the opening, and it recirculates within the enclosure before it exits. Similarly, there is a wide variation in the spatial distribution of air velocity (highest in the core where it strikes the floor and declining towards the lateral and longitudinal sides away from the centre) near the floor surface. These typical distribution patterns of velocity and temperature profile obtained for the assumed geometrical, and boundary conditions result in a distinctive spatial distribution of the heat flux at the floor of the enclosure as demonstrated in Figure 4-18.

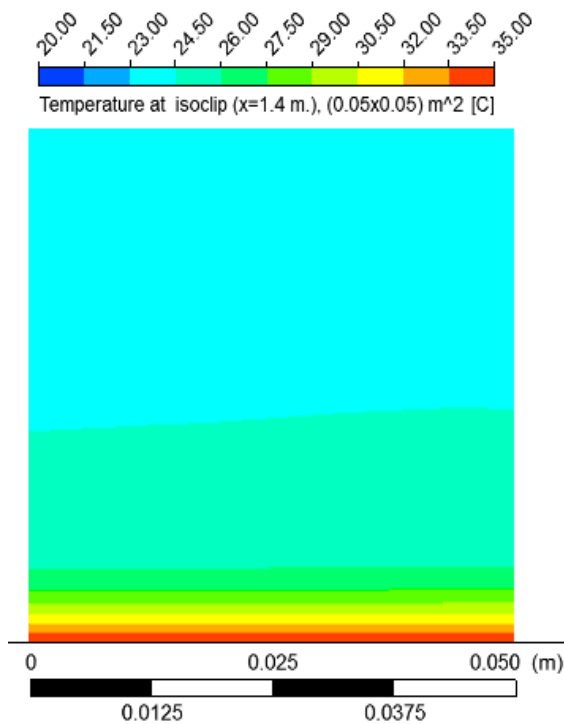


Figure 4-17. High-resolution temperature Contour (Isoplane  $x = 1.4$  m)

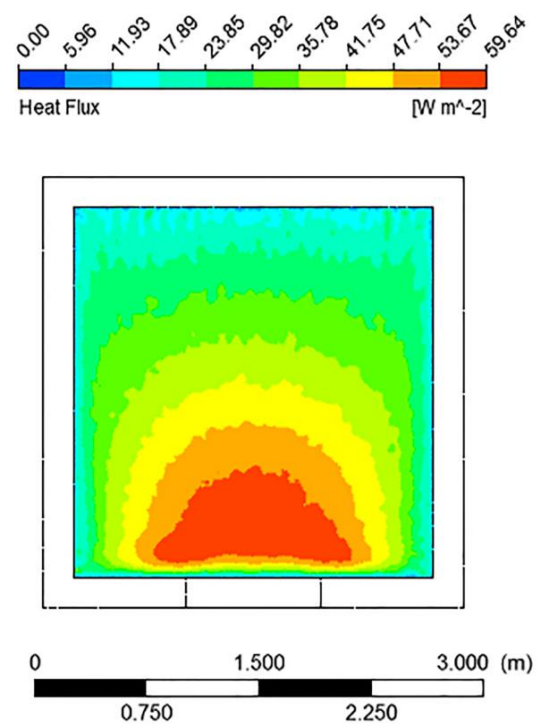


Figure 4-18. Spatial distribution of floor heat flux

The distribution pattern indicates that the heat flux decreases in both the lateral and longitudinal directions away from the initial strike core of the incoming air plume. It shows that as long as there exists a buoyancy effect due to a positive temperature difference between floor and the outside environment, this type of typical spatial distribution pattern of heat flux remains; however, the magnitude of heat flux varies relative to the extent of the buoyancy effect. Hence, if the window opening area changes, the flow fields inside the enclosure also change resulting in a deviation in the magnitude of the heat flux.

In summary, Table 4-1 presents the heat transfer behaviour of 12 different cases in terms of floor average  $Nu$  number and  $CHTC(s)$  due to different level of buoyancy forces. These differences in buoyancy forces are due to the relatively hot floor at 35°C compared to the outdoor ambient temperature conditions (10°C, 15°C and 20°C ) and considering the WOF values of (1, 0.75, 0.5 and 0.25) assumed within the threshold in the model. While doing this, the analysis considers the average air temperature between floor and ambient outside to define the air properties and reference temperature.

Table 4-1 Convective heat transfer behaviour of floor due to buoyancy-driven force

WOF	Temperature difference [K]	Rayleigh number ( $Ra$ )	Floor average Nusselt Number ( $Nu$ )	Floor average $CHTC$ ( $h_{c, floor}$ ) [ $W/m^2.K$ ]
1	15	1.9E+10	424	4.7
0.75	15	1.9E+10	402	4.5
0.5	15	1.9E+10	372	4.1
0.25	15	1.9E+10	319	3.5
1	20	2.7E+10	470	5.2
0.75	20	2.7E+10	450	5.0
0.5	20	2.7E+10	421	4.7
0.25	20	2.7E+10	369	4.1
1	25	3.6E+10	513	5.7
0.75	25	3.6E+10	493	5.5
0.5	25	3.6E+10	465	5.2
0.25	25	3.6E+10	433	4.8

Figure 4-19 demonstrates the results in terms of the floor average  $Nu$  number corresponding to different values of WOF and  $Ra$  number. Figure 4-19 illustrates the generic tendency of increased heat transfer potential at the heated floor (represented as higher  $Nu$  number) with relatively higher values of both WOF value and  $Ra$  number representing the somewhat higher magnitude of natural convection phenomena. There is a lower potential for heat transfer at the heated floor surface if the enclosure is exposed to minimum window opening area (minimum WOF) and  $Ra$  number.

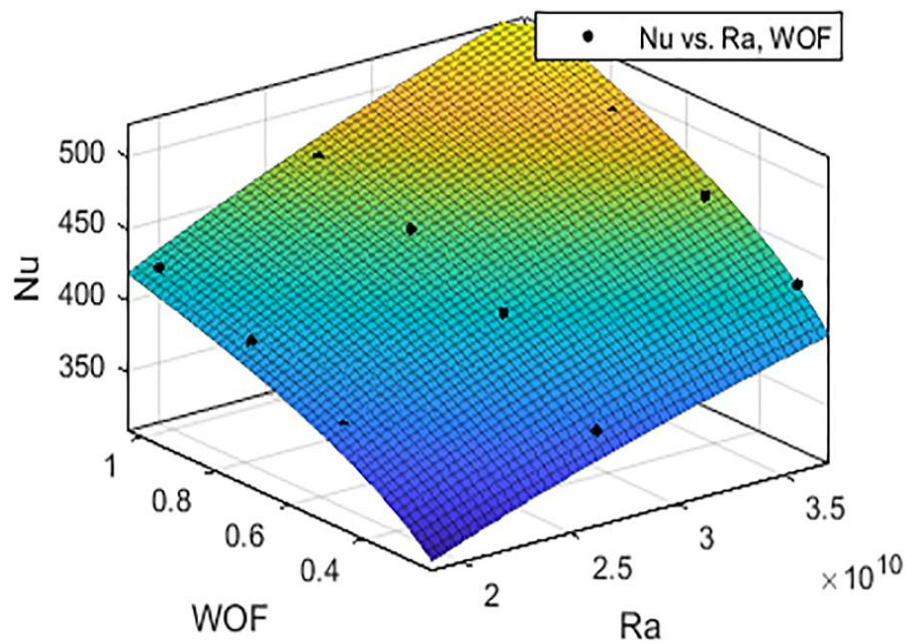


Figure 4-19. Average Nu with respect to WOF and Ra

Summarising these results in terms of a typical single-sided natural ventilated BES application such that for a room/building exposed to underfloor heating or solar radiation, the heat transfer rate at the floor might not remain constant throughout the simulation period. Instead, it varies with both the window opening area and the  $Ra$  number (temperature difference between outdoor air and floor surface considering other properties remains constant). Besides this, the performance of the underfloor heating system can also vary significantly concerning a relative exposure to natural ventilation in terms of WOF value and  $Ra$  number in particular or window opening area and outside temperature in general.

#### 4.5 Empirical relationship and the robustness of the result

It is apparent from the results that  $Nu$  increases with  $Ra$  and WOF. The correlation presented in terms of Equation (4-7) (coefficients with 95% confidence bounds) can generalise the convective heat transfer behaviour of the floor within the ambient temperature range ( $10^{\circ}\text{C}$ ,  $15^{\circ}\text{C}$  and  $20^{\circ}\text{C}$ ) and WOF values of (1, 0.75, 0.5 and 0.25) threshold assumed in the model.

$$Nu = 0.1593.Ra^{0.33}.WOF^{0.18} \quad (4-7)$$

Alternatively, in terms of the aspect ratio of the opening ( $d'/D'$ ) ( $d'$  is the opening height and  $D'$  is the overall enclosure height), the Equation (4-8) can also express the heat transfer behaviour of the floor.

$$Nu = 0.17.Ra^{0.33}.\left(\frac{d'}{D'}\right)^{0.18} \quad (4-8)$$

This expression is similar to the relationship developed by Anderson and Norris [112, 113, 114] for natural convection in a partly open cube in the form of Equation (4-9) for  $1 \times 10^8 \leq Ra \leq 5 \times 10^8$  and characteristic length of 1 m.

$$Nu = 0.12.Ra^{0.34}.\left(\frac{d'}{D'}\right)^{0.4} \quad (4-9)$$

A comparison of the respective constants and exponents in these two relationships demonstrates that the size of the geometry is an essential aspect of heat transfer behaviour. Further, the value of the exponent of the  $Ra$  number  $\approx 1/3$  suggests that a turbulent flow regime is dominant in both studies. This research also confirms that the flow fields are principally recirculating in nature in both of the works and that heat transfer at the floor of the single-sided naturally ventilated house varies significantly in a spatial context within the floor.

#### 4.6 Remarks

This work examines the variation of flow fields of a computational model of a single-sided partially opened 3D air-filled room. Corroborating the previous studies, the work demonstrates that the  $Ra$  and the  $WOF$  values strongly influence the heat transfer behaviour of a partly open room. There is also a significant variation in flow field in 3D space resulting in a non-uniform distribution of floor heat flux on spatial context. As such, there is a considerable scope for increasing the robustness of thermal models of naturally ventilated buildings by greater utilisation of empirical relationships developed specifically for this purpose. Furthermore, a substantial reduction on the uncertainty of estimating heat transfer seems possible by considering the localised distribution of the heat flux on the floor.

Nevertheless, a further improvement in the proposed correlation is necessary so as to include the effect of the varying enclosure length, width and different height. In addition to that, further research is essential to understand the impact on heat transfer behaviour due to external wind conditions, the transient temperature inside the space, thermal mass of the envelope, solar gains, internal heat loads and furnishings/flow restrictions in the interior spaces.

## Chapter 5 The influence of the wind conditions on the heat transfer behaviour of the floor

### 5.1 Introduction

Depending on the location of the window openings in a residential house, the natural ventilation phenomena can be classified as single-sided, adjacent sided or cross-ventilated. In a mild climatic zone, the rooms are often ventilated by a window on a single exterior wall. However, when a room is naturally ventilated with an opening on a single side, a bi-directional airflow prevails, and the “pulsation” and “penetration of eddies” due to the wind are also major driving mechanism of the ventilation [120]. The airflow mechanism is complicated due to the turbulence created at the opening [121] and it also involves buoyancy-driven forces. Similarly, the fluctuating nature of the associated driving forces and the resultant airflow movement, combined with different geometric dimensions and window configurations, makes assessment and prediction of natural ventilation complex [42]. Furthermore, the wind can reinforce or restrict the buoyancy-driven natural ventilation [27], resulting in difficulty in accurately predicting the potential for natural ventilation and its effect on the heat transfer from surfaces within the space.

In this respect, researchers conducted a series of studies [113, 114, 122] including the work discussed in Chapter 4 of this thesis considering buoyancy-driven flows in partially open cubical cavities. Their work indicates that the buoyancy-induced flow fields inside the enclosure are principally recirculating in nature with a dominant turbulent flow regime. The work also confirms that the heat transfer behaviour varies significantly across the floor spectrum. This led to the development of an empirical relationship for expressing convective heat transfer behaviour of a partly opened room as a function of  $Ra$  and WOF. This research demonstrates that the convective heat transfer behaviour of a hot floor in a partially opened enclosure can have significantly different characteristics than for the sealed enclosure. Although these research works indicate that the size of an opening and buoyancy influences the convective heat transfer from the floor of a partly open enclosure, in reality, a naturally ventilated building is subject to several external conditions: perhaps most importantly, the wind.

A typical building can be exposed to air movement from ventilation systems, wind or draughts, resulting in the existence of forced or mixed convection heat transfer regimes inside the enclosure. In order to predict the airflow through opening(s) and evaluate the thermal behaviour of a naturally ventilated house, BES programs require modelling of convective heat transfer from surfaces within the natural ventilated space. However, there is a significant challenge in identifying the value of the CHTC, because it is influenced by various factors: the flow regime, the properties of the fluid, and the geometry of the specific system under consideration.

Researchers [123, 124, 125, 126, 127] contributed several correlations to describe forced and mixed convection. Furthermore, Beausoleil-Morrison [128, 129] developed an adaptive convection algorithm to manage the selection of different convection correlations as appropriate for a given surface at a given time. Despite these numerous correlations available for modelling the forced and mixed convective heat transfer behaviour of internal surfaces of a building, it is difficult to determine a suitable heat transfer correlation applicable to a naturally ventilated building (analogous to a single room with underfloor heating, or where the floor has been heated by solar radiation) and exposed to the external environment.

The consequence of these effects on indoor flow-fields, and particularly convective heat transfer on the floor, needs further examination. To understand the influence of wind conditions, this research work further examines the flow in, and heat transfer from the floor of, a single-sided partly open air-filled cubical enclosure considering both wind and buoyancy forces. In particular, this chapter presents the influence of outdoor wind conditions (different wind speed and direction) on the flow fields and convective heat transfer behaviour of the floor of a naturally ventilated building. This research aims to further contribute to improving the relationships used to estimate the convective heat transfer from the floor of naturally ventilated buildings.

## **5.2 Methodology**

In order to develop an understanding of how wind affects the heat transfer from the floor of a single-side ventilated enclosure, the research work uses the same

computational physical geometric model of a three-dimensional air-filled room in a commercial finite-volume CFD solver (ANSYS Fluent V17.2). The Navier-Stokes equations along with the turbulence model and energy equation are solved at each node of the mesh. The fluid is incompressible and the Boussinesq approximation was employed. However, the flow field is considered transient.

As shown in Figure 5-1, the dimensions of the room are  $L = 2.4$  m,  $W = 2.4$  m and  $H = 2.4$  m. A simulation domain with open boundaries (a distance of  $5L$  upstream of the external wall, as well as to the sides and top and  $15L$  downstream from the rear wall), encompass the room space. The simulation work considers the floor at a temperature of  $35^{\circ}\text{C}$ , and the ambient temperature at  $20^{\circ}\text{C}$ . Besides, the simulation work assumes all other walls as adiabatic to limit the influences of other variables.

For this study, the computational model considers a single window ( $W' = 0.9$  m and  $H' = 1.5$  m) in the upstream wall; however, the simulations assume a WOF value of 0.5. The work considers discrete wind speeds of 0, 2, 4, 6 and 8 m/s at a reference height of 10 m. The limit of 8 m/s applied for this research sufficiently covers the average median annual average wind speed for NZ based on the 30-year average. [130].

The wind impinges at an angle of attack (the angle between the wind direction and a line normal to the window opening) of  $0^{\circ}$  (i.e. wind impinging normal to the opening) to create an atmospheric boundary layer based on a power-law profile, with an exponent value of 0.218 (for rough terrain).

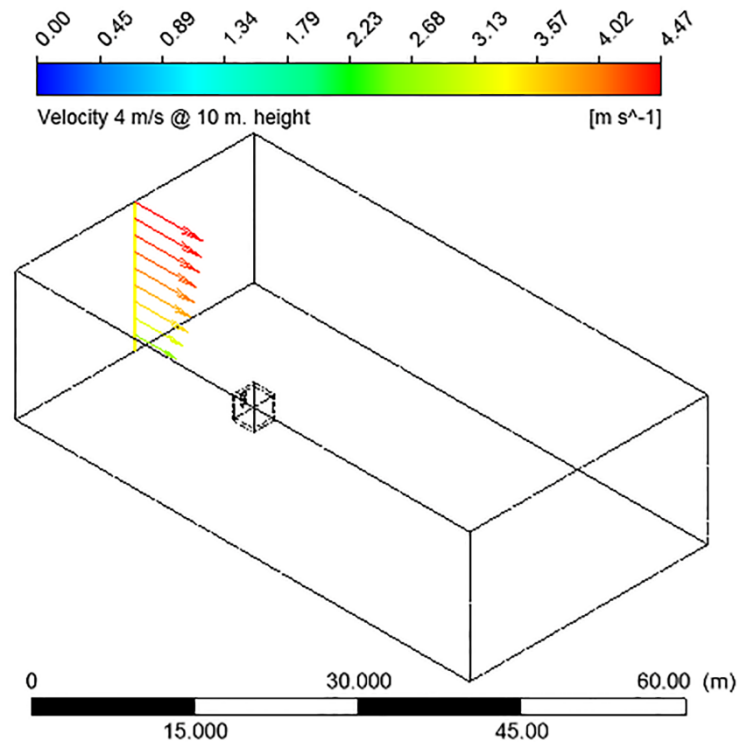


Figure 5-1. Schematic representation of the computational domain and model

In order to assess the effect of wind direction on the flow field, and the heat transfer from the floor due to the window, the computational model, is rotated at intervals of  $30^\circ$  from  $0^\circ$  to  $180^\circ$  (wind impinging on the leeward side of the building) for a wind speed of 4 m/s at the reference height. To illustrate this point, Figure 5-1 shows the 3D simulation domain with an atmospheric boundary layer with a wind speed of 4 m/s at the reference height and a wind direction of  $0^\circ$ .

Similar to the meshing structure presented in Chapter 4, the modelling work utilises a predominantly unstructured 3D tetrahedron mesh type model resulting in approximately 1.8 million control volumes in the computational domain. In addition, the boundary layer close to the floor was resolved with the same discretisation scheme to ensure the average  $y^+$  value significantly less than 1 ( $\approx 0.3$ ).

The transient  $k - \omega SST$  with Low Reynolds Number viscous model, addresses the turbulence field. The SIMPLEC scheme resolves the coupling between pressure and velocity distribution. Spatial discretisation considers the PRESTO pressure scheme, and other variables employ a second-order linear upwind difference scheme. This process mirrors that of [118, 119], which illustrates that the  $k - \omega SST$  turbulence model is one

of the most accurate models to capture not only the effect of natural and forced convection heat transfer at the surface exposed to different wind flow conditions.

A sensitivity study helps determine an appropriate time step value (0.01 second), and Figure 5-2 shows the time-averaged transient solution for 10 seconds.

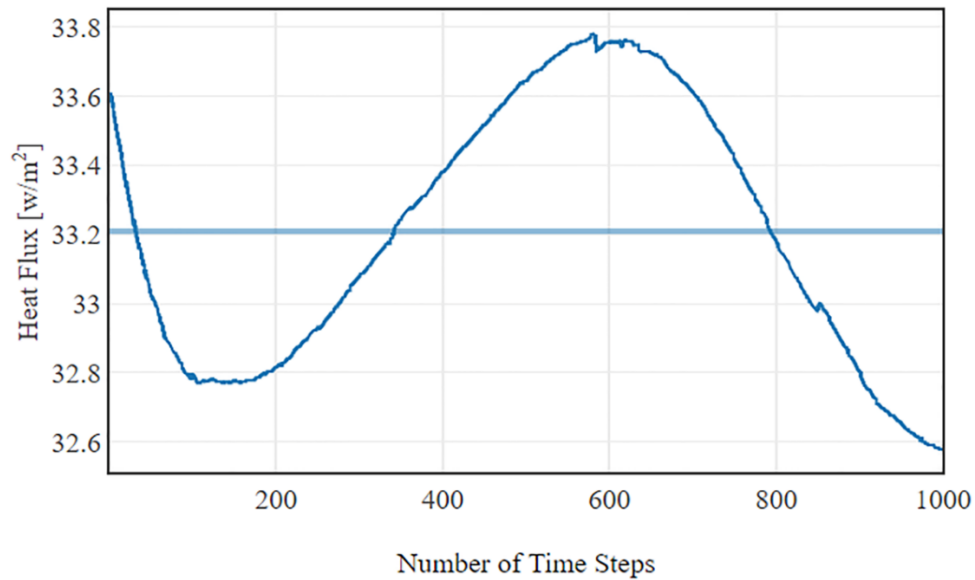


Figure 5-2. An example of the time-averaged estimation of the floor heat flux (wind speed 4m/s at 120°)

The convergence criterion ensures the reduction of all scaled solution residuals under a threshold of  $10^{-3}$  for all time steps and cases. For all cases, the simulation work considers mid-plane ( $x = 1.4$  m), as shown in Figure 5-3 to post-processes the 3D behaviour of the flow fields inside the enclosure.

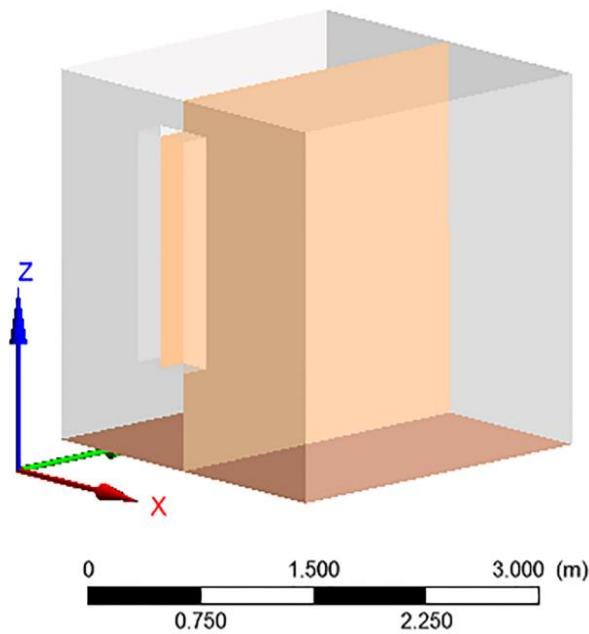


Figure 5-3. Schematic representation of the 3D air space and the mid-Isoplane ( $x = 1.4$  m)

### 5.3 Model Validation

In order to validate the model, a wind speed of 4 m/s at a reference height of 10 m and an angle of attack of  $0^\circ$ , help creates an atmospheric boundary layer profile as described previously. The research undertakes simulations with similarly defined conditions (but without the window open) to determine the localised and surface averaged pressure coefficients ( $C_p$ ) on the external surfaces of the enclosure. The rotation of the computational model between  $0^\circ$  to  $90^\circ$  at intervals of  $30^\circ$  determines the effect of varying wind direction on  $C_p$ . The surface averaged  $C_p$  values of the unventilated enclosure is then compared with the surface averaged  $C_p$  values of [49, 50, 47].

Figure 5-4 shows the variation of the computed surface averaged  $C_p$  values with respect to the wind direction and shows that the computational model is capable of quantitatively capturing the aerodynamic behaviour of a closed enclosure. The results demonstrate that the surface averaged values of  $C_p$  lie well within the possible positive and negative extremes of  $C_p$  determined by [49] for wind on a low-rise building.

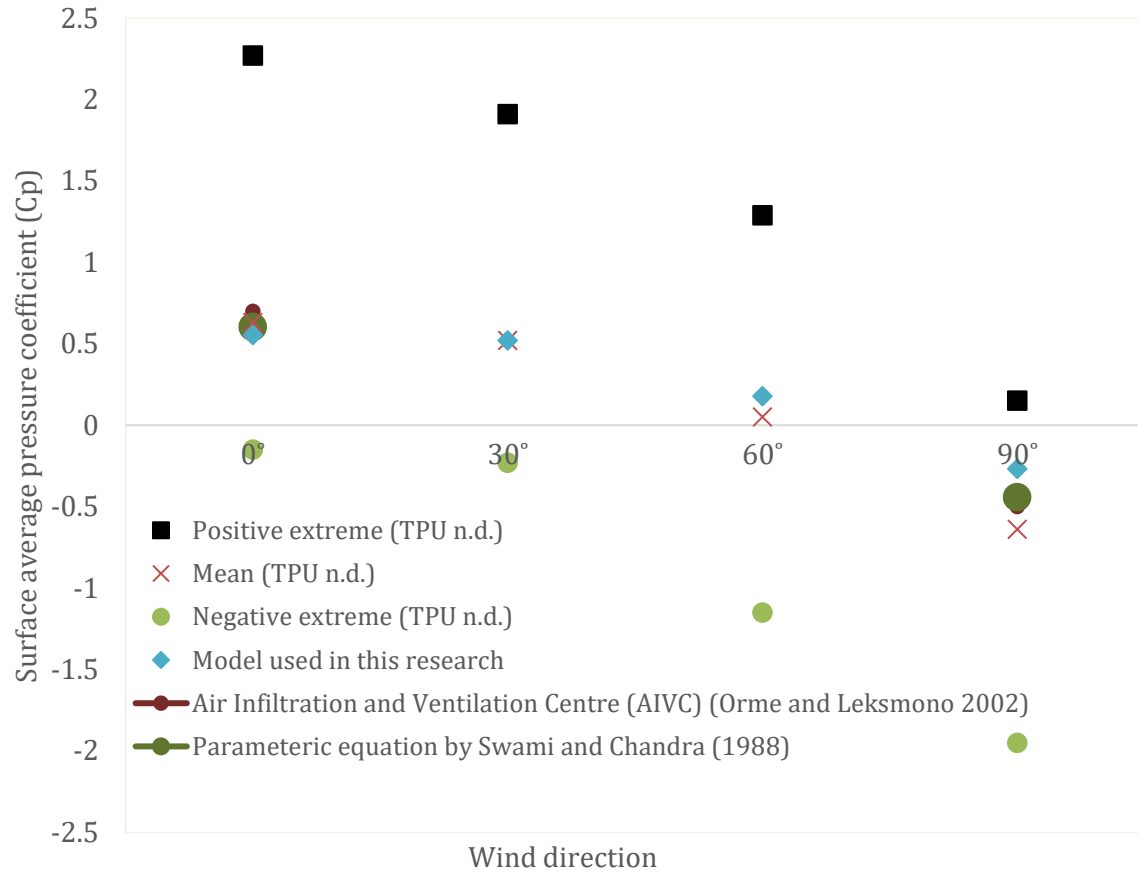


Figure 5-4. Surface averaged pressure coefficient with respect to wind direction

Figure 5-5 illustrates the localised  $C_p$  contours for the face exposed to the wind. It compares qualitatively and quantitatively with the contours experimentally produced by [49], as shown in Figure 5-6. The similarity of these results confirms the robustness of the computational modelling technique.

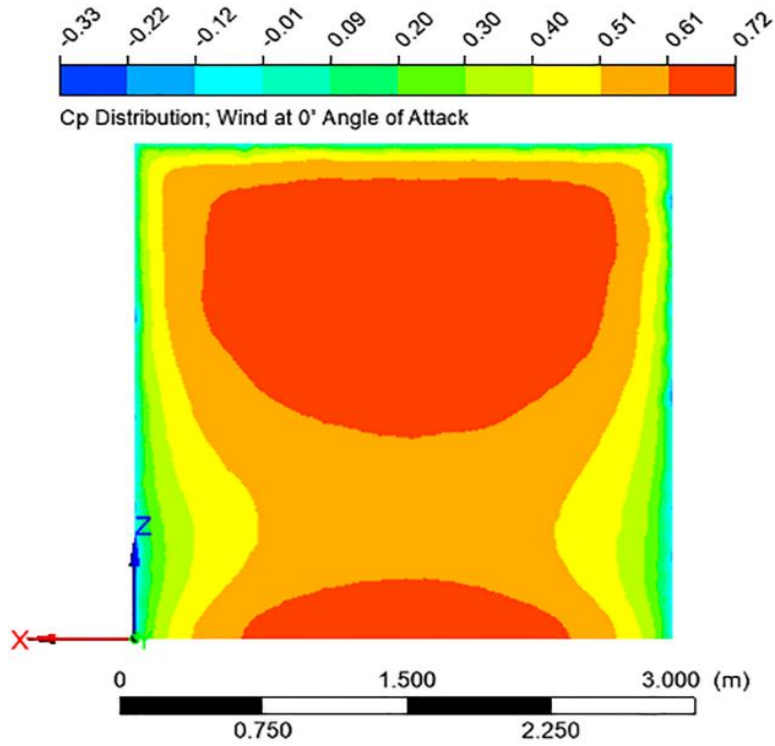


Figure 5-5. Localised pressure coefficient distribution on a closed enclosure [face orthogonal to upstream wind at  $0^\circ$  angle of attack]

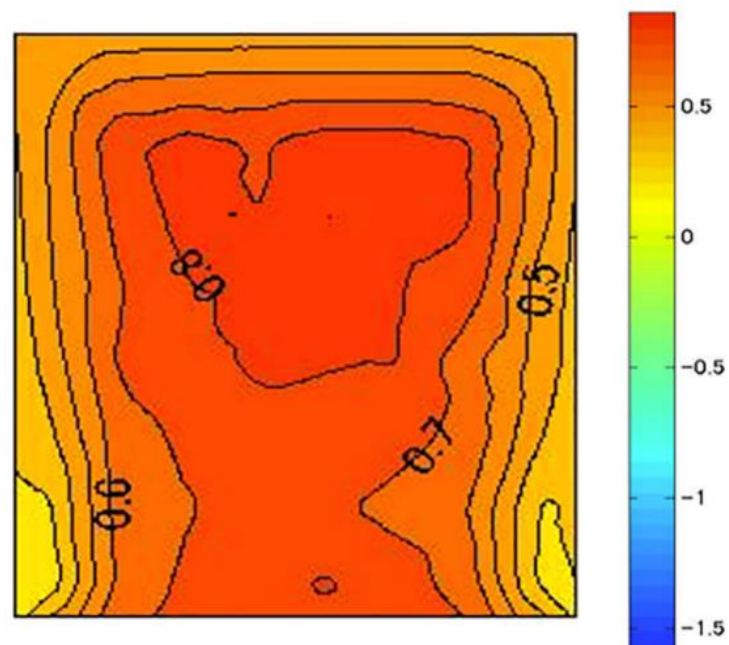


Figure 5-6. Localised pressure coefficient distribution on a closed enclosure (face orthogonal to upstream wind at  $0^\circ$  angle of attack) (Adapted from TPU (n. d.))

## 5.4 Results and Discussion

Having validated the computational model, it was decided to explore the effect of the opening on the heat transfer from the floor of the enclosure. By examining the flow fields of the 3D space on the mid-plane ( $x = 1.4$  m), the effect of wind speeds from 0 to 8 m/s at intervals of 2 m/s, with an angle of attack of  $0^\circ$ , can be analysed.

As a baseline for comparison, Figure 5-7 shows the recirculating nature of the velocity flow field generated at the mid plane of the room for the no-wind (0 m/s) condition. This clearly illustrates the buoyancy effect, whereby a fresh air plume is drawn into the lower part of the room from outside the enclosure to maintain continuity as air exits the room. This contributes significantly to the turbulent nature of the flow impinging on the floor adjacent to the window.

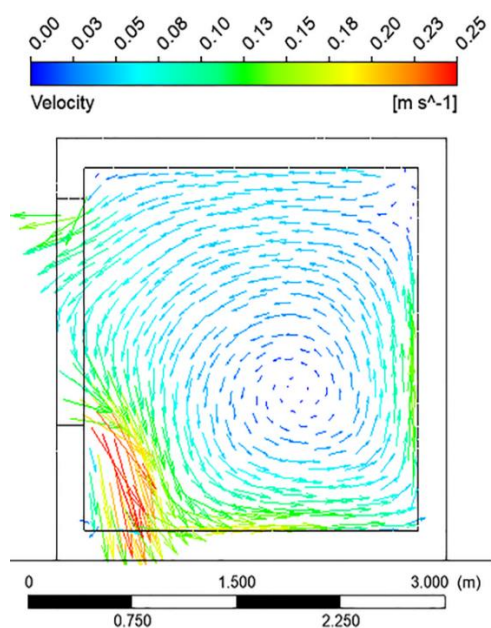


Figure 5-7. Velocity vectors  
[Isoplane  $x = 1.4$  m & no wind]

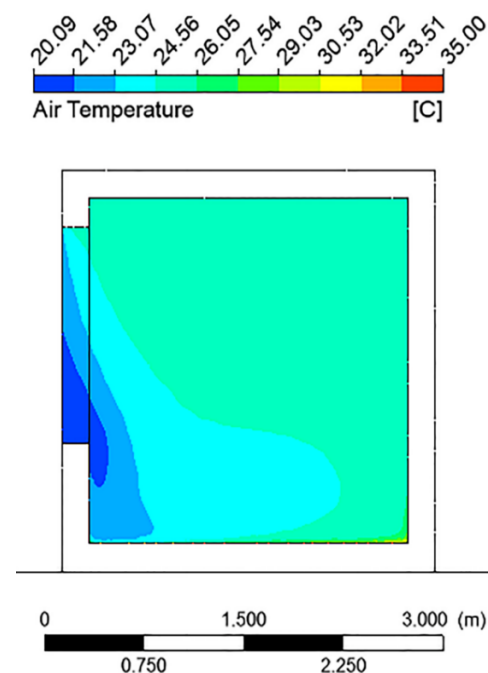


Figure 5-8. Air temperature contours  
[Isoplane  $x = 1.4$  m & no wind]

Similarly, examining the air temperature profile on the same plane, Figure 5-8 indicates there is an increase in temperature from the opening toward the opposite wall and from the floor to the ceiling of the enclosure. The uneven velocity and temperature

distributions indicate that the resulting heat transfer from the floor would be weak and non-uniform. Chapter 4 (Figure 4-5 and Figure 4-6) and the publication [122] demonstrated this in detail for a larger opening area, equivalent to a WOF 1.

Developing this further in Figure 5-9, with a wind speed of 4 m/s at angle of attack  $0^\circ$  and the reference height of 10 m, the recirculating indoor flow field appears to be 'squeezed'. This is due to the wind force acting on the top portion of the opening, countering the buoyancy-driven flow in the lower part of the enclosure. This increased penetration of the wind into space strengthens the mixing within the enclosure, resulting in an increased velocity near the floor compared to the case with no wind.

Moreover, Figure 5-10 shows the effect of the wind on the temperature distribution in the enclosure, principally that cold outside air has penetrated quite far into the enclosure. The net effect of this is a lowering of the bulk temperature of the air and an increase in the temperature difference between the floor and the surrounding fluid. Though these phenomena support a move towards increased convective heat transfer from the floor, the wind force is unable to completely disrupt the buoyancy-driven flow.

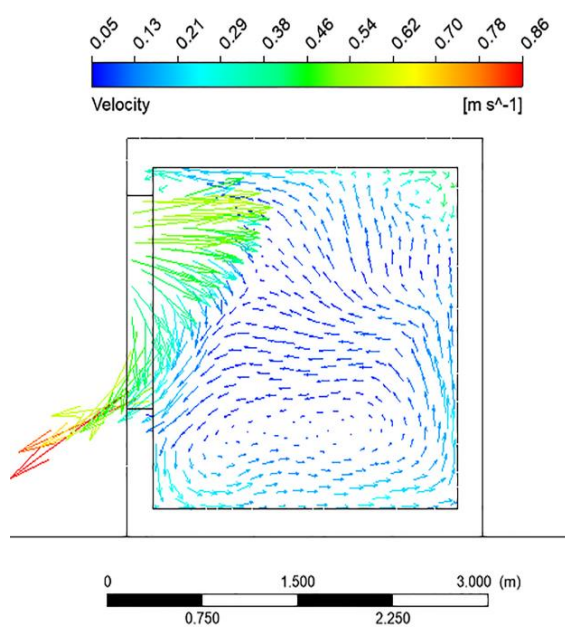


Figure 5-9. Velocity vectors  
[Isoplane  $x = 1.4$  m, wind speed = 4 m/s]

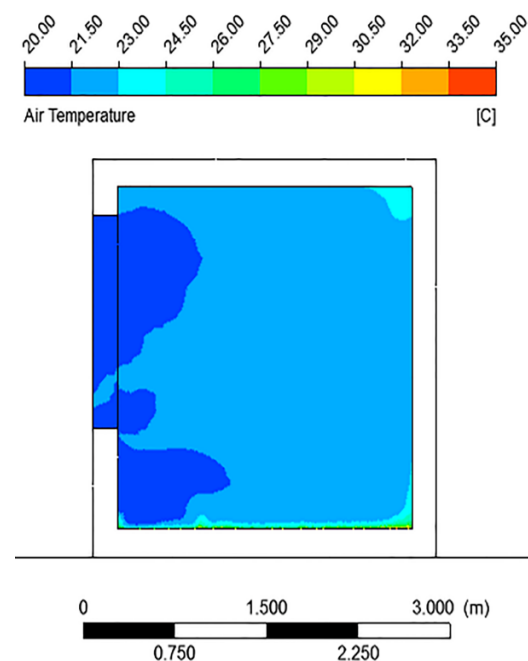


Figure 5-10. Air temperature contours  
[Isoplane  $x = 1.4$  m, wind speed = 4 m/s]

Finally, in Figures 5-11 and 5-12, with a wind speed 8 m/s at the reference height, there is a noticeable disruption of the flow in the room. Figure 5-11 shows that the increased wind speed reverses the direction of the flow field, indicating a dominant wind-driven force throughout the space. Similarly, Figure 5-12 shows that the entire space is filled with air close to the outside temperature. This reduction in the bulk air temperature in the enclosure ultimately increases the temperature difference between the air and the floor, which leads to an increased level of heat transfer from the floor.

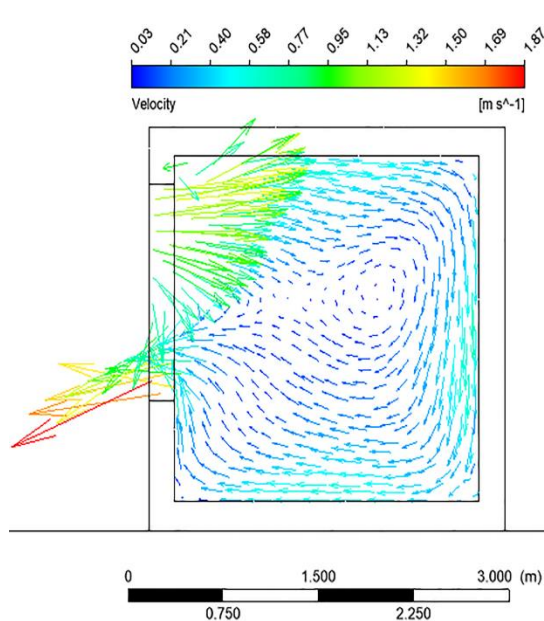


Figure 5-11. Velocity vectors  
[Isoplane  $x = 1.4$  m, wind speed = 8 m/s]

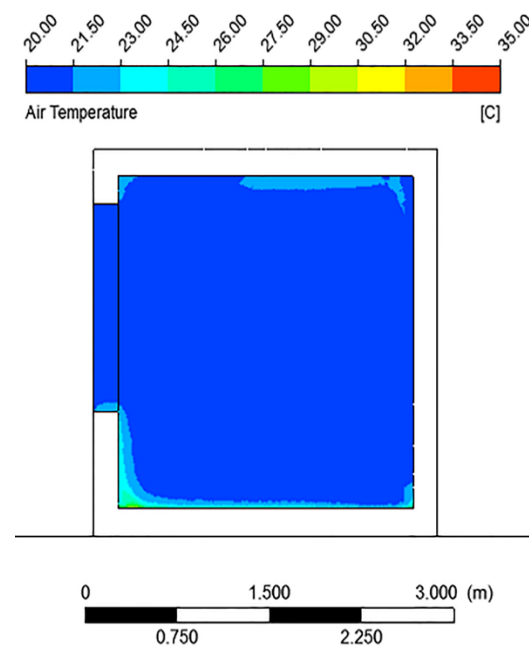


Figure 5-12. Air temperature contours  
[Isoplane  $x = 1.4$  m, wind speed = 8 m/s]

To illustrate this point, Table 5-1 summarises the impact of different wind speeds on average heat flux and the respective  $Nu$  number on the floor.

Table 5-1 Effect of wind speed on heat transfer behaviour from the floor

Wind velocity at 10-metre reference height [m/s]	Floor average heat flux [W/m <sup>2</sup> ]	Floor average Nusselt number ( $Nu$ )
0	32.4	388
2	34.2	410
4	37	444
6	46	551
8	57	682

Plotting the results, Figure 5-13 illustrates the effect of wind speed on the average  $Nu$  number on the floor. The increase in the average  $Nu$  number and heat transfer coefficient at the floor is relatively small if buoyancy is the dominant driving force. However, this value increases when forced convection (i.e. the wind) begins to dominate. In this case, the transition in the rate of heat transfer behaviour appears to be between wind speeds of 3 and 4 m/s, at the 10 m reference height. Beyond these speeds, the rate of increase of the average  $Nu$  number at the floor indicates that the wind has become the dominant driving force for the heat transfer.

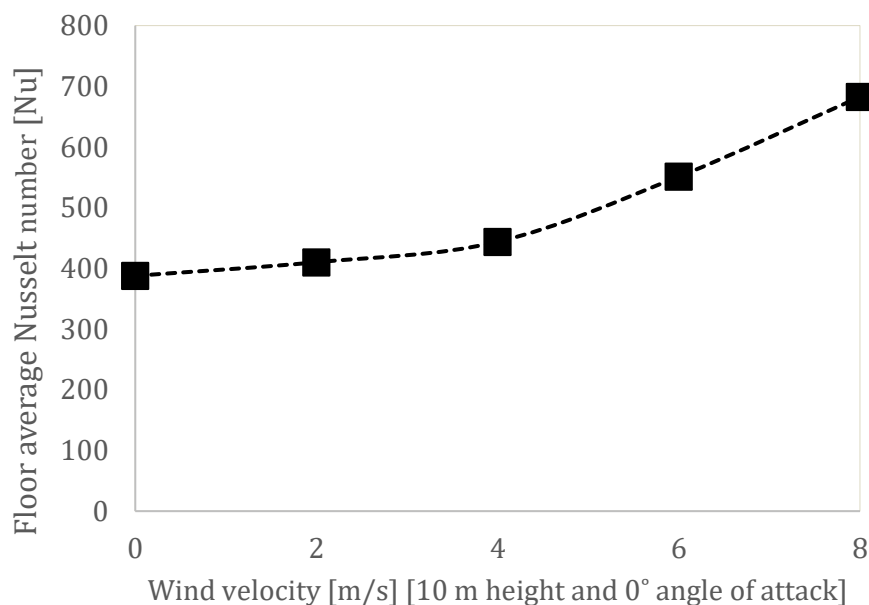


Figure 5-13. Effect of external wind speed on the floor's average  $Nu$  number [Wind condition at reference height of 10 m and angle of attack 0°]

Since the wind can approach the single-sided opening of the building from any direction, the influence of the wind angle of attack on the flow fields and the floor heat transfer is examined. Six different cases with varying angles of attack are analysed at intervals of  $30^\circ$  with a wind speed of 4 m/s (at the 10 m reference height).

By examining the flow fields of the enclosure on the mid-plane ( $x = 1.4$  m), it is apparent that varying the wind direction greatly influences the indoor flow field and floor heat transfer behaviour. For example, Figure 5-14 shows the influence of a leeward opening (an angle of attack of  $180^\circ$ ), and from this it can be seen that the flow field does not get 'squeezed' like the windward opening presented in Figure 5-9. Consequently, the flow inside the space behaves more like the natural convection flow seen in Figure 5-7 and Figure 5-8. By comparing Figure 5-14 and Figure 5-9, it can also be seen that the velocity of the flow near the floor is  $\approx 0.18$  m/s in the leeward case compared to  $\approx 0.30$  m/s for the windward case, again suggesting lower convective heat transfer. This low velocity in the enclosure is due to the window residing in the wake of the enclosure, meaning that it is not subject to the flow apparent in a windward facing opening. The results also show that the temperature inside the enclosure is higher ( $\approx 23$ - $24^\circ\text{C}$ ) in the leeward case (Figure 5-15) than the corresponding windward case ( $\approx 20$ - $21^\circ\text{C}$ ) (Figure 5-10). From this, it is apparent that the convective heat transfer from the floor is lower in the leeward facing window scenario than for the windward case.

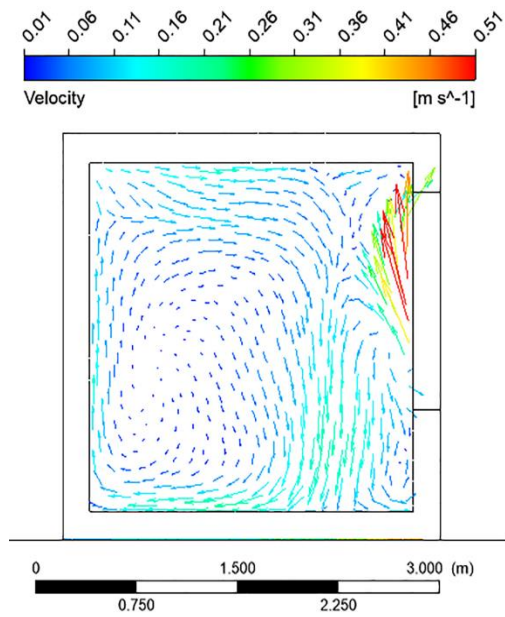


Figure 5-14. Velocity vectors [Wind speed = 4 m/s, angle of attack = 180°]

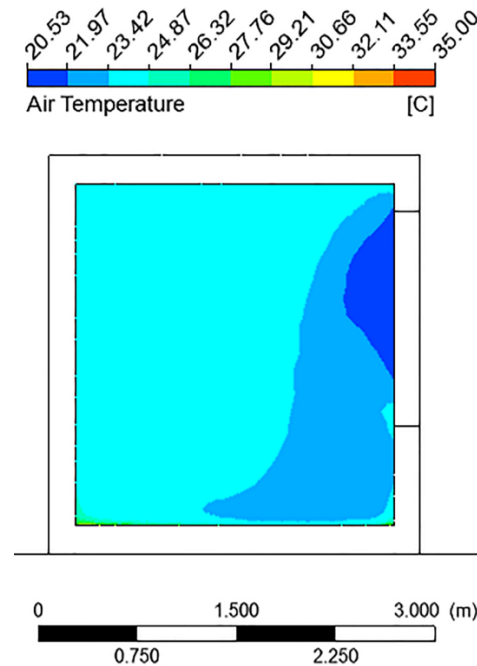


Figure 5-15. Air temperature [Wind speed = 4 m/s, angle of attack = 180°]

Supporting this assertion, an examination of the  $Nu$  numbers (Figure 5-16) indicates that the convective heat transfer from the floor is at a maximum if the angle of attack is 0°, and it gradually decreases to a minimum value for an angle of attack 90°. This might be due to the flow and the smaller temperature differences in the enclosure between the floor and the air as the angle of attack is changed from 0° to 90°. Alternatively, it might be due to the crosswind preventing air from exiting the room at 90°, thus suppressing the convective heat loss (as was observed for an open enclosure subject to wind [118]).

In contrast to this observation, for angles of attack between 120° and 180°, there is little variation in the  $Nu$  number. This suggests that the heat transfer for these angles is governed mainly by the buoyancy-driven flow. This assertion corresponds to the recirculating nature of the flow field observed inside the enclosure, for the leeward facing condition.

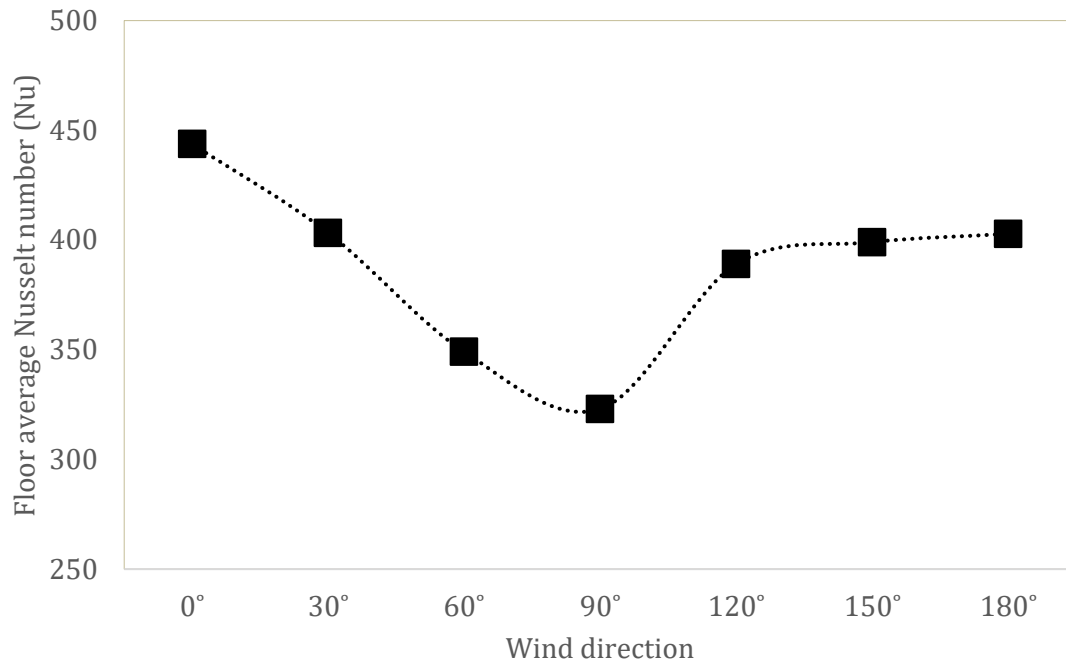


Figure 5-16. Effect of varying wind direction on the floor's average  $Nu$  Number [Wind speed of 4 m/s at a reference height of 10 m]

## 5.5 Remarks

The results of this study indicate that wind conditions strongly influence both the indoor flow-fields and convective heat transfer from the floor of single-sided naturally ventilated room-like spaces. The investigation shows that changes in the wind conditions, such as speed and direction, can result in significantly different flow regimes and temperature distributions inside these spaces, leading to a significant variation in the convective heat transfer from the floor. Furthermore, changes in the strength of the wind-driven force, with respect to the buoyancy-driven force, can lead to the reinforcement of, or resistance to, flow through the opening, resulting in different natural convection mechanisms. Further scrutiny is needed on the method to precisely evaluate the dominant force (buoyancy or wind) to implement the respective empirical relationship in building simulations. Chapter 6 presents how the research approach this aspect.

The generalisation of these results requires further study with an extended range of wind conditions, opening areas, building dimensions and Rayleigh numbers.

Nonetheless, there is significant scope for improving the prediction of the convective heat transfer from the floor of naturally ventilated spaces by including the effect of the outdoor wind conditions in the existing empirical correlations.

## Chapter 6 Improving the robustness of the naturally ventilated house model

### 6.1 Introduction

Chapter 3 presented simulation results of the coupled thermal-airflow behaviour of a model house in TRNSYS dynamic simulation environment. The research indicated that there is a significant potential for regulating the thermal behaviour of a relatively airtight and insulated natural ventilated house with a single-sided opening located in a temperate climatic region [99, 131].

This simplified approach of examining the thermal behaviour of the natural ventilated building possesses a risk of higher uncertainty due to the many influencing factors and complexity involved in natural ventilation driving forces. Studies of the combined effect of wind and buoyancy on indoor surfaces' convective heat transfer behaviour of natural ventilated building are sparse in the literature. Additionally, the choice of the heat transfer correlation for convection strongly affects the energy use and thermal comfort predictions of BES programs [108, 106, 109].

Despite this, there are many research works [132, 133, 134, 88, 135, 136, 137, 138, 139, 140] published analysing the effect of single-sided ventilation on volume flow rate through the opening(s) of a naturally ventilated building. In one of the most recent works, Park et al. [132] investigated a combined effect of them on an isolated building by applying CFD  $k - \omega SST$  model. The research work concludes that the combined interaction produces a destructive effect, reducing the volume flow rate when applying a positive (indoor-outdoor) temperature difference. Whereas, when applying negative temperature difference, it is always constructive, producing a reinforcing effect and improving volume flow rate through the opening.

The work presented earlier in Chapter 4 and Chapter 5 demonstrated that airflow through a partially opened enclosure space, due to both wind and buoyancy conditions, can greatly influence the heat transfer behaviour of a relatively heated floor [141, 122, 142, 143]. In summary, the research initially established an empirical relationship of heat transfer from a hot floor based on the buoyancy-driven numerical experimental

setup. The study further examined the heat transfer behavior of the floor due to the combined effect of buoyancy and wind-driven flow with increased wind velocity for a particular window opening case when exposed to different wind conditions (speed and direction).

Applying these specifically derived relationships of convective heat transfer to the coupled thermal and airflow model presented in Chapter 3, can significantly influence and improve the robustness of the developed building thermal-airflow model, including the dynamic simulation results.

As such, this chapter intends to apply these relationships and research outcome to improve the building model developed in TRNSYS environment in Chapter 3. Besides, this chapter aims to re-examine the improved model house to understand the implications and improve the accompanying results and database under different operating conditions.

## **6.2 Convective heat transfer relationship for a floor**

The results of the numerical experiment in terms of empirical correlations presented in Chapter 4 and Chapter 5, addresses three different possible categories of influences on the heat transfer behaviour for a specific case of floor: buoyancy only, buoyancy and wind speed at perpendicular to the opening, buoyancy and wind impinging from different directions.

The first category of the influence refers to the heat transfer behaviour from the floor due to a buoyancy-driven airflow from outside to the partially opened enclosure/room without any presence of external wind. Recalling from Chapter 4, the result confirms that the  $Ra$  and the WOF influences the heat transfer behaviour of a heated floor of a buoyancy-driven partly opened enclosure. The empirical relationships presented in Equation (4-7) and Equation (4-8) can help determine the heat transfer behaviour of the floor.

From an application point of view, this result could be analogous to a single room with underfloor heating, or where the floor is heated by solar radiation and exposed to natural ventilation driven by buoyancy forces with the single-sided opening without any external wind conditions. Equation (6-1) simplifies this correlation further with 95%

confidence bounds for the heated floor as demonstrated in Figure 6-1 (analogous to Figure 4-19) so that a multi-zone building energy model can simulate the floor convection heat transfer.

$$h_{c,floor} = 1.557 \cdot |T_{s,floor} - T_o|^{0.4069} \cdot WOF^{0.1781} \quad (6-1)$$

Where,  $h_{c,floor}$  = CHTC of floor [W/m<sup>2</sup>.K]

$T_{s,floor}$  = Inside surface temperature of floor [K]

$T_o$  = Outdoor ambient air temperature [K]

As the TRNSYS building model Type 56 requires an input of CHTC in terms of the unit [k]/hr.m<sup>2</sup>.K], Equation (6-1) is further simplified to Equation (6-2) including the necessary conversion factor.

$$h_{c,floor} = 5.61 \cdot |T_{s,floor} - T_o|^{0.4069} \cdot WOF^{0.1781} \quad (6-2)$$

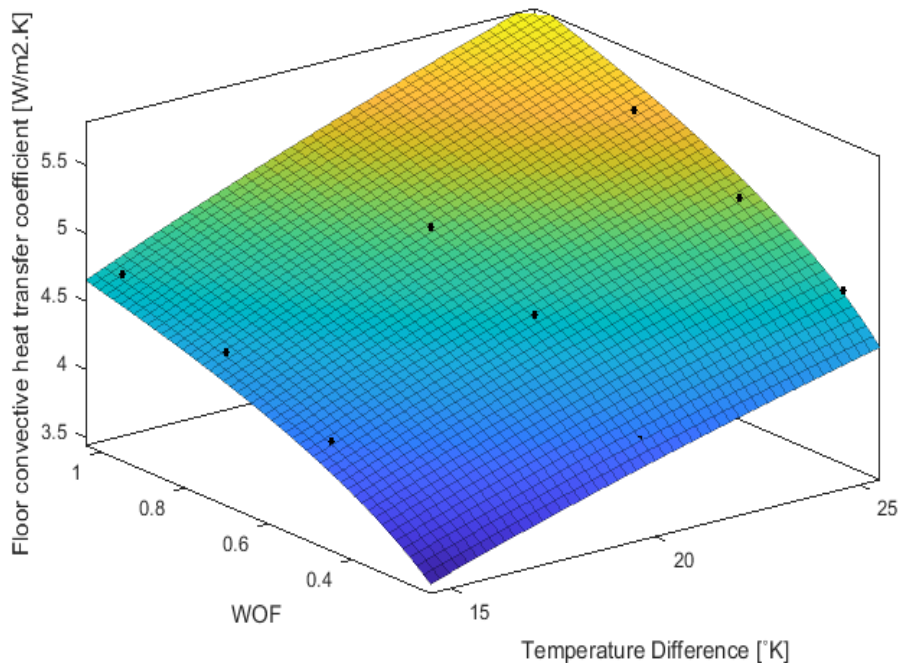


Figure 6-1. Floor CHTC with respect to WOF and temperature difference for the buoyancy-driven case

To address the issue related to floor convective heat transfer behaviour in case of cold floor ( $T_{s, floor} < T_{a,i}$ ) or window shut position (WOF value of 0) and other vertical and ceiling inside surfaces, the work considers the default standard correlations as in Equation (6-3) [80] with respective constants and exponents as presented in Table 6-1.

$$h_{c,j} = \frac{C}{3.6} |T_{s,j} - T_{a,i}|^n \quad (6-3)$$

Where,  $h_{c,j}$  = CHTC of surface  $j$  [W/m<sup>2</sup>.K]

$C$  = Constant

$n$  = Exponent

$T_{a,i}$  = Ambient air temperature for zone  $i$  [K]

$T_{s,j}$  = Temperature at inside wall surface  $j$  [K]

Table 6-1. Default values of constants and exponents [80]

Surface	Thermal status	Constant ( $C$ ) [k]/m <sup>2</sup> K	Exponent ( $n$ )
Floor	Cold ( $T_{s, floor} - T_{a,i} < 0$ )	3.888	0.31
Ceiling	Hot ( $T_{s, ceiling} - T_{a,i} > 0$ )	3.888	0.31
Ceiling	Cold ( $T_{s, ceiling} - T_{a,i} < 0$ )	7.2	0.31
Vertical	Any	5.76	0.3

Nevertheless, the openable window of naturally ventilated house exposes it to different wind conditions with unpredictable wind speed and direction. The wind speed can vary from zero to a powerful wind in the case of a cyclone. In the NZ context, the maximum applicable design standard of wind speed for a timber-framed house for the low zone is 32 m/sec (115 km/hour) [144]. Though the structure of the house can withstand relatively higher wind speeds, the ASHRAE standard [14] advocates that, from a thermal comfort perspective, the resulting indoor airspeed should be less than 0.8 m/s for a light primary sedentary activity. The median annual average wind speed spectrum for NZ based on the 30-year average [130] is below 8 m/s in most of the locations.

Therefore, the research limits a maximum wind speed consideration of 8 m/s (30

km/hr) at standard meteorological station height of 10 metres for the necessary assessment for this research.

However, the involvement of wind-driven forces makes the problem more complicated. The initial results presented in Chapter 5 define the second category of influence by performing a micro analysis of convective heat transfer behaviour at the floor of the partially opened enclosure/room due to varying external wind speeds in addition to the buoyancy-driven forces. The results as presented in Table 5-1 and Figure 5-13 demonstrate two patterns of the rate of increase in heat transfer behaviour such that it is significantly low at lower wind speed range 0-2 m/s compared to the higher wind speed range above 2 m/s.

Based on the impinging strength of wind speed, the combined wind and buoyancy-driven airflow might complement or restrict each other, resulting in a further and intricate nature of convective heat transfer process that could be either mixed or forced convection. In this context, applying a dimensionless Archimedes Number ( $Ar$ ) can help to identify the predominant driving force (wind or buoyancy) and use the respective generalised empirical correlation of the convective heat transfer from the floor.

The influence of variation in wind speed is not sufficient to provide a full representation of external wind conditions as the wind might impinge at a certain speed from any direction with respect to the opening. In this regard, the results in Chapter 5 presented the third category of influence by performing a micro analysis of convective heat transfer behaviour at the floor of the partially opened enclosure/room due to varying wind direction for a particular external wind speed 4 m/s in addition to the buoyancy-driven forces. Figure 5-16 demonstrates a typical pattern of the influence on heat transfer behaviour such that floor average  $Nu$  number is minimum when the wind impinges from the transverse direction ( $90^\circ$  angle of attack), and maximum when it impinges perpendicular ( $0^\circ$  angle of attack) to the face of the opening. Generalising the behaviour for other wind speeds- 2, 6 and 8 m/s, Figure 6-2 illustrates the variation of floor average  $Nu$  number with respect to different wind speeds and directions.

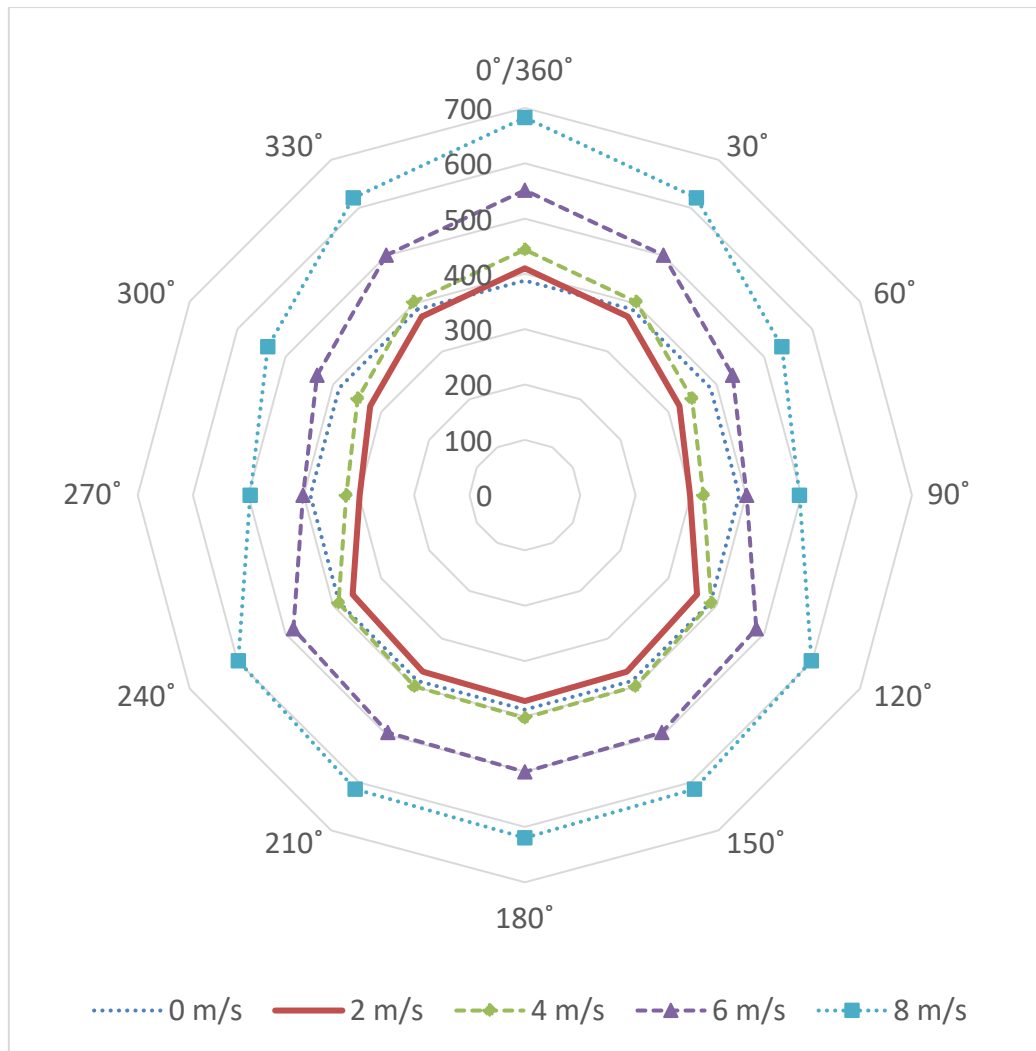


Figure 6-2. Average floor  $Nu$  with respect to different wind reference conditions at the height of 10 m.

Transforming the respective results in compliance with the input structure of TRNSYS Type 56 building model, Figure 6-3 illustrates the threshold of floor average  $CHTC(s)$  with respect to different wind speed and direction along with the no-wind condition (0 m/s).

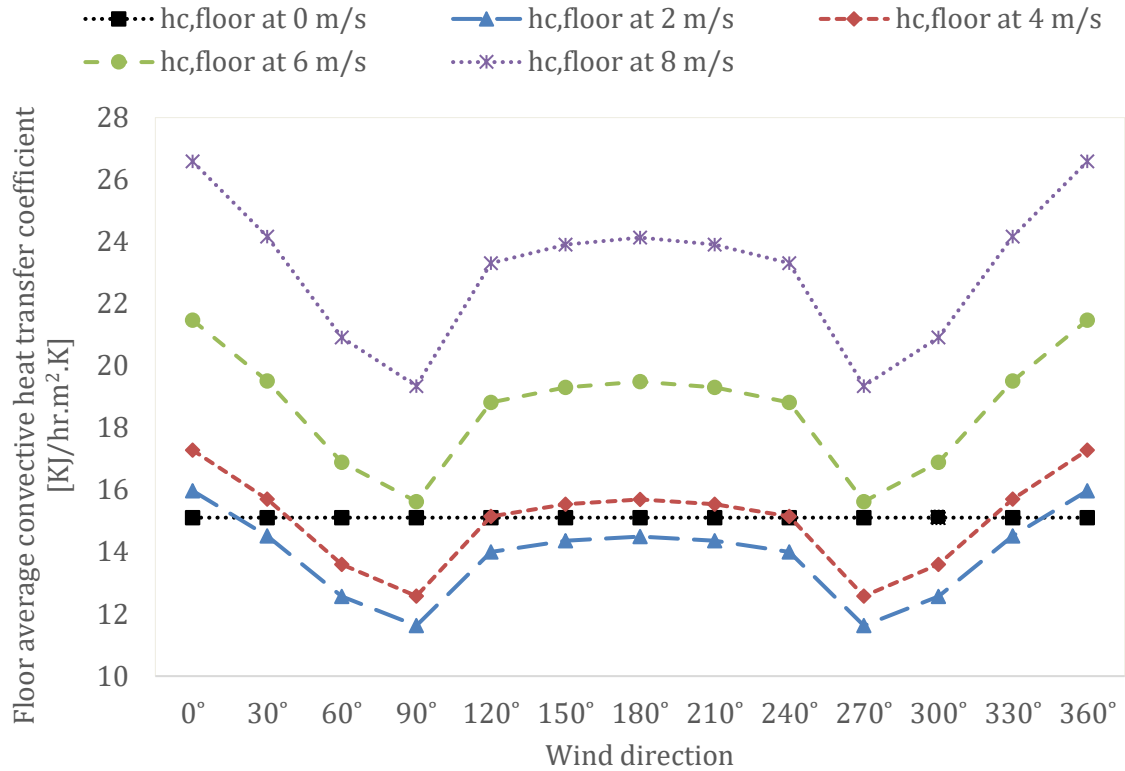


Figure 6-3. Average floor CHTC with respect to different wind reference conditions at the height of 10 m

Figure 6-3 illustrates that there is a similar rate of change of heat transfer behaviour for a particular range of wind direction (0°-90°; 90°-120°; 120°-240°, 240°-270°; and 270°-360°). In order to estimate the average floor heat transfer coefficient, the research derives multiple polynomial equations for these ranges of wind directions within the threshold of wind speed 0-8 m/s. Equation (6-4) represents these multiple polynomial equations by a typical relationship.

$$h_{c, floor} = a + (b.V_m) + (c.\phi) + (d.V_m^2) + (e.V_m.\phi) + (f.\phi^2) \quad (6-4)$$

Where,  $h_{c, floor}$  = Floor CHTC [K].hr/m<sup>2</sup>.K]

$V_m$  = Wind speed at meteorological mast height (10m) [m/s]

$\phi$  = Wind direction [°]

The set of constants (a, b, c, d, e and f) associated with a particular range of wind direction as mentioned in Table 6-2 can be plugged into the Equation (6-4) to estimate the respective floor average CHTC within that particular range of wind direction.

Table 6-2. Constants of polynomial Equation (6-4) for the different range of wind direction

Wind Direction ( $\theta$ )	Constants					
	a	b	c	d	e	f
$\theta \leq 90^\circ$	15.4	-0.2347	-0.03551	0.2063	-0.005625	0
$90^\circ < \theta < 120^\circ$	6.984	-1.399	-0.05632	0.1907	-0.008929	0
$120^\circ \leq \theta \leq 240^\circ$	9.044	-0.5154	0.06234	0.2122	-3.02E-18	0.0001732
$240^\circ < \theta < 270^\circ$	27.26	1.815	-0.05632	-0.1907	-0.008929	0
$\theta \geq 270^\circ$	2.621	-2.29	0.03551	0.2063	0.005625	0

### 6.3 Methodology

To systematically analyse the effect of buoyancy and wind on single-sided ventilation, this research applies a dimensionless  $Ar$ , defined as the ratio of buoyancy to inertia forces (Equation (6-5)) considering the floor as the surface of interest. A similar relationship has been used by many researchers [134, 140, 145] to decide whether the flow is predominantly buoyancy or wind-driven in the ventilation domain.

$$Ar = \frac{g|\Delta T| \cdot H'}{T_{av} \cdot V_o^2} \quad (6-5)$$

Where,  $g$  = Acceleration due to gravity [ $m/s^2$ ]

$\Delta T$  = Temperature difference between indoor floor surface to ambient [K]

$H'$  = Height of the opening [m]

$T_{av}$  = Average of the indoor room floor surface and outdoor ambient temperature [K]

$V_o$  = Wind speed at building reference height [m/s]

The power-law profile as presented in the Equation (6-6) estimates the wind speed at building reference height,  $V_o$ .

$$V_o = V_m \cdot \left(\frac{h_o}{h_m}\right)^\alpha \quad (6-6)$$

Where,  $V_m$  = Wind speed at meteo mast height [m/s]

$h_o$  = Building reference height [m]

$h_m$  = Meteo mast reference height [m]

$\alpha$  = Wind velocity profile exponent = 0.22 (Rough profile)

Interpreting the Equation (6-5), when wind dominates the natural ventilation,  $Ar$  tends to zero and airflow due to buoyancy becomes independent of  $Ar$ ; whereas with increasing  $Ar$ , the buoyancy force is dominant for delivering airflow through the opening.

Applying this concept, Figure 6-4 presents a plot of average  $Nu$  number of the floor with respect to the square root of Archimedes number ( $\sqrt{Ar}$ ) as an extension of the results of increasing wind speed presented in Table 6-3 for a WOF value of 0.5. The plot indicates that there is a significant rate of increase on floor average convective heat transfer rate when the impinging wind speed at a meteo mast (reference height of 10 m) increases above 2.5 m/s compared to the wind speed range between 0 to 2.5 m/s. For this case of the window opening (WOF 0.5), the transition point is equivalent to a value of 1.4 for  $\sqrt{Ar}$ . Now, this value is generalised to decide whether the convective heat transfer from the floor is predominantly due to wind or buoyancy-driven airflow.

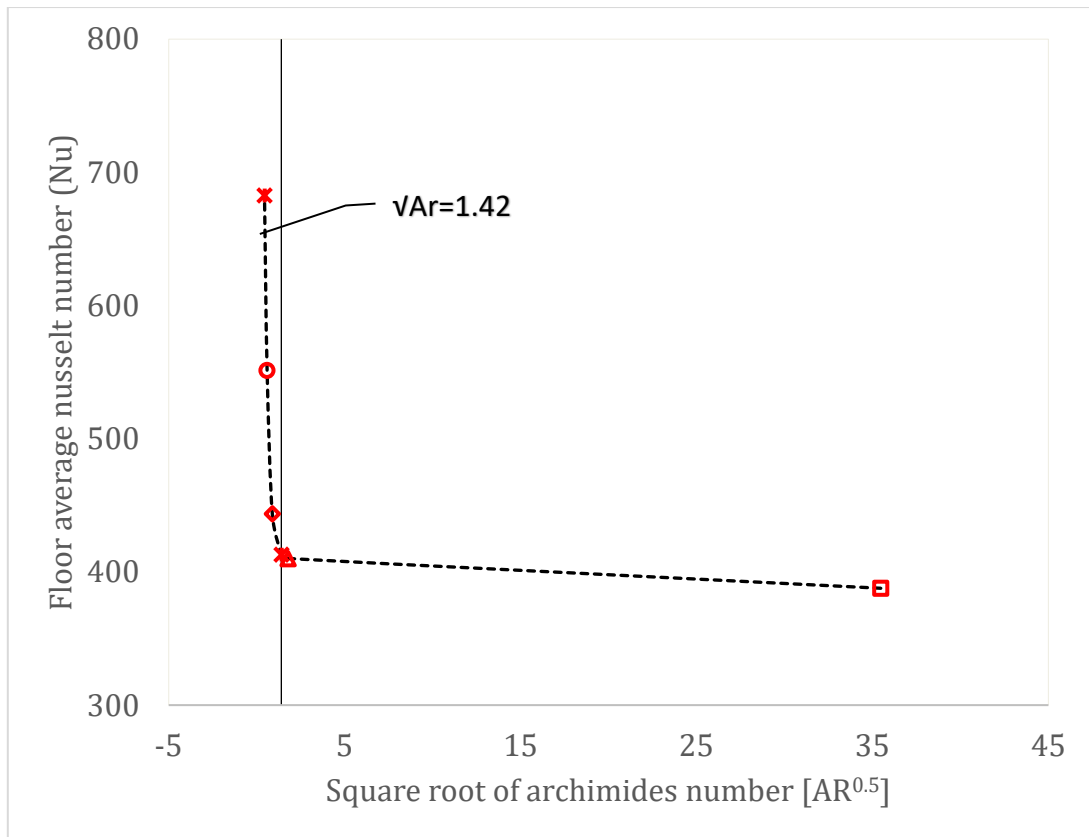


Figure 6-4. Floor average heat transfer behaviour with respect to the square root of Ar

Table 6-3 Floor average Nu and  $\sqrt{Ar}$  with respect to increasing wind speed

Wind Speed at Meteorological height of 10 m ( $V_m$ ) [m/s]	Wind speed at building reference height ( $V_o$ ) [m/s]	Floor average Nusselt Number ( $Nu$ )	Square root of Archemedis Number ( $\sqrt{Ar}$ )
0.1	0.08	388	35
2	1.6	410	1.77
2.5	2	413	1.42
4	3.2	444	0.89
6	4.8	551	0.59
8	6.4	682	0.44

A mini-program developed in TRNSYS according to the flowchart shown in Figure 6-5 helps select the necessary relationships to model the convective heat transfer behaviour of the floor of the building model. As such, if the window is open ( $WOF > 0$ ), and positive temperature difference exists between the indoor floor and outdoor ambient temperature ( $\Delta T > 0$ ), the mini-program selects the empirical relationships developed in this research work. In particular, the mini-program picks the empirical relationship related to buoyancy-driven airflow (Equation (6-2)) for modelling convective heat transfer behaviour of the floor if the square root of Archimedes number ( $\sqrt{Ar}$ ) is greater than 1.4. If wind driven ventilation force is predominant (the value of  $\sqrt{Ar}$  is less than or equal to 1.4), the mini-program picks Equation (6-4) with appropriate constants (a, b, c, d, e and f) according to the input wind direction at that time step to model the floor average CHTC. Similarly, for the remaining cases (window shut, cold floor than ambient) the mini-program selects the empirical correlation that is similar to the default setting of TRNSYS for the floor as defined by Equation (6-3) and Table 6-1. The convective heat transfer behaviour of the vertical and ceiling surfaces are modelled as default standard setting for the respective surfaces as mentioned in Equation (6-3) and Table 6-1.

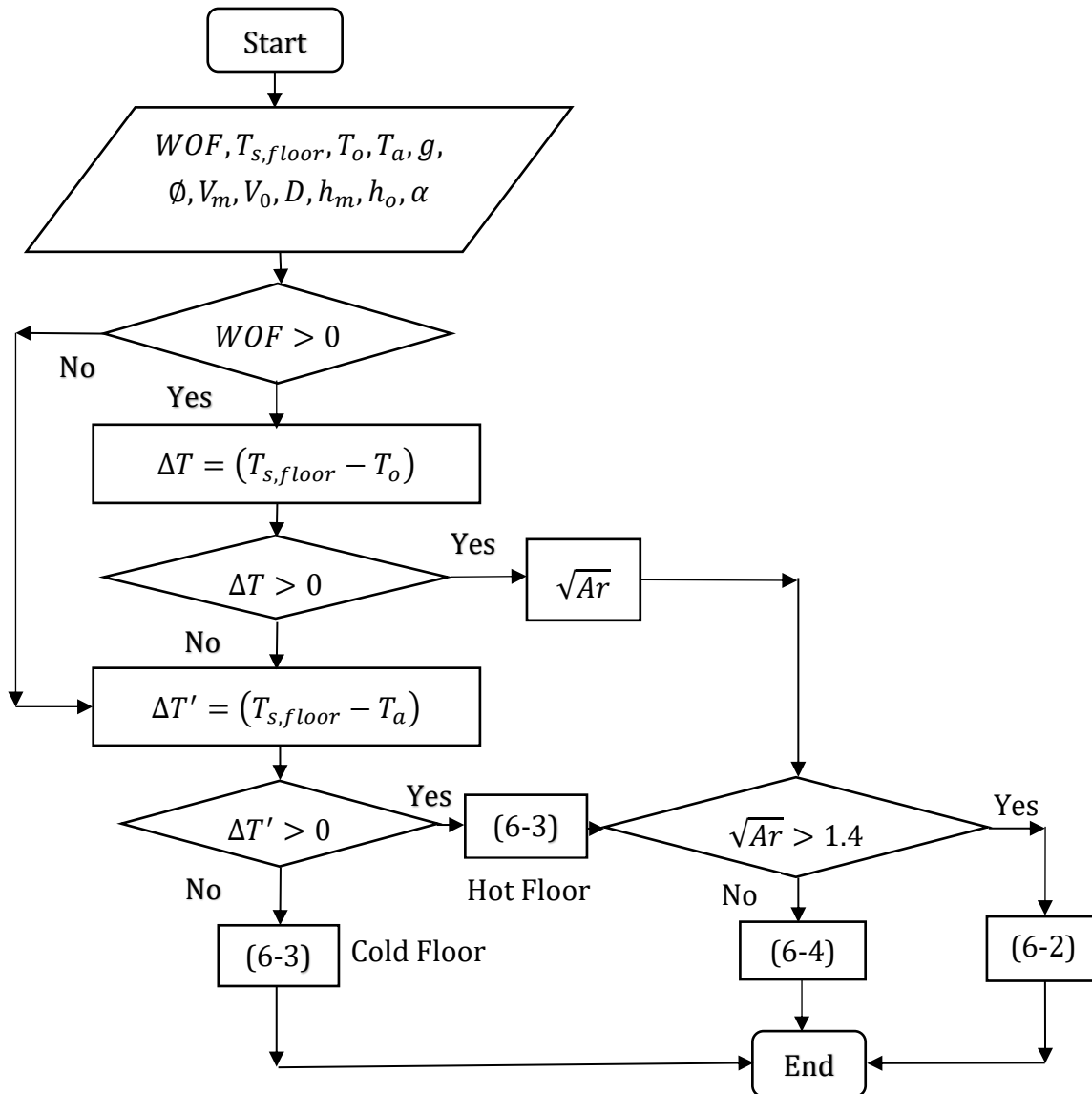


Figure 6-5. Flowchart for switching floor convective heat transfer correlations

The research work re-simulates all the different operating conditions of envelope airtightness (UAT, AT, AVG, LKY, DTY) level and average envelope thermal resistance ( $R_{avg}$ ) value of (2.01, 2.6, 3.22 and 3.4) for different WOF values.

## 6.4 Results

To re-examine the level of thermal comfort regulation potential of the model house, the work simulates a baseline scenario equivalent to different discrete values of openable window area equal to  $WOF$  (0, 0.125, 0.25, 0.5, 0.75 and 1) for 8,760 hours. It generates

an hourly time-series of occupied zone air temperature and the PMV profile for different values of  $R_{avg}$  (2.01, 2.6, 3.22 and 3.4) and airtightness level (0.03, 0.3, 0.5, 0.7 and 3.4) ACH as defined earlier in Chapter 3.

Comparing the simulation results, Figure 6-6 and Figure 6-7 illustrate an improved potential for thermal comfort regulation by opening windows in well-insulated houses ( $R_{avg}$  3.4) compared to a baseline insulated ( $R_{avg}$  2.01) house for the summer month of January.

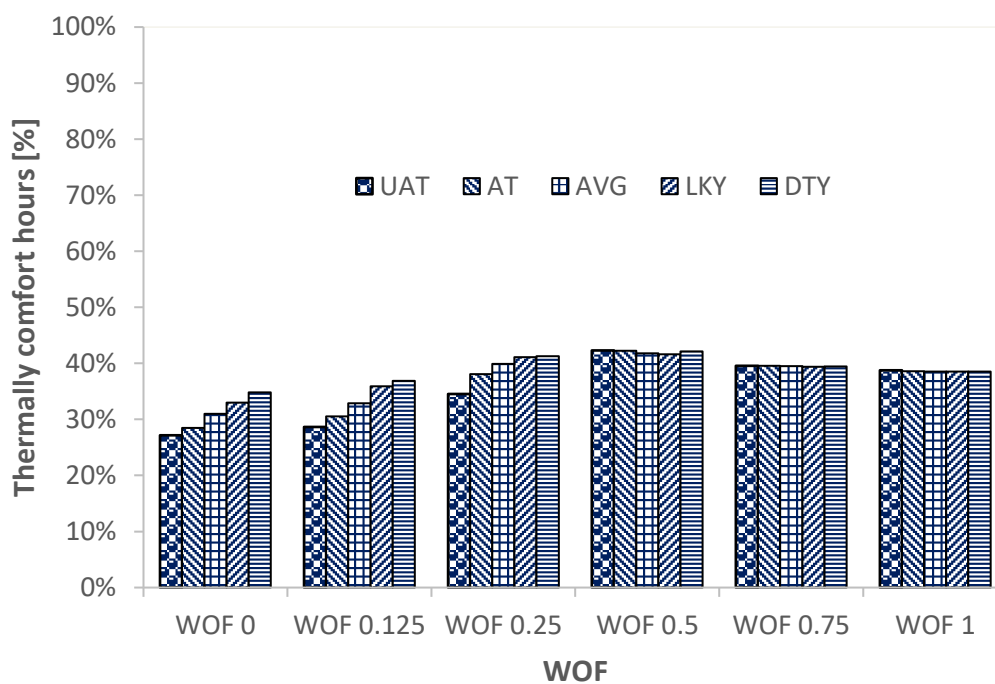


Figure 6-6. Percentage thermal comfort duration ( $-0.7 < PMV < 0.7$ ) with respect to WOF ( $R_{avg}$  2.01, January)

Nevertheless, close examination of Figure 6-6 shows that there is only a marginal gradual improvement in the average percentage of thermally comfortable hours from 31% for window shut (WOF 0) to a maximum of 42% for half-open (WOF 0.5) window positions. This is an average result for houses with differently airtight envelopes with a thermal resistance value of  $R_{avg}$  2.01.

In comparison to this, Figure 6-7 shows the respective performance of the model house with the thermal resistance value of  $R_{avg}$  3.4. Figure 6-7 demonstrates that there is a relatively sharp improvement on the average percentage of thermally comfort hours from 14% for window shut (WOF 0) to a maximum of 42% for half-open (WOF 0.5) window positions.

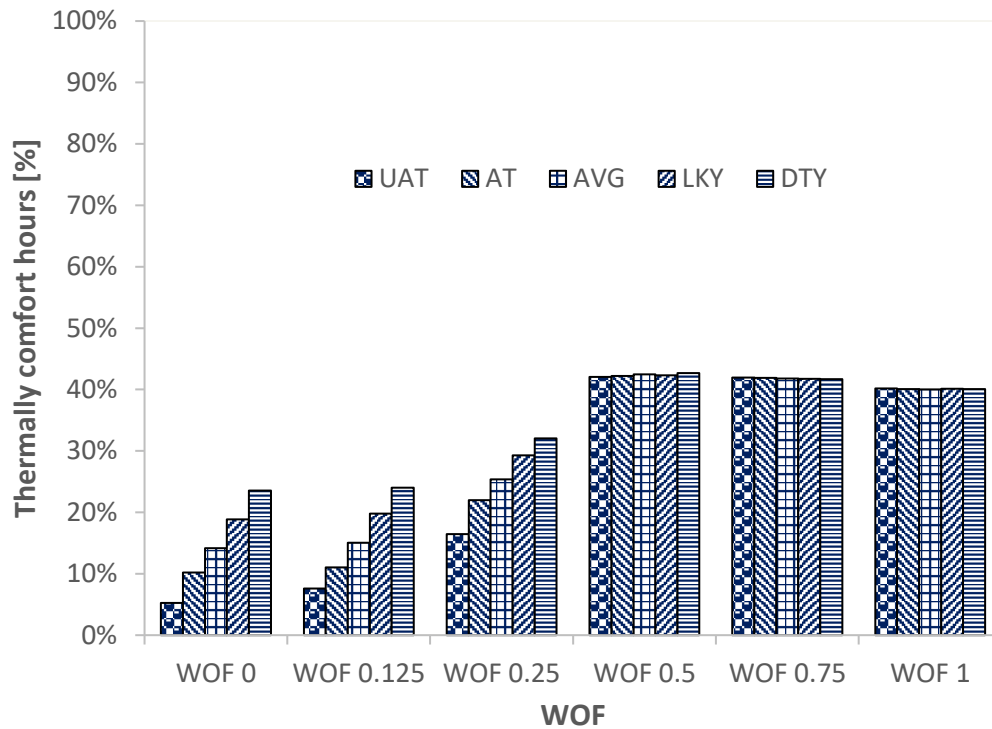


Figure 6-7. Percentage of thermal comfort duration ( $-0.7 < PMV < 0.7$ ) with respect to WOF ( $R_{avg}$  3.4, January)

In both cases, the results of WOF values of 0.75 and 1 illustrate a marginal decrease in the average percentage of thermal comfort hours (39-40%) compared to the 42% at half-open window position (WOF 0.5). This result indicates that bigger openings do not necessarily improve the average percentage of thermal comfort hours; instead, they can permit more than the natural ventilation required for free cooling. It might result in transitioning some instances that sit on the lower range of thermal comfort index (PMV slightly greater than -0.7 might transition to less than -0.7) and starts worsening the average performance of thermal comfort of the house as seen for the WOF values of 0.75 and 1.

Despite having a well-insulated and airtight house, it reveals that a large proportion of the instances (more than 58%) still fall into either an uncomfortable cold or hot range. It shows the prospect of any position of fixed openable area is limited for improving the thermal comfort of the naturally ventilated house.

Examining the results further for the same set of virtual houses, mainly focusing on the percentage of the uncomfortable hot period, Figure 6-8 and Figure 6-9 demonstrate that envelope airtightness can also play a significant role in regulating thermal comfort behaviour of the naturally ventilated house.

Close examination of Figure 6-8 shows that there is only a marginal gradual decline on the average percentage of thermally uncomfortable hot hours from 62% for window shut (WOF 0) to 35% for half-open (WOF 0.5) window positions. This is an average result for houses with differently airtight envelopes with the thermal resistance value of  $R_{avg}$  2.01.

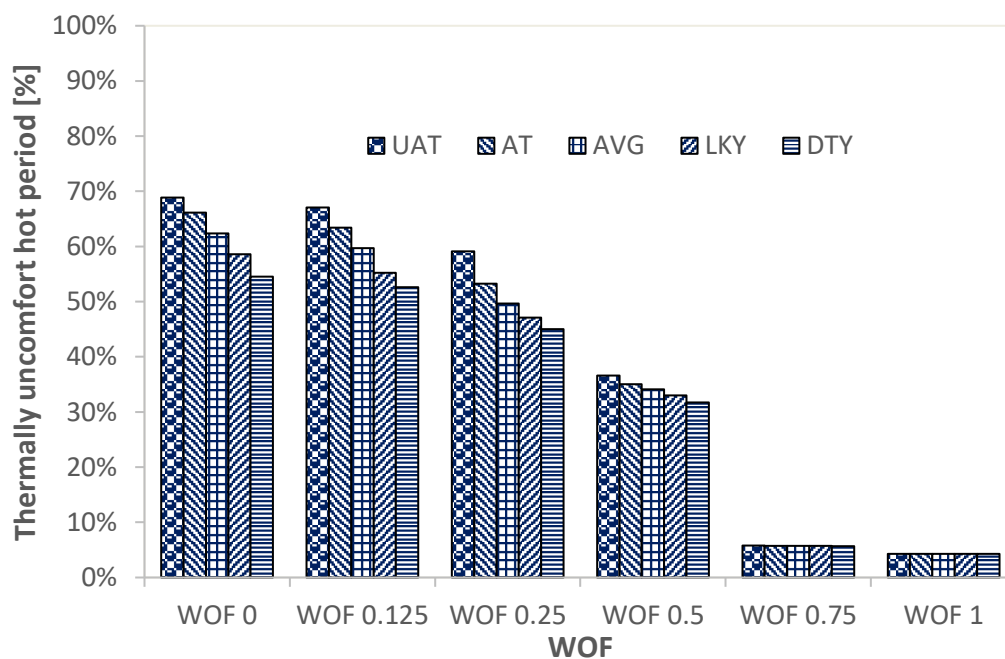


Figure 6-8. Percentage of thermally uncomfortable hot duration (PMV>0.7) with respect to WOF & airtightness ( $R_{avg}$  2.01, January)

In comparison to this, Figure 6-9 shows the respective performances of the model house with thermal resistance value of  $R_{avg}$  3.4. Figure 6-9 demonstrates that there is a

relatively sharp decline on the average percentage of thermally uncomfortable hours from 85% for window shut (WOF 0) to 45% for half-open (WOF 0.5) window positions.

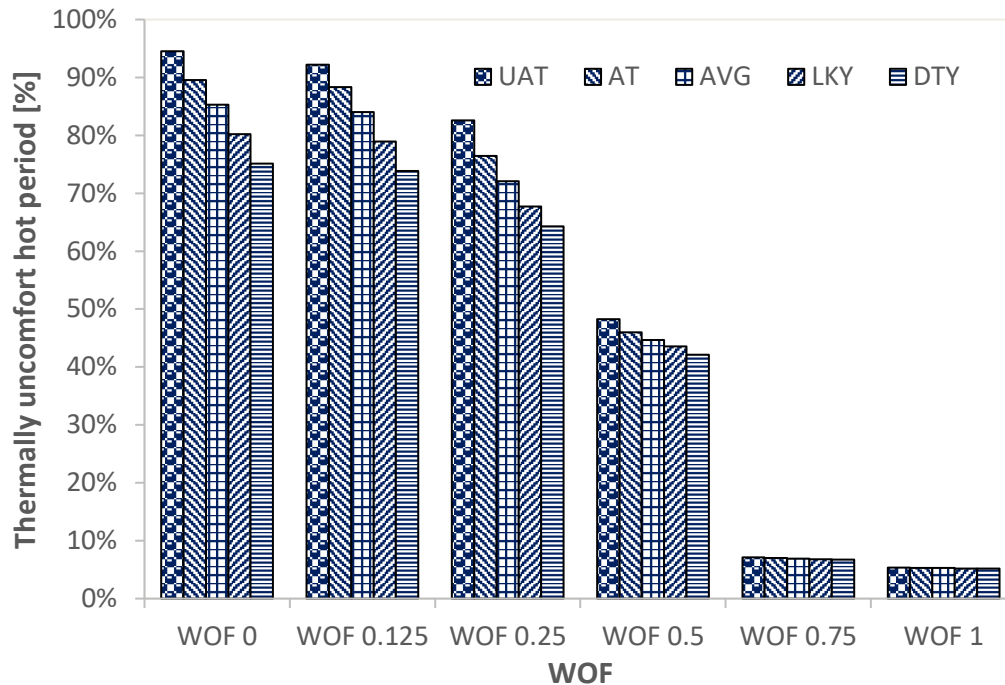


Figure 6-9. Percentage of thermally uncomfortable hot duration (PMV>0.7) with respect to WOF & airtightness ( $R_{avg}$  3.4, January)

In both cases, the results of WOF values of 0.75 and 1 illustrate a significant drop (30-40%) in the average percentage of thermally uncomfortable hours compared to the half-open window position (WOF 0.5). This result indicates that bigger openings reduce the average percentage of thermal uncomfortable hours sharply as they permit a very high exchange of natural ventilation for free cooling. It might result transitioning some instances that sit on the lower range of thermal comfort index (PMV slightly greater than -0.7 might transition to less than -0.7) and starts worsening the average performance of thermal comfort of the house as seen for the WOF values of 0.75 and 1.

Besides, the degree of thermal comfort regulating potential reduces with reducing the level of the airtightness in both cases. For illustration, an UAT house results in a 14% higher number of uncomfortably hot hours compared to DTY house with the same window shut position (WOF 0) and thermal resistance of  $R_{avg}$  2.01 as presented in Figure 6-8.

However, this value increases to 20% for a more insulated house ( $R_{avg}$  3.4) as shown in Figure 6-9 indicating that there exists a relatively higher likelihood of overheating the indoor environment in well-insulated and airtight dwellings. Furthermore, the difference of percentage of uncomfortable hot hours gradually decreases to 5-6% for half-open window position and disappears as the window openable area further increases for greater values of WOF (WOF 0.75 and 1) irrespective to envelope thermal insulation level.

In naturally ventilated houses, the fixed opening of the window during unnecessary periods might also affect the indoor thermal behaviour by making it uncomfortably cold. To assess this further, Figure 6-10 demonstrates an increasing percentage of uncomfortably cold instances for higher values of WOF for the similar set up of virtual houses having different values of envelope airtightness for a baseline-insulated house ( $R_{avg}$  2.01).

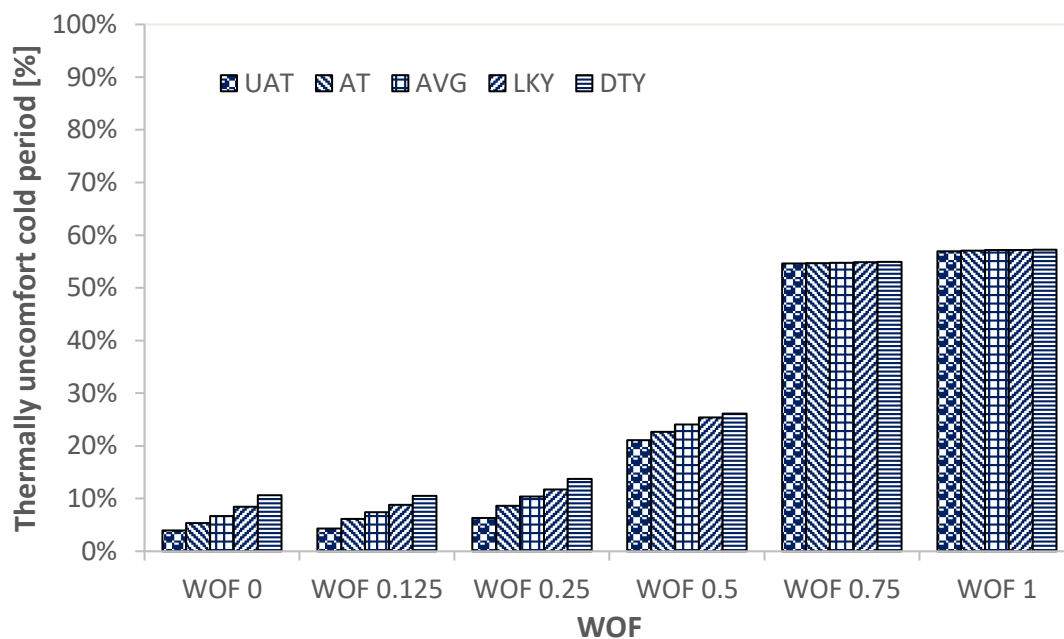


Figure 6-10. Percentage of thermally uncomfortable cold (PMV<-0.7) duration with respect to WOF & airtightness ( $R_{avg}$  2.01, January)

However, for well-insulated ( $R_{avg}$  3.4) houses, the resilience to instances having uncomfortable-cold periods improves (up to WOF value of 0.25) as shown in Figure 6-11. Figure 6-11 also demonstrates the relatively lower value of the thermally

uncomfortable cold period (4 %) at WOF value of 0.25 for DTY house. Moreover, the influence of various level of airtightness for a specific window opening condition is also not significant despite being well-insulated house ( $R_{avg}$  3.4) making them more favourable for regulating indoor thermal behaviour by adjusting the window opening area.

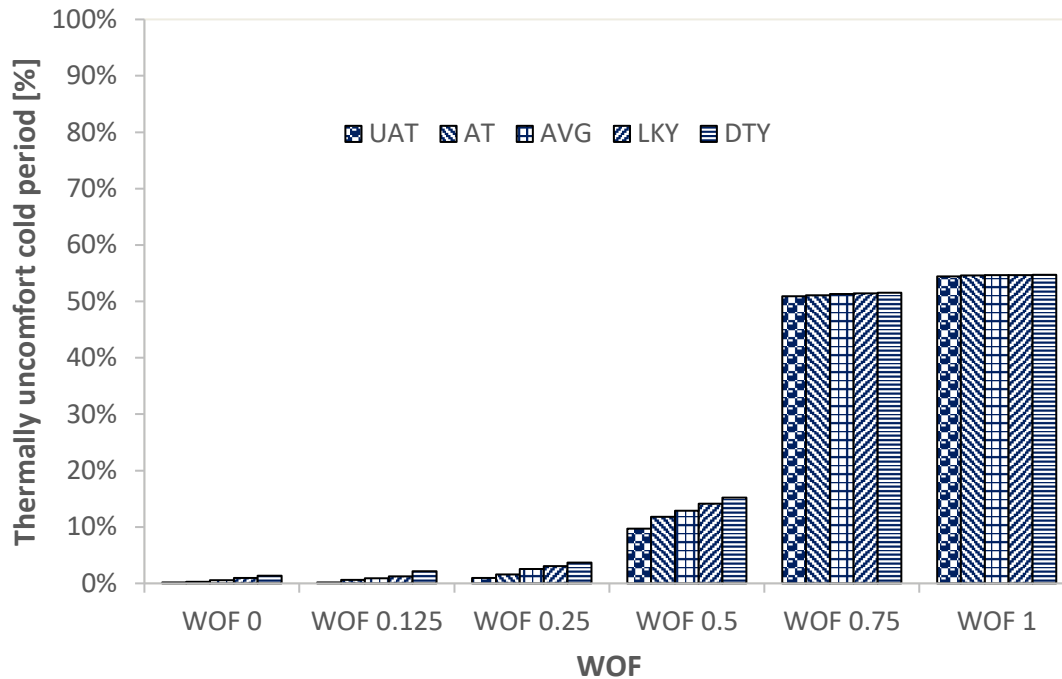


Figure 6-11. Percentage of thermally uncomfortable cold (PMV<-0.7) duration with respect to WOF & airtightness ( $R_{avg}$  3.4, January)

In both cases, the results of WOF values of 0.75 and 1, illustrate a significant increase in the average percentage of thermally uncomfortably cold hours (55-57%) compared to the (13- 24%) at the half-open window position (WOF 0.5). By letting more than necessary natural ventilation exchange occur, the relatively more significant openings exploit the outdoor free cooling and worsen the average percentage of thermal uncomfortable cold hours. Generally, the instances related to lower values of thermally comfortable PMV index range ( $0.7 > PMV > -0.7$ ) transitions to thermally uncomfortable cold PMV range (PMV<-0.7).

Compiling the thermally comfortable period together with both the thermally uncomfortable hot and cold duration, Figure 6-12 to Figure 6-15 demonstrate the impact of the increasing envelope thermal resistance values from  $R_{avg}$  2.01 to  $R_{avg}$  3.4

respectively. Each of these figures consists of results for different window opening positions including WOF values (0, 0.125, 0.25, 0.5, 0.75 and 1) and envelope airtightness (UAT, AT, AVG, LKY, DTY) cases together for a particular envelope thermal resistance.

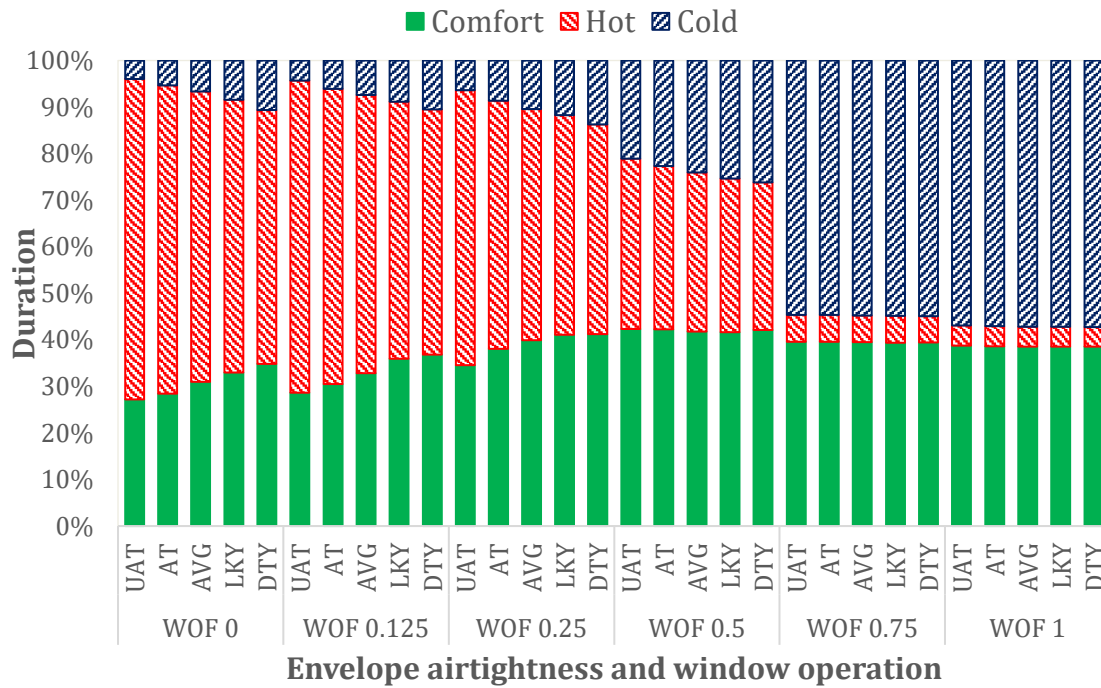


Figure 6-12. Percentage of thermally comfortable and uncomfortable duration (with respect to WOF & airtightness ( $R_{avg}$  2.01, January))

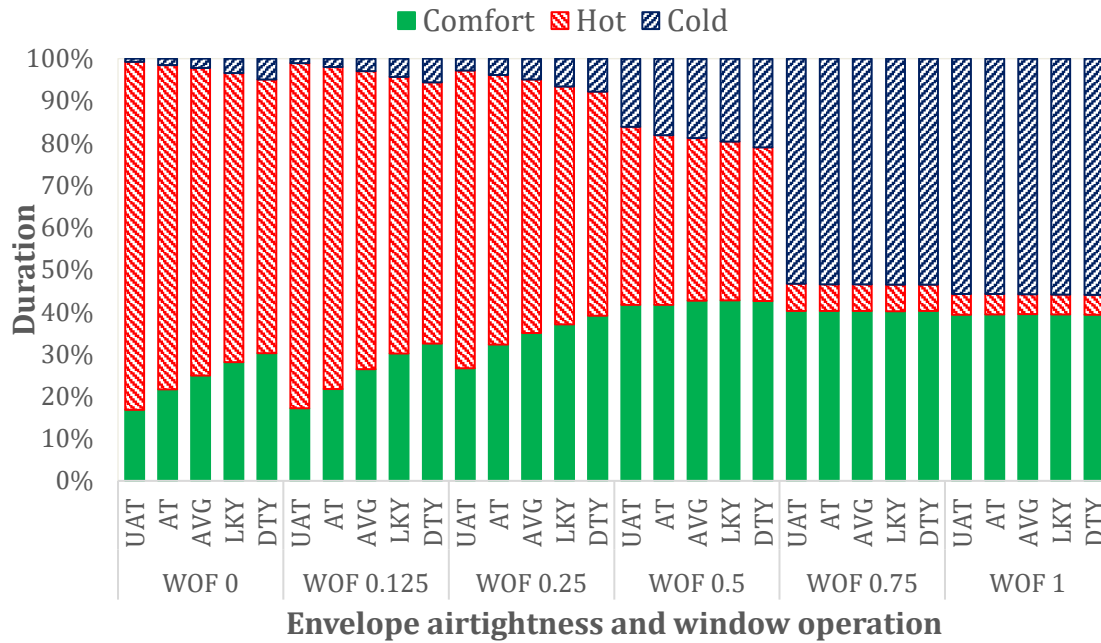


Figure 6-13. Percentage of thermally comfortable and uncomfortable duration (with respect to WOF & airtightness ( $R_{avg}$  2.6, January))

These graphs (Figure 6-12 to Figure 6-15) illustrate that there is a gradual increase in thermally uncomfortable hot and decrease in cold duration in a well-insulated house. As such, there is a somewhat better prospect of regulating the thermal behaviour of the uncomfortable hot period in the well-insulated house. Also, these results confirm that a maximum of 43% thermal comfort duration is achievable, typically for half opening window position (WOF 0.5) irrespective of any envelope airtightness and thermal resistance values. These results are an outcome of the annual simulation (8,760 hours) with a time step of 1 hour for each particular window opening position and airtightness combination without any control system.

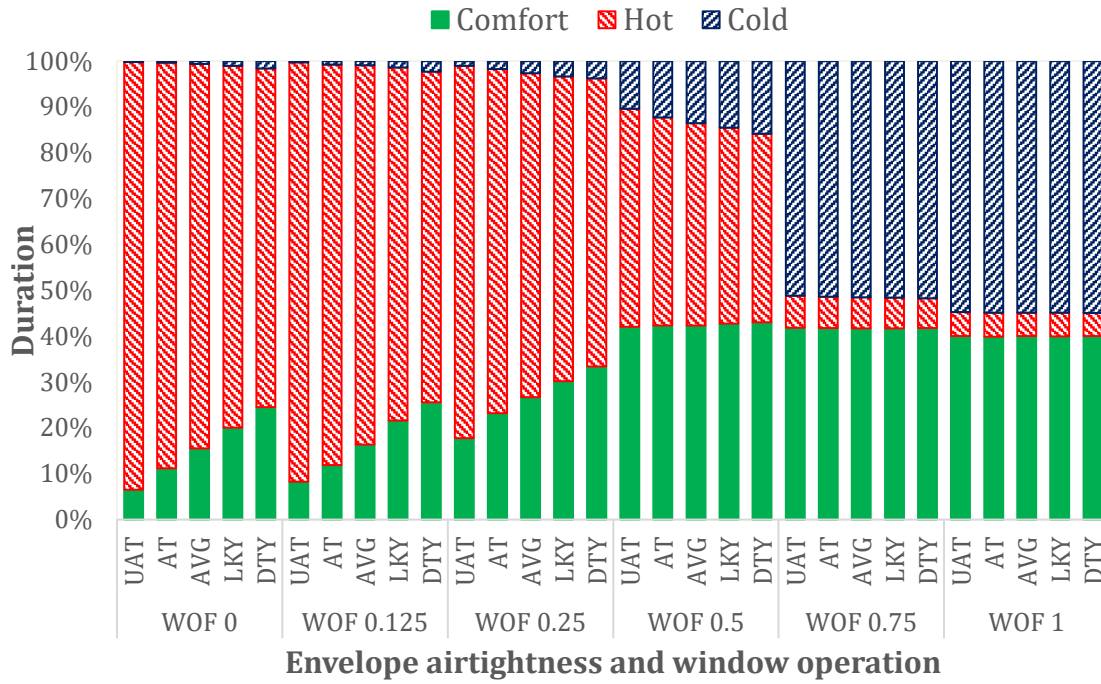


Figure 6-14. Percentage of thermally comfortable and uncomfortable duration (with respect to WOF & airtightness ( $R_{avg}$  3.22, January))

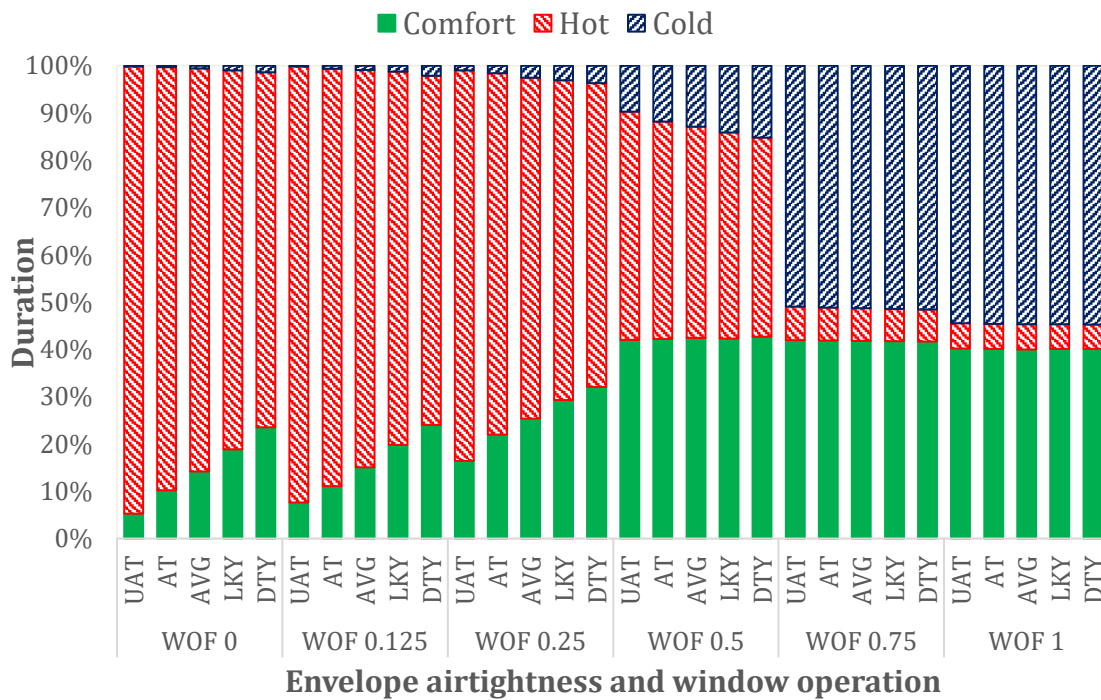


Figure 6-15. Percentage of thermally comfortable and uncomfortable duration (with respect to WOF & airtightness ( $R_{avg}$  3.4, January))

In summary, the results demonstrate that the improved thermal resistance and airtightness of the envelope helps to store thermal energy generated internally by occupants, solar load and thermal load due to air temperature. Furthermore, the stored thermal energy can either reduce uncomfortably cold periods or increase in uncomfortably warm periods. However, as the fixed window opening increases, it essentially increases the leakiness of the room by allowing higher air exchange rates to occur. Ultimately, opening the window can help reduce uncomfortably warm periods, but it might worsen uncomfortably cold periods.

## 6.5 Remarks

Exerting the developed convective heat transfer relationships for the floor of a partially opened enclosure improves the robustness of the coupled multi-zone thermal and airflow model. Re-examining the thermal comfort behaviour presented in this chapter validates that there is a significant scope for regulating the thermal behaviour of naturally ventilated residential houses in particular by opening windows. The capacity improves considerably for a relatively airtight and insulated house during the summer period.

The improved model still uses the default convective heat transfer relationships for the vertical indoor and ceiling surfaces based on the natural convection mechanism ideally developed in the closed room operating conditions. A partially opened naturally ventilated building would result in a stream of airflow exchange from outdoor to indoor and vice-versa through the opening. This stream of incoming airflow with the dynamic outdoor weather condition, in particular, the outdoor air temperature, relative humidity, wind speed and direction might result in a completely different convective heat transfer behaviour of the vertical indoor surfaces. Therefore, it is possible to improve the robustness of such thermal-airflow models further. In particular, the method for determining the CHTC of vertical indoor surfaces and ceiling.

From the application perspective, the simulation results are helpful for understanding the influence and limits of opening, closing and regulating the window to control and improve the indoor thermal behaviour to some extent. Manually varying the WOF across the day, month-wise and season wise might help move towards obtaining a more comfortable indoor environment. Nevertheless, it does not seem practical to

continuously adjust the window position manually in a quest to maintain thermal comfort.

In this context, further investigation is necessary to identify a technique to intelligently actuate the windows and regulate the values of WOF for maximising the percentage of thermal comfort period by minimising both thermally uncomfortable hot and cold period. This is the subject of Chapter 7.

## **Chapter 7 Developing and applying intelligent control concept**

### **7.1 Introduction**

The research work presented in earlier chapters has already developed and improved the methodology to model natural ventilation of a typical house located in mild climatic zone. The research also confirmed that there is a significant potential for regulating the thermal behaviour of relatively insulated and airtight naturally ventilated spaces by modulating windows actively in the summer. However, maintaining the indoor thermal comfort characteristics of the house by modulating natural ventilation is particularly challenging, as the solution is not explicit.

One of the key rationales behind this is the highly fluctuating nature of associated driving forces of natural ventilation along with many other influencing factors. Despite this, occupants attempt to improve the indoor comfort condition by manually adjusting the window openable area in order to modulate natural ventilation. Nevertheless, the changing thermal behaviour of the occupied space due to the various non-linear, dynamic and random nature of thermal loads raises the complexity. As a result, an occupant's decision to manually operate the window(s) cannot ensure the desired thermal comfort level all the time.

Therefore, determining a solution requires a technique that adjusts the openable window area while encapsulating the complexity, dynamics, nonlinearity and randomness associated with the natural ventilation driving forces and the building's thermal behaviour. To resolve the issue of complexity and non-linearity in many challenging problems, researchers widely use and recognise artificial intelligence techniques, in particular, ANN.

In this respect, by using a co-simulation platform of TRNSYS and MATLAB, an initial investigation of this research demonstrated that the ANN-NARX technique with the model predictive intelligent window control approach might be able to actuate the windows of the naturally ventilated house for maintaining thermal comfort [146]. The preliminary findings indicated that the ANN technique appeared to be able to address

the issue of nonlinearity and complexity associated with natural ventilation, as well as to predict the thermal behaviour of the occupied space. However, the work used the simulation results from the initial un-improved building thermal model as training information and there is a level of uncertainty associated with the results. Particularly those initial results did not consider the effect of natural ventilation on the convective heat transfer behaviour of the floor.

By applying the results from dynamic simulations of the improved building model, this chapter aims to present the research on developing and applying the ANN-based model predictive technique to actuate the window and modulate the natural ventilation intelligently in order to maintain the indoor thermal comfort level. This research work included simulation results of the improved building thermal model including the specific correlation developed to model the convective heat transfer effect of wind and buoyancy on the floor of the house. Besides, this chapter also presents an extension of the technique to trigger and regulate other heating appliances as necessary to maintain year-round comfort condition of a naturally ventilated building.

## **7.2 Artificial Neural Networks**

The ANN tool provides an alternative way to tackle complex, ill-defined and nonlinear problems [147]. Researchers use ANN in the fields of approximation, modelling, prediction, classification, recognition, data compression and signal processing, particularly in engineering. This tool is also useful in physics, medicine, statistics, and economics [148]. Once trained, ANNs can perform predictions and generalisations at high speed, making them well suited for dealing with these situations [147].

The Multi Layer Perceptron (MLP), MLP ensemble, Radial Basis Function (RBF) ANN, Nonlinear auto-regressive model with exogenous input (NARX), RBFs used as NARX, Feedforward multi-layer self-growing ANN, Artificial Neuro-Fuzzy Inference System (ANFIS) types of ANN are used in ANN-MPC development of building control having HVAC system [149].

The MLP feedforward (all the signals flow from the inputs to the output) ANN structure is the most popular [148]. There is no feedback in the MLP network, and output signals are entirely calculated from the present values of input signals [149]. The MLP with only

one nonlinear hidden layer can make a Double Layer Perceptron (DLP) feed-forward ANN structure [148, 150, 151]. The DLP network can approximate any continuous function with an arbitrary degree of accuracy, provided that the number of hidden nodes is sufficient [148]. The climatologic sector widely adopts them due to their property of being able to fit measurable functions with reasonable accuracy [151].

Figure 7-1 illustrates a typical structure of a feedforward ANN. It consists of  $K$  outputs ( $y_1, \dots, y_k, \dots, y_K$ ), transferred from the  $I$  inputs ( $x_1, \dots, x_i, \dots, x_I$ ) through the hidden layers with  $J$  neurons ( $z_1, \dots, z_j, \dots, z_J$ ). Equations (7-1) and (7-2) [150] can determine the output of an ANN model.

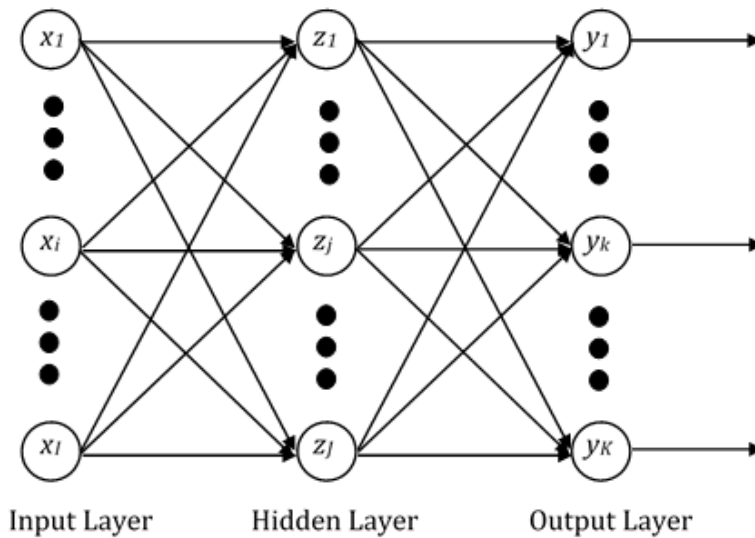


Figure 7-1. Typical structure of the MLP-ANN (adapted from [150])

$$y_k = f_y \left( \sum_{j=1}^J w_{kj} z_j + c_k \right) \quad (7-1)$$

$$z_j = f_z \left( \sum_{i=1}^I w_{ji} x_i + b_j \right) \quad (7-2)$$

Where,  $w_{kj}$  = Weight from neuron  $z_j$  to neuron  $y_k$

$c_k$  = Bias for the neurons  $y_k$

$w_{ji}$  = Weight from neuron  $x_i$  to neuron  $z_j$

$b_j$  = Bias for the neurons  $z_j$

$f_y$  &  $f_z$  = Non-linear activation functions with a sigmoid shape

The identification procedure of a neural model consists of three steps: a selection of the model structure (i.e. the choice of model inputs and the number of hidden nodes), model training (i.e. optimisation of model parameters-weights) and model validation [148]. Defining an ANN configuration requires identifying appropriate values of the weights and the biases; training the ANN [151] helps to find them. Different training methods, (nonlinear gradient optimisation, steepest descent, the conjugated gradients, the quasi-Newton variable metric or the Levenberg-Marquardt algorithm) [148], are available.

Most of the ANN's modelling works use a back-propagation learning algorithm [147, 150, 151, 152, 153, 154] for climate forecasting or for PMV computation research. It is a supervised iterative training method based on searching the global minimum in the error surface, i.e. the difference between the ANN's output and the target, as a function of the ANN's weights and biases using the gradient descent approach [150, 151]. The errors help to backwardly adjust each weight, starting from the output layer, through the hidden layer, toward the input layer [151]. The weights (initialised with random values), change during the training phase to minimise the Mean Square Error (MSE) between the ANN and the target output [151].

The ANN-based technique can address the complexities and nonlinearity associated with natural ventilation for optimising the size and location of windows and also for evaluating the airflow through a naturally ventilated test set up [64, 65, 67]. Similarly, Atthajariyakul and Leephakpreeda [150, 155] used an ANN to compute the PMV of a HVAC system and real-time determination of optimum indoor air for air quality, energy-efficiency and optimum thermal comfort condition. In their work of predicting PMV, researchers [150] approximate mean radiant temperature by global temperature and water vapour pressure by relative humidity. Another study [156] also corroborated the capability of modelling thermal comfort PMV of building using the ANN technique.

Previous studies [69, 70] have successfully demonstrated the use of ANNs for predicting and controlling the indoor building environment, typically the air temperature in a closed occupied space. ANN models are suitable for modelling building dynamics due to their ability to deal with nonlinear, multivariable modelling problems [157]. In achieving this, the researchers used an ANN technique to predict solar radiation and the outdoor air temperature. In other studies [158, 159], researchers used the ANN technique to assess predictive control of multizone HVAC systems in non-residential buildings and also to estimate PMV to apply model-based predictive control of HVAC systems. The recurrent neural network is ANN that uses previous input and output signals [149, 157]. This can be applied to many dynamic systems [149, 157], including building. NARX is a type of recurrent network that uses previous input and output signals formed by passing them through time-delay networks before connecting to the network inputs [149, 157]. NARX has feedback connections enclosing several layers of the network [149]. In a naturally ventilated building, the wind (speed and direction), air temperature and relative humidity are also influential climatic parameters affecting indoor thermal comfort. Forecasting these climate variables for the short-term is essential from a control perspective. The ANN tool with MLP input-output mapping approach and backpropagation or Levenberg-Marquardt learning algorithm are used for predicting external climatic variables [69, 70, 151, 152, 153, 154, 160, 161, 162]. Similarly, a recent study for forecasting time series global solar irradiance in NZ locations verified the applicability of the neural network technique with specific reference to Nonlinear Autoregressive with Exogenous Input (NARX) ANNs [163].

The thermal behaviour of naturally ventilated residential house is dynamic and highly nonlinear, involving many uncertainties of parameters. Simple physical models cannot capture the actual dynamics of the system. Since ANNs are nonlinear, they can learn sophisticated mappings between inputs and outputs and can be chosen to model in this work. In the case of a building, the system's output (indoor air temperature) is highly dependent on the previous temperature. The NARX structure is also recognised to have a better performance in learning long-term dependencies than the other structures of ANN [164]. In 2018, Erfani et al. demonstrated a non linear model predictive controller for optimising a multi zone air handling unit [164]. Similarly, Yang et al. also used NARX recurrent neural network-based approximate MPC for energy-efficient building

control without solving the optimisation problem that otherwise could have required significant computational power for finding optimum signal [165].

In this respect, an initial investigation of this research demonstrated that the ANN technique with the NARX approach could predict a time series of the occupied space air-temperature of a naturally ventilated house [166]. While doing this, the author considered the non-linearity and dynamics of the relevant weather quantities, random occupancy, and discrete values of WOF as input quantities to successfully model the ANN and predict the time series of the indoor air temperature. In addition, reviewing the housing stock of NZ [2, 3], the author revealed a considerable nonlinearity prevailing in building fabric and envelope airtightness of residential houses in NZ. Therefore, the author further demonstrated that the ANN-NARX technique could predict the occupied space indoor air temperature time-series of the naturally ventilated house irrespective of any envelope thermal resistance and airtightness level [131, 146]. This review indicates that the ANN-NARX approach can forecast both external and internal climate variables and also could help establish a base for controlling indoor conditions.

### 7.3 Methodology

To predict the occupied space air-temperature time-series, the author develops an ANN model in MATLAB using the NARX [167] approach, similar to that described by [163].

Figure 7-2 illustrates a typical series-parallel architecture of ANN-NARX technique.

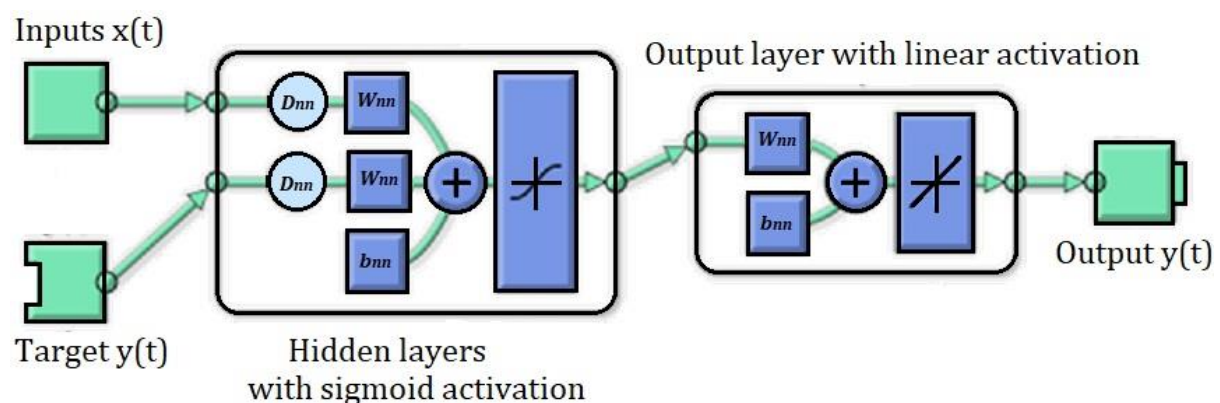


Figure 7-2. A typical ANN-NARX structure

To do this, the work investigates the possibility of predicting future values of a time series  $y(t)$  from  $d'$  past values of that time series and  $d'$  past values of another time series  $x(t)$  as shown in Equation (7-3) [167].

$$y(t) = f(y(t-1), \dots, y(t-d'), x(t-1), \dots, (t-d')) \quad (7-3)$$

### 7.3.1 Developing ANN-NARX model of the house

To develop the ANN, the author eliminates the input quantities having low correlation with the indoor air temperature so that the final ANN model is as simple as possible without compromising the accuracy. The final NARX model comprises a set of time series databases of hourly values of different input quantities, as shown in Table 7-1. Similarly, the hourly values of the indoor room air temperature predicted by the TRNSYS simulations forms the database for the target time series.

Table 7-1 Input quantities for the ANN model

Input quantities	Unit	Abbreviation	Range
Outdoor temperature	°C	$T_o$	-
Wind speed	m/s	$V_m$	-
Wind direction	°	$\phi$	0-360
Outdoor relative humidity	%	$RH_o$	0-100
Window opening factor		WOF	0, 0.25, 0.5, 1
Envelope airtightness	ACH	UAT, AT, LKY	0.03, 0.3, 0.7
Hour of the day		$HRS$	0-23
Global horizontal radiation		$GHR$	-
Random number of occupants		$OCC$	0-5
Weighted average envelope thermal resistance		$R_{avg}$	2.01, 2.6, 3.44

Subsequently, the author divides the input and target vectors randomly into three sets such that 70% of the data refers to the network for training, 15% for validation and 15% for generalisation. In performing the training, the author implements the Levenberg-Marquardt algorithm in a bid to fit the input and target. While doing this, the work constructs the first network considering default values for the number of hidden layers (10) and delays (2). Illustrating the Regression (R) values, Figure 7-3

demonstrates the performance of training, validation, and testing, of the NARX model with default NARX architecture.

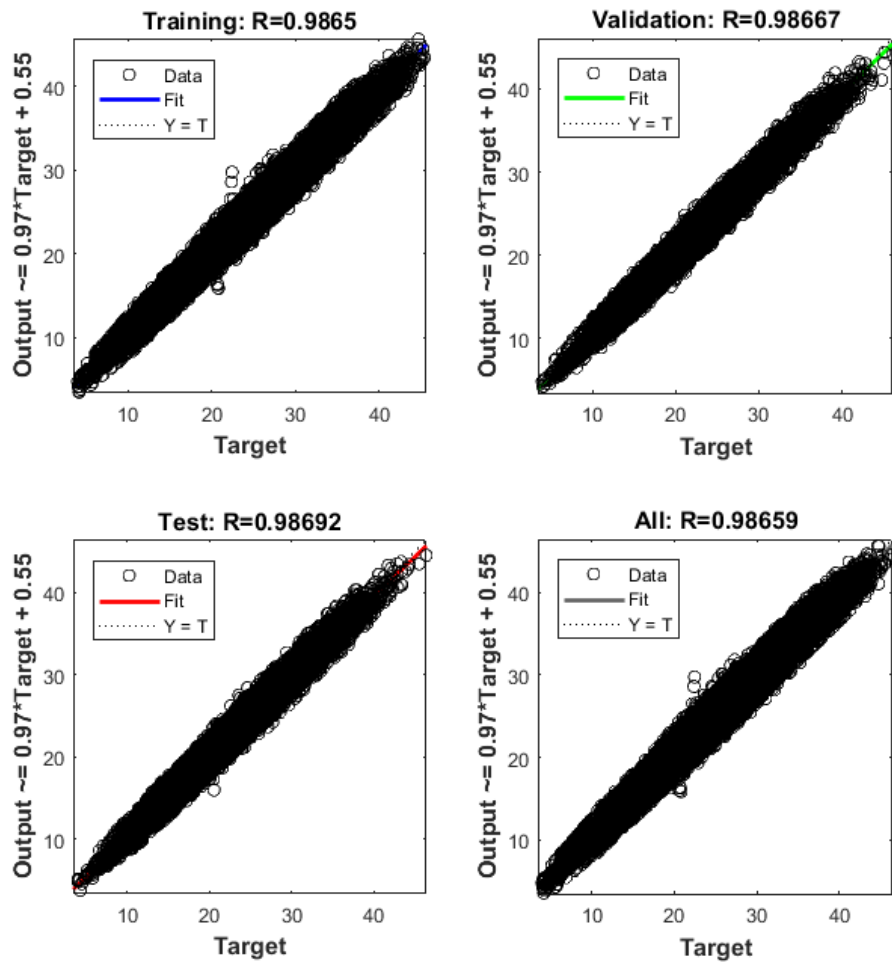


Figure 7-3. Neural network performance with default architecture

### 7.3.2 Optimising the architecture of the ANN-NARX model

Despite the excellent performance demonstrated by the default values, to identify the most appropriate values of hidden layers and delays for the proposed NARX network, a sensitivity study was carried out with various combinations of their values. While doing this, the author accesses the average values of the R and corresponding MSE for each combination of hidden layers and delay for at least three training runs. The work ensures that the maximum threshold of MSE is less than 1.5 as demonstrated in Figure 7-4.

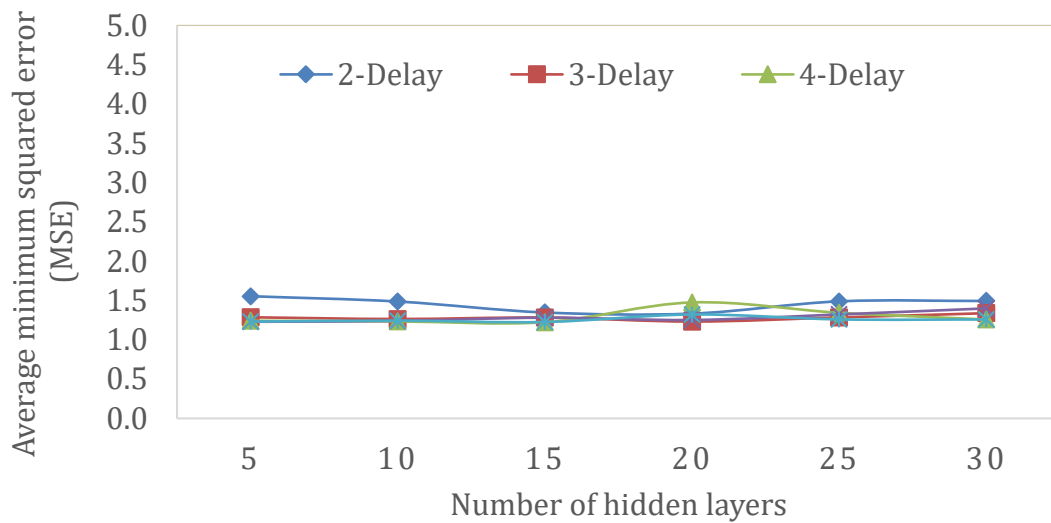


Figure 7-4. Sensitivity of average minimum squared error values for different values hidden layers and delays

Now, increasing both the number of hidden layers and delays results in better performance (R close to 1) as demonstrated in Figure 7-5.

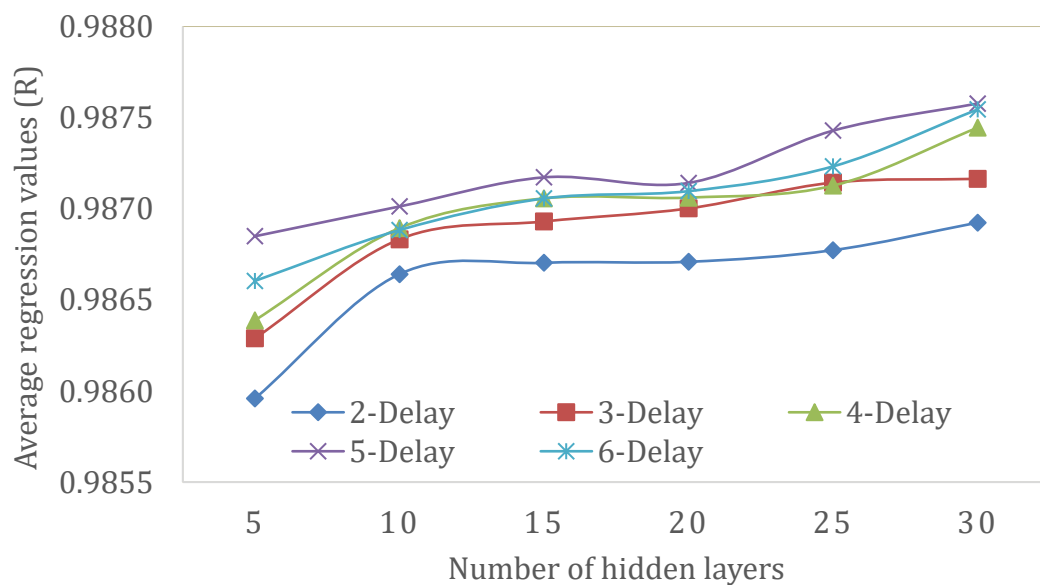


Figure 7-5. Sensitivity of average regression values for different values hidden layers and delays

However, this is offset with the expense of increased time required for the training as demonstrated in Figure 7-6; and it also increased likelihood of overfitting the network.

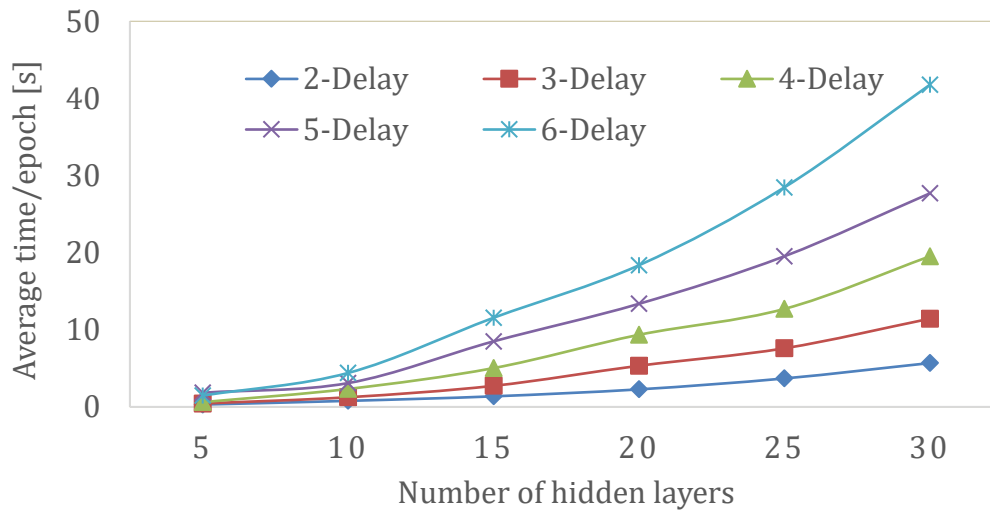


Figure 7-6. The sensitivity of training time for different values of hidden layers and delays

The research work further verifies the architecture for an additional set of the database (not used before for initial training purposes). In particular, the envelope airtightness (AVG & DTY), and envelope resistance ( $R_{avg}$  2.6 and 3.44) for WOF values of 0.125, 0.25 and 0.75 for this additional verification. The results, as demonstrated in Figure 7-7, indicate that the average regression values with this additional verification though are slightly lower than the values achieved during the initial training phase (Figure 7-5) with average regression values (0.978-0.98) in terms of forecasting capability of the ANN function. Besides, we can observe the falling average regression values for the relatively higher hidden number of layers and delays (Figure 7-7) recognising that increasing the number of hidden layers does not necessarily improve respective regression values or the predictability of the ANN function.

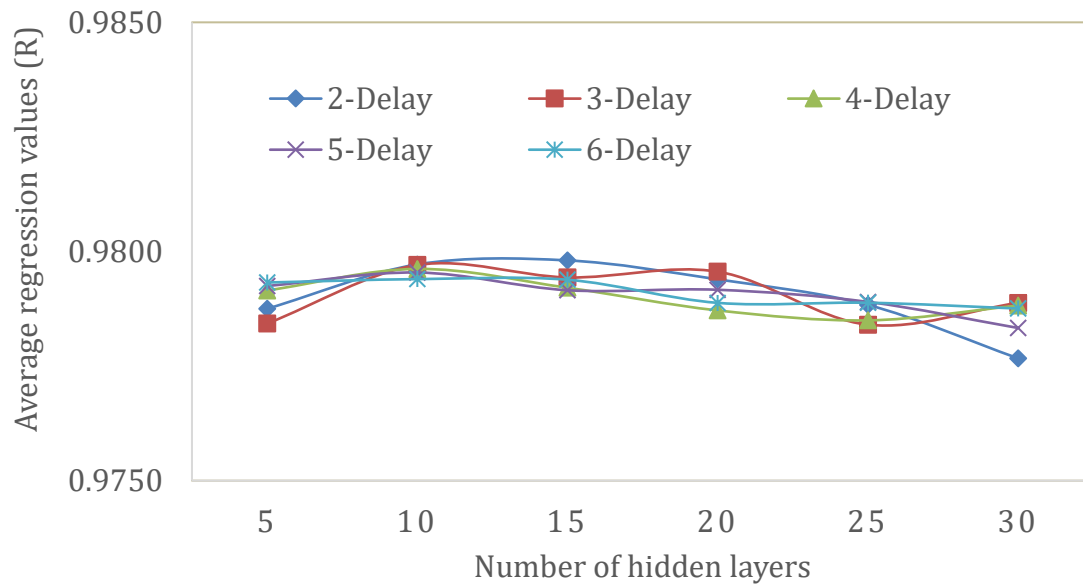


Figure 7-7. The sensitivity of regression values of supplementary tests for different values of hidden layers and delays

Therefore, considering a balance between the times required for the training and achievable performance, the research considers an ANN-NARX open-loop (series-parallel) architecture, as shown in Figure 7-8, with 15 hidden layers and 5 delays for further assessment. While doing the network training to minimise the MSE, the weights- $W_{nn}$  and biases- $b_{nn}$ , are optimised as illustrated in Figure 7-8.

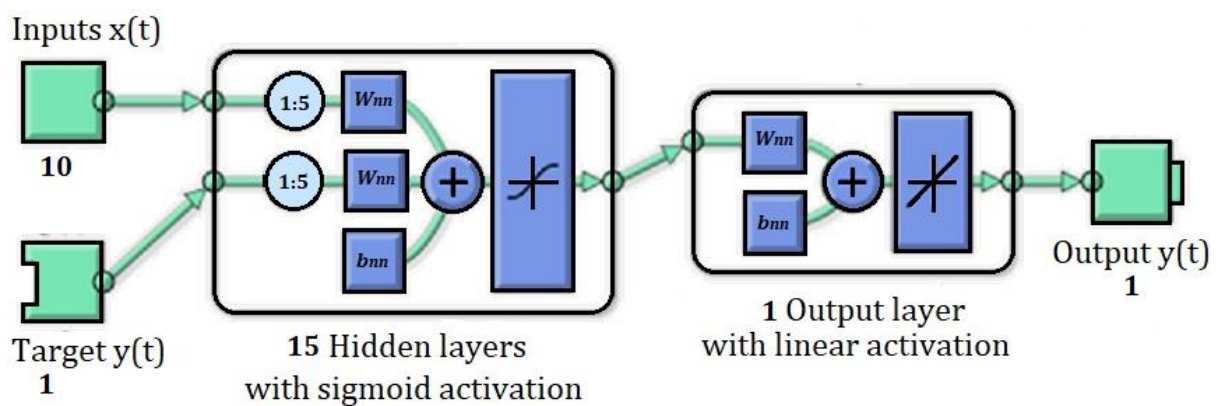


Figure 7-8. The optimum neural network architecture

### 7.3.3 Applying the ANN-NARX model predictive control strategy

By reversing the operation of the ANN (i.e., determining the WOF required to achieve a desired indoor temperature with given ambient conditions), the research conceptualises a controller based on the simple model predictive control concept with a one-time step ahead prediction. The concept is implemented by co-simulating the developed ANN and the coupled thermal-airflow models of the naturally ventilated house by calling a MATLAB program to execute the ANN model from TRNSYS model as demonstrated in Figure 7-9.

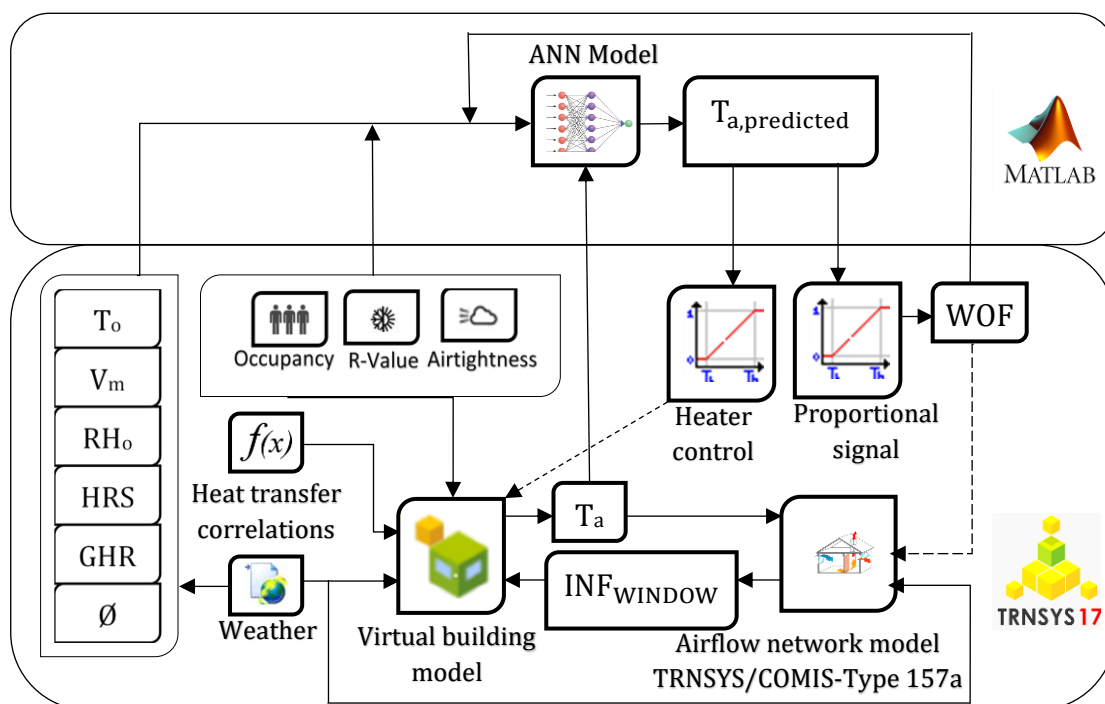


Figure 7-9. A schematic demonstrating the co-simulation strategy of ANN and coupled thermal & airflow model

While doing this, the predicted value of the room air temperature from the ANN model is compared with the desired indoor room temperature setpoint such that it generates a proportional control signal. The control signal is then used to define the value of WOF for the next time step in the coupled thermal and airflow model. It helps optimally adjust the WOF in advance while obtaining the desired indoor temperature.

## 7.4 Results and Discussion

### 7.4.1 Examining the predicting capability of air temperature time series by ANN

Having developed the coupled thermal-airflow model leading to the ANN-NARX model of the naturally ventilated building, the research work explores how well the ANN model predicts the indoor room temperature in comparison to the coupled thermal-airflow model developed in the TRNSYS. Initially, the ANN model is trained with the hourly input and target values corresponding to the WOF (0, 0.25, 0.5 and 1), average envelope thermal insulation ( $R_{avg}$  2.01,  $R_{avg}$  2.6 and  $R_{avg}$  3.44) and envelope airtightness level (LKY - 0.7, AT - 0.3 and UAT - 0.03) ACH for a year. As the generated function is the core for the deployment of the control concept, the robustness of the function requires verification. It ensures a further use of the function for any value of WOF, airtightness and  $R_{avg}$  within the upper and lower threshold of the respective variables defined in the model.

Figure 7-10 and Figure 7-11, illustrate the time series of the indoor air temperature generated by both models with WOF values of 0.75 and 0.4, respectively. In saying this, it considers  $R_{avg}$  3.2 and AVG house for the first week of January and July as representative months at the peak summer and winter respectively.

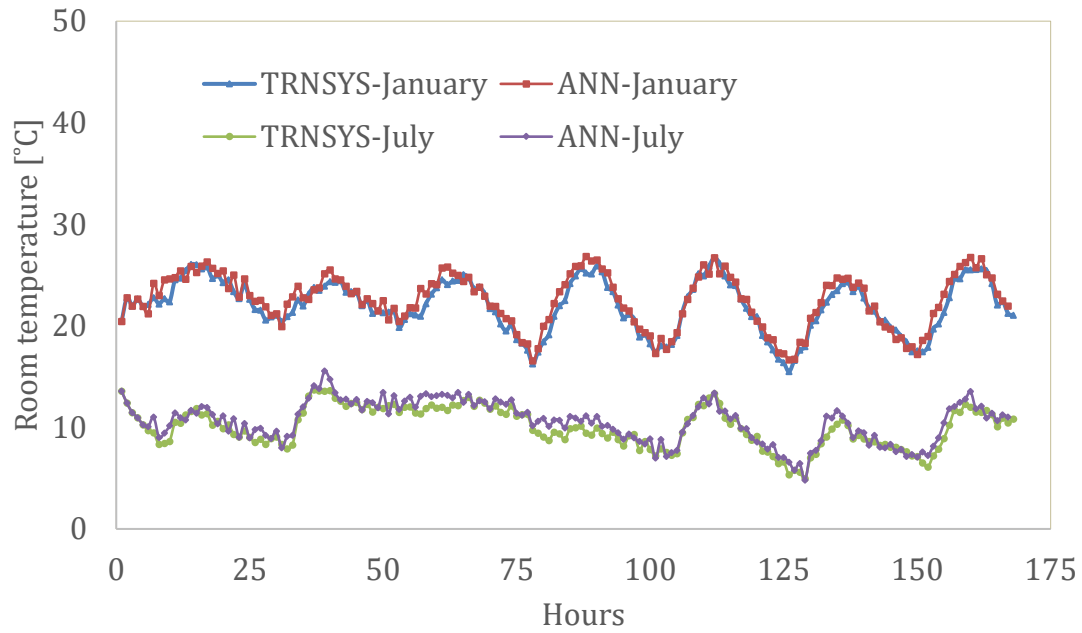


Figure 7-10. Indoor air temperature from the ANN and TRNSYS model (WOF 0.75, AVG house with  $R_{avg}$  3.2, first week of January and July)

Both Figure 7-10 and Figure 7-11 demonstrate that the predicted time series from the ANN model agrees quite well with the time series generated by the TRNSYS thermal model of the house. This confirms that the prediction capability of the ANN model for the indoor room air temperature is quite reliable at a relatively higher value of WOF 0.75 and also at a medium value of 0.4.

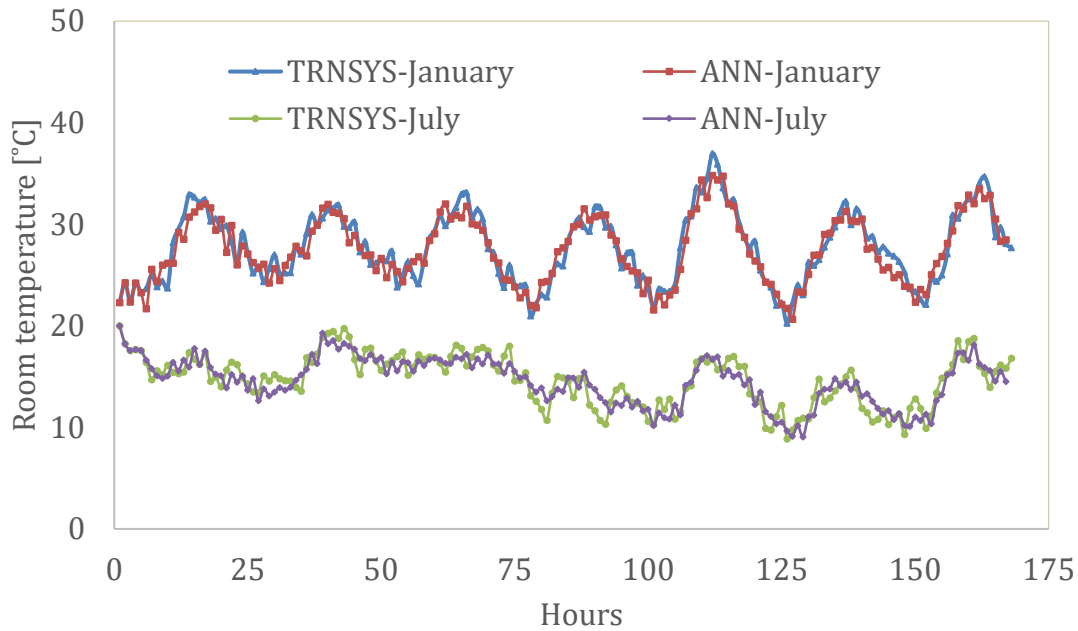


Figure 7-11. Indoor air temperature from the ANN and TRNSYS model (WOF 0.4, AVG house with  $R_{avg}$  3.2, first week of January and July)

By exploring this further, a comparison of time series of the indoor air temperature generated by both models for WOF values of 0.1 for the first week of January and July is shown in Figure 7-12 as a representation of peak summer and winter respectively. Figure 7-12 again demonstrates that the predicted time series from the ANN model matches the time series generated by the thermal model of the house in TRNSYS. It re-confirms that the prediction capability of the ANN model for the indoor room air temperature is quite reliable even for small opening areas (WOF = 0.1), where the balance of the inward and outflow from the space is restricted and thus increases the nonlinearity.

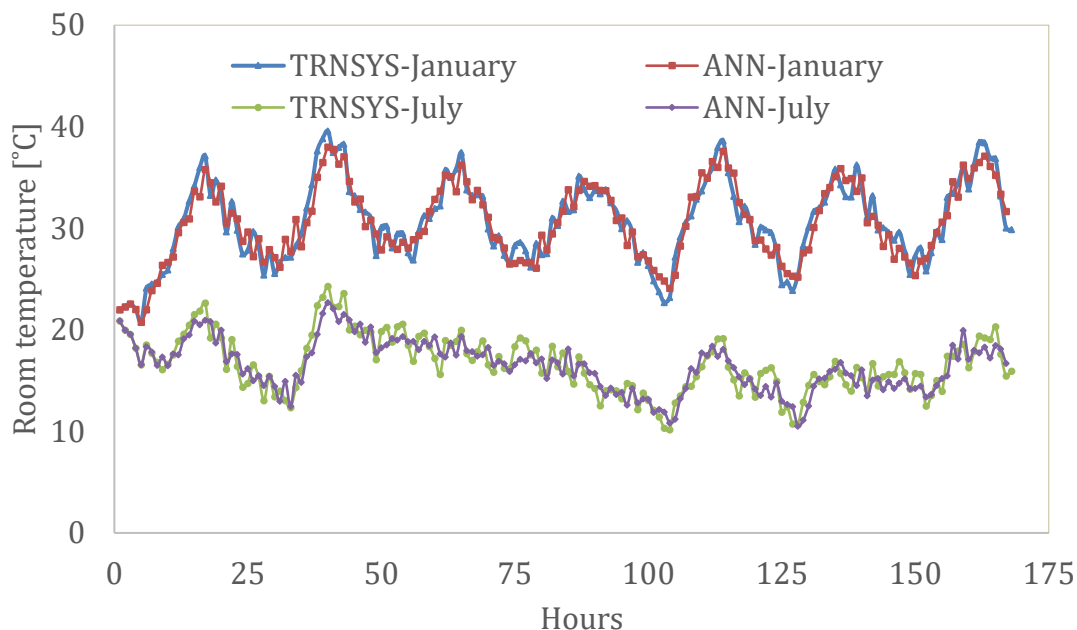


Figure 7-12. Indoor air temperature from the ANN and TRNSYS model (WOF 0.1, AVG house with  $R_{avg}$  3.2, first week of January and July)

To illustrate the reliability of the prediction for an extended period, covering entire months and throughout the year, the work extends comparisons for January, July, April, and October representing different seasons for a UAT house with  $R_{avg}$  3.2 for a value of WOF 0.1. As expected, the time series of the indoor room temperature produced from the TRNSYS model is in excellent agreement with the time series created from the ANN model as shown in Figure 7-13 as a representative month of October. It illustrates that the prediction holds exceptionally well for an extended period and throughout the year for the smaller opening area.

Further investigations show that an increased opening area of WOF values of (0.4 and 0.75) correlates even better. Thus, it confirms that the prediction holds exceptionally well for any opening area with better prediction at higher values of WOF throughout the year.

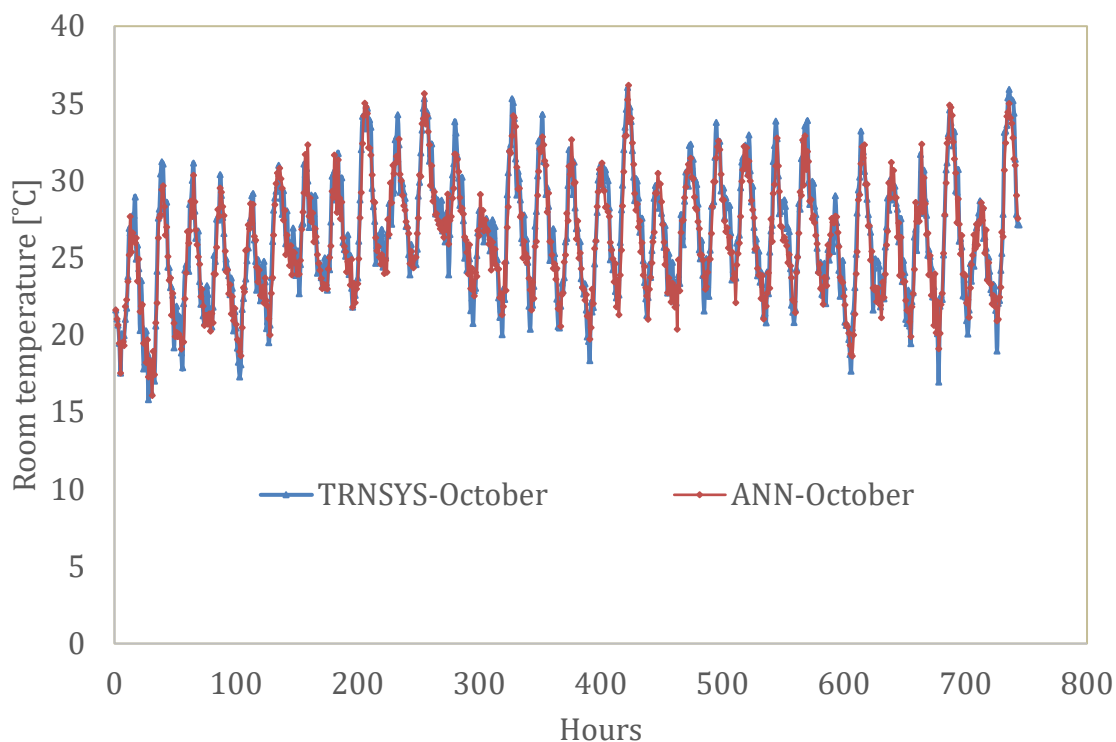


Figure 7-13. Indoor air temperature from the ANN and TRNSYS model (WOF 0.1, UAT house with  $R_{avg}$  3.2, October)

ANN is well known for solving complexity and non-linearity issues; this work once again successfully demonstrates that the ANN technique, as a black box, can predict the indoor air temperature time-series for the differently airtight and insulated naturally ventilated occupied space. Thus, applying its excellent prediction ability, we can conceive the ANN-based model predictive intelligent window control strategy for the next generation of sustainable, naturally ventilated residential houses.

The prediction of the time series of zone air temperature from the proposed ANN-NARX model is adequate for actuating windows of the naturally ventilated house irrespective of any value of WOF and time of a year, building envelope airtightness and thermal resistance value. The performance depends on the extent of robust information trained from the thermal model. The enrichment of the ANN-NARX model regarding training, including various operating conditions, different geometries, size and location of windows and orientation is necessary for an improved and more comprehensive predictive model. However, in summary, the use of ANN appears to offer a positive outlook in the development of intelligent control of actuated windows in naturally ventilated buildings.

### 7.4.2 Applying the ANN-NARX model for intelligently actuating a window

Given the satisfactory outcome of the ANN model for predicting the indoor air temperature of the naturally ventilated house, this work investigates the potential for it to perform an intelligent control concept. In particular, to actuate windows of a naturally ventilated house by applying the co-simulation strategy as demonstrated earlier in Figure 7-9. As such, the work further co-simulates the model houses with different combinations of airtightness level and  $R_{avg}$  values. Figure 7-14 demonstrates the window actuator performance for a typical day in January for an AVG house with  $R_{avg}$  3.2. The Figure 7-14 shows that how the regulation of the values of the WOF between 0 and 1 modulates the natural ventilation (infiltration) to help to sustain the indoor room temperature ( $T_a$ ) around the desired indoor set point of 24°C.

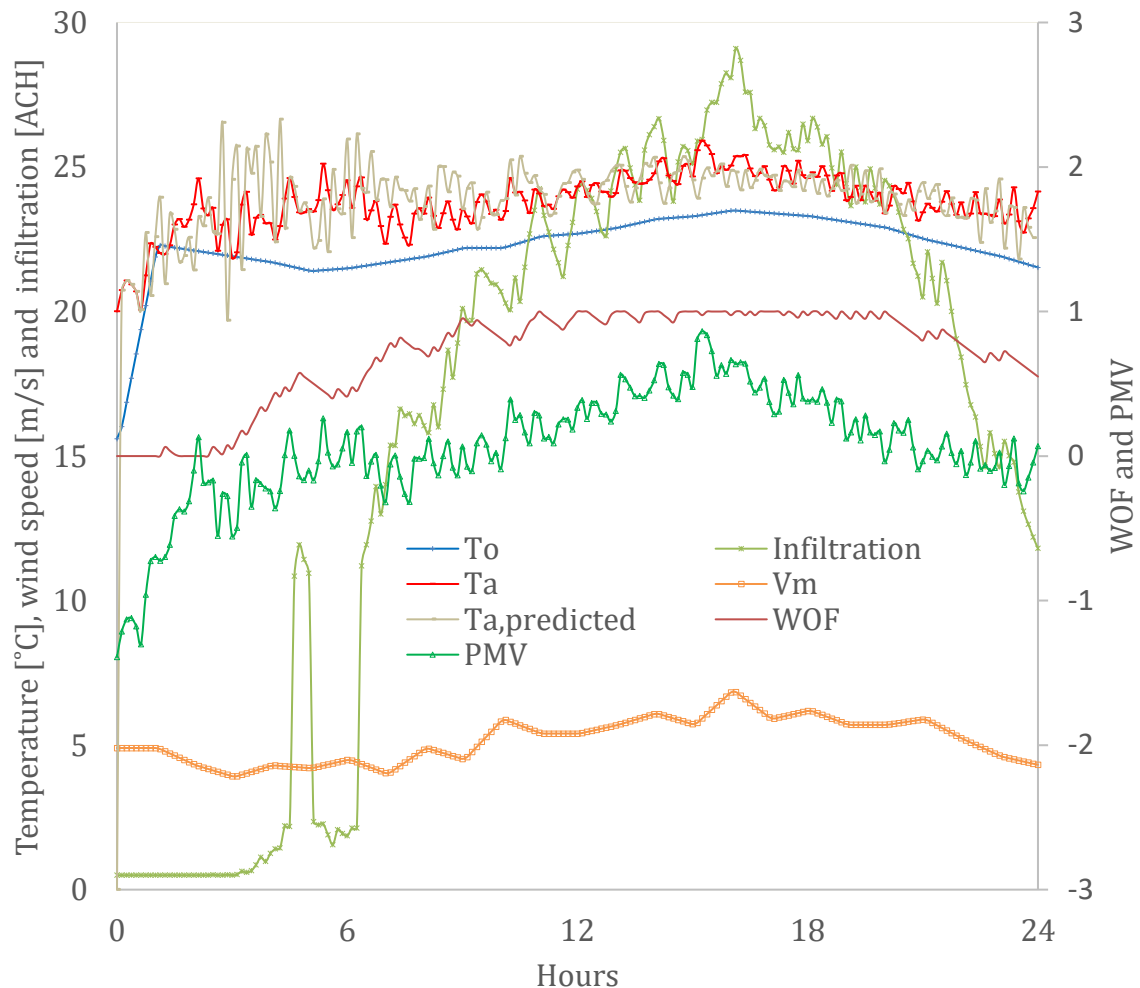


Figure 7-14. Actuator performance for the model (AVG house with  $R_{avg}$  3.2) for a typical day in January

By keeping the settings of envelope thermal resistance and airtightness intact, the research work extends the co-simulation of the thermal and the ANN model for the first week of January, to observe the actuator performance for an extended period. The resulting frequency distribution as shown in Figure 7-15 illustrates that the implementation of the actuator can alone achieve maintaining of the thermal comfort level ( $-0.7 < PMV < 0.7$ ) of the model house in 96% of the instances.

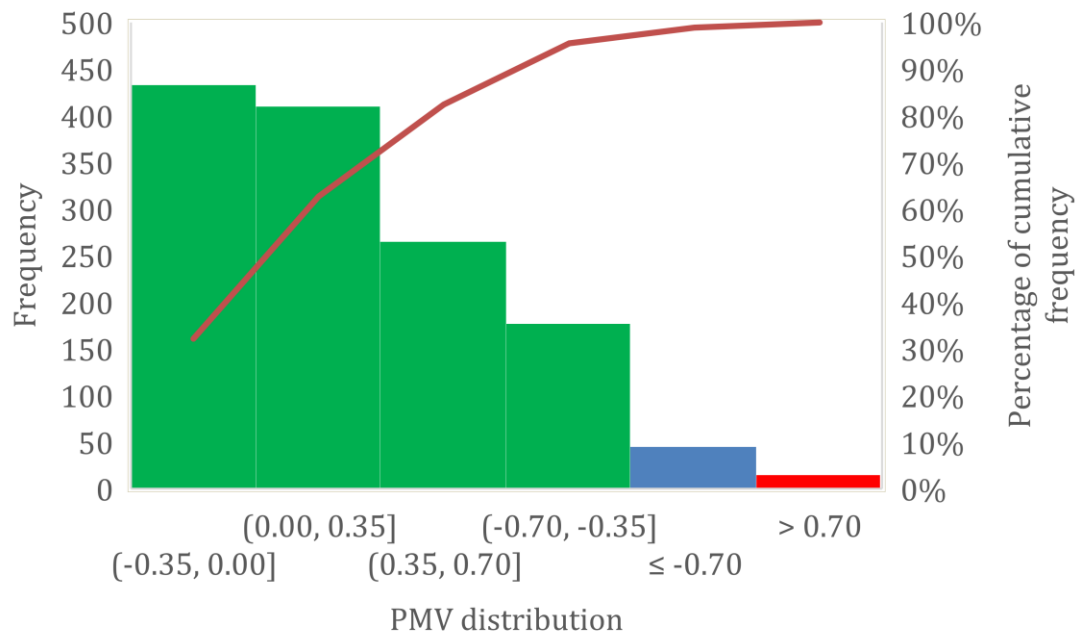


Figure 7-15. Frequency distribution of PMV after using window actuator (AVG house with  $R_{avg}$  3.2 for first week of January)

The lower and upper set points of the input values for the proportional signal generator are fixed at indoor room air temperatures of 23.5 and 24.5 respectively so that it generates respective proportional WOF values between 0 and 1. Besides, the research considers a relatively small time step size of 7.5 minutes as an optimum value from a sensitivity study on the time-step interval producing the best performance.

Comparing the performance of the window actuator driven by ANN system with respect to different discrete settings of WOF values of 0, 0.125, 0.25, 0.5, 0.75 and 1, Figure 7-16 demonstrates a frequency distribution of PMV values (maximum 60 % within  $-0.7 < PMV < 0.7$  range) for WOF value of 0.75.

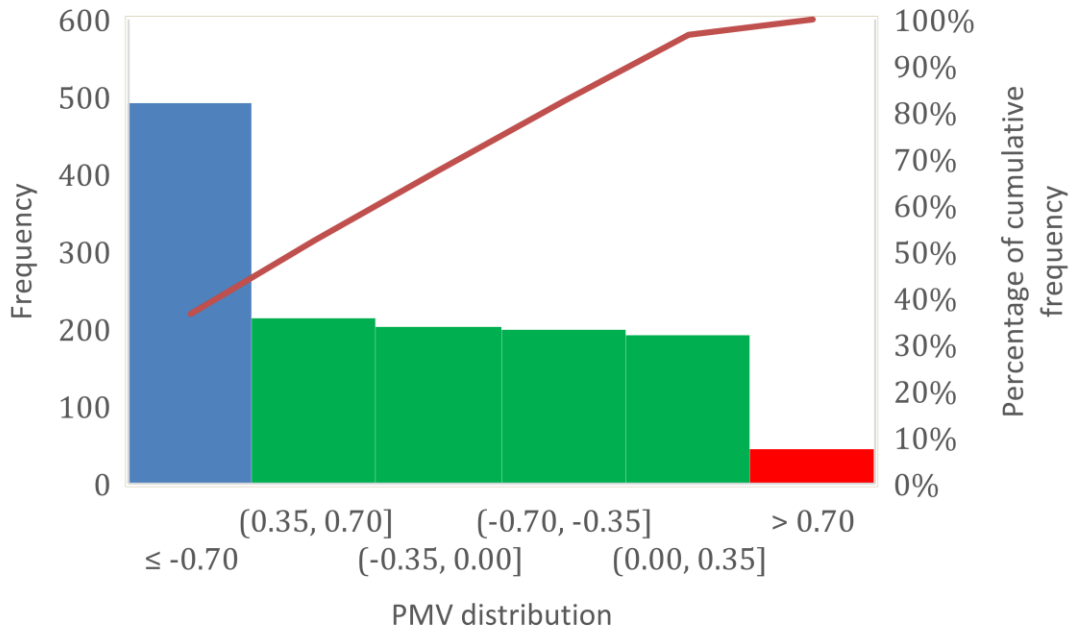


Figure 7-16. Frequency distribution of PMV for fixed WOF 0.75 (AVG house with  $R_{avg}$  3.2 for first week of January)

Similarly, Table 7-2 lists the percentage of thermally comfortable instances for different discrete values of WOF for the AVG house with  $R_{avg}$  3.2. In comparing this, exactly similar settings (including time step size of 7.5 minutes) and input values were ensured.

Table 7-2. Comfort period proportion for different values of WOF and window actuation (AVG house with  $R_{avg}$  3.2 for first week of January)

WOF	Window Actuation	Comfort period Proportion ( $-0.7 < PMV < 0.7$ ) [%]
1	OFF	58.6
0.75	OFF	60.1
0.5	OFF	41.7
0.25	OFF	21
0.125	OFF	10
0	OFF	8.2
Varies between 0 and 1	ANN model predictive control actuation	95.6

Figure 7-17 illustrates the effectiveness of the intelligent window actuation across the entire range of envelope airtightness for envelope thermal resistance of  $R_{avg}$  3.2 for first week of January). The figure reveals that the performance maintains a high level of comfort duration ( $\approx 96\%$ ) for window control (WC) case irrespective of changes in envelope airtightness. This result further corroborates the fact that the intelligent window actuation can have a considerable potential to improve the comfort period compared to any discrete window opening case of WOF values of 0 to 1, as shown.

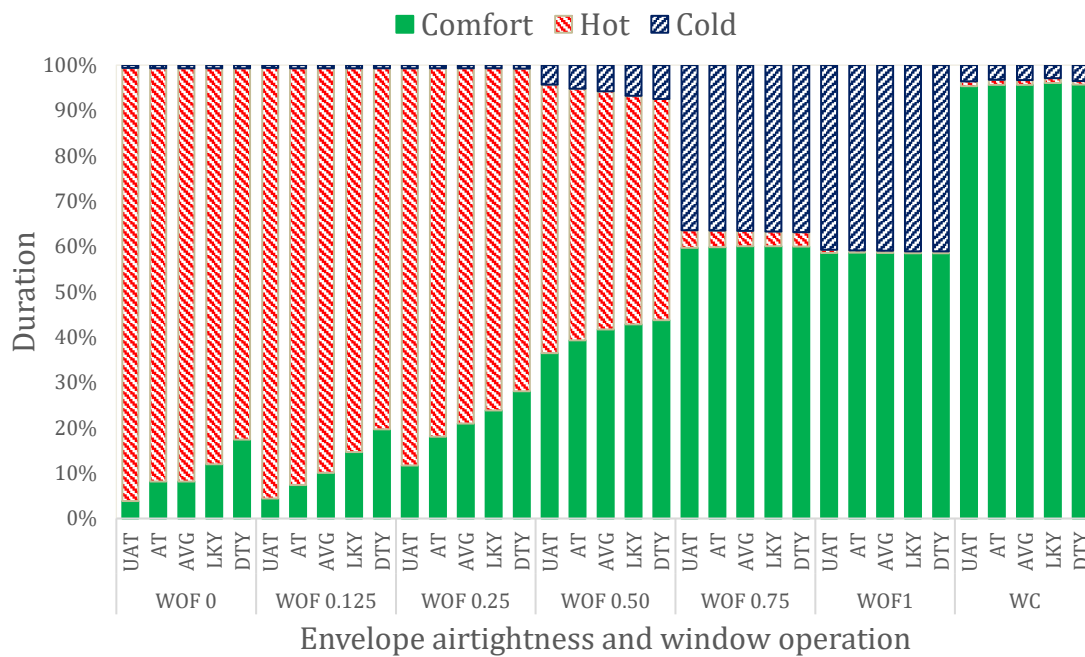


Figure 7-17. Thermal comfort distribution of house ( $R_{avg}$  3.2) with and without window control for first week of January

Similarly, Figure 7-18 presents the performance of intelligent window actuation performance for a typical day of peak winter July. However, WOF value remains 0 (window shut) position throughout the day because the ANN model predictive control system always forecast the indoor temperature to be below the lower minimum set point of  $23.5^{\circ}\text{C}$  during the evaluation period of the day.

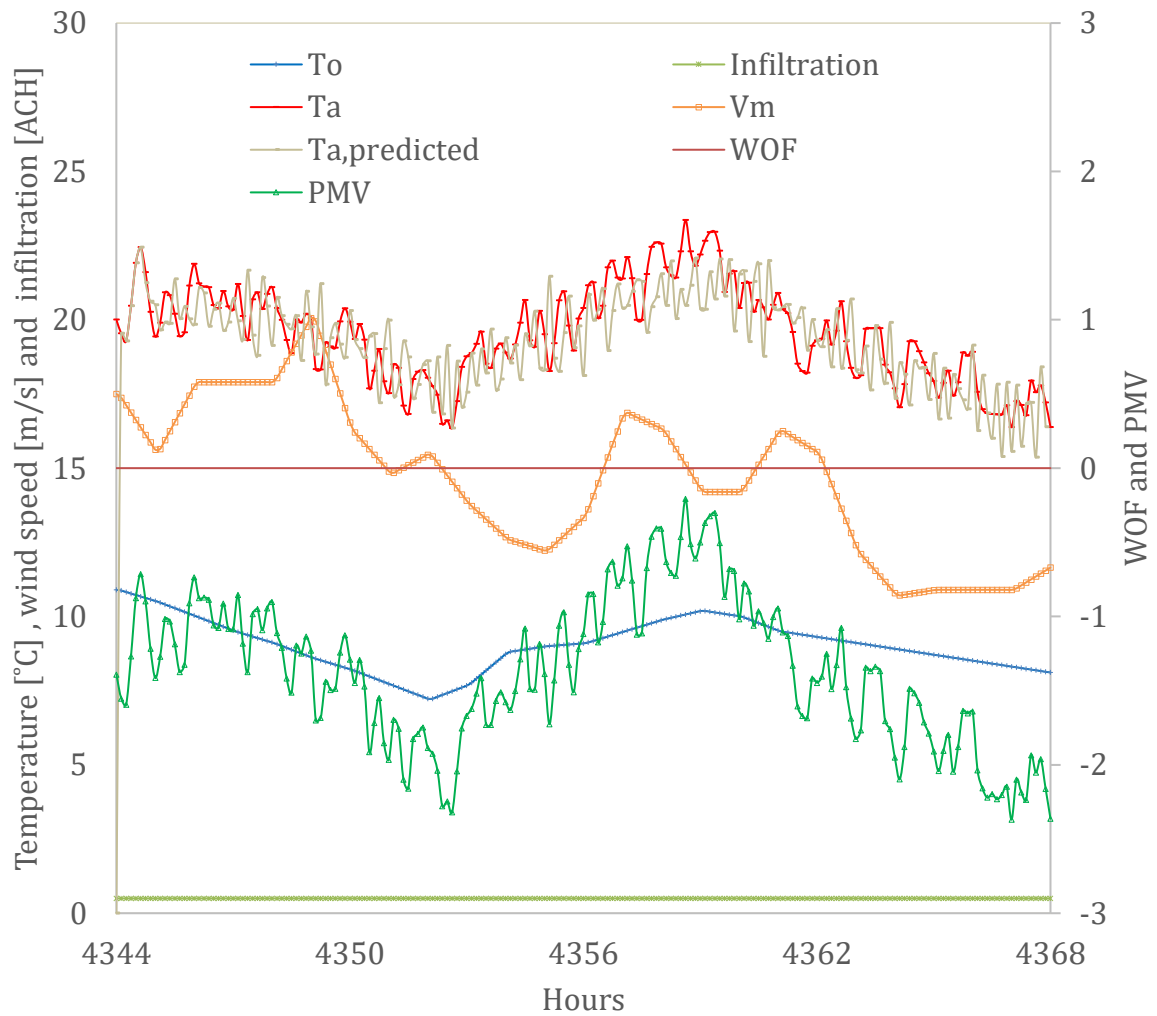


Figure 7-18. Actuator performance for the model (AVG house with  $R_{avg}$  3.2) for a typical day in July

Figure 7-19 also presents the extension of the simulation results for entire duration of the first week of July. It demonstrates that 98.14 % of the evaluated period remains at thermally uncomfortable cold condition ( $PMV < -0.7$ ) and 1.83% belongs to thermal comfort condition ( $0.7 < PMV < 0.7$  range). It also indicates the fact that there are no instances related to thermally uncomfortable hot duration ( $PMV > 0.7$ ).

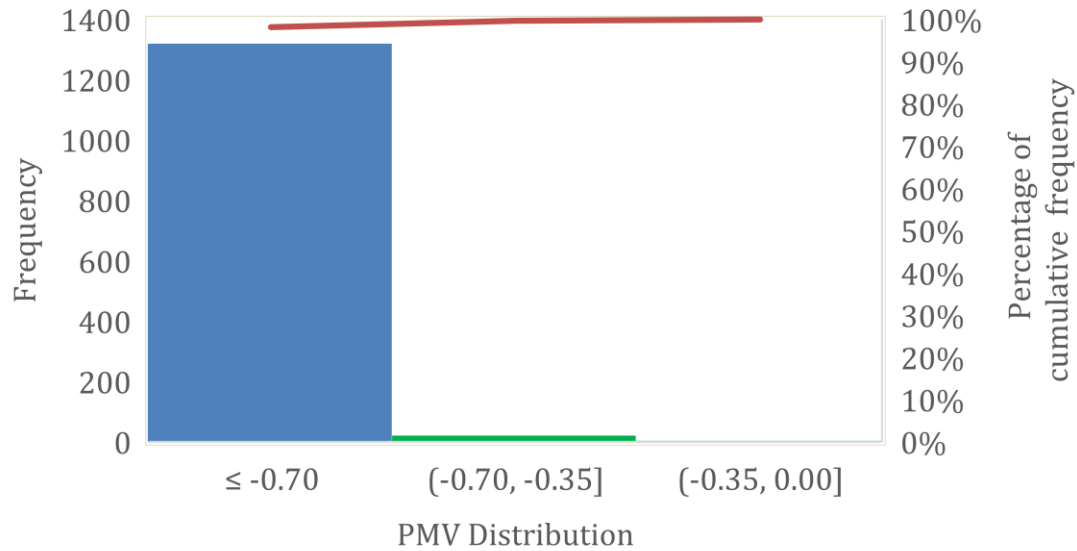


Figure 7-19. Frequency distribution of PMV after using window actuator (AVG house with  $R_{avg}$  3.2 for first week of July)

In contrast to this result, Figure 7-20 presents simulation results of a base case operation of an AVG airtight house with envelope thermal resistance of  $R_{avg}$  3.2 whereby window always remains in shut position (WOF 0) for the entire duration of the first week of July.

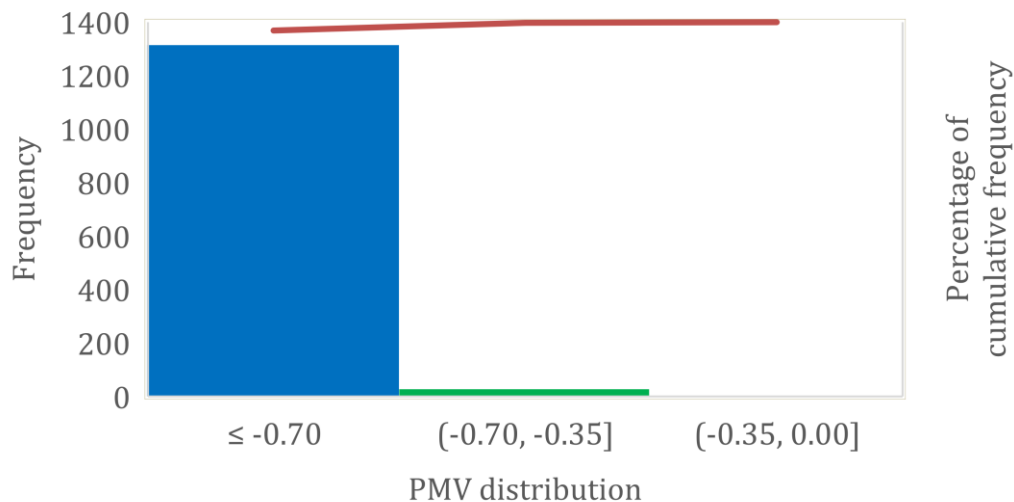


Figure 7-20. Frequency distribution of PMV with window shut (WOF value 0) of the model (AVG house with  $R_{avg}$  3.2 for first week of July)

It demonstrates that 97.7 % of the evaluated period remains at a thermally uncomfortable cold condition ( $PMV < -0.7$ ) and 2.23% belongs to thermal comfort condition ( $0.7 < PMV < 0.7$  range). It also indicates the fact that there are no instances related to thermally uncomfortable hot durations ( $PMV > 0.7$ ). Opening the window (WOF values  $> 0$ ) worsens the base case situation with further increase in the period of the thermally uncomfortable cold condition ( $PMV < -0.7$ ).

Figure 7-21 demonstrates the effectiveness of the intelligent window actuation across the entire range of envelope airtightness for envelope thermal resistance of  $R_{avg}$  3.2 for first week of July). The figure reveals that the thermal comfort duration does not improve for Window Control (WC) case as compared to any of the fixed window opening case (WOF values  $\geq 0$ ) irrespective of change in envelope airtightness in peak winter months.

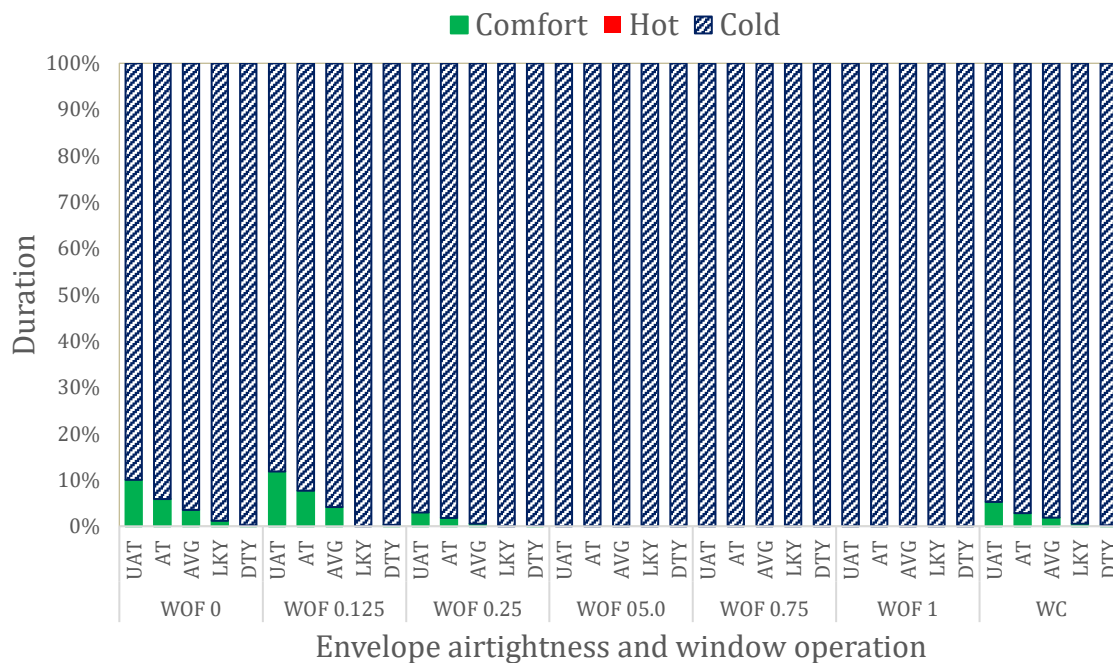


Figure 7-21. Thermal comfort distribution of house ( $R_{avg}$  3.2) with and without window control for first week of July

Figure 7-22 demonstrates the effectiveness of the intelligent window actuation across the year for the AVG house with envelope thermal resistance of  $R_{avg}$  3.2 for the first week of each month. The figure reveals that the performance of the window actuation

system in terms of its ability to maintain thermal comfort condition of the model house is maximum ( $\approx 96\%$ ) on peak summer month of January and gradually reduces to a minimum ( $\approx 2\%$ ) in the peak winter month of July.

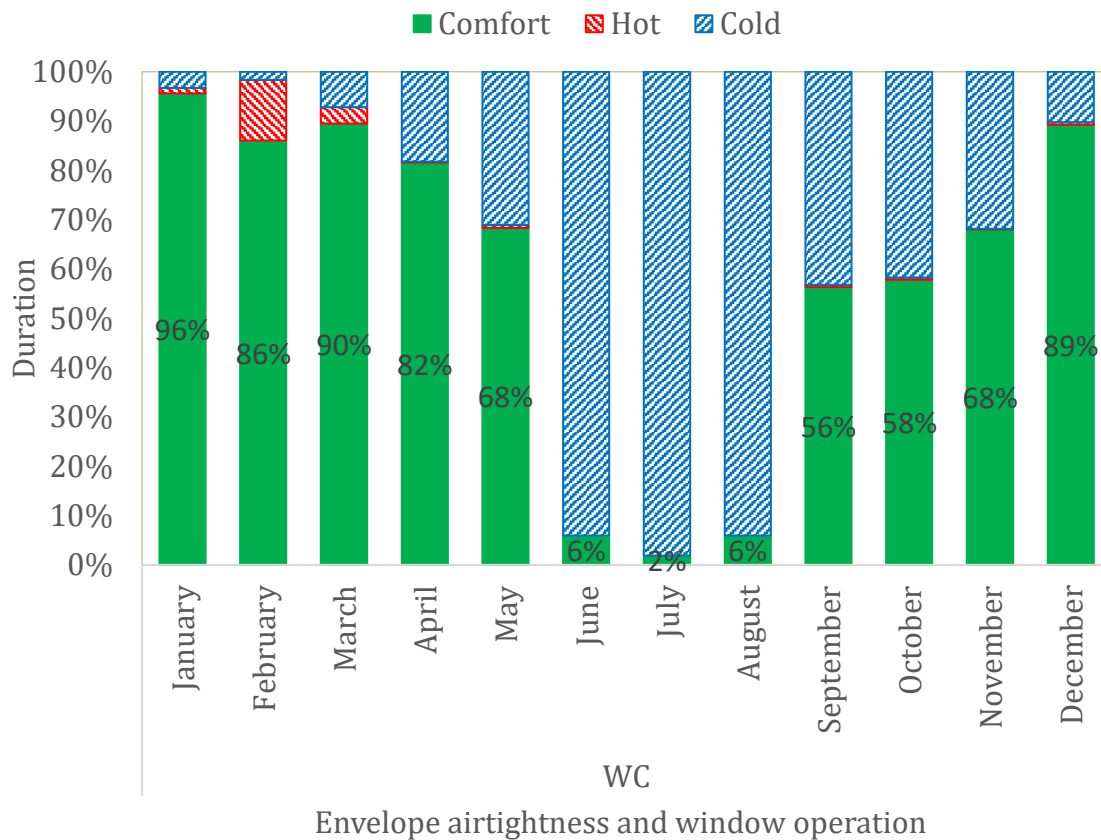


Figure 7-22. Impact of window control on thermal comfort distribution of house (AVG house with  $R_{avg}$  3.2 for first week of each month)

These results illustrate that natural ventilation can help in maintaining a comfortable indoor room temperature in a summer season by using the outside air free cooling potential. The comfort duration of the house gradually decreases as the summer season transition to shoulder and then to the winter period. The outdoor free cooling is not required to maintain indoor thermal comfort condition in the peak winter period.

In summary, the intelligent window actuation possesses a significant potential of maintaining thermal comfort in summer season for a typical average thermally insulated and airtight house located in a temperate climatic region like Auckland, NZ. In comparison to the basic scenario of window operating in fixed window position

throughout a typical day without any window actuating automation (manual or controlled) resulting in a maximum of 60% thermal comfort duration, the intelligent window actuation system can ensure the thermal comfort for 90% of the peak summer period (December to March). However, as the summer season transitions to shoulder and finally to the winter season, the role of intelligent window actuation system gradually reduces and becomes completely redundant for maintaining indoor thermal comfort conditions during the peak winter period. Nevertheless, the intelligent actuation system ensures that the window remains shut position during the winter period as there is no potential application of free cooling of outdoor air in maintaining indoor thermal comfort conditions.

### **7.4.3 Expanding the ANN capability for heating**

Despite a good potential of actuating windows intelligently for improving the thermal comfort duration particularly in summer period by using the free cooling potential of outdoor air, there are many instances when the thermal comfort condition of the house can remain cold. Those instances depend on many factors like relatively colder weather condition, lower level of building envelope resistance, weak envelope airtightness and less internal loads. In those situations or operating condition of the house, any opening of the window resulting natural airflow would potentially worsen the indoor thermal comfort level making it more uncomfortably cold. For those instances, besides, completely shut the window or open it minimum to let necessary fresh airflow, the actuator needs to trigger any other available auxiliary heating sources (electric heater or heat pump).

To simulate such a situation, this work includes an idealised heating device (inbuilt in TRNSY Type 56 building model) with a limited thermal capacity of 2 kW in the model. The research work controls the heater based on the predicted room temperature from ANN model. While doing this, the author fixes the lower and upper set point of the input values for a proportional signal generator as 22 °C and 24 °C respectively so that it generates a respective proportional control signal value between 1 and 0. When the temperature is lower than or equal to 22 °C the heater works on its full capacity of 2 kW and proportionally decreases to 0 when the predicted room temperature by the ANN model reaches 24°C.

In addition to this heating control, the actuation of the window was simultaneously tested. While doing this, this work also fixes the lower and upper set point of the input values for a proportional signal generator as 23.5 °C and 24.5 °C respectively so that it generates a respective proportional WOF value between 0 and 1 to regulate the window actuation when the predicted indoor temperature is higher than 23.5°C.

While observing this closely, Figure 7-23 demonstrates the window actuator performance for a typical day in January for the AVG house with  $R_{avg}$  3.2. The heating controller triggers the auxiliary heater to maintain the desired indoor temperature according to the lower and upper set points based on indoor air temperature prediction of the ANN model.

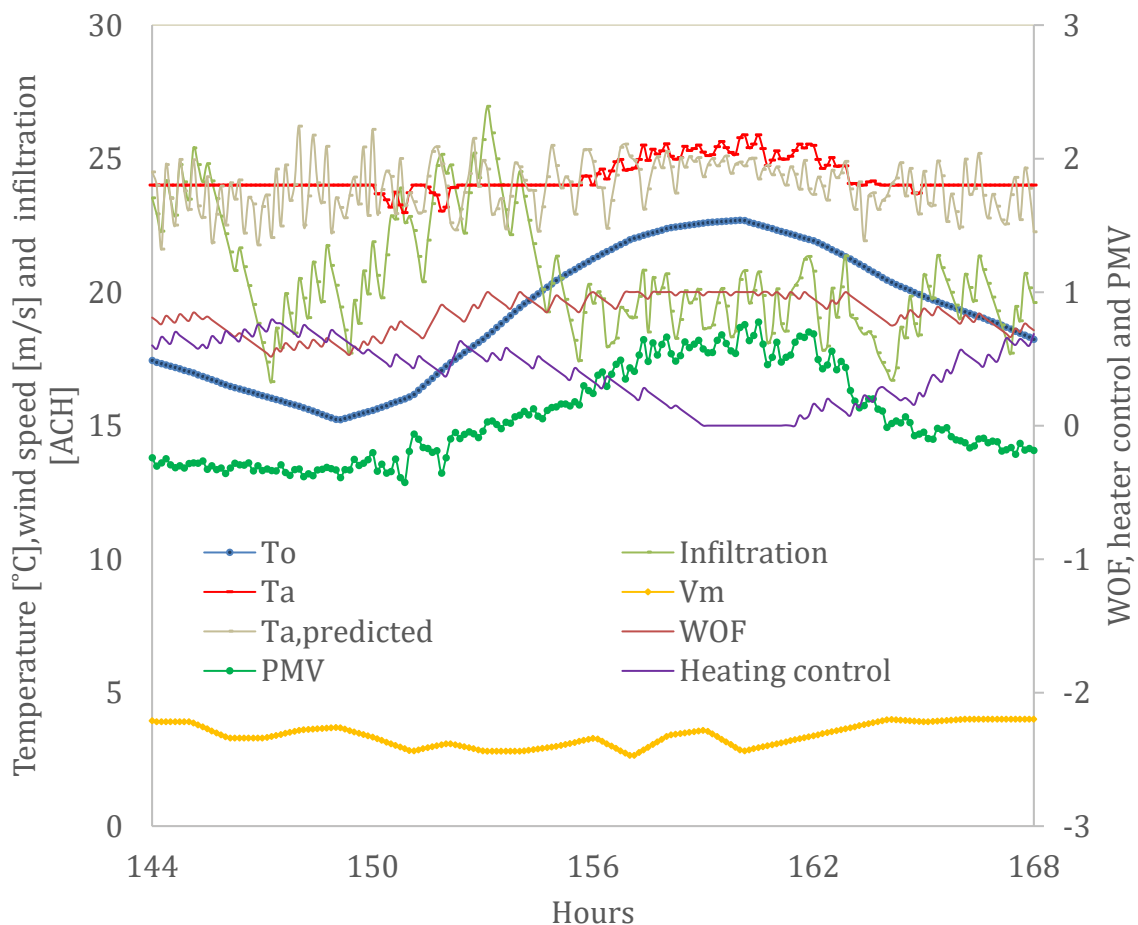


Figure 7-23. Performance of actuator and heating device working together for the model (AVG house with  $R_{avg}$  3.2) for a typical day in January

Similarly, Figure 7-23 also illustrates that the window actuator regulates the value of WOF between 0 and 1 and modulates the natural ventilation (infiltration). The operation of both the window and heating control results in outdoor airflow to the house. The airflow is dependent on both the thermal buoyancy effect (outdoor and ANN predicted indoor temperature difference) and outdoor wind conditions. The incoming cold outdoor air requires an auxiliary heating device to work harder to maintain indoor room temperature ( $T_a$ ) around the desired indoor set points.

By keeping the settings of envelope thermal resistance and airtightness intact, the co-simulation of the thermal and the ANN model for the first week of January was extended to observe the combined performance of the intelligent window and heating control. The resulting frequency distribution as shown in Figure 7-24 illustrates that the implementation of both the window actuator and heater control can achieve maintaining the thermal comfort level ( $-0.7 < PMV < 0.7$ ) of the model house for  $\approx 99\%$  of the assessed period, with 7.5 minute time steps. The heater comes online to address some occasional cold instances that might occur in the assessed period of 1 week of January. However, these rare cold instances in the summer period are usually in the night, and practically heating devices might not be necessary.

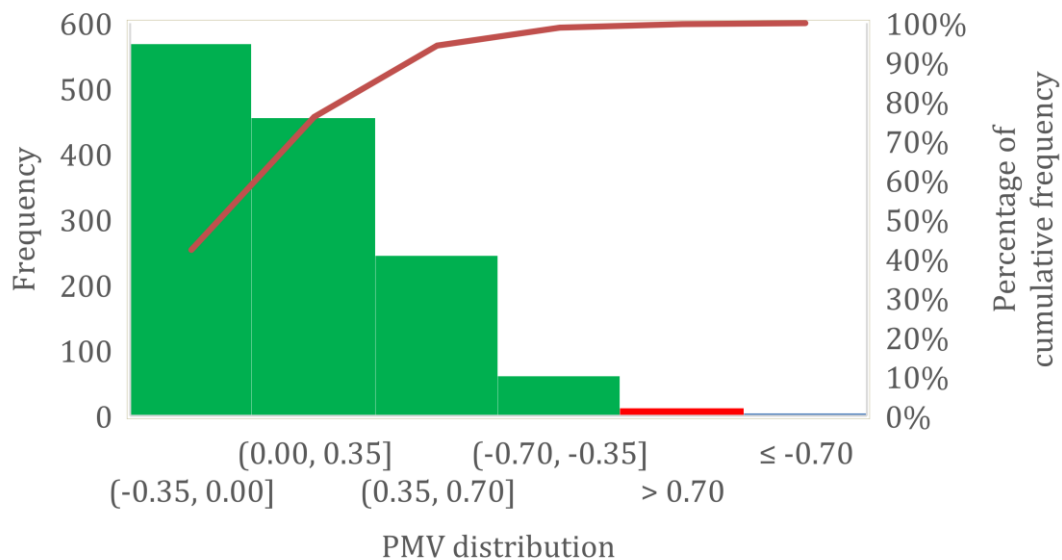


Figure 7-24. Frequency distribution of PMV after using window actuator (AVG house with  $R_{avg}$  3.2 for first week of January)

Figure 7-25 demonstrates the effectiveness of the intelligent window actuation and heater control across the entire range of envelope airtightness for envelope thermal resistance of  $R_{avg}$  3.2 for first week of January. The figure reveals that the performance further improves and sustains at the high level of comfort duration ( $\approx 99\%$ ) by including intelligent Heater Control (HC) on top of intelligent window control irrespective of the change in envelope airtightness. This result further corroborates that there is a significant potential for expanding the ANN model predicted control system further to intelligently control additional auxiliary pieces of equipment so as to improve the indoor thermal comfort condition further.

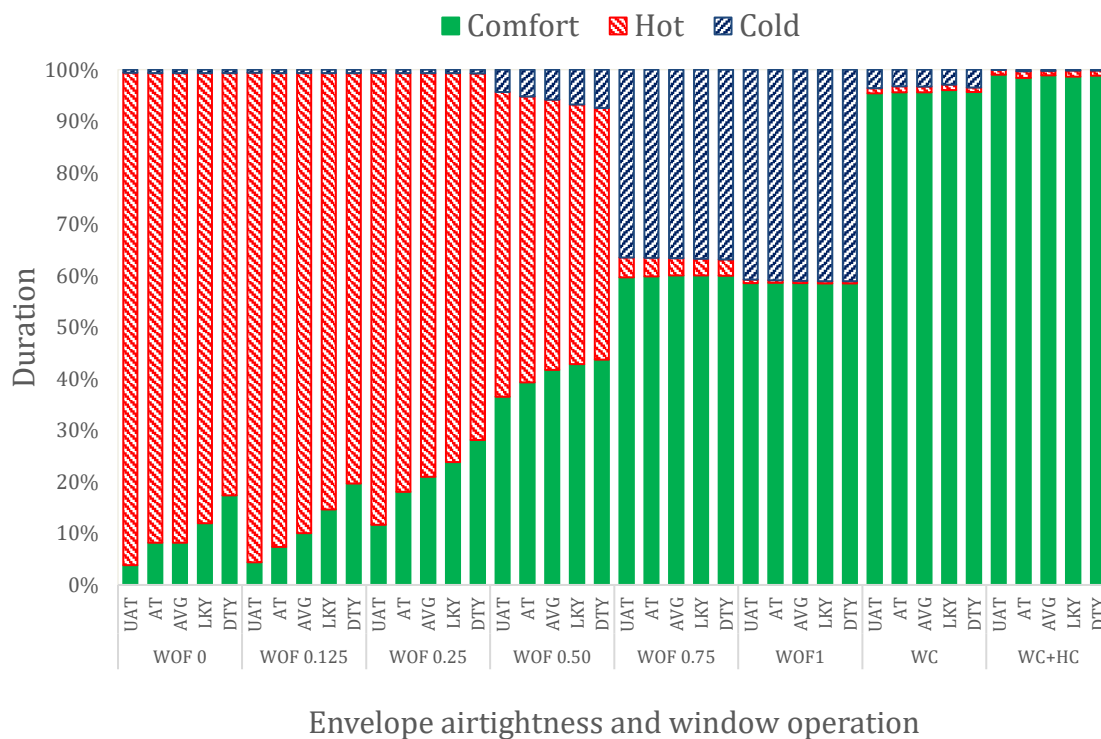


Figure 7-25. Thermal comfort distribution of house ( $R_{avg}$  3.2) with and without window control and heater control for first week of January

Despite this improved result for a typical summer period, the uncomfortable cold duration is significantly at higher proportion compared to hot and comfort duration mostly in winter season as illustrated before in Figure 7-21 and Figure 7-22. This makes the need for heating far more than for cooling to obtain and ensure a complete thermal comfort condition throughout the winter period. As such, verifying the combined performance of the ANN model predictive control system for intelligently operating

both window and auxiliary heating device during the peak winter period of June, July and August are quite crucial from an application perspective. While observing this closely, Figure 7-26 demonstrates the window actuator performance for a typical day in July for the AVG house with  $R_{avg}$  3.2. The heating controller triggers and modulates the capacity of the auxiliary heater to maintain the desired indoor temperature according to the lower and upper set points based on indoor air temperature predicted by the ANN model.

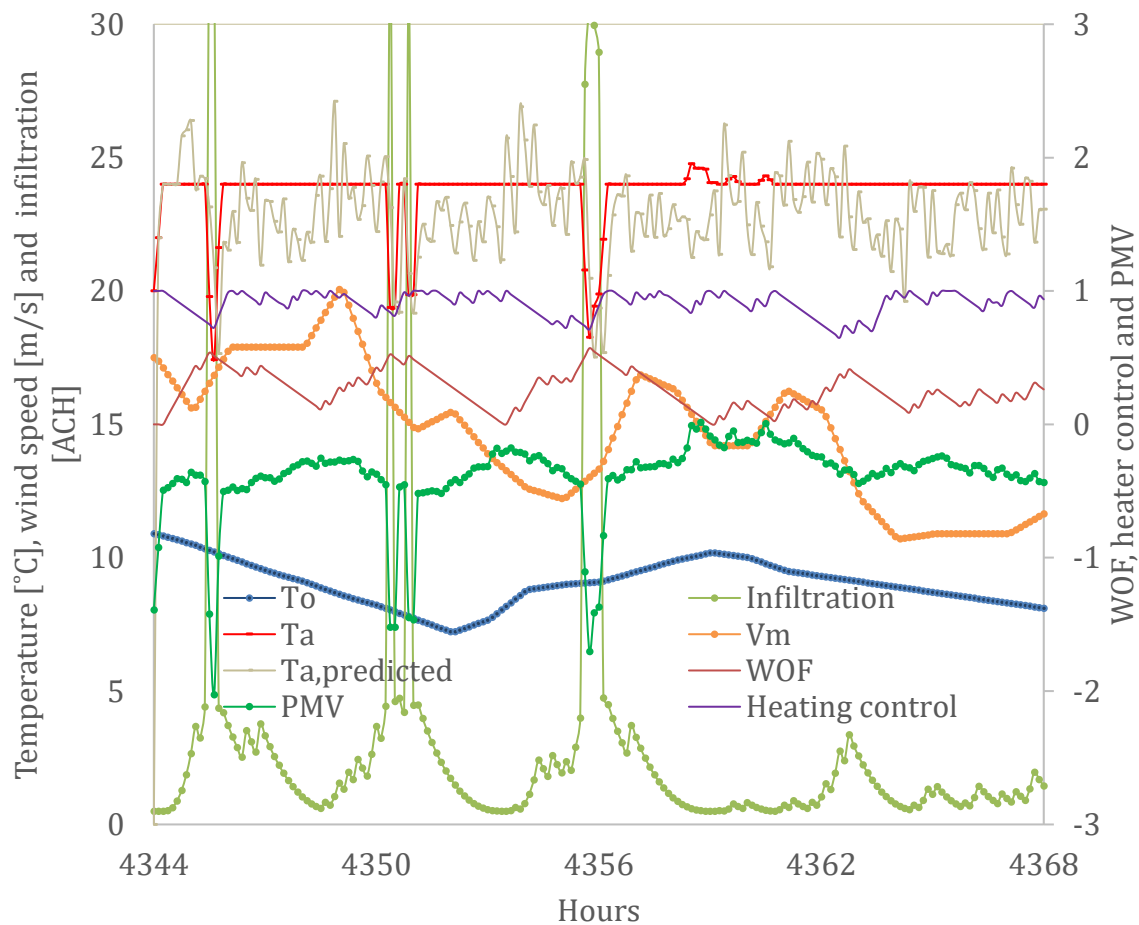


Figure 7-26. Performance of actuator and heating device working together for the model (AVG house with  $R_{avg}$  3.2) for a typical day in July

Similarly, Figure 7-26 also illustrates that the window actuator regulates the value of WOF between 0 and 1 and modulates the natural ventilation (infiltration). Also, the operation of both the window and heating control results in outdoor airflow to the house. The airflow is dependent on both the thermal buoyancy effect (outdoor and ANN predicted indoor temperature difference) and the outdoor wind conditions. Noticeably,

the incoming cold outdoor air requires an auxiliary heating device to work harder to maintain indoor room temperature ( $T_a$ ) around the desired indoor set points.

By illustrating the implementation of both auxiliary heating device and window actuator, Figure 7-27 shows that it is possible to maintain the indoor comfort level within ( $-0.7 < PMV < 0.7$ ) up to 95.3 % of instances for the first week of July. The figure also shows that there is no duration of a thermally uncomfortable hot condition ( $PMV > 0.7$ ) indicating that the remaining 4.7 % of duration is entirely related to the uncomfortable cold period. It also corroborates that in peak winter period there is no significant contribution of an actuating window to maintaining indoor thermal comfort of the house. Increasing the capacity of auxiliary heating equipment or adjusting other building operating conditions might help reduce the percentage of uncomfortable cold instances.

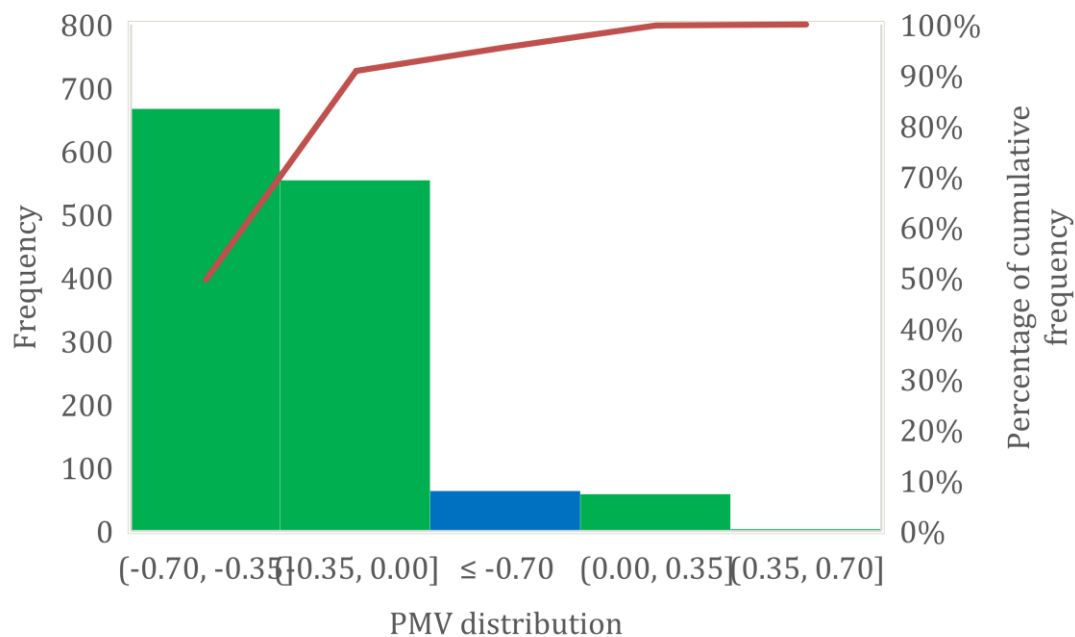


Figure 7-27. Frequency distribution of PMV applying both auxiliary heating device and window actuation (AVG house with  $R_{avg}$  3.2 for first week of July)

To add value on the assessment, Figure 7-28 presents simulation results of another case of operation of the average airtight house with the envelope thermal resistance of  $R_{avg}$  3.2 whereby window always remains in a minimum open position (WOF 0.25) for a typical day of July. While doing this, the ANN model predictive system controls the auxiliary heating equipment intelligently, similar to the earlier lower and upper set

points to maintain the thermal comfort condition of the house. The purpose of this assessment is to observe the impact of leaving window at a minimum fixed opening position without actuation so that there is always an availability of outdoor air that can contribute to maintaining indoor air quality.

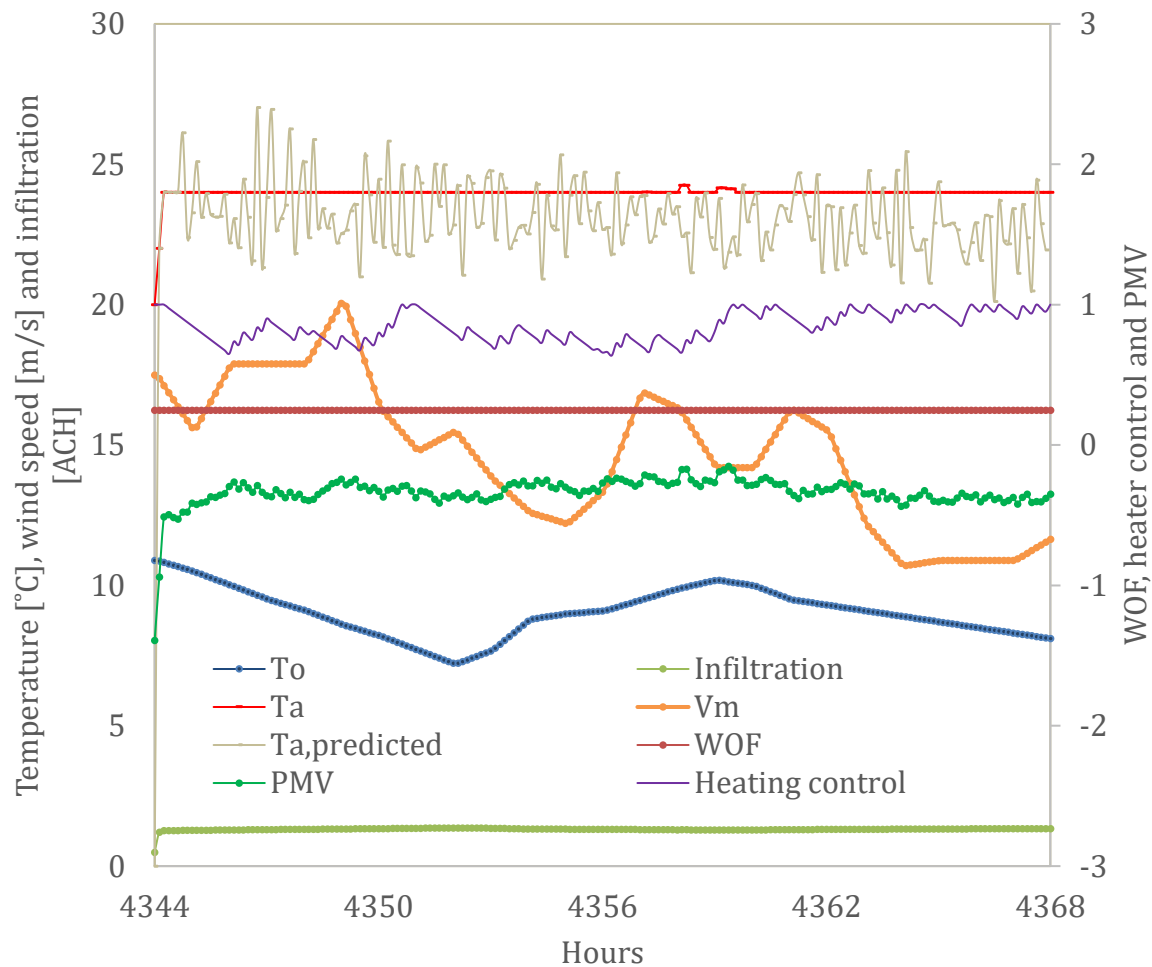


Figure 7-28. Performance of window fixed opening (WOF 0.25) with intelligent control of the heating device for the model (AVG house with  $R_{avg}$  3.2) for a typical day in July

By illustrating the implementation of both auxiliary heating device and fixed window opening position (WOF value 0.25), Figure 7-29 shows that it is possible to maintain the indoor comfort level within the range ( $-0.7 < PMV < 0.7$ ) in up to 99.85 % of instances for the first week of July. The figure also shows that there is no duration of thermally uncomfortable hot modes ( $PMV > 0.7$ ) indicating that the remaining 0.15 % of instances are entirely related to thermally uncomfortable cold instances.

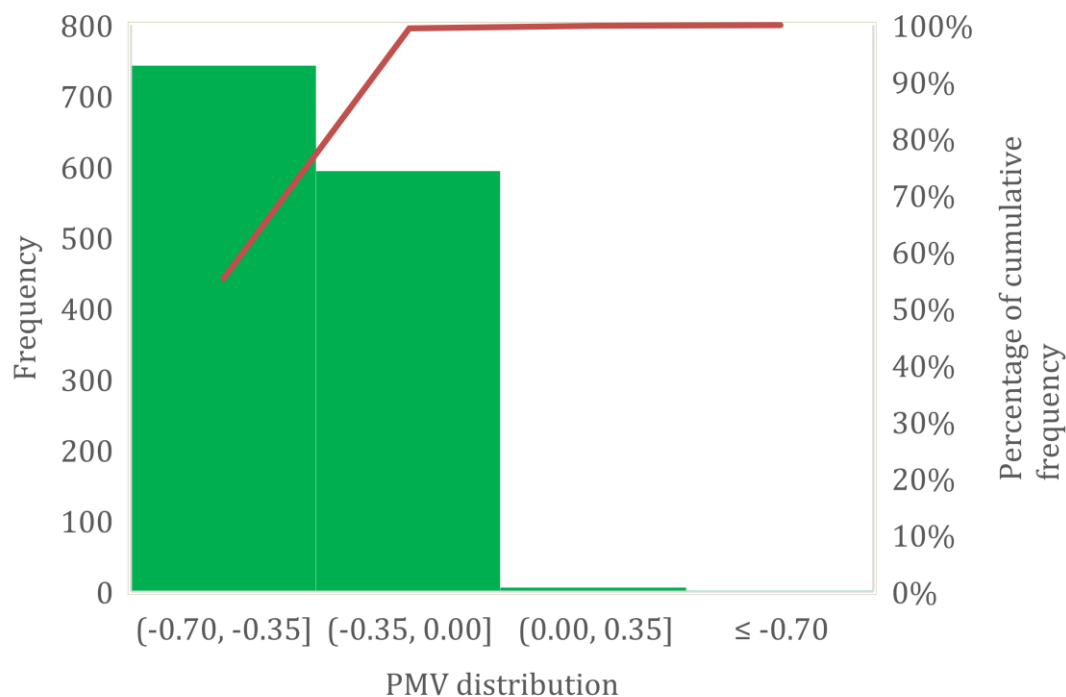


Figure 7-29. Frequency distribution of PMV applying auxiliary heating device and fixed window opening at WOF value of 0.25 (AVG house with  $R_{avg}$  3.2 for first week of July)

This result indicates that the thermal comfort level is sustained at the higher range even when the window is open to a minimum value to let airflow for contributing/maintaining indoor air quality. The auxiliary heating equipment works hard to compensate for the additional impact of the airflow through the fixed window opening.

To summarise the impact of implementing both the window and heating control system simultaneously or separately across the entire range of envelope airtightness for envelope thermal resistance of  $R_{avg}$  3.2 for first week of July), the Figure 7-21 is further expanded to Figure 7-30. The figure reveals that the thermal comfort performance improves and sustains at the high level of comfort duration ( $\approx 95\%$ ) by including intelligent heater control (HC) on top of intelligent window control irrespective of change in envelope airtightness. This result further upholds that the ANN model predicted control system could control additional auxiliary heating equipment to improve the indoor thermal comfort condition in the winter period.

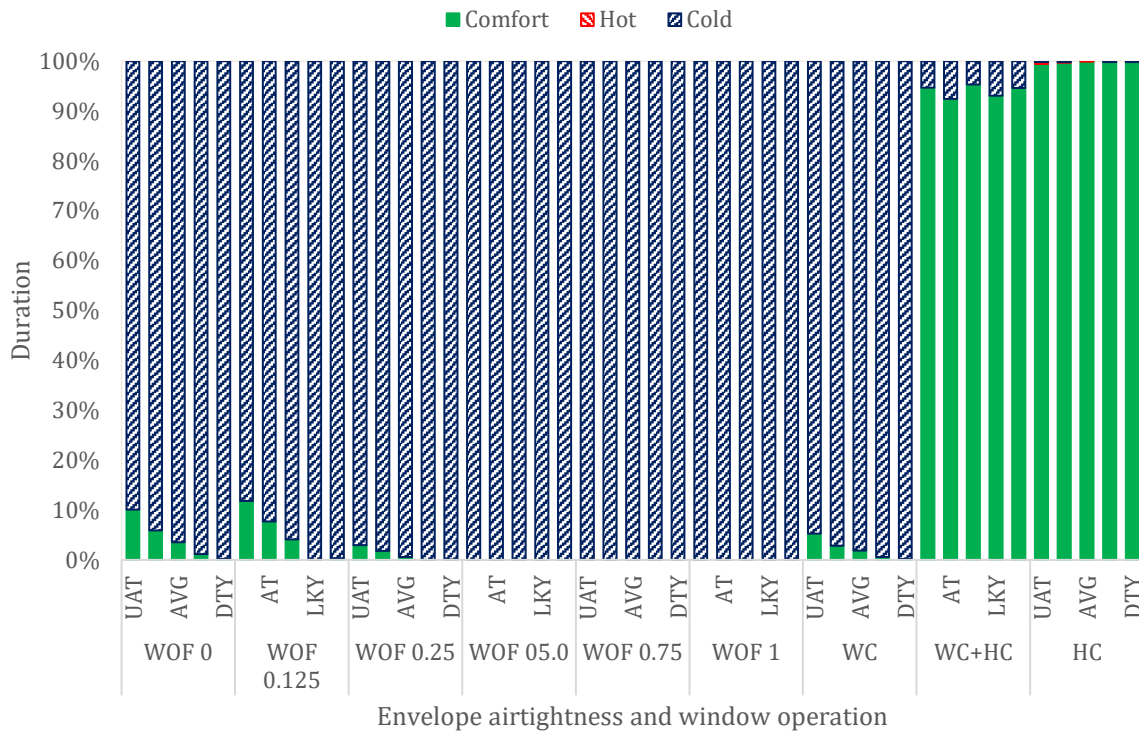


Figure 7-30. Thermal comfort distribution of house ( $R_{avg}$  3.2) with and without window control and heater control for first week of July

Further extending the verification for the entire year, Figure 7-31 demonstrates the effectiveness of operating both the intelligent window actuation and heating control for AVG airtight house with envelope thermal resistance of  $R_{avg}$  3.2 for the first week of each month. The figure reveals that implementing both systems ensures a very high level of thermal comfort condition with an annual average value of ( $\approx 96.43\%$ ) throughout the year.

The performance can further improve to 100% comfort winter period (June, July, August) if we include the intelligent heating control (HC) as heating is the only requirement during those periods as shown in Figure 7-32.

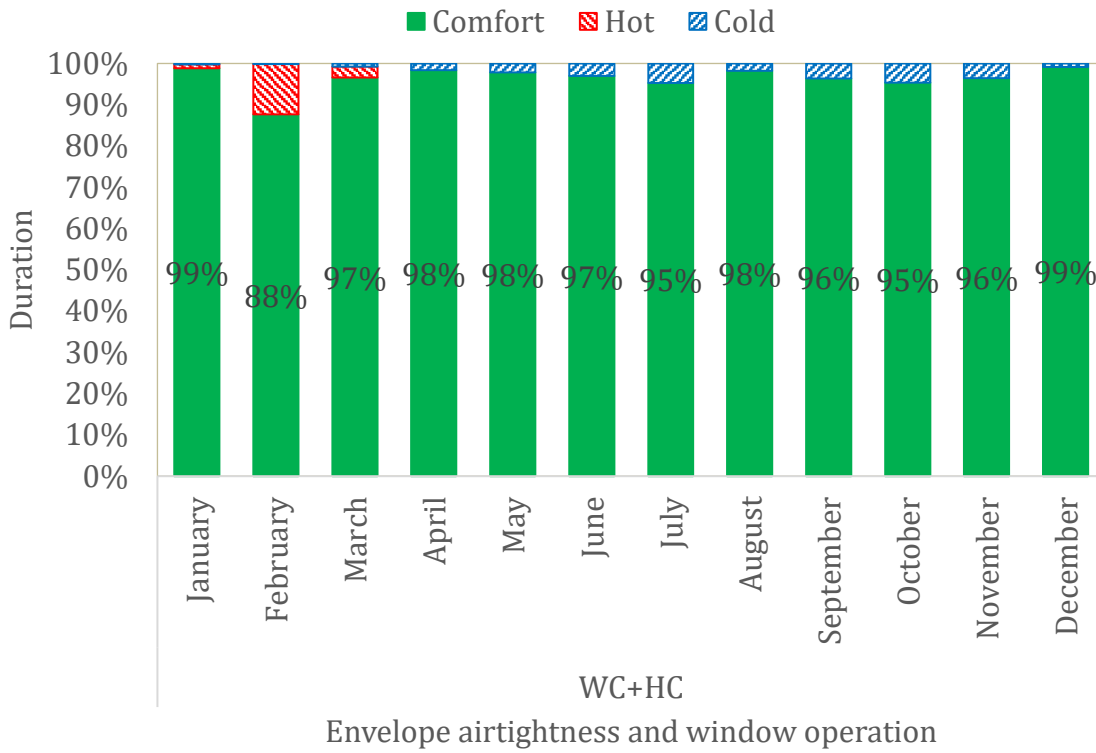


Figure 7-31. Impact of intelligent control of both window and auxiliary heater on thermal comfort distribution of house (AVG house with  $R_{avg}$  3.2 for first week of each month)

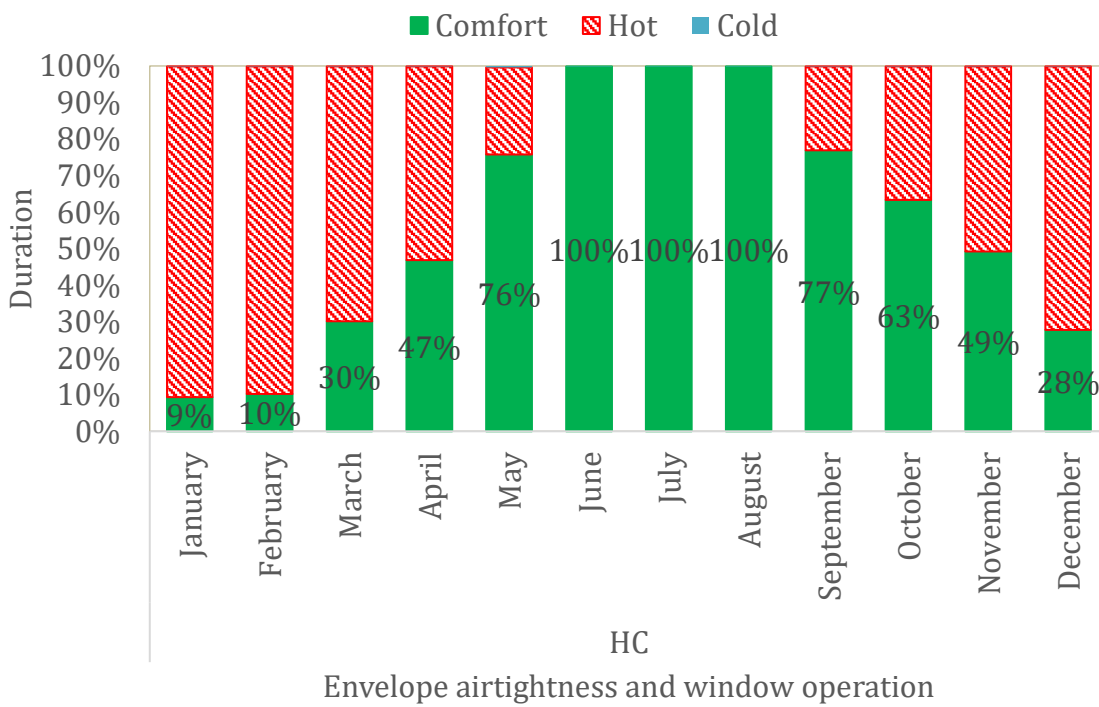


Figure 7-32. Impact of intelligent control only on the auxiliary heater on thermal comfort distribution of house (AVG house with  $R_{avg}$  3.2 for first week of each month)

## 7.5 Remarks

It is possible to use the ANN technique to predict the occupied space indoor air temperature time-series of the naturally ventilated house. This technique can work as part of an intelligent window control strategy for maintaining the thermal comfort of naturally ventilated residential houses. In general, this technique helps actuate the windows of a residential house and vary the windows' opening area to effectively regulate the leakiness of the building by changing the air exchanges rates and ultimately helping to reduce uncomfortably warm or cold periods. Overall, there is a significant improvement in the indoor thermal comfort condition by actuating the window intelligently during the summer indoor condition.

It is also possible to use the technique to reduce the indoor uncomfortable cold condition by limiting the window opening area, thereby reducing the air exchange rate. It ultimately keeps the stored thermal energy in the occupied space to maintain indoor thermal comfort during a mild winter condition. Likewise, there is a reasonable prospect of using this technique to trigger further and modulate auxiliary heating devices (electric heater, heat pumps). The extension can help maintain indoor thermal comfort conditions for extreme winter condition or other instances when necessary. Applying the extension can help keep the thermal comfort well above the annual average 96% across the year.

In a summary, the use of ANN appears to offer a positive outlook in the development of intelligent control of actuated windows for the next generation naturally ventilated sustainable buildings.

## Chapter 8 Conclusions and Recommendations

### 8.1 Conclusions

Many residential houses in New Zealand's mild climatic region, have been found to perform poorly from thermal and health perspectives. As an overwhelming proportion of these houses are ventilated naturally and maintaining a comfortable thermal environment using just natural ventilation is a challenging proposition. Though numerous studies have examined the problem of ventilation in buildings, few have attempted to modulate the thermal behaviour of naturally ventilated spaces actively using only the windows. Also, there is considerable diversity in housing stock in terms of building characteristics, operating conditions, user dynamics, environment influences, etc., making it difficult to use a prescriptive analytical solution addressing the problem for all houses and climatic conditions.

To understand the problem more and explore a better solution, an overarching research question was posed: **How can we actively control the window (s) to modulate the natural ventilation of a residential house and as a component in maintaining thermal comfort?** To find the answers to the research question, the author divided the research question into achieved following specific objectives.

- 1) Examined the thermal comfort characteristics of a single-sided naturally ventilated model house
- 2) Investigated the influence of the driving forces (thermal buoyancy and wind) of natural ventilation and develop specific relationship(s) to improve the estimation of heat transfer behaviour of the floor of a single-sided partially opened model enclosure
- 3) Improved the robustness of the single-sided naturally ventilated model house by applying the specifically developed relationship(s) for estimating convection heat transfer behaviour of the floor and re-examine the thermal comfort characteristics
- 4) Developed and apply an intelligent control concept based on an Artificial Neural Network (ANN) to actuate the window to modulate the natural ventilation and maintain the thermal comfort of the naturally ventilated model house.

The researcher realised the set objectives within the spectrum, covering the necessary depth and breadth of coverage of the subject matter. Considering an overarching nature of the problem that might come across many open-ended questions in three different exciting subjects of natural ventilation, thermal comfort and intelligent control, the researcher embraced some limitations while investigating the issue within the prescribed scope of the objectives. As such, the research work used the NZ context (housing types, construction method, climate, standards, building codes) to identify the thermal comfort dynamics of NZ residential houses. In particular, the research work considered a simple suspended timber floor cubical shape and single-sided naturally ventilated house situated in temperate climate conditions of Auckland, NZ.

Approaching the issue at a macroscopic level with a recognised dynamic building simulations software tool TRNSYS (used by ASHRAE standard 140 to set the acceptable range of building performance), this research performed a preliminary examination of the thermal comfort characteristics of a coupled thermal and airflow single-sided naturally ventilated room. The investigation helped understand the relative influences of variations of internal and external operating conditions on the thermal behaviour of naturally ventilated house by using numerical experiment method. With sufficient level of depth, breadth and robustness, the research established that there is a significant scope for regulating the thermal behaviour of naturally ventilated residential houses by opening windows. The research also confirmed the possibility to improve comfort considerably for a relatively airtight and insulated house during the summer in a temperate climatic region like Auckland.

Other than what the research contemplated under the scope of this research objective, there are still many open-ended questions on the thermal comfort dynamics of naturally ventilated NZ houses. Researchers should explore the subject to improve the knowledge base about the thermal comfort dynamics of naturally ventilated NZ houses operated in complex, real-life conditions. Finding the answers requires examining more complex building model (multiple zones) and the associated operating conditions (cross window, adjacent window, natural and mechanical hybrid ventilation, plug loads, occupancy schedules, various house orientation, location of the window, size and type of windows etc.). Nevertheless, this work might help better inform planners and

policymaker to conceive necessary instruments and standards to improve the thermal performance of the existing housing stock of NZ.

Despite this, this simplified approach of examining the thermal behaviour of the natural ventilated building poses a risk of higher uncertainty in the investigation. This is because the dynamic simulation with building simulation tool used simplifies the process of modelling the convective heat transfer behaviour of internal surfaces which is based on empirical relationships developed by researchers considering only either the unventilated enclosure or flat surface. However, a partially opened naturally ventilated house results in a stream of airflow exchange from outdoor to indoor and vice-versa through the opening. This stream of incoming airflow combined with the dynamic outdoor weather conditions, in particular the outdoor air temperature, relative humidity, wind speed and direction might result in a completely different convective heat transfer behaviour on the indoor surfaces.

Despite the numerous correlations for the convection-driven heat transfer to and from a building's internal surfaces, the resulting heat transfer from the floor is unlikely to be accurately determined by any of these relationships for a naturally ventilated building. In this vein, a particular case of a simple naturally ventilated house where the floor has been heated by solar radiation and is exposed to the external environment (for example, by an open window) was investigated. This research focused on improving the robustness of such thermal-airflow models by developing appropriate empirical relationships for determining the indoor floor Convective Heat Transfer Coefficient (CHTC).

To address this, a computational model of a single-sided partially opened 3D air-filled cubical enclosure (analogous to a single room with underfloor heating, or where the floor had been heated by solar radiation), was examined initially for the variation of flow fields considering only buoyancy-driven air-exchange between indoors and outdoors. The results indicated that the heat transfer behaviour of the floor in terms of Nusselt number ( $Nu$ ) could be determined by a generalised correlation  $Nu = 0.1593 \cdot Ra^{0.33} \cdot WOF^{0.18}$  for a range of Rayleigh Numbers ( $1.9 \times 10^{10} \leq Ra \leq 3.6 \times 10^{10}$ ) and Window Opening Fractions (WOF) ( $0.25 \leq WOF \leq 1$ ). Highlighting that there is significant variation in flow field inside the enclosure resulting in a non-uniform

distribution of floor heat flux on spatial context, the work concentrated on improving the correlation further, including the effect of wind-driven air-exchange.

The wind driving force on single-sided opening could result in a complex air-exchange due to pulsation, penetration of eddies and turbulence at the opening. Furthermore, the wind can reinforce or restrict the buoyancy-driven natural ventilation resulting in difficulty in accurately predicting the potential for natural ventilation and its effect on the heat transfer from surfaces within the space. Therefore, this research further investigated the computational model by including the impact of wind conditions. The results confirmed that wind conditions strongly influence both the indoor flow-fields and convective heat transfer from the floor of single-sided naturally ventilated room. The investigation showed that changes in the wind conditions, such as speed and direction, can result in significantly different flow regimes and temperature distributions inside such spaces, leading to a significant variation in the convective heat transfer from the floor. Furthermore, the research also corroborated that changes in the strength of the wind-driven force, with respect to the buoyancy-driven force, can lead to the reinforcement of, or resistance to, flow through the opening, resulting in different natural convection mechanisms. The numerical simulation work concluded that there is a significant scope for increasing the robustness of thermal models of naturally ventilated buildings by greater utilisation of empirical relationships developed particularly for that purpose. The generalisation of these results requires further study with an extended range of wind conditions, opening areas, building dimensions and Rayleigh numbers.

Applying the developed convective heat transfer relationships for the floor of a partially opened enclosure further helped improve the robustness of the coupled multi-zone thermal and airflow model. Re-examining the thermal comfort behaviour with the updated results from the improved model corroborated the significant scope of regulating the thermal behaviour of relatively airtight and insulated naturally ventilated residential houses during the summer season. However, from the application perspective, the result could not be used to continuously adjust the window position manually to maintain thermal comfort. Therefore, the research investigated a technique to intelligently actuate the windows and regulate the values of WOF for maximising the

percentage of thermal comfort periods by minimising both thermally uncomfortably hot and cold periods.

Due to the complex nature of dynamic and nonlinear driving forces and many influencing factors, the problem applied Artificial Neural Network (ANN) technique. The research work used the results of the thermal simulations of the improved model to train an adaptive ANN to the building model and using an appropriate window opening strategy and to maintain the desired thermal environment. The research work also constructed the ANN predictive algorithm on the simulation platform of Matrix Laboratory (MATLAB). It tested the whole process of an intelligently actuated window for the coupled thermal airflow house model in a co-simulation environment of Transient Simulation System tool (TRNSYS) and MATLAB. The conclusion was that the ANN technique could predict the occupied space indoor air temperature time-series of the naturally ventilated house reasonably well. The research further developed an ANN-based function/algorithm to actuate the window intelligently for maintaining thermal comfort.

In comparison to the basic scenario with the operating window in a fixed window position throughout a typical day without any window actuating automation (manual or controlled), the intelligent window actuation system (using the developed function) demonstrated the thermal comfort was ensured for 95% of the summer period. However, the research found the effectiveness of the intelligent system diminished as the summer season transitioned to shoulder and finally, to the winter season. Nevertheless, the technique actively reduced the indoor uncomfortable cold condition by limiting the window opening area, thereby reducing the air exchange rate and ultimately keeping stored thermal energy in the occupied space. The research work also demonstrated that the technique could help enhance thermal comfort over the whole year by controlling additional heating equipment.

Corroborating the recognition of ANN on solving a complex problem and accurate prediction capability, the proposed ANN-based predictive window actuation system demonstrated a unique and simple solution for actively actuating windows modulating natural ventilation and as a component of maintaining thermal comfort. The research indicated that the solution could address the complexity of natural ventilation and the

non-linearity involved in building dynamics due to changing operating conditions. It could also address the diversity in housing stock in terms of building characteristics, orientation, size and location of window etc., and provide a unique solution applicable to all houses irrespective of building typologies, climate and user dynamics.

Though the research used NZ, in particular the Auckland regional climatic context, with a single-sided one-room building model limitation, the solution can be generalised to the different context of location, climate, building size and operating characteristics. Deploying a robust thermal-airflow modelling method to create the necessary training database for ANN predictive model is the most crucial aspect requiring attention. This research addressed improving robustness by specifically treating methods for evaluating convection heat transfer behaviour of the house floor exposed to natural ventilation.

However, many other aspects in the real-life operation of a building (influence of different window type, size, location, heat transfer of vertical surface and ceiling, multi-zone multi-window operation, etc.) might exist. The more robust and comprehensive is the set of building models and simulations database used for the training of the ANN, the better the generalisation capability of the proposed system.

In summary, the research demonstrated that it is possible to actuate the window intelligently with the ANN-based model predictive technique to help maintain thermal comfort of a relatively insulated and airtight naturally ventilated house during the summer period and the method can be expanded to optimally control other auxiliary systems or equipment and maintain the thermal comfort of the house for the entire year.

## **8.2 Recommendations**

In this work, the author used a macro level coupled thermal and airflow modelling approach for dynamic building performance simulations of the natural ventilated model house. Also, the author used the relevant inputs and outputs to develop the ANN model predictive system for actuating window intelligently. To do this, the author considered a range of typical envelope characteristics, in particular, envelope airtightness and thermal resistance of a cubical model house analogous to the size of a room with single-

sided sliding window for Auckland, NZ weather conditions. In reality, besides the considered envelope characteristics, there exists a wide variation of geometry, operating conditions and characteristics of residential houses. Parameters such as size of house, types and sizes of openings, weather conditions for these naturally ventilated houses operate, vary significantly. Therefore, to corroborate and generalise the technique with robust ANN function/algorithm for a wide range of environment, built and operating conditions, the author recommends to further develop the database input to the ANN model. In this regard, additional simulation databases capturing the following influences may help enrich the ANN model:

- Influence of the single-sided window located in a different direction (South, East, North and West) facing envelopes
- Influence of adjacent sided and cross-ventilation of naturally ventilated residential houses
- Influence of different window types (awning, casement, hopper) and their respective effective opening aperture
- Influence of increased height, width and depth of the ventilated space of the house
- Influence of multiple zones having multiple windows and doors.

Similarly, as part of this thesis, the author numerically examined a partially opened rectangular opening with a cubical enclosure. This model is analogous to a particular case of a simple naturally ventilated partially opened enclosure with the floor heated by solar radiation and exposed to the external environment with a single-sided sliding window. The examination resulted in empirical relationships for convective heat transfer behaviour at the floor for a limited range of operating conditions threshold. The generalisation of these results requires further study with an extended range of wind conditions, opening areas, building dimensions and Rayleigh numbers in particular as follows:

- Influence of different geometries of opening for different types of windows (hopper, casement, awning )
- Influence of different geometrical shape of the cavity analogous to different shape of occupied space (rectangular, spherical, cylindrical )
- Influence of widening the size of the cavity geometry (length, breadth, height)

- Influence of opening(s) of cavity analogous to adjacent sided and cross ventilation principle
- Influence of small to large temperature differences between inside surfaces and the outside environment.

Further verification of the influence of wind direction on convective heat transfer behaviour at the surface exposed to the different opening area and wind speed . would help to further corroborate the empirical relationships developed. Including possible effects due to transient temperature inside the space, thermal mass of the envelope, solar gains, internal heat loads and furnishings/flow restrictions in the interior spaces might also be useful to improve the robustness of the heat transfer relationship. Furthermore, a substantial reduction on the uncertainty of estimating heat transfer seems possible by considering the localised distribution of the heat flux on the floor.

As a potential future work, the author further recommends examining the robustness of the existing convective heat transfer correlations for vertical surfaces and ceilings used in existing building dynamic simulation software from the perspective of natural ventilation. Furthermore, a substantial reduction of the uncertainty of estimating heat transfer behaviour of internal surfaces seems possible by considering the localised distribution of the heat flux on these surfaces.

Besides low-rise residential building, there exist many high-rise apartment buildings and commercial hotels/office space with the possibility of varying the openable area of the window(s) to control indoor comfort. The actuating system might be useful to drive window(s) for those occupied spaces, specifically high rise residential or hotel apartment using a modular approach. However, the natural ventilation-influencing factors, in particular the driving force of the wind at an elevated height, the behaviour of wind in the cityscape possess particular challenges requiring further examination both in terms of macro and micro-level modelling approaches. Besides, the operating conditions of the building, for example, the envelope and fabric, airtightness level, existing centralised heating, ventilation and cooling (HVAC) systems are different from low rise buildings. As such, there is an opportunity to examine further the possibility of using this technique of intelligently actuate opening(s) of high rise building for maximising the use of free cooling and reducing the use of the energy by reducing the loads of HVAC systems/subsystems.

The author performed the work mainly on numerical and dynamic building performance on well-recognised simulation platforms. These platforms have already been sufficiently validated by several researchers and provided a standard approach to complete the scope of the work in this research work. Finally, the author recommends performing an experimental evaluation of the work, particularly the physical realisation of the actuation system and confirming the theoretical results presented in this thesis.

For future work, the research recommends conceptualising a more advanced controller such that it modulates the thermal comfort of the residential house in terms of PMV or adaptive thermal comfort index criteria rather than only the indoor air temperature. As such, the resulting time series function/algorithm of the thermal comfort index can be used as a basis to devise an intelligent model predictive control strategy having a window actuation optimisation strategy using an objective function to directly maximise the indoor thermal comfort level of a naturally ventilated residential house and minimise the heating or cooling energy consumption.

## Chapter 9 References

- [1] N. Buckett and J. Burgess, "Real Experience of Retrofitting for Sustainability," in *SB07 NZ Conference: Transforming our Built Environment*, Auckland, November 14-16, 2007.
- [2] V. Ryan, G. Burgess and L. Easton, "New Zealand House Typologies to Inform Energy Retrofits," Beacon Pathway Ltd, 2008.
- [3] M. Bassett, "Naturally Ventilated Houses in New Zealand: Simplified Air Infiltration Prediction," in *CIB world building conference*, Wellington, April 2-6, 2001.
- [4] Passive House Institute, "Criteria for the Passive House, EnerPHit and PHI Low Energy Building Standard," 2016.
- [5] M. Boulic, I. Hosie and R. Phipps, "Effects on Indoor Environment in 30 Auckland Homes from the Installation of a Positive Pressure Ventilation Unit," in *SB10 New Zealand Sustainable Building Conference*, 2010.
- [6] C. Rode and M. Woloszyn, "Common Exercises in Whole Building HAM Modelling," in *Eleventh International IBPSA Conference*, Glasgow, 2009.
- [7] M. Cunningham, "Indoor Moisture-Causes and Cures," *Build*, no. 127, p. 46, 2012.
- [8] P. Leardini and T. Van Raamsdonk, "Design for airtightness and moisture control in New Zealand housing," in *New Zealand Sustainable Building Conference*, Wellington, May 26-28, 2010.
- [9] P. Howden-Chapman, A. Matheson, J. Crane, H. Viggers, M. Cunningham, T. Blakely, C. Cunningham, A. Woodward, K. Saville-Smith, D. O'Dea, M. Kennedy, M. Baker, N. Waipara, R. Chapman and G. Davie, "Effect of insulating existing

houses on health inequality: cluster randomised study in the community," *BMJ (Clinical research ed.)*, vol. 334, no. 7591, p. 460, 2007.

- [10] K. Rosemeier, "Introduction of the passive house standard in New Zealand: opportunities and barriers," Auckland, 2007.
- [11] P. Howden-Chapman, K. Saville-Smith, J. Crane and N. Wilson, "Risk factors for mold in housing: a national survey.," *Indoor Air*, vol. 15, no. 6, pp. 469-476, 2005.
- [12] W. B. Fitzgerald, M. Fahmy, I. J. Smith, M. A. Carruthers, B. R. Carson, Z. Sun and M. R. Bassett, "An assessment of roof space solar gains in a temperate maritime climate," *Energy and Buildings*, vol. 43, no. 7, pp. 1580-1588, 2011.
- [13] NIWA, "Climate Overview," 2016.
- [14] ASHRAE Standard 55, "Thermal Environmental Conditions for Human Occupancy," ANSI, 2010.
- [15] MBIE: G4 Ventilation, "Acceptable Solutions and Verification Methods for New Zealand Building Code Clause G4 Ventilation," Ministry of Business, Innovation & Employment, 2014.
- [16] NZS 4303, "Ventilation for Acceptable Indoor Air Quality," Standards New Zealand, 1990.
- [17] ASHRAE Standard 62.2, "Ventilation and Acceptable Indoor Air Quality for Low Rise Building," ANSI, 2016.
- [18] ASHRAE Standard 62.1, "Ventilation for Acceptable Indoor Air Quality," ANSI, 2016.

- [19] AS 1668.2, "The use of mechanical ventilation and air conditioning in building part-2 Mechanical ventilation for acceptable indoor air quality," Standards Australia, 1991.
- [20] NZS 4218, "Energy Efficiency-Housing and small building envelope," Standards New Zealand, 1996.
- [21] NZS 4218, "Minimum thermal insulation requirements for residential buildings," Standards New Zealand, 1977.
- [22] MBIE: H1 Energy Efficiency, "Acceptable Solutions and Verification Methods for Building Code Clause H1 Energy Efficiency," Ministry of Business, Innovation & Employment, 2011.
- [23] NZS 4218, "Energy Efficiency-Small building envelope," Standards New Zealand, 2004.
- [24] NZS 4218, "Thermal Insulation-Housing and small buildings," Standards New Zealand, 2009.
- [25] C. Ghiaus, F. Allard, M. Santamouris, C. Georgakis, C. A. Roulet, M. Germano and F. Tillenkamp, "URBVENT Natural Ventilation in Urban Areas-Potential Assessment and Optimal Facade Design: Work Package 1-Soft Computing of Natural Ventilation Potential," 2004.
- [26] P. F. Linden, "The Fluid Mechanics of Natural Ventilation," *Annual Review of Fluid Mechanics*, vol. 31, pp. 201-238, 1999.
- [27] G. R. Hunt and P. F. Linden, "The Fluid Mechanics of Natural Ventilation: Displacement Ventilation by Buoyancy-Driven Flows Assisted by Wind," *Building and Environment*, vol. 34, no. 6, pp. 707-720, 1999.

- [28] H. Breesch, "Natural Night Ventilation in Office Buildings: Performance Evaluation Based on Simulation, Uncertainty and Sensitivity Analysis," 2006.
- [29] Q. Zhao, Z. Lian and D. Lai, "Thermal comfort models and their developments: A review," *Energy and Built Environment*, vol. 2, no. 1, pp. 21-33, 2021.
- [30] P. O. Fanger, *Thermal Comfort-Analysis and Applications in Environmental Engineering*, McGraw-Hill Book, 1970.
- [31] J. Cigler, S. Prívvara, Z. Váňa, D. Komárková and M. Šebek, "Optimization of predicted mean vote thermal comfort index within Model Predictive Control framework," in *51st IEEE Conference on Decision and Control (CDC)*, Maui, HI, USA, 2012.
- [32] J. F. Nicol and M. A. Humphreys, "Adaptive thermal comfort and sustainable thermal standards for buildings," *Energy and Buildings*, vol. 34, no. 6, pp. 563-72, 2002.
- [33] R. d. Dear and G. S. Brager, "Thermal Comfort in Naturally Ventilated Buildings: Revisions to ASHRAE Standard 55," *Energy and Buildings*, vol. 34, no. 6, pp. 549-561, 2002.
- [34] H. B. Rijal, P. Tuohy, M. A. Humphreys, J. F. Nicol, A. Samuel and J. Clarke, "Using results from field surveys to predict the effect of open windows on thermal comfort and energy use in buildings," *Energy and Buildings*, vol. 39, no. 7, pp. 823-836, 2007.
- [35] EN ISO 7730, "Ergonomics of the thermal Environment-Analytical determination and interpretation of thermal comfort using calculation of the PMV and PPD indices and local thermal comfort criteria".
- [36] T. Yang and D. J. Clements-Croome, "Natural Ventilation in Built Environment," in *Encyclopedia of Sustainability Science and Technology*, Springer, 2012.

- [37] C. Ghiaus and F. Allard, "Potential for free-cooling by ventilation," *Solar Energy*, vol. 80, no. 4, pp. 402-413, 2006.
- [38] A. I. Dounis, M. Bruant, G. Guarracino, P. Michel and M. Santamouris, "Indoor Air-Quality Control by a Fuzzy-Reasoning Machine in Naturally Ventilated Buildings," *Applied Energy*, vol. 54, no. 1, pp. 11-28, 1996.
- [39] T. Kleiven, "Natural Ventilation in Buildings-Architectural Concepts, Consequences and Possibilities," 2003.
- [40] M. W. Liddament, "A Guide to Energy Efficient Ventilation," Air Infiltration and Ventilation Centre (AIVC), 1996.
- [41] G. V. Fracastoro, G. Mutani and M. Perino, "Experimental and theoretical analysis of natural ventilation," *Energy and Buildings*, vol. 34, no. 8, p. 817-827, 2002.
- [42] G. Tan, "Study of Natural Ventilation Design by Integrating the Multizone Model with CFD Simulation," 2001.
- [43] H. Montazeri and B. Blocken, "New generalized expressions for forced convective heat transfer coefficients at building facades and roofs," *Building and Environment*, vol. 119, pp. 153-168, 2017.
- [44] H. E. Feustel and A. R. Hooson , "COMIS Fundamentals," Lawrence Berkeley Laboratory, 1990.
- [45] TRNFLOW , "A module of an air flow network for coupled simulation with TYPE 56 (multi-zone building of TRNSYS)," Transsolar Energietechnik GmbH, 2009.
- [46] D. Cóstola and B. Blocken, "Overview of pressure coefficient data in building energy simulation and airflow network programs," *Building and Environment*, vol. 44, no. 10, pp. 2027-2036, 2009.

- [47] M. Orme and N. Leksmono, "AIVC Guide 5: Ventilation Modelling Data Guide," Air Infiltration and Ventilation Centre, 2002.
- [48] ASHRAE, "ASHRAE Handbook-Fundamentals," Atlanta, 2001.
- [49] TPU (Tokyo Polytechnic University), n.d.. [Online]. Available: [http://www.wind.arch.tokugei.ac.jp/info\\_center/windpressure/lowrise/mainpage.html](http://www.wind.arch.tokugei.ac.jp/info_center/windpressure/lowrise/mainpage.html). [Accessed 29 4 2019].
- [50] M. V. Swami and S. Chandra, "Correlations for pressure distribution of buildings and calculation of natural-ventilation airflow," *ASHRAE Transactions*, vol. 94, pp. 243-266, 1988.
- [51] F. Amara, K. Agbossou, A. Cardenas, Y. Dubé and S. Kelouwani, "Comparison and Simulation of Building Thermal Models for Effective Energy Management," *Smart Grid and Renewable Energy*, vol. 6, no. 4, pp. 95-112, 2015.
- [52] X. Li and J. Wen, "Review of building energy modeling for control and operation," *Renewable and Sustainable Energy Reviews*, vol. 37, pp. 517-537, 2014.
- [53] J. D. Spitler, Load Calculation Application Manual, ASHRAE, 2014.
- [54] M. Hiller, S. Holst, T. Welfonder, A. Weber and M. Koschenz, "TRNFLOW: Integration of the airflow model COMIS into the multi-zone building model of TRNSYS," TRANSOLAR Energietechnik GmbH, 2002.
- [55] A. Ghaffarianhoseini, U. Berardi, H. AlWaer, H. Chang, S. Halawa, A. Ghaffarianhoseini and D. ClementsCroome, "What is an intelligent building? Analysis of recent interpretations from an international perspective," *Architectural Science Review*, vol. 59, no. 5, pp. 238-257, 2016.

- [56] A. H. Buckman , M. Mayfield Stephen and B. M. Beck, "What is a Smart Building?," *Smart and Sustainable Built Environment*, vol. 3, no. 2, pp. 92-109, 2014.
- [57] A. Ghaffarianhoseini, H. AlWaer, A. Ghaffarianhoseini, D. Clements-Croome, U. Berardi, K. Raahemifar and J. Tookey, "Intelligent or smart cities and buildings: a critical exposition and a way forward," *Intelligent Buildings International*, pp. 1756-6932, 2017.
- [58] A. I. Dounis, M. J. Santamouris and C. C. Lefas, "Implementation of artificial intelligence techniques in thermal comfort control for passive solar buildings," *Energy Conversion and Management*, vol. 33, no. 3, pp. 175-182, 1992.
- [59] A. I. Dounis and C. Caraiscos, "Advanced control systems engineering for energy and comfort management," *Renewable and Sustainable Energy Reviews*, vol. 13, no. 6-7, pp. 1246-1261, 2009.
- [60] S. Prívarva, J. Šíroky', L. Ferkl and J. Cigler, "Model predictive control of a building heating system: The first experience," *Energy and Buildings*, vol. 43, no. 2-3, pp. 564-572, 2011.
- [61] Z. Wang, R. Yang and L. Wang, "Multi-agent Intelligent Controller design for Smart and Sustainable Buildings," in *2010 IEEE International Systems Conference*, San Diego, 2010.
- [62] B. Dong and K. P. Lam, "A real-time model predictive control for building heating and cooling systems based on the occupancy behavior pattern detection and local weather forecasting," *Building Simulation*, vol. 7, no. 1, pp. 89-106, 2014.
- [63] Y. H. Song and A. T. Johns, "Application of fuzzy logic in power systems. II. Comparison and integration with expert systems, neural networks and genetic algorithms," *Power Engineering Journal*, vol. 12, no. 4, pp. 185-190, 1998.

- [64] G. M. Stavrakakisa, P. L. Zervas, H. Sarimveis and N. C. Markatos, "Optimization of window-openings design for thermal comfort in naturally ventilated buildings," *Applied Mathematical Modelling*, vol. 36, no. 1, pp. 193-211, 2012.
- [65] G. M. Stavrakakis, D. P. Karadimou, P. L. Zervas, H. Sarimveis and N. C. Markatos, "Selection of window sizes for optimizing occupant comfort and hygiene based on computational fluid dynamics and neural network," *Building and Environment*, vol. 46, no. 2, pp. 298-314, 2011.
- [66] J. I. Kindangen, "Artificial neural network and naturally ventilated buildings-A method of predicting window size and location with subsequent effect on interior air motion using neural networks," *Building Research & Information*, vol. 24, no. 4, pp. 203-208, 1996.
- [67] S. A. Kalogirou, M. M. Eftekhari and D. J. Pinnock, "Artificial neural networks for predicting air flow in a naturally ventilated test room," *Building Services Engineering Research and Technology*, vol. 22, no. 2, pp. 83-93, 2001.
- [68] S. Kalogirou, M. Eftekhari and L. Marjanovic, "Predicting the pressure coefficients in a naturally ventilated test room using artificial neural networks," *Building and Environment*, vol. 38, no. 3, pp. 399-407, 2003.
- [69] T. Salque, D. Marchio and P. Riederer, "Neural predictive control for single-speed ground source heat pumps connected to a floor heating system for typical French dwelling," *Building Services Engineering Research and Technology*, vol. 35, no. 2, pp. 182-197, 2013.
- [70] J. Krauss, M. Bauer, N. Morel and M. EL-Khouri, "NEUROBAT Predictive Neuro:Fuzzy Building Control System," CSEM and EPFL, 1998.
- [71] S. Hou, T. Wu, D. Hu, X. Xiao and Y. Liu, "Intelligent Window System for Obtaining Weather Information Based on Internet," in *2018 3rd International*

*Conference on Mechanical, Control and Computer Engineering (ICMCCE)*, Huhhot, China, 2018.

- [72] Z. Sun, S. Wei and X. Zhang, "Intelligent Window Control System Design Based on Single Chip Microcomputer," in *2020 IEEE International Conference on Progress in Informatics and Computing (PIC)*, Shanghai, China, 2020.
- [73] K. Zhang, G. Shi and Z. Zhai, "Design and Implementation of Automatic Window Closer Based on Intelligent Control Algorithm," in *2019 IEEE International Conference on Mechatronics and Automation (ICMA)*, Tianjin, China, 2019.
- [74] S. P. Medeiros, J. J. P. C. Rodrigues, M. A. A. da Cruz, R. A. L. Rabêlo, K. Saleem and P. Solic, "Windows Monitoring and Control for Smart Homes based on Internet of Things," in *2019 4th International Conference on Smart and Sustainable Technologies (SpliTech)*, Split, Croatia, 2019.
- [75] F. Stazi, F. Naspi, G. Ulpiani and C. D. Perna, "Indoor air quality and thermal comfort optimization in classrooms developing an automatic system for windows opening and closing," *Energy and Buildings*, vol. 139, pp. 732-746, 2017.
- [76] M. Han, R. May, X. Zhang, X. Wang, S. Pan, D. Yan and Y. Jin, "A novel reinforcement learning method for improving occupant comfort via window opening and closing," *Sustainable Cities and Society*, vol. 61, 2020.
- [77] M. Fiorentini, G. Kokogiannakis, W. Jackson, Z. Ma and P. Cooper, "Evaluation methodology and implementation for natural ventilation control strategies," in *CLIMA 2016 - proceedings of the 12th REHVA World Congress*, Aalborg, Denmark, 2016.
- [78] M. Fiorentini, G. Serale, G. Kokogiannakis, A. Capozzoli and P. Cooper, "Development and evaluation of a comfort-oriented control strategy for thermal management of mixed-mode ventilated buildings," *Energy and Buildings*, vol. 202, 2019.

- [79] J. Chen, G. Augenbroe and S. Song, "Lighted-weighted model predictive control for hybrid ventilation operation based on clusters of neural network models," *Automation in Construction*, vol. 89, pp. 250-265, 2018.
- [80] University of Wisconsin (Solar Energy Laboratory), "TRNSYS 17 Documentation," Madison, 2012.
- [81] L. Nielsen, "Analysis of the radiant heating and cooling System in the Green Energy," 2015.
- [82] D. G. Stephenson and G. P. Mitalas, "Calculation of heat conduction transfer functions for multi-layer slabs," *ASHRAE Transactions*, vol. 77, no. 2, p. 117-126, 1971.
- [83] P. Voit, T. Lechner and M. Schuler, "Common EC validation procedure for dynamic building simulation programs - application with TRNSYS," in *Conference of international simulation societies*, Zürich, 1994.
- [84] D. Saelens, "Energy performance assessment of single storey multiple-skin facades," Leuven, 2002.
- [85] J. E. Seem, "Modeling of heat transfer in buildings," Madison, 1987.
- [86] E. Dascalaki, M. Santamouris, M. Bruant, C. A. Balaras, A. Bossaer, D. Ducarme and P. Wouters, "Modeling large openings with COMIS," *Energy and Buildings*, vol. 30, no. 1, pp. 105-115, 1999.
- [87] A. Haas, A. Weber, V. Dorer, W. Keilholz and R. Pelletret, "COMIS v3.1 simulation environment for multizone air flow and pollutant transport modelling," *Energy and Buildings*, vol. 34, no. 9, pp. 873-882, 2002.
- [88] E. Dascalaki, M. Santamouris, A. Argiriou, C. Helmis, D. N. Asimakopoulos, K. Papadopoulos and A. Soilemes, "Predicting single sided natural ventilation rates in buildings," *Solar Energy*, vol. 55, no. 5, pp. 327-341, 1995.

- [89] H. E. Feustel and B. V. Smith, "COMIS 3.2 Users Guide," EMPA, 2005.
- [90] F. Allard and Y. Utsumi, "Airflow through large openings," *Energy and Buildings*, vol. 18, no. 2, pp. 133-145, 1992.
- [91] P. Heiselberg, K. Svdt and P. V. Nielsen, "Characteristics of airflow from open windows," *Building and Environment*, vol. 36, no. 7, p. 859-869, 2001.
- [92] H. Wang and Q. Y. Chen, "Modeling of the impact of different window types on single-sided natural ventilation," in *Energy Procedia*, 2015.
- [93] H. Wang, P. Karava and Q. Chen, "Development of simple semiempirical models for calculating airflow through hopper, awning, and casement windows for single-sided natural ventilation," *Energy and Buildings*, vol. 96, pp. 373-384, 2015.
- [94] A. Tecele, G. T. Bitsuamlak and T. E. Jiru, "Wind-driven natural ventilation in a low-rise building: A Boundary Layer Wind Tunnel study," *Building and Environment*, vol. 59, pp. 275-289, 2013.
- [95] ANSI/ASHRAE Standard 140-2017, "Standard Method of Test for the Evaluation of Building Energy Analysis Computer Programs," 2017.
- [96] "Auckland Design Manual," Auckland Council, [Online]. Available: <http://www.aucklanddesignmanual.co.nz/sites-and-buildings/mixed-use/guidance/thebuilding/buildingform/floortoceilingheights>.
- [97] "New Zealand Legislations," Housing improvement regulation, 1947. [Online]. Available: <https://www.legislation.govt.nz/regulation/public/1947/0200/latest/whole.html>. [Accessed 2018].

- [98] M. Orme, M. W. Liddament and A. Wilson, "Numerical Data for Air Infiltration and Natural Ventilation Calculations," Air Infiltration and Ventilation Center (AIVC), 1998.
- [99] M. K. Pokhrel, T. N. Anderson, J. Currie and T. T. Lie, "Examining the Thermal Comfort Characteristics of Naturally Ventilated Residential Buildings in New Zealand," in *Asia Pacific Solar Research Conference*, Canberra, Australia, 2016.
- [100] Y. A. Cengel and J. G. Afshin, *Heat and Mass Transfer: Fundamentals and Applications*, 5 ed., Mc-Graw Hill Education, 2015.
- [101] F. Alamdari and G. P. Hammond, "Improved data correlations for buoyancy-driven convection in rooms," *Building Services Engineering Research and Technology*, vol. 4, no. 3, pp. 106-112, 1983.
- [102] A. J. N. , Khalifa and R. H. Marshall, "Validation of heat transfer coefficients on interior building surfaces using a real-sized indoor test cell," *International Journal of Heat and Mass Transfer*, vol. 33, no. 10, pp. 2219-2236, 1990.
- [103] A. J. N. Khalifa, "Heat transfer processes in buildings," Cardiff, 1989.
- [104] R. K. Calay, A. E. Holdø and G. P. Hammond , "Natural convective heat transfer rates in rectangular enclosures," *Building and Energy*, vol. 27, no. 2, pp. 137-146, 1998.
- [105] H. B. Awbi and A. Hatton, "Natural convection from heated room surfaces," *Energy and Buildings*, vol. 30, no. 3, pp. 233-244, 1999.
- [106] K. Goethals , H. Breesch and A. Janssens, "Sensitivity analysis of predicted night cooling performance to internal convective heat transfer modelling," *Energy and Building*, vol. 43, no. 9, pp. 2429-2441, 2011.
- [107] A. Rincón-Casado, F. J. Sánchez de la Flor, E. Chacón Vera and J. Sánchez Ramos, "New natural convection heat transfer correlations in enclosures for

building performance simulation," *Engineering applications of computational fluid mechanics*, vol. 11, no. 1, pp. 340-356, 2017.

- [108] K. J. Lomas, "The U.K. applicability study: an evaluation of thermal simulation programs for passive solar house design," *Building and Environment*, vol. 31, no. 3, pp. 197-206, 1996.
- [109] M. Mirsadeghi, D. Costola, B. J. E. Blocken and J. L. M. Hensen, "Review of External Convective Heat Transfer Coefficient Models in Building Energy Simulation Programs: Implementation and Uncertainty," *Applied Thermal Engineering*, vol. 56, no. 1-2, pp. 134-151, 2013.
- [110] E. Bilgen and A. Muftuoglu, "Natural convection in an open square cavity with slots," *International Communications in Heat and Mass Transfer*, vol. 35, no. 8, pp. 896-900, 2008.
- [111] M. Prakash, S. B. Kedare and J. K. Nayak, "Numerical study of natural convection loss from open cavities," *International Journal of Thermal Sciences*, vol. 51, pp. 23-30, 2012.
- [112] T. N. Anderson, "Natural convection heat transfer from a partly open enclosure," in *8th Australian Natural Convection Workshop (8ANCW)*, Sydney, December 16-17, 2013.
- [113] S. E. Norris and T. N. Anderson, "A CFD Model of Natural Convection in a Partially Open Enclosure," in *9th Australasian Heat and Mass Transfer Conference (AHMT 2015)*, Melbourne, December 14-15, 2015.
- [114] T. N. Anderson and S. E. Norris, "Natural convection heat loss from a partly open cubic enclosure," in *10th Australasian Heat and Mass Transfer Conference (AHMT2016)*, Brisbane, 2016.

- [115] J. Franke , A. Hellsten , H. Schlünzen and B. Carissimo, “Best Practice Guideline for the CFD Simulation of Flows in the Urban Environment,” Brussels: COST Office, 2007.
- [116] C. Teodosiu, F. Kuznik and R. Teodosiu, “CFD modeling of buoyancy driven cavities with internal heat source-Application to heated rooms,” *Energy and Buildings*, vol. 68, pp. 403-411, 2014.
- [117] M. Omri and N. Galanis, “Numerical analysis of turbulent buoyant flows in enclosures: Influence of grid and boundary conditions,” *International Journal of Thermal Sciences*, vol. 46, no. 8, pp. 727-738, 2007.
- [118] M. Uzair, T. Anderson and R. Nates, “The impact of the parabolic disc concentrator on the wind induced heat loss from its receiver,” *Solar Energy*, vol. 151, pp. 95-101, 2017.
- [119] M. Uzair, “Wind induced heat losses from solar dish-receiver system,” Auckland, 2018.
- [120] T. Yamanaka, H. Kotani, K. Iwamoto and M. Kato, “Natural, Wind-Forced Ventilation Caused by Turbulence in a Room with a Single Opening,” *International Journal of Ventilation*, vol. 5, no. 1, pp. 179-187, 2006.
- [121] T. Stabat, T. M. Caciolo and D. Marchio, “Progress on Single-Sided Ventilation Techniques for Buildings,” *Advances in Building Energy Research*, vol. 6, no. 2, pp. 212-241, 2012.
- [122] M. K. Pokhrel, T. N. Anderson and T. T. Lie, “Improving the Robustness of the Thermal Models of Natural Ventilated Buildings,” in *The Asia-Pacific Solar Research Conference 2017*, Melbourne, Australia, 2017.
- [123] J. Spitler, C. Pedersen, D. Fisher, P. Menne and J. Cantillo, “An experimental facility for investigation of interior convective heat transfer,” *ASHRAE Transactions*, vol. 97, no. 1, pp. 497-504, 1991.

- [124] J. Spitler, C. Pedersen and D. Fisher, "Interior convective heat transfer in buildings with large ventilative flow rates," *ASHRAE Transactions*, vol. 97, no. 1, pp. 505-515, 1991.
- [125] D. E. Fisher, "An experimental investigation of mixed convection heat transfer in a rectangular enclosure," Urbana, USA, 1995.
- [126] D. E. Fisher and C. O. Pedersen, "Convective heat transfer in building energy and thermal load calculations," *ASHRAE Transactions*, vol. 103, no. 2, pp. 137-148, 1997.
- [127] H. B. Awbi and A. Hatton, "Mixed convection from heated room surfaces," *Energy and Buildings*, vol. 32, no. 2, pp. 153-166, 2000.
- [128] I. Beausoleil-Morrison, "Modelling mixed convection heat transfer at internal building surfaces," in *International Building Performance Simulation Association*, Kyoto, 1999.
- [129] I. Beausoleil-Morrison, "The adaptive coupling of heat and air flow modelling within dynamic whole-building simulation," Glasgow, UK, 2000.
- [130] Macara, G. R., "The climate and weather of New Zealand," NIWA, 2018.
- [131] M. K. Pokhrel, T. N. Anderson and T. T. Lie, "Improving Thermal Comfort Regulating Potential in Naturally Ventilated Residential House," in *Asia Pacific Solar Research Conference*, Sydney, Australia, 2018.
- [132] J. Park, X. Sun, J. Choi and G. H. Rhee, "Effect of wind and buoyancy interaction on single-sided ventilation in," *Journal of Wind Engineering & Industrial Aerodynamics*, vol. 171, pp. 380-389, 2017.
- [133] C. Allocca, Q. Chen and L. R. Glicksman, "Design analysis of single-sided natural ventilation," *Energy and Buildings*, vol. 35, no. 8, pp. 785-795, 2003.

- [134] P. Warren and L. Parkins, "Single-sided ventilation through open windows," *ASHRAE*, vol. SP 49, pp. 209-228, 1985.
- [135] M. Dascalaki, M. Santamouris, A. Argiriou, C. Helmis, D. N. Asimakopoulos, K. Papadopoulos and A. Soilemes, "On the combination of air velocity and flow measurements in single sided natural ventilation configurations," *Energy and Buildings*, vol. 24, no. 2, pp. 155-165, 1996.
- [136] A. A. Argiriou, C. A. Balaras and S. P. Lykoudis, "Single-sided ventilation of buildings through shaded large openings," *Energy*, vol. 27, no. 2, pp. 93-115, 2002.
- [137] T. S. Larsen and P. Heiselberg, "Single-sided natural ventilation driven by wind pressure and temperature difference," *Energy and Buildings*, vol. 40, no. 6, pp. 1031-1040, 2008.
- [138] M. Caciolo, P. Stabat and D. Marchio, "Full scale experimental study of single-sided ventilation: Analysis of stack and wind effects," *Energy and Buildings*, vol. 43, no. 7, pp. 1765-1773, 2011.
- [139] M. Caciolo, P. Stabat and D. Marchio, "Numerical simulation of single-sided ventilation using RANS and LES and comparison with full-scale experiments," *Building and Environment*, vol. 50, pp. 202-213, 2012.
- [140] M. Caciolo, S. Cui, P. Stabat and D. Marchio, "Development of a new correlation for single-sided natural ventilation adapted to leeward conditions," *Energy and Buildings*, vol. 60, pp. 372-382, 2013.
- [141] M. K. Pokhrel and T. N. Anderson, "Spatial Distribution of Heat Transfer in Naturally Ventilated Buildings Surfaces," in *10th Australasian Natural Convection Workshop (10 ANCW)*, Auckland, New Zealand, 2017.
- [142] M. K. Pokhrel, T. N. Anderson and T. T. Lie, "Influence of wind on indoor convective floor heat transfer of single-sided naturally ventilated cubical enclosures,"

in *52nd International Conference of the Architectural Science Association (ANZAScA)*, Melbourne, 2018.

- [143] M. K. Pokhrel, T. N. Anderson and T. T. Lie, "The effect of wind on the convective heat transfer from the floor of single-sided naturally ventilated cubical enclosures," *Architectural Science Review*, 2020.
- [144] NZS 3604, "Timber Framed Buildings," Standards New Zealand, 2011.
- [145] P. R. Warren, "Ventilation through openings on one wall only," in *Energy Conservation in Heating, Cooling and Ventilating Buildings*, Dubrovnik, Yugoslavia, 1977.
- [146] M. K. Pokhrel, T. N. Anderson and T. T. Lie, "MAINTAINING THERMAL COMFORT OF A SINGLE-SIDED NATURALLY VENTILATED MODEL HOUSE BY INTELLIGENTLY ACTUATING WINDOWS," in *The 24th International Conference of the Association for Computer-Aided Architectural Design Research in Asia (CAADRRIA) 2019*, Wellington, 2019.
- [147] S. A. Kalogirou, "Applications of artificial neural networks in energy systems: A review," *Energy Conversion & Management*, vol. 40, pp. 1073-1087, 1999.
- [148] M. Lawrynczuk, *Computationally Efficient Model Predictive Control Algorithms- A Neural Network Approach*, Springer, 2014.
- [149] A. Afram, F. Janabi-Sharifi, A. S. Fung and K. Raahemifar, "Artificial neural network (ANN) based model predictive control (MPC) and optimization of HVAC systems: A state of the art review and case study of a residential HVAC system," *Energy and Buildings*, vol. 141, pp. 96-113, 2017.
- [150] S. Atthajariyakul and T. Leephakpreeda, "Neural computing thermal comfort index for HVAC systems," *Energy Conversion and Management*, vol. 46, no. 15-16, pp. 2553-2565, 2005.

- [151] E. F. Alsina, M. Bortolini, M. Gamberi and A. Regattieri, "Artificial neural network optimisation for monthly average daily global solar radiation prediction," *Energy Conversion and Management*, vol. 120, pp. 320-329, 2016.
- [152] I. Tasadduq, S. Rehman and K. Bubshait, "Application of neural networks for the prediction of hourly mean surface temperatures in Saudi Arabia," *Renewable Energy*, vol. 25, no. 4, pp. 545-554, 2002.
- [153] S. A. Kalogirou, "Artificial neural networks in renewable energy systems applications: a review," *Renewable and Sustainable Energy Reviews*, vol. 5, no. 4, pp. 373-401, 2001.
- [154] E. Cadenas and W. Rivera, "Short term wind speed forecasting in La Venta, Oaxaca, México, using artificial neural networks," *Renewable Energy*, vol. 34, no. 1, pp. 274-278, 2009.
- [155] S. Atthajariyakul and T. Leephakpreeda, "Real-time determination of optimal indoor-air condition for thermal comfort, air quality and efficient energy usage," *Energy and Buildings*, vol. 36, no. 7, pp. 720-733, 2004.
- [156] J. V. Grabe, "Potential of artificial neural networks to predict thermal sensation votes," *Applied Energy*, vol. 161, pp. 412-424, 2016.
- [157] H. Huang, L. Chen and E. Hu, "A new model predictive control scheme for energy and cost savings in commercial buildings: An airport terminal building case study," *Building and Environment*, vol. 89, pp. 203-216, 2015.
- [158] P. M. Ferreira, S. M. Silva, A. E. Ruano, A. T. Négrier and E. Z. Conceição, "Neural network PMV estimation for model-based predictive control of HVAC systems," in *The 2012 International Joint Conference on Neural Networks (IJCNN)*, Brisbane, QLD, Australia, 2012.

- [159] A. Garnier, J. Eynard, M. Caussanel and S. Grieu, "Predictive Control of Multizone HVAC Systems in Non-residential Buildings," in *IFAC Proceedings Volumes*, 2014.
- [160] A. Sfetsos and A. H. Coonick, "Univariate and multivariate forecasting of hourly solar radiation with artificial intelligence techniques," *Solar Energy*, vol. 68, no. 2, pp. 169-178, 2000.
- [161] R. Marquez and C. F. Coimbra, "Forecasting of global and direct solar irradiance using stochastic learning methods, ground experiments and the NWS database," *Solar Energy*, vol. 85, no. 5, pp. 746-756, 2011.
- [162] A. Khotanzad, M. H. Davis, A. Abaye and D. J. Maratukulam, "An artificial neural network hourly temperature forecaster with applications in load forecasting," *IEEE Transactions on Power Systems*, vol. 11, no. 2, pp. 870-876, 1996.
- [163] A. Ahmad and T. N. Anderson, "Hourly global solar irradiation forecasting for New Zealand," *Solar Energy*, vol. 122, pp. 1398-1408, 2015.
- [164] A. Erfani, A. Rajabi-Ghahnaviyeh and M. Boroushaki, "Design and construction of a non-linear model predictive controller for building's cooling system," *Building and Environment*, vol. 130, pp. 237-245, 2018.
- [165] S. Yang, M. P. Wan, W. Chen, B. F. Ng and S. Dubey, "Experiment study of machine-learning-based approximate model predictive control for energy-efficient building control," *Applied Energy*, vol. 288, 2021.
- [166] M. K. Pokhrel, T. N. Anderson, J. Currie and T. T. Lie, "An Intelligent System for Actuating Windows of Naturally Ventilated Residential Houses," in *51st International Conference of the Architectural Science Association (ANZAScA)*, Wellington, New Zealand, 2017.

- [167] MathWorks, "Shallow Neural Network Time-Series Prediction and Modeling," 2018.
- [168] D. E. Fisher, "An Experimental Investigation of Mixed Convection Heat Transfer in a Rectangular Enclosure," Urbana, USA, 1995.